



SRF2011
C H I C A G O
15th International Conference on RF Superconductivity

Chicago, Illinois USA
July 25-29, 2011

Hosted by

Argonne National Laboratory
9700 S. Cass Avenue
Argonne, IL 60439

and

Fermi National Accelerator Laboratory
P.O. Box 500
Batavia, IL 60510



WELCOME

Dear Attendee,

On behalf of the International Program Committee (IPC), we would like to welcome you to Chicago for the 15th International Conference on RF Superconductivity (SRF2011) hosted by Argonne National Laboratory and Fermi National Accelerator Laboratory.

We are truly gratified to have more than 350 registered attendees this year, nearly 100 tutorial attendees and more than 45 students participating in the student poster sessions. The IPC has tried to be receptive to the community desire to expand time for posters, and provide genuinely useful and stimulating "hot topic" discussions. We hope you agree.

We also acknowledge up front the generous support of our worldwide sponsors.

Lastly, we hope you enjoy the conference and your stay in our city.

Sincerely,



Michael Kelly
Program Committee Co-Chair



Robert Kephart
Program Committee Co-Chair

INTERNATIONAL PROGRAM COMMITTEE

Claire Antoine (CEA-Saclay)
Jia-er Chen (Peking Univ.)
Jean Delayen (Old Dominion Univ.)
Helen Edwards (FNAL)
Walter Hartung (MSU)
Michael Kelly (ANL) **SRF 2011 Co-Chair**
Robert Kephart (FNAL) **SRF 2011 Co-Chair**
Jens Knobloch (HZB) **IPC Chair**
Matthias Liepe (Cornell Univ.)
Wolf-Dietrich Moeller (DESY)
Shuichi Noguchi (KEK)
Vincenzo Palmieri (INFN-LNL)
Charlie Reece (JLAB)
Tsuyoshi Tajima (LANL)
Wolfgang Weingarten (CERN)

LOCAL ORGANIZING COMMITTEE

Shilpee Arora (FNAL)
Janet Bergman (ANL)
Tony Favale (SPAFOA)
Scott Gerbick(ANL)
Michael Kelly (ANL)
Robert Kephart (FNAL)
Jacque LeBreck (ANL)
Shekhar Mishra (FNAL) **Co-Chair**
Jim Norem (ANL) **Co-Chair**
Alireza Nassiri (ANL)
Maria Power (ANL)
Thomas Prolier (ANL)
Cynthia Sazama (FNAL)
Jen Seivwright (ANL)
Suzanne Weber (FNAL)

Contact E-mail: SRF2011@anl.gov

TABLE OF CONTENTS

General Information	5
Conference Venue	5
Registration/Information Desk.....	5
Welcome Reception	5
Breaks and Lunches	5
Internet & Wireless Service.....	5
Information for Speakers	6
Tours of Argonne and Fermilab.....	7
Group Photograph	8
List of Participants	8
Security	8
Vendor Exhibits	8
Tipping	8
No-Smoking Policy	8
About Chicago.....	8
About Argonne National Laboratory.....	9
About Fermi National Accelerator Laboratory.....	9
Transportation	9
Architectural River Cruise	10
Banquet Venue	11
Lunch Options	12
Sheraton Floor Plans	14
Sponsors	15
Exhibitors	17
Abstract Contents.....	25
Program	33
Abstracts.....	47
Author Index.....	145
List of Registrants.....	154

GENERAL INFORMATION

CONFERENCE VENUE

Sheraton Chicago Hotel & Towers
301 East North Water Street
Chicago, IL 60611 USA
Phone: 1-312-464-1000
Fax: 1-312-464-9140
E-mail: info@sheratonchicago.com
URL: www.sheratonchicago.com/

REGISTRATION/INFORMATION DESK

Registration materials (i.e., conference badge, banquet tickets) will be available at the registration desk located outside the Sheraton Chicago Ballroom Promenade.

Sunday, July 24	16:00 – 20:00	Wednesday, July 27	07:30 – 15:00
Monday, July 25	07:00 – 17:00	Thursday, July 28	07:30 – 17:00
Tuesday, July 26	07:30 – 17:00	Friday, July 29	07:30 – 13:00

WELCOME RECEPTION - SUNDAY, JULY 24TH

You are invited to join us for a Welcome Reception on Sunday, July 24, at 18:00 in the Sheraton Chicago Ballroom Promenade. While there you can check-in, receive your conference materials and enjoy refreshments.

BREAKS AND LUNCHES

Refreshment breaks are at 10:15 each day and 16:00 during poster sessions. Lunch breaks are from 13:00–14:30. A list of restaurants near the Sheraton Chicago Hotel & Towers is included with the information you received at registration. Please feel free to ask the concierge for additional recommendations.

INTERNET & WIRELESS SERVICE

Internet service is available at The Link @ Sheraton Café located on Level 2. Complimentary wireless networking is available in the SRF meeting rooms.

An online agenda/program is available at <http://appora.fnal.gov/pls/srf11/agenda.html>

INFORMATION FOR SPEAKERS

All presentations should be submitted through the SRF2011 Author Account at <http://appora.fnal.gov/pls/srf11/profile.html> ahead of time. A monitor will be available near the registration area to view the editing status of your paper.

Invited Talks

Invited talks will take place in Sheraton Ballrooms IV & V starting at 08:00 each morning. Speakers should upload a PDF of their slides through the SRF2011 Author Account 45 minutes prior to the talk. Slides will be available to participants online during the presentation via the SRF2011 website.

Poster Sessions

Poster Sessions will take place in Sheraton Ballrooms I, II, & III. Presenters should upload a PDF of their poster for inclusion in the proceedings.

Student Poster Session	Sunday, July 24	16:00-18:00 (displayed until 20:00)
Poster Session 1	Monday, July 25	14:30-18:00
Poster Session 2	Tuesday, July 26	14:30-18:00
Poster Session 3	Thursday, July 28	14:30-18:00

Poster Display and Removal

You may put your poster up any time after 08:00 on the day of your poster session. Your poster must be on display by 14:30 on the day of your presentation. The poster Paper IDs will be displayed on the boards. Mount your poster on the board labeled with your Paper ID. **Please remove your poster at the end of your poster session.**

Proceedings

All contributions properly presented at the conference are eligible for publication in the conference proceedings at the JACoW site. Upload of contributions is via the SRF2011 Author Account and detailed instructions can be found at the SRF2011 website. **The deadline for the submission of contributions to the proceedings is the first day of the conference Monday, July 24, 2011.**

The preliminary proceedings will be available on the SRF2011 web site. The final version will be posted on the JACoW site at <http://accelconf.web.cern.ch/accelconf/>. Questions concerning the proceedings may be addressed to the Proceedings Editor, Maria Power.

The Proceedings Office will be located in the Missouri Room on Level 2 of the Sheraton.

TOURS OF ARGONNE AND FERMILAB – FRIDAY, JULY 29

Tours to the SRF facilities at Argonne National Laboratory and Fermi National Accelerator Laboratory have been organized. Attendees can choose to go to one or the other, but not both. The buses will leave on Friday, July 29th, at 13:00 from the Lower Lobby of the hotel in the bus/departure area. The tour will last approximately two hours and the buses will return to the Sheraton at ~17:30. Assorted boxed lunches will be provided on the buses.

In order to attend the tour at Argonne National Laboratory, you **MUST** be pre-registered. All visitors (except children under the age of 17) are required to present photo identification, such as a driver's license or passport, to receive a gate pass.

Gate passes will be issued by Jennifer Seivwright upon entering the bus.

****IMPORTANT****

FOR THE ARGONNE TOUR: If you are not a U.S. citizen, you will be **REQUIRED** to present a copy of your **passport, visa and/or I-94 documentation** in order to attend the tour. You may scan and e-mail these documents in advance to srf2011@anl.gov or provide them upon registration in a sealed envelope addressed to **Jennifer Seivwright**.

GROUP PHOTOGRAPH

A group photograph will be taken place on Monday, July 25th, just before lunch.

LIST OF PARTICIPANTS

A list of SRF2011 registrants is included in the back of this book. The list of participants will be posted on the SRF2011 website following the conference.

SECURITY

Participants are asked not to leave their baggage or conference bags unattended and to wear conference badges at all times. The conference organizers cannot accept liability for personal injuries sustained, or for loss of, or damage to, property belonging to conference participants (or accompanying persons), either during or as a result of the conference.

VENDOR EXHIBITS

Vendor Exhibits are located in Sheraton Ballrooms 1, 2, and 3.

TIPPING

Tipping in the United States is generally 15-20% for restaurant service; more for exceptional service. Tips are typically 10-15% for taxis and \$1.00 per bag for luggage.

NO-SMOKING POLICY

Illinois has a no-smoking policy that restricts smoking in all public and work places; smoking is only permitted outside (15 feet beyond building entrances).

ABOUT CHICAGO

Chicago is the third largest city in the United States, with a population of nearly three million people. Its scenic lakeside location, world-class cultural offerings and unique architecture are just a few of the reasons why Chicago is a great place to live and visit. You can explore the city by bus, boat, or on foot. There are many attractions such as the John Hancock and Willis Towers, Millennium Park, Navy Pier, The Art Institute of Chicago, Shedd Aquarium, Field Museum, Adler Planetarium, Lincoln Park Zoo, and the Museum of Science & Industry.

Please visit the conference website at <http://conferences.fnal.gov/srf2011/chicago.html> for more information.

ABOUT ARGONNE NATIONAL LABORATORY (ARGONNE)

Argonne National Laboratory (Argonne) is a U.S. Department of Energy Laboratory managed by UChicago Argonne, LLC, under contract number DE-AC02-06CH11357. Argonne is located southwest of Chicago at 9700 S. Cass Avenue, Argonne, IL 60439. See www.anl.gov for information about Argonne.

ABOUT FERMI NATIONAL ACCELERATOR LABORATORY (FERMILAB)

Fermilab, is a U.S. Department of Energy National Laboratory specializing in high-energy particle physics. As of January 1, 2007, Fermilab is operated by the Fermi Research Alliance, a joint venture of the University of Chicago and the Universities Research Association (URA). Fermilab is located just outside Batavia near Chicago, Illinois. See www.fnal.gov for information about Fermilab.

TRANSPORTATION

Within Chicago, transportation is usually by taxi cab or through the Chicago Transit Authority (CTA) bus and rail systems. Transit Cards can be purchased and value can be added to Transit Cards at vending machines located at all CTA rail stations. Vending machines accept \$1, \$5, \$10, and \$20 USD bills, and all coins except pennies and half dollars. Credit cards cannot be used to purchase transit cards at the station.

Taxicabs are available outside the main hotel entrance. Currently, the base Chicago taxi fare is \$2.25 and increases \$.20 for each additional 1/9 of a mile (or 36 seconds). Plus, there is a \$1 charge for the first additional passenger ages 12-65, \$.50 for each additional passenger, and a \$1 fuel surcharge. Tips are accepted for good service.

Taxicab Phone Numbers:

American-United Taxi	773-248-7600	Yellow Cab	312-829-4222
Checker Cab	312-243-2537	Flash Cab	773-561-1444

The CTA provides bus and 'L' (subway) service. See www.transitchicago.com/ for more information.

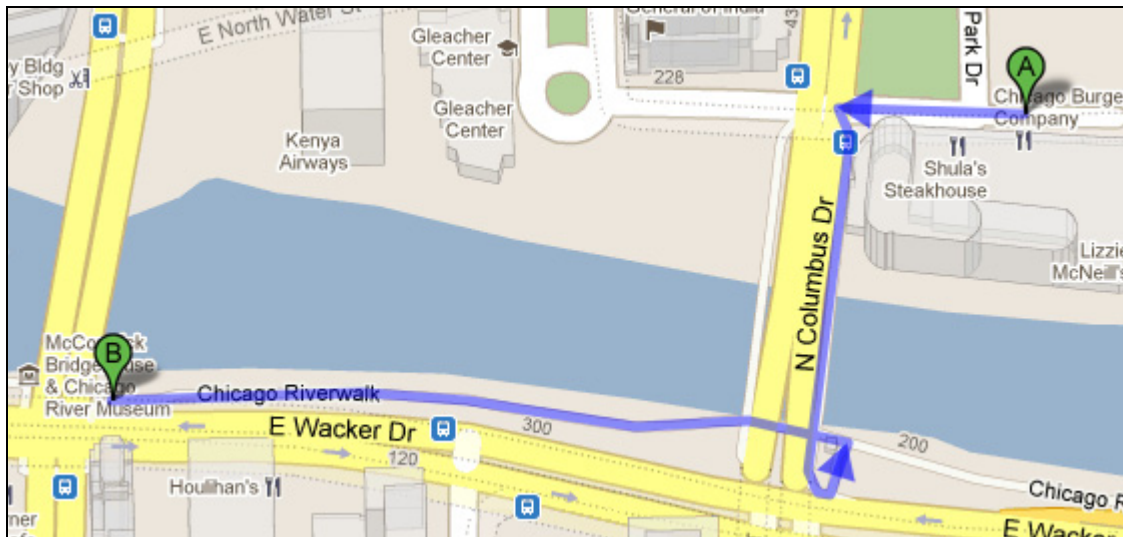
Airport and additional travel information can be found on the conference web page: conferences.fnal.gov/srf2011/hotel.html

ARCHITECTURAL RIVER CRUISE

The 90 minute architectural river cruise of downtown Chicago is scheduled for the afternoon of Wednesday, July 27, 2011. The river tour includes all three branches of the Chicago river and highlights more than 53 historic and architecturally significant sites such as the Wrigley Building, the Tribune Tower, the Merchandise Mart, the Trump Tower, 333 W. Wacker Drive, the Willis (formerly Sears) Tower, River City, Marina City, the Aqua, The Montgomery (formerly the world headquarters for Montgomery Ward), the Chicago Tribune printing press plant, and Goose Island. The boats have outdoor viewing on the upper deck, as well as an air conditioned main deck.

The cost for the river tour is \$26/person (\$22/child under 3 yrs), and will be collected in cash on Sunday, July 24th during the conference registration. There is a full service cash bar on board offering everything from water to mixed drinks. Light snacks are also available for purchase.

If you are participating, we will leave together from the lobby of the Sheraton and walk to the NE corner of Michigan Ave. and E. Wacker Dr. Look for the blue awnings along the river. **Please check your ticket for the boat departure time.**



BANQUET VENUE

The SRF 2011 banquet will be held at the Mid-America Club on Wednesday, July 27th. The Mid America Club is located on the 80th floor in the Aon Center where it enjoys a wonderful panoramic view of the lake, Navy Pier, and the famous Chicago Skyline.

Mid-America Club

200 East Randolph Drive, 80th Floor, Chicago, IL 60601
(847-582-0289)

Reception: 18:00-19:00

Dinner Served: 19:30-20:30

Invited Speaker, Hasan Padamsee, Cornell University
"50 Years of RF Superconductivity"

NOTES: Before being allowed to enter the elevator to the banquet floor, you will need to present picture identification to a Security Guard (*i.e.*, passport, drivers license, etc.)

Required Dress code: NO Blue jeans, shorts, or tennis shoes are allowed

For those interested, at 21:30 there will be a fireworks display at Navy Pier, which is only a short walk away.

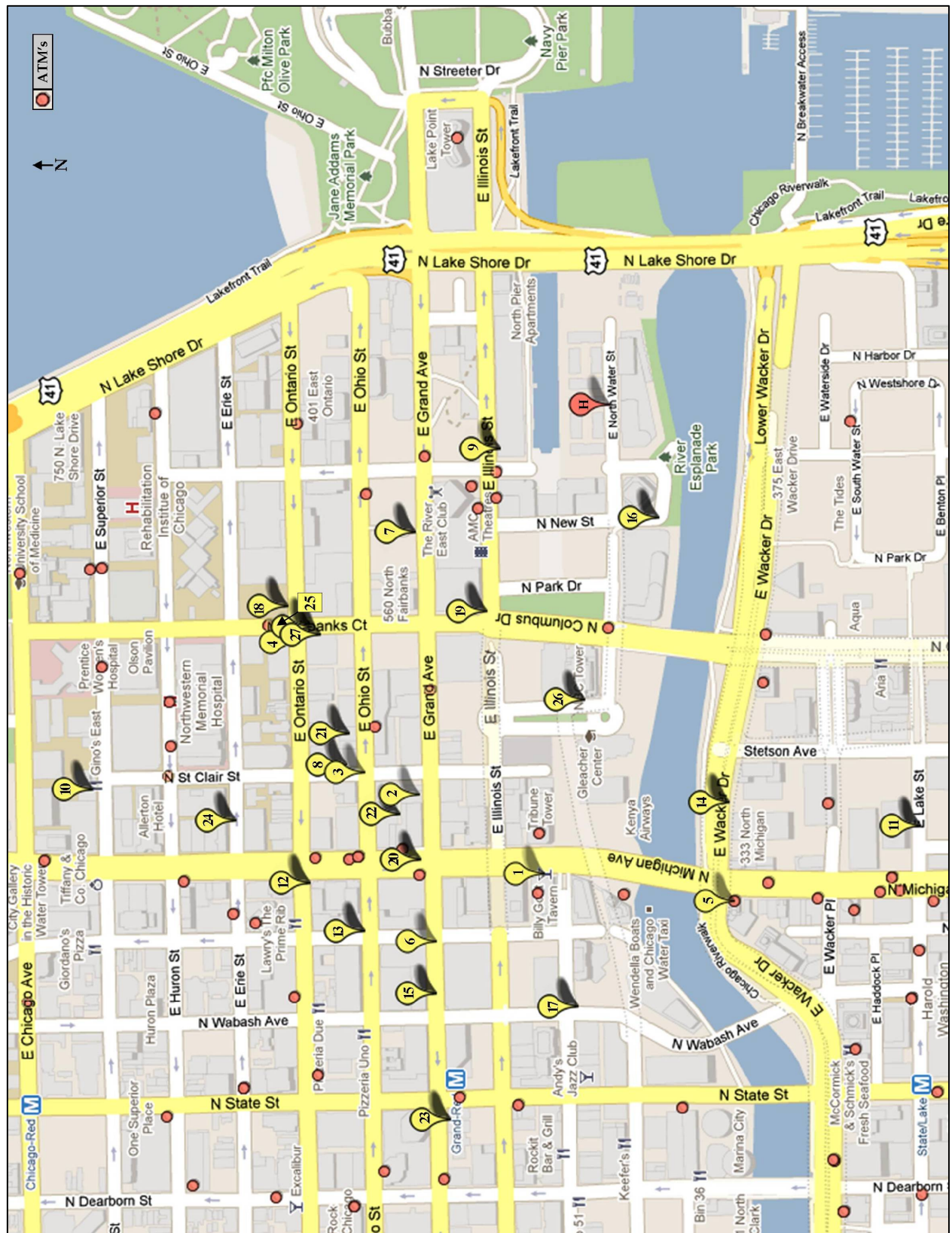


10 Minute Walking Directions

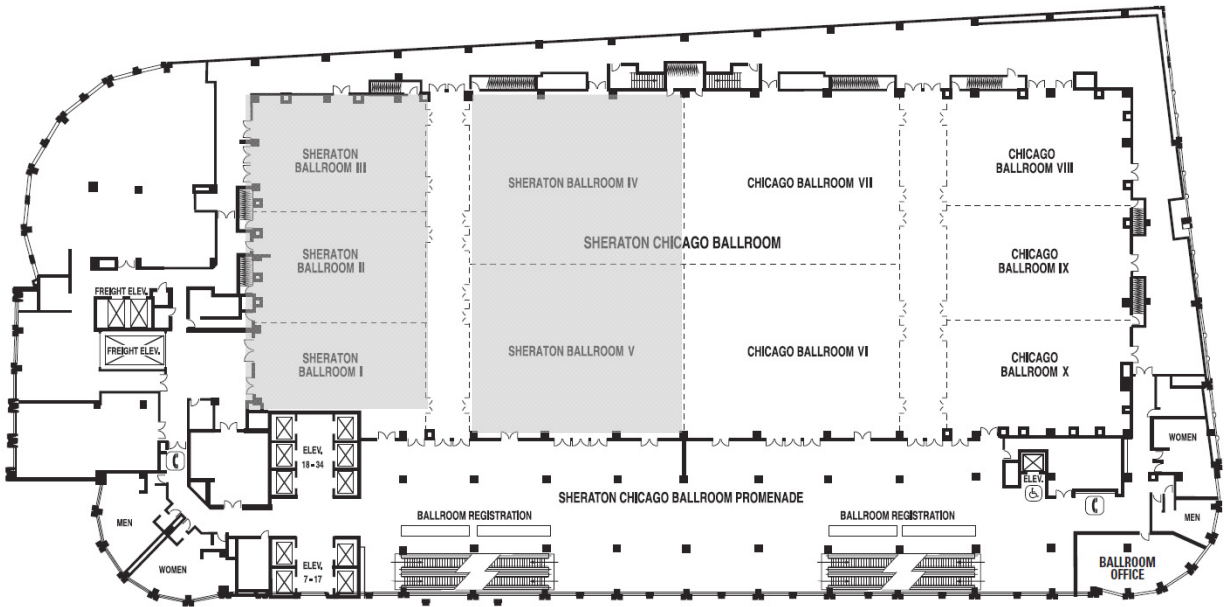
1. Be careful crossing streets!
2. Go west on E. North Water St. (100 m)
3. Turn left and go south on Columbus Dr. (500 m)
4. Turn right and go west on E. Lake St. (100 m)

LUNCH OPTIONS

- 1** **Billy Goat Tavern (Bar/Hamburgers \$5-8)** Walk out the front doors and turn left, walk on to Michigan Ave. Walk across Michigan Ave. to the set of stairs on the other side. Go down the stairs to the bottom and walk forward to Water Street. Billy Goat Tavern will be on the right.
- 2** **Boston Blackies (Bar/Burgers \$8-15)** Walk out the front door and turn left. Turn right onto Columbus and walk down the hill to Grand. Turn left onto Grand Street and walk to St. Clair Street. Boston Blackies is on the right just past St. Clair.
- 3** **Burrito Beach (Casual Mexican \$8-15)** Walk out the front door and turn left. At Columbus Dr. turn right and walk 3 blocks to Ohio St., left on Ohio to St. Clair. Burrito Beach is on the right.
- 4** **Chipotle (Burritos \$8-15)** See directions to West Egg Café. At the corner of Columbus and Ontario, turn left. Chipotle is on the left side of the street.
- 5** **Corner Bakery (Bakery/Sandwiches/Salads under \$8)** Walk out the front door and turn left, follow two blocks to Michigan Avenue. Turn left and proceed across the Michigan Avenue bridge. At the corner of Michigan Avenue and Wacker, cross the street to the left and The Corner Bakery is on the right corner.
- 6** **Costi (Sandwiches/Salads/Flatbreads under \$15)** Walk out the front doors and turn left. At Columbus Dr. turn right. Proceed 2 blocks to Grand Ave. Turn left on Grand and continue for 3 blocks. Costi is on your left hand side across Rush St.
- 7** **D4 (Upscale Irish Pub \$10-25)** At Columbus Dr. turn right. 2 blocks to Grand Ave. Right on Grand ½ block down on the left hand side.
- 8** **Dunkin Donuts/Baskin Robbins(Coffee, donuts, ice cream)** Walk out the front door and turn left. At Columbus Dr. turn right and walk 3 blocks to Ohio St., turn left on Ohio to St. Clair.
- 9** **Fox & Obel Café (inside gourmet grocery store \$8-25)** Walk out front door. Walk straight down the Taxi Ramp to Illinois Street. Turn right on Illinois and walk to McClurg Court. The entrance to Fox & Obel grocery is on the corner of the building on the right. Proceed down the sidewalk in front of the grocery to enter the café.
- 10** **(P) Gino's East (Pizza \$10-25)** Walk out the front door and turn left. Turn right on Columbus Ave and walk for seven blocks to Superior St. Turn left on Superior and walk two blocks. Gino's will be at 162 E. Superior.
- 11** **Giordano's (Pizza \$10-25)** Walk out the front door and turn left. Continue on to Michigan Ave. Turn left onto Michigan Ave. and walk two blocks to Lake Street. Turn left onto Lake Street. Giordano's will be on your right.
- 12** **(P) Grand Lux Café (American \$8-25)** Walk out front doors and turn left. Proceed past NBC Tower, across plaza to Michigan Ave. Cross Michigan Ave and turn right. Proceed 3 blocks to Ontario. Grand Lux is on left, above Ann Taylor.
- 13** **(R) Heaven on Seven (Cajun \$8-15)** Walk out the front doors and turn to your left. Cross Columbus Ave. and continue walking through the courtyard area to Michigan Ave. Cross Michigan Ave. and go to your right down Michigan Ave. Walk 2 blocks to Ohio Street. Turn left on Ohio and walk it is on your right.
- 14** **Houlihan's (American \$8-20)** Walk out the front door and turn left. Continue forward to Michigan Ave. Turn left onto Michigan and walk to Wacker Drive. Turn Left onto Wacker Dr. Houlihan's will be on your right.
- 15** **Jimmy John's (sandwiches under \$8)** Walk out the front door and turn left. Make an immediate right onto Columbus. walk two blocks to Grand Ave. and turn left. Walk 3 ½ blocks down to Rush. Just past Costi.
- 16** **Lizzie McNeil's (pub under \$8)** Walk out the front door and down the cab ramp onto Illinois street. Turn left and proceed forward two blocks. At Marketplace make a right and proceed forward on the Left side past the street just past the stop sign is Lizzie McNeil.
- 17** **McDonalds (Burgers under \$10)** Walk out the front door and turn left. Continue forward to Michigan Ave. Cross Michigan Ave. to the Wrigley Building. Go through the middle of the Wrigley Building and walk forward to McDonalds.
- 18** **Panera Bread (casual American \$6-\$10)** Follow the same directions as West Egg Café, walk one block further north, the restaurant is on the right side at 635 N. Fairbanks.
- 19** **PJ Clarke's (casual American \$8-15)** Walk out front doors. Turn left and walk to Columbus Drive. Turn right on Columbus and walk down the hill, one block, to Illinois Ave. PJ Clarke's is on the corner.
- 20** **Popeye's Chicken/Subway Sandwiches (Fast Food \$5-10)** Walk out the front door and turn left. Turn right on Columbus Dr. 2 blocks to Grand Ave. turn left. One block down on right hand side.
- 21** **Pompei (Casual Italian \$4-\$10)** Turn right on Columbus drive 3 blocks to Ohio St. turn left on Ohio and continue for one block. The restaurant is on the right at 212 East Ohio
- 22** **Reagle Beagle (All American under \$15)** Follow directions to Popeyes and Subway.
- 23** **Rock Bottom (Micro Brewery and American food \$8-20)** Walk out the front doors and turn left to Columbus Drive. Turn right onto Columbus and walk 2 blocks to Grand Ave. Turn left on Grand Ave. and walk about 5 blocks to State Street and Grand.
- 24** **TGI/Fridays (Casual American \$8-20)** Walk out the front doors, turn left. Turn right on Columbus and walk 5 blocks to Erie St. Turn left on Erie and proceed to a block down towards Michigan. TGI/Fridays will be on your left at 153 E. Erie.
- 25** **Timothy O'Tooles (Irish Sports bar/American cuisine \$8-20)** Follow directions to West Egg Café. Timothy O'Tooles is at the corner downstairs.
- 26** **Urban Kitchen (Deli under \$15)** Walk out the front door and turn left. Walk across the street to The NBC Building. Walk into the NBC Building it is up the stairs and on your left. **(Monday-Friday)**
- 27** **West Egg Cafe (Casual American, breakfast anytime under \$8)** Walk out the front door and turn left, then turn right onto Columbus Drive. Walk down on Columbus for four blocks to Ontario Street. West Egg is on your left on the corner of Ontario and Columbus

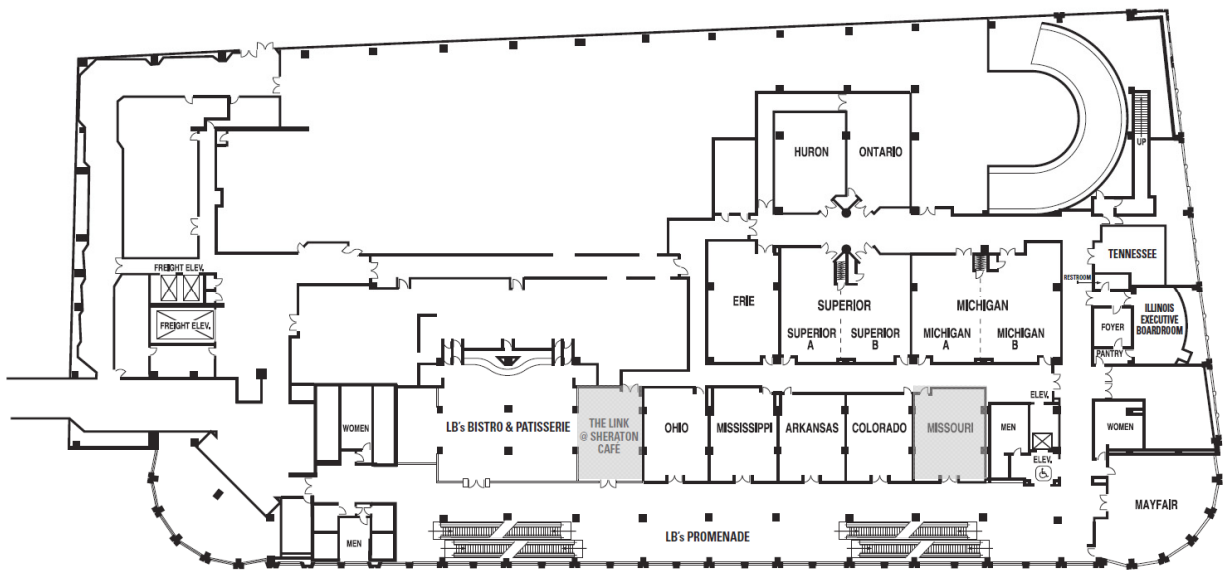


SHERATON FLOOR PLANS



Ballroom – Level 4

General Sessions – Sheraton Ballrooms IV & V
 Poster Sessions / Exhibitors – Sheraton Ballrooms I, II, & III



Meeting Rooms– Level 2

Internet Access – The Link @ Sheraton Café
 Proceedings Office – Missouri Room

SPONSORS

Advanced Energy Systems, Inc.

27 Industrial Blvd., Unit E
Medford, NY 11763
Phone: 631-345-6264 x100
URL: www.aesys.net/
Contact: Tony Favale

Amuneal Manufacturing Corp.

4737 Darrah Street
Philadelphia, PA 19124
Phone: 215-535-3000 ext. 242
URL: www.amuneal.com/
Contact: Stuart Koch

ATI Wah Chang

PO Box 460
Albany, OR 97321
Phone: 541-812-7102
URL: www.wahchang.com/
Contact: Barry Valder

Communications & Power Industries (CPI)

607 Hansen Way
Palo Alto, CA 94304-1015
Phone: 650-846-2900
URL: www.cpii.com/
Contact: Todd Treado

Cryogenic Society of America, Inc.

218 Lake Street
Oak Park, IL 60302-2609
Phone: 708-383-6220 ext. 222
URL: www.cryogenicsociety.org/
Contact: Theresa Boehl

Everson Tesla

615 Daniels Road
Nazareth, PA 18064
Phone: 610-746-1520
URL: www.eversontesla.com/
Contact: Greg Naumavich

Helmholtz Zentrum Berlin

Hahn-Meitner-Platz 1
D-14109 Berlin
Germany
Phone: 49-30-8062-14883
URL: www.helmholtz-berlin.de/
Contact: Jens Knobloch

Incodema, Inc.

407 Cliff Street
Ithaca, NY 14850
Phone: 607-277-7070
URL: www.incodema.com/IncodemaMainSite/
Contact: Illa Burbank

Linde Cryogenics

A Division of Linde Process Plants, Inc.
6100 South Yale Avenue, Suite 1200
Tulsa, OK 74136
Phone: 918-477-1200
URL: www.lppusa.com
Contact: John Urbin

Meyer Tool & Manufacturing, Inc.

4601 W. Southwest Highway
Oak Lawn, IL 60453
Phone: 708-425-9080
URL: www.mtm-inc.com/
Contact: Ed Bonnema

Muons, Inc.

552 N. Batavia Avenue
Batavia, IL 60510
Phone: 757-870-6943
URL: www.muonsinc.com/
Contact: Rolland Johnson

Niowave

1012 N. Walnut St.
Lansing, MI 48906
Phone: 517-944-6772
URL: www.niowaveinc.com/
Contact: Vance Fennell

Parsons

100 West Walnut Street
Pasadena, CA 91124
Phone: 626-440-3738
URL: www.parsons.com/pages/default.aspx
Contact: Bruce Shelton

Pavac Industries, Inc.

12371 Horseshoe Way
Unit 105
Richmond, BC,
Canada V7A 4X6
Phone: 604-231-0014
URL: www.pavac.com/
Contact: Ralf Edinger

PTR-Precision Technologies, Inc.

120 Post Road
Enfield, CT 06082
Phone: 860-741-2281
URL: www.ptreb.com/
Contact: John Rugh

RI Research Instruments GmbH

Friedrich-Ebert-Strasse 1
Bergisch Gladbach
51429 Germany
Phone: 49-22-0484-2583
URL: www.research-instruments.de
Contact: Hanspeter Vogel

Sciaky, Inc.

4915 W. 67th Street
Chicago, IL 60638
Phone: 708-594-3800
URL: www.sciaky.com/
Contact: Mike McGuire

Thales Electron Devices

2, rue Marcel Dassault
Vélizy Villacoublay - Cedex
78141 France
Phone: 33-0-(1)-30-70-3581
URL: [www.thalesgroup.com/Markets/
Security/What we do/](http://www.thalesgroup.com/Markets/Security/What%20we%20do/)
Contact: James VcVea

Titanium Fabrication Corporation

110 Lehigh Drive
Fairfield, NJ 07004-3044
Phone: 973-227-5300
URL: www.tifab.com/
Contact: Greg Dunn

W. C. Heraeus GmbH

Heraeusstraße 12 - 14
63450 Hanau
Germany
Phone: 49-61-81-35-5809
URL: wc-heraeus.com/en/home/hmt_hpm.aspx
Contact: Ursula Weitzel Hoefler

EXHIBITORS

Advanced Energy Systems, Inc.

27 Industrial Blvd., Unit E
Medford, NY 11763
Phone: 631-345-6264 x100
URL: www.aesys.net/
Contact: Tony Favale

Bruker BioSpin

34 rue de l'Industrie BP 10002
67166 Wissembourg Cedex
France
Phone: 33-388-06-6081
URL: www.bruker-biospin.com/
Contact: Pascal Dupire

Meyer Tool & Manufacturing Inc.

4601 W. Southwest Highway
Oak Lawn, IL 60453
Phone: 708-425-9080
URL: www.mtm-inc.com/
Contact: Ed Bonnema

Mitsubishi Heavy Industries, Ltd.

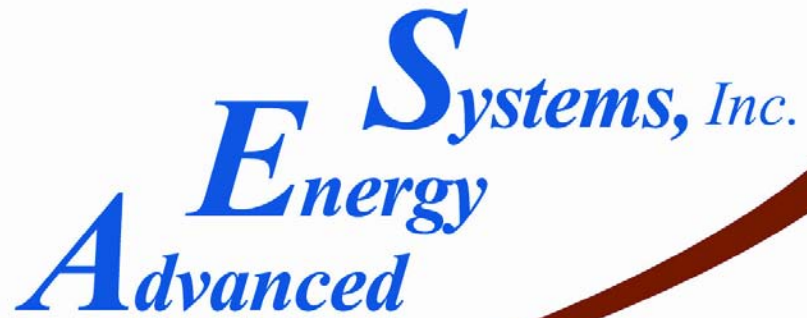
16-5, Konan 2-Chome
Minato-Ku
Tokyo 108-8215
Japan
Phone: 81-78-672-5832
URL: www.mhi.co.jp/en/tsat/index.html
Contact: Tatsunori Watanabe

RI Research Instruments GmbH

Friedrich-Ebert-Strasse 1
Bergisch Gladbach
51429 Germany
Phone: 49-22-0484-2583
URL: www.research-instruments.de
Contact: Hanspeter Vogel

Toshiba Electron Tubes & Devices

1-1-1, Shibaura, Minato-ku
105-8001, Tokyo
Japan
Phone: 81-33-457-4870
URL: www.toshiba-tetd.co.jp/tetd/eng/
Contact: Osamu Yushiro



Advanced Energy Systems, Inc.

Website

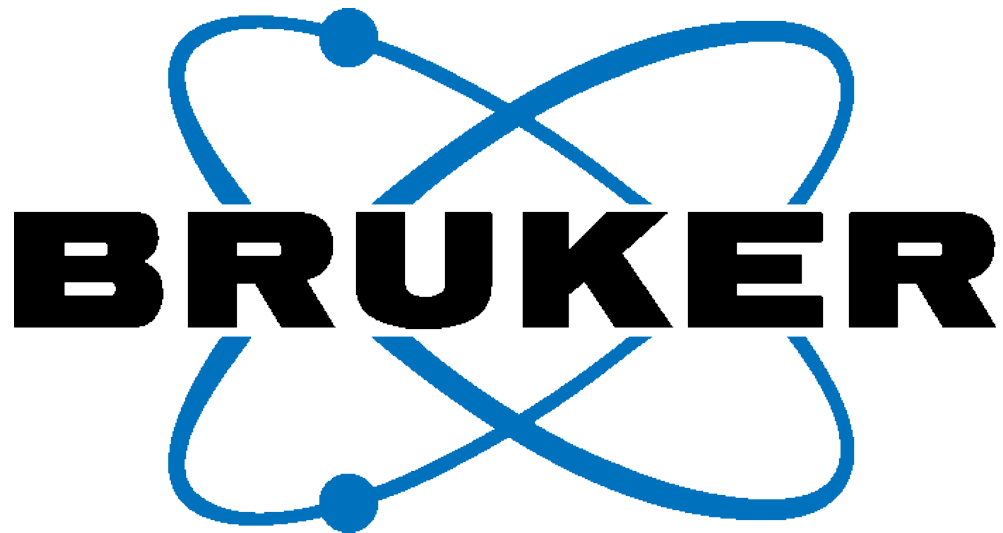
<http://www.aesys.net/>

Mailing Address

27 Industrial Blvd., Unit E
Medford, NY 11763
631-345-6264 x100

Telephone Number

(631) 345-6264 x100



Website

<http://www.bruker-est.com/>

Mailing Address

34 rue de l'Industrie BP 10002
67166 Wissembourg Cedex

Telephone Number

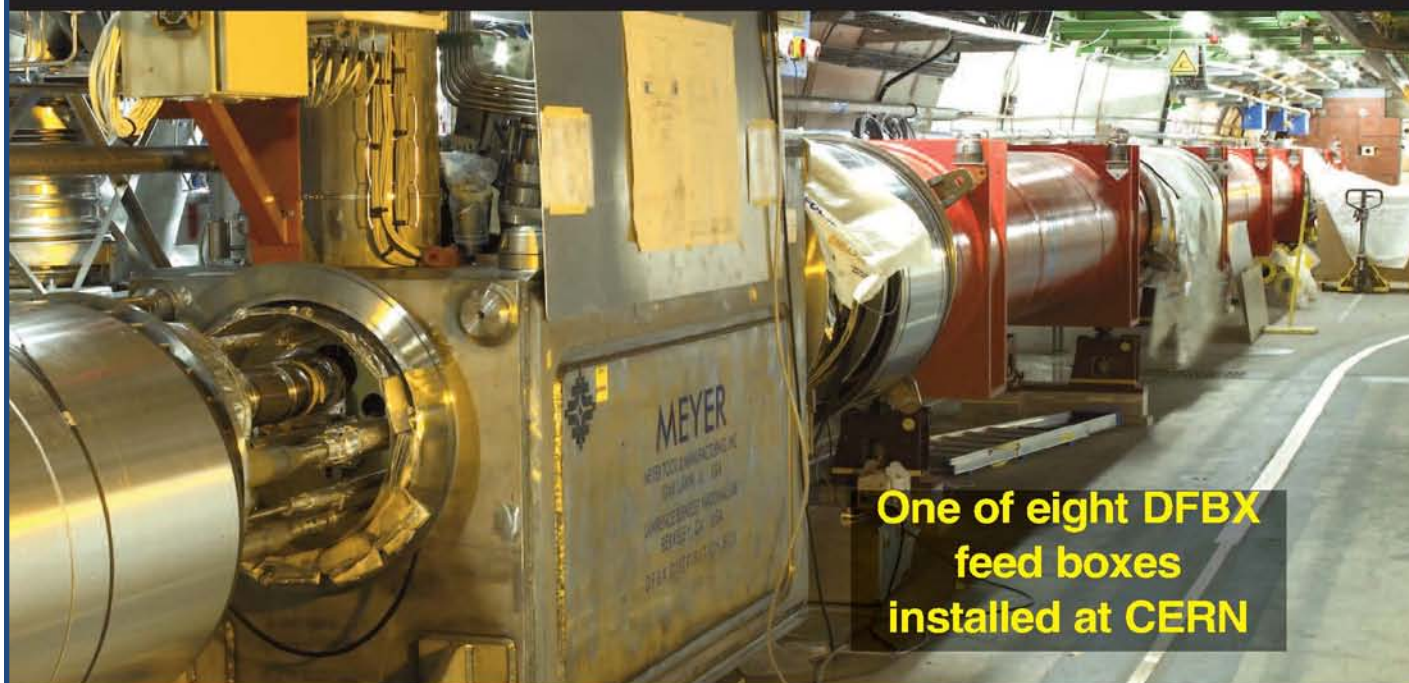
+33-388-06-6081

Fax Number

+33-388-73-6879

Reducing Project Risk Since 1969.

Specialists in Cryogenic, Vacuum and Pressure Technology



One of eight DFBX
feed boxes
installed at CERN

Serving Basic Science, R&D, High Tech Industrial

Achieve
the Lowest
Total Cost
of Ownership

Meyer components are installed at the world's most powerful particle accelerator, laser and neutron source, at the South Pole and in other harsh environments. All these components are installed with no surprises and working without fault.

Our commitment to quality in engineering and manufacturing makes it possible for us to build things that others say cannot be built.

*Free technical information and advice at
www.mtm-inc.com/ReduceProjectRisk*

"Just saw your newsletter and discussion of shields. Great Stuff!" *ANL physicist*

MEYER

Meyer Tool & Mfg., Inc.

Sign up for our eNewsletter: www.mtm-inc.com/signup

Talk with an engineer about your needs at
708-425-9080 or sales@mtm-inc.com



Our Technologies, Your Tomorrow

Website

<http://www.mhi.co.jp/en/tsat/index.html>

Mailing Address

Advanced Mechanical Systems Department
Transportation Systems & Advanced Technology Division
1-1, Wadasaki-cho, 1-chome
Hyogo-ku, Kobe 652-8585 Japan

Telephone Number

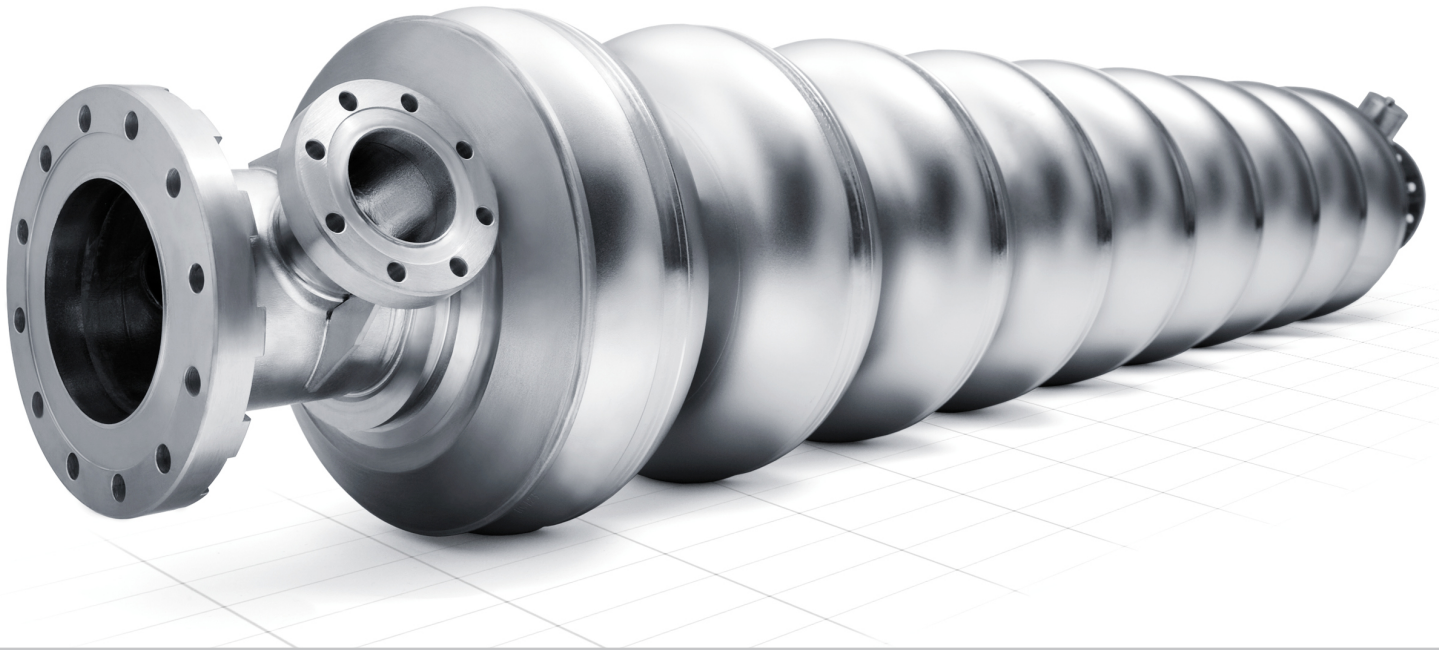
+81-78-672-5832

Facsimile Number

+81-78-672-2750



research
instruments



Discover precision

RI Research Instruments GmbH

- Linear accelerators
- Accelerator modules
- RF cavities and couplers
- Particle sources
- Beamlines and diagnostics
- Special manufacturing projects

TOSHIBA

Leading Innovation >>>

Toshiba Electron Tubes & Devices is the leading suppliers of the high power microwave tubes like Klystrons and Gyrotrons, and high power input couplers and windows. Toshiba Klystrons and high power couplers have been adapting for scientific researches in the world main laboratories, and also for medical applications in the world. Toshiba is ready to develop new types of RF sources. If you have any requirements, please contact.

<http://www.toshiba-tetd.co.jp/tetd/eng/>

[contact information in USA]

Toshiba America Electronic Components, Int.

Buffalo Grove, IL (Chicago)

2150 East Lake Cook Road, Suite 31, Buffalo Grove,
IL 60089, USA

Tel(847)484-2400 Fax(847)541-7287

E-mail:

John kurzydlo: john.kurzydlo@glb.toshiba.co.jp

Hazuo Watanabe: Hazuo.Watanabe@taec.toshiba.com



Multi-Beam Klystron E3736H

1.3GHz/10MW/1.5msec/10pps

[contact information outside USA]

Toshiba Electron Tubes & Devices Co., Ltd

1-1-1, Shibaura, Minato-ku, Tokyo 105-8001, Japan

Tel:+81-33457-4870, Fax:+81-33457-4871

E-mail:

Osamu Yushiro: osamu.yushiro@toshiba.co.jp



Input Coupler E4278

805MHz/550kW/11.3msec

Contents

Program

MOIOA — Overview of SRF Challenges

MOIOA01	Challenges in SRF Module Production for the European XFEL	47
MOIOA02	Advances in SRF Development for ILC	47
MOIOA03	Recent SRF Developments for ERLs	47
MOIOA04	SRF Challenges for Improving Operational Electron Linacs	47

MOIOB — Overview of SRF Challenges

MOIOB01	SRF Development for High Energy Physics	48
MOIOB02	Advances in SRF for Low Beta Ion Linacs	48
MOIOB03	Advances in SRF for Neutron Sources	48
MOIOB04	Survey of SRF Guns	48
MOIOB05	Operational Experience with SRF Cavities for Light Sources	49
MOIOB06	Hot Topics: Source of Quench Producing Defects	49

MOPO — Poster Session

MOPO001	Commercial Superconducting Electron Linacs	50
MOPO002	A Superconducting Cavity for a Flux Coupled Cyclotron That Drives a Power Plant Based on a Spent Nuclear Fuel	50
MOPO003	650 MHz Cryomodules for Project X at Fermilab – Requirements and Concepts	50
MOPO004	Modified SRF Photoinjector for the ELBE at HZDR	51
MOPO005	Conceptual Design of the Superconducting Proton Linac (SPL) Short Cryo-module	51
MOPO006	Status and Plans for an SRF Accelerator Test Facility at Fermilab	51
MOPO007	Test of Components for the S-DALINAC Injector Upgrade*	52
MOPO008	RF and SRF Layout of BERLinPro	52
MOPO009	Design Status of the Superconducting Driver Linac for the Facility for Radioactive Isotope Beams	52
MOPO010	Update on Module Measurements for the XFEL Prototype Modules	52
MOPO011	Status of SARAF Superconducting Acceleration Module	53
MOPO012	Overview of ILC High Gradient Cavity R&D at Jefferson Lab	53
MOPO013	RF Test Results from Cryomodule 1 at the Fermilab SRF Beam Test Facility	53
MOPO014	Design of the Fundamental Power Coupler and Photocathode Inserts for the 112 MHz Superconducting Electron Gun	54
MOPO015	IHEP 1.3GHz SRF Technology R&D Status	54
MOPO016	Superconducting RF R&D for the Cornell ERL Main Linac	54
MOPO017	Performance Limitation Studies on ISAC-II QWR's and e-Linac Elliptical Cavities at TRIUMF	55
MOPO018	The Upgraded Injector Cryostat-Module and Upcoming Improvements at the S-DALINAC	55
MOPO019	Minimizing Microphonics Detuning by Optimization of Stiffening Rings	55
MOPO020	Nine-cell Elliptical Cavity Development at TRIUMF	56
MOPO021	Electromechanical Design of 704MHz β 0.65 SC Proton Cavity	56
MOPO022	Higher Order Mode Properties of Superconducting Two-Spoke Cavities	56
MOPO023	Low Temperature Test of a Low-Beta Elliptical Cavity for PEFP Linac Extension	57
MOPO024	Design of Single Spoke Resonators at Fermilab	57

Contents

MOPO025	High-Frequency and Mechanical Basic Analysis of Conical Half-Wave Resonator	57
MOPO026	$\beta = 0.285$ Half-Wave Resonator for FRIB	58
MOPO027	Analysis of HOM Properties of Superconducting Parallel-Bar Deflecting/ Crabbing Cavities	58
MOPO028	Design of CW Superconducting Buncher for RIKEN RI-Beam Factory	58
MOPO029	Some Concerns on the Development of Spoke Cavity	59
MOPO030	The sc cw -LINAC Demonstrator - First section of a sc cw -LINAC	59
MOPO031	Electro-Magnetic Optimization and Analyses of Etching for HIRFL Quarter- Wave Resonators	59
MOPO032	Development of a Frequency Map for the WiFEL SRF Gun	60
MOPO033	Design of Superconducting Multi-Spoke Cavities for High-Velocity Applications	60
MOPO034	Optimized RF Design of 704 MHz $\beta=1$ Cavity for Pulsed Proton Drivers	60
MOPO035	Structural Mechanical Analysis of Superconducting CH-Cavities	60
MOPO036	Design Optimization of Spoke Cavity of Energy-Recovery Linac for Non- Destructive Assay Research	61
MOPO037	Development of Superconducting CH Cavities	61
MOPO038	Development of the Demountable Damped Cavity	61
MOPO039	Low- β Triple Spoke Cavity Design Improvement for Proton Linac	62
MOPO040	SRF Cavity Design for High Current Linacs	62
MOPO041	Conceptual Design of the $\beta = 0.86$ Cavities for the Superconducting Linac of ESS	62
MOPO042	Coupler Design for a Sample Host TE Cavity	63
MOPO043	Mechanical Study of Superconducting Parallel-Bar Deflecting/Crabbing Cavities	63
MOPO044	Electromagnetic Design Optimization of a Half-Wave Resonator	63
MOPO045	Coupled Electromagnetic and Mechanical Simulations for Half-Wave Resonator Design	64
MOPO046	Design of a 322 MHz $\beta=0.29$ Half Wave Resonator	64
MOPO047	HOM Cavity Design for the TRIUMF E-LINAC	64
MOPO048	The Dipole Steering Effect With New Ways: Shifting Inside and Outside Pole of QWR Cavity Method	65
MOPO049	Electro-Magnetic Optimization of a Quarter-Wave Resonator	65
MOPO050	Design of a 1500 MHz Bunch Lengthening Cavity for NSLS-II	65
MOPO051	Design for Manufacture of a Superconducting Half Wave Resonator $\beta=0.53$	66
MOPO052	Studies on a Plunger Tuner System for a Double Spoke Cavity	66
MOPO053	Designs of Superconducting Parallel-Bar Deflecting Cavities for Deflecting/ Crabbing Applications	66
MOPO054	Superconducting 112 MHz QWR Electron Gun	67
MOPO055	Superconducting Resonator Production for Ion Linac at Michigan State University	67
MOPO056	Beam Break Up Studies for Cornell's Energy Recovery Linac	67
MOPO057	Coupler Kick Studies in Cornell's 7-Cell Superconducting Cavities	68
MOPO058	Analysis of Beam Damage to FRIB Driver Linac	68
MOPO059	Design and Test of HOM Coupler for High Current SRF Cavity	68
MOPO060	Using Cavity Higher Order Modes for Beam Diagnostics in Third Harmonic 3.9 GHz Accelerating Modules	69
MOPO061	Effects of Elliptically Deformed Cell Shape in the Cornell ERL Cavity	69
MOPO062	BEPcII Superconducting RF System Operation Status	69
MOPO063	HOM Measurements with Beam at the Cornell Injector Cryomodule	70
MOPO064	Adaptive Lorentz Force Detuning Compensation in the ILC S1-G Cryomodule at KEK	70
MOPO065	Systems Testing of Cryomodules for an Ion Reaccelerator Linac	70
MOPO066	SCREAM – Modified Code SCREAM to Simulate the Acceleration of a Pulsed Beam Through the Superconducting Linac	70
MOPO067	CW Measurements of Cornell LLRF System at HoBiCaT	71
MOPO068	Reliability Improvements of the Diamond Superconducting Cavities	71
MOPO069	Operation Status of SRF System at SSRF	71
MOPO070	Preliminary Test Results from 650 MHz Single Cell Medium Beta Cavities for Project X	72

MOIOC — Hot Topics

HOT TOPIC	Source of Quench Producing Defects	73
-----------	------------------------------------	----

TUIOA — New Materials/Techniques

TUIOA01	Athmospheric Surface Treatments to SC cavities	74
TUIOA02	Multilayer Coatings: Opportunities and Challenges.	74
TUIOA03	Magnetic Screening of NbN Multilayers Samples	74
TUIOA04	MgB2 Thin Film Studies	75
TUIOA05	The Superheating Field of Niobium: Theory and Experiment	75
TUIOA06	Deposition of Niobium and Other Superconducting Materials With High Power Impulse Magnetron Sputtering: Concept and First Results	75

TUIOB — New Materials/Techniques

TUIOB01	Energetic Condensation Growth of Nb Films	76
TUIOB02	Summary of the Symposium on Ingot Nb and New Results on Fundamental Studies of Large Grain Nb	76
TUIOB03	Testing the RF Properties of Novel Super Conducting Materials	76
TUIOB04	Muon Spin Rotation/Relaxation Studies of Niobium for SRF applications	77
TUIOB05	New Approaches to Nb Thin Film Coating	77
TUIOB06	Nb Films: Substrates, Nucleation & Crystal Growth	77
TUIOB07	Magnesium Diboride Films for SRF Cavity Applications	78
TUIOB08	Hot Topics: Medium Field Q-Slope and Paths to High-Q Operation	78

TUPO — Poster Session

TUPO001	Development of Quality Assurance Procedures for the Fast/Slow Tuners on the 1.3 GHz SRF Cavities for the SRF Accelerator Test Facility at Fermilab	79
TUPO002	High Power Pulsed Tests of a $\beta=0.5$ 5-Cell 704 MHz Superconducting Cavity	79
TUPO003	Cooling Properties of HOM Absorber Model for cERL in Japan	79
TUPO004	Development and Testing of Prototype Fundamental Power Couplers for FRIB Half Wave Resonators	80
TUPO005	High Power Tests of KEK-ERL Input Coupler for Main Linac Under LN2 Condition	80
TUPO006	High Power Couplers for the Project X Linac	80
TUPO007	Development of STF Input Couplers for ILC	81
TUPO008	Vertical Test Facility for Superconducting RF Cavities at Daresbury Laboratory	81
TUPO009	How to Increase Average Power of Main Coupler	81
TUPO010	Conditioning the Fundamental Power Coupler for ERL SRF Gun	81
TUPO011	Coupler Cleaning Machine	82
TUPO012	Niobium Electropolishing in an Aqueous, Non-Viscous HF-Free Electrolyte: A New Polishing Mechanism	82
TUPO013	Assembly of the International ERL Cryomodule at Daresbury Laboratory	82
TUPO014	High Gradient Results of ICHIRO 9-Cell Cavity in Collaboration With KEK and Jlab	83
TUPO015	Standard Procedures of ILC High Gradient Cavity Processing at Jefferson Lab	83
TUPO016	Study Correlating Niobium Surface Roughness with Surface Particle Counts	83
TUPO017	Development and Scale-Up of an HF Free Electropolishing Process in Single-Cell Niobium SRF Cavities	84
TUPO018	Update of the DESY Infrastructure for Cavity Preparation	84
TUPO019	Fabrication, Tuning, Treatment and Testing of Two 3.5 Cell Photo-Injector Cavities for the ELBE Linac	85

Contents

TUPO020	CMP Polishing of a Niobium SRF Cavity	85
TUPO021	Current State of Electropolishing at ANL	85
TUPO022	Effects of Cathode Shapes on BEP and EP During Vertical Surface Treatments on Niobium	86
TUPO023	Development of the Superconducting Cavity for ILC at TOSHIBA	86
TUPO024	Sulfur Residues in Niobium Electropolishing	86
TUPO025	Integrated Cavity Processing Apparatus at Fermilab: SRF Cavity Processing R&D	87
TUPO026	Nine - Cell Tesla Shape Cavities Produced From Hydroformed Cells	87
TUPO027	A New Home for SRF Work at JLab—the Technology and Engineering Development Facility	87
TUPO028	Qualification of the Second Batch Production 9-Cell Cavities Manufactured by AES and Validation of the First US Industrial Cavity Vendor for ILC	88
TUPO029	Gradient Improvement by Removal of Identified Local Defects	88
TUPO030	Status of the 9-Cell Superconducting Cavity R&D for ILC at Hitachi	88
TUPO031	Update on the R&D of Vertical Buffered Electropolishing on Nb Samples and SRF Single Cell Cavities	89
TUPO032	Updates on R&D of Nondestructive Inspection Systems for SRF Cavities	89
TUPO033	Study of I-V Characteristics at Different Locations Inside a Demountable Nb SRF Cavity During Vertical BEP and EP Treatments	89
TUPO034	High Pressure Rinse System for Multiple SRF Cavities	90
TUPO035	Cryogenic Test of a Two-Cell Passive SRF Cavity for NSLS-II	90
TUPO036	Material for European XFEL Resonators	90
TUPO037	Study on Electro-Polishing Process by Niobium-Plate Sample With Artificial Pits	91
TUPO038	Superconducting RF Cavity Development With UK Industry	91
TUPO039	Long-Term Monitoring of 2nd-Period EP-Electrolyte in STF-EP Facility at KEK	91
TUPO040	The Status of Cavity-Fabrication Study for ILC at KEK	91
TUPO041	Investigation on Cavity String Assembly and Repair	92
TUPO042	SLAC/FNAL TTF3 Coupler Assembly and Processing Experience	92
TUPO043	Optimization of Ar/CL2 Plasma Parameters Used for SRF Cavity Etching	92
TUPO044	Correction of a Superconducting Cavity Shape Due to Etching, Cooling Down and Tuning	92
TUPO045	Status of Investigations on Degradation of Cavities in DESY Acceleration Modules	93
TUPO046	Update on Large Grain Cavities with 45 MV/m in a Nine-Cell Cavity at DESY	93
TUPO047	Progress in Developing 500MHz Nb Cavity at SINAP	93
TUPO048	Commissioning and Upgrade of Automatic Cavity Tuning Machines for the European Xfel	94
TUPO049	Q0 Improvement of Large-Grain Multi-Cell Cavities by Using JLab’s Standard ILC EP Processing	94
TUPO050	Studies on Transportation of Superconducting Resonators and Beam Position Monitors - Quadrupol Units for the XFEL Project	94
TUPO051	High-Temperature Heat Treatment Study on a Large-Grain Nb Cavity	95
TUPO052	Fabrication and Test of 500MHz Nb Cavity for BEPCII	95
TUPO053	Optical Inspection of SRF Cavities at Fermilab	95
TUPO054	SRF Cavity Surface Topography From Optical Inspection	96
TUPO055	Horizontal SRF Cavity Testing at Fermilab	96
TUPO056	Dewar Testing of $\beta = 0.53$ Half Wave Resonators at MSU	96
TUPO057	Buffered Chemical Polishing Development for the $\beta=0.53$ Half-Wave Resonator for the Facility for Rare Isotope Beams	97
TUPO058	CERN SRF Assembling and Test Facilities	97
TUPO059	SRF Cavity Processing and Cleanroom Facility Upgrades at Michigan State University	97
TUPO060	Dewar Testing of $\beta = 0.085$ Quarter Wave Resonators at MSU	98
TUPO061	Preparation and Testing of the SRF Cavities for the CEBAF 12 GeV Upgrade	98
TUPO062	Vertical Electro-Polishing at CEA Saclay: Commissioning of a New Set-Up and Modeling of the Process Applied to Different Cavities	98

TUPO063	MgB ₂ Films on Metallic Substrates with Different Surface Roughness	99
TUPO064	Large-Area MgB ₂ Films by Hybrid Physical Chemical Vapor Deposition	99
TUPO065	Economical Manufacture of Seamless High-Purity Niobium	99
TUPO066	Analysis of Recent Results from Second Sound, Temperature Mapping and Optical Inspection of 1.3 GHz Cavities at DESY	100
TUPO067	E HIE ISOLDE QWR: Progress in Magnetron and Bias Diode Sputtered Niobium Thin Film Coating	100
TUPO068	Electropolishing of Niobium to Obtain Defect Free Surface	100

TUIOC — Hot Topics

HOT TOPIC	Medium Field Q-Slope and Paths to High-Q Operation	101
-----------	--	-----

WEIOA — R&D/Diagnostics

WEIOA01	Quantitative EP Studies and Results for SRF Nb Cavity Production	102
WEIOA02	Centrifugal Barrel Polishing (CBP) of SRF Cavities Worldwide	102
WEIOA03	A New Electropolishing System For Low-Beta SC Cavities	102
WEIOA04	Review of RF - Sample - Test Equipment and Results	103
WEIOA05	X-Ray Tomography Inspection of SRF Cavities	103
WEIOA06	Effect of Deformation and Heat Treatment on the Thermal Conductivity of Large Grain Superconducting Niobium	103

WEIOB — R&D/Diagnostics/Fabrication

WEIOB01	Guided Cavity Repair with Laser, E - Beam and Grinding	104
WEIOB02	Cavity Inspection and Repair Techniques	104
WEIOB03	Improvement in Cavity Fabrication Technology and Cost Reduction Methods	104
WEIOB04	XFEL Cavity Procurement as an Example of Technology Transfer	105
WEIOB05	Large Grain Cavities: Fabrication, RF Results and Optical Inspection	105
WEIOB06	IHEP 1.3GHz Low-Loss Large Grain 9-cell cavity R&D for ILC	105

THIOA — $\beta=1$ Cavities

THIOA01	Test Results of the International S1-Global Cryomodule	106
THIOA02	Gradient R&D in the US	106
THIOA03	Compact Superconducting Cavities for Deflecting and Crabbing Applications	106
THIOA04	QWR for $\beta \sim 1$ Accelerators	107
THIOA05	The sc cw-LINAC Demonstrator - SRF-Technology finds the way into GSI	107
THIOA06	Mechanical Design Considerations for $\beta=1$ Cavities	107
THIOA07	Single-cell SC Cavity Development in India	108

THIOB — $\beta < 1$ Cavities

THIOB01	Project X Cavity and Cryomodule Development	109
THIOB02	Vertical Tests Results of the IFMIF Cavity Prototypes and Cryomodule Development	109
THIOB03	Status of the ReAccelerator Facility ReA for Rare Isotopes	110
THIOB04	SRF Advances for ATLAS and other $\beta < 1$ Applications	110
THIOB05	SPL Cavity Development	110
THIOB06	Recent Developments in SRF at TRIUMF	111
THIOB07	HIE-ISOLDE quarter wave Nb/Cu cavity	111
THIOB08	Hot topics: Recipes for 9-cell cavity fabrication and preparation	111

Contents

THPO — Poster Session

THPO001	Quench Simulation Using a Ring-Type Defect Model	112
THPO002	Defect-Induced Local Heating of Superconducting Cavity Surface	112
THPO003	Multipacting in HOM Couplers at the 1.3GHz 9-cell TESLA Type SRF Cavity	112
THPO004	Electro- or Chemical- Polishing and UHV Baking of Superconducting rf Nb Cavities and Q(H) Dependencies	113
THPO005	Exploration of Very High Gradient Cavities	113
THPO006	Study of Trapped Magnetic Flux in Superconducting Niobium Samples	113
THPO007	Novel Deflecting Cavity Design for eRHIC	114
THPO008	Post-Baking Losses in Niobium Cavities Studied by Dissection	114
THPO009	Quench Studies in Large and Fine Grain Nb Cavities	114
THPO010	Multipactor Studies for DIAMOND Storage Ring Cavities	114
THPO011	Improving the Intrinsic Quality Factor of SRF Cavities by Thermal Cycling	115
THPO012	Influence of Foreign Particles on the Quality Factor of a Superconducting Cavity	115
THPO013	Investigation of 9-Cell Cavity Performance Problem by Facilities in KEK AR East 2nd Experimental Hall	115
THPO015	Repair SRF Cavity by Re-Melting Surface Defects via High Power Laser Technique	115
THPO016	Preliminary Results on the Laser Heating Investigation of Hotspots in a Large-Grain Nb Cavity	116
THPO017	Probing the Fundamental Limit of Niobium in High Radiofrequency Fields by Dual Mode Excitation in Superconducting Radiofrequency Cavities	116
THPO018	Quench Studies of ILC Cavities	116
THPO019	Design, Construction, and Initial Test of High Spatial Resolution Thermometry Arrays for Detection of Surface Temperature Profiles on SRF Cavities in Super Fluid Helium	117
THPO020	Exploration of Quench Initiation Due to Intentional Geometrical Defects in a High Magnetic Field Region of an SRF Cavity	117
THPO021	Measurement of H_{c1} in Superconducting Thin Films	117
THPO022	Temperature and Surface Treatment Dependence of Medium Field Q-Slope	118
THPO023	External Magnetic Fields and Operating SRF Cavity	118
THPO024	Quench Dynamics in SRF Cavities	118
THPO025	Effects of Anodization on Field Emission on Nb Surfaces	119
THPO026	Second Sound Triangulation for SPL Cavity Quench Localization	119
THPO027	Optical Observation of Geometrical Features and Correlation With RFTest Results	119
THPO028	SIMS and TEM Analysis of Niobium Bicrystals	120
THPO029	Commissioning Cornell OSTs for SRF Cavity Testing at JLab	120
THPO030	Microphonics Compensation for a 325MHz Single Spoke Cavity at Fermilab	120
THPO031	Second Sound as an automated Quench Localisation Tool at DESY	121
THPO032	TOF-SIMS Analysis of Hydrogen in Niobium, From 160i $\frac{1}{2}$ K to 475i $\frac{1}{2}$ K	121
THPO033	Measurements of HOM Spectrum a 1.3 GHz ILC SC Cavity	121
THPO034	Vertical Test Results on KEK-ERL 9-Cell L-Band Superconducting Cavity	122
THPO035	Comparison of Field Emission at Different SRF Cavity Assembly States and Test Stands	122
THPO036	A Machine for High-Resolution Inspection of SRF Cavities at JLab	122
THPO037	Lorentz Force Detuning Compensation in Fermilab Cryomodule 1	122
THPO038	Detailed Nb Surface Morphology Evolution During Electropolishing for SRF Cavity Production	123
THPO039	Niobium Surface Resistance Measurement by Thermometric Method With a TE011 Cavity	123
THPO040	A Wire Position Monitor System for the 1.3GHz Tesla-Style Cryomodule at the Fermilab New Muon Lab	123
THPO041	HOM Identification and Bead Pulling on the Brookhaven ERL	124
THPO042	Crystallographic Orientation of Epitaxial Transition Observed for Nb (BCC) on Cu and MgO (FCC) Single-Crystals	124

THPO043	Understanding of Suppressed Superconductivity on SRF Quality Niobium	124
THPO044	Structural Characterization of Nb Films Deposited by ECR Plasma Energetic Condensation on Crystalline Insulators	125
THPO045	Nb Surface Nonlinear Properties Under Localized High RF Magnetic Field	125
THPO046	Characterization of Scale-Dependent Roughness of Niobium Surfaces as a Function of Surface Treatment Processes	126
THPO047	Growth Mode and Strain Effects in the Superconducting Properties of Nb Thin Films on Sapphire	126
THPO048	RF Surface Impedance of MgB ₂ Thin Films at 7.5 GHz	127
THPO049	Atomic-Scale Characterization of Niobium for SRF Cavities Using Ultraviolet Laser-Assisted Local- Electrode Atom-Probe Tomography	127
THPO050	TE Sample Host Cavities Development at Cornell	127
THPO051	Laser Re-Melting Influence on Nb Properties: Geometrical and Chemical Aspects	128
THPO052	Investigation of Near-Surface Interstitial Hydrogen in Cavity-Grade Niobium	128
THPO053	Material for Fabrication of DESY Large Grain/Single Crystal Cavities	128
THPO054	Magneto-Optical and Electromagnetic Study Different Forms of Nb for SRF Application	129
THPO055	Investigation of Samples Separated From Prototype Cavities of the European XFEL	129
THPO056	Thermal-Vacuum Variations of the Surface Oxide Complex on Cu	129
THPO057	Superconducting DC and RF Properties of Ingot Niobium	130
THPO058	Phase-Sensitive Nonlinear Near-Field Microwave Microscopy on MgB ₂ Thin Films	130
THPO059	Correlation of Microstructure, Chemical Composition and RRR-Value in High Purity Niobium (Nb-RRR)	130
THPO060	First Principles Investigation of Hydrogen in Niobium	131
THPO061	Activation of Field Emitters on Clean Nb Surfaces	131
THPO062	Epitaxial Niobium Thin Films for Accelerator Cavities	132
THPO063	Study of the Impurity Species in Niobium Films Grown by ECR Technique Employing Secondary Ion Mass Spectrometry	132
THPO064	Structural Properties of Niobium Thin Films Deposited on Metallic Substrates by ECR Plasma Energetic Condensation	133
THPO065	Anomalous Morphological Scaling in Epitaxial Nb Thin Films on MgO(001)	133
THPO066	Stoichiometric Nb ₃ Sn in First Samples Coated at Cornell	133
THPO067	Characterization of Large Grain Nb Ingot Microstructure Using OIM and Laue Methods	134
THPO068	Experimental Investigation and CPFE Modeling of Single Crystal Niobium for Tube Hydroforming	134
THPO069	Nb Film Growth on Crystalline and Amorphous Substrates	135
THPO070	Effect of Fabricate Condition on Properties of Bi-2212 Thin Films	135
THPO071	Detailed Surface Analysis of Incremental Centrifugal Barrel Polishing (CBP) and EP of Single-Crystal Niobium Samples	135
THPO072	Raman Spectroscopy as a Probe of Surface Oxides and Hydrides on Niobium	136
THPO073	Laser Melt Smoothing of Niobium Superconducting Radio-Frequency Cavity Surfaces	136
THPO074	NbTiN Films for SRF Multilayer Structures	136
THPO075	Does Annealing Reduce or Remove Defects Observed After Electropolishing?	137
THPO076	Measurement of the Loss Tangent and Heat Capacity of a Large Single Crystal Sapphire	137
THPO077	Mo-Re Films for SRF Applications	137
THPO078	Surface and Thin Film Characterization of Superconducting Multilayer Films for Application in RF Accelerator Cavities	138
THPO079	Surface Preparation of Metallic Substrates for Quality SRF Thin Films	138

THIOC — Hot Topics

HOT TOPIC	Recipes for 9-cell cavity fabrication and preparation	139
-----------	---	-----

Program

FRIOA — SRF Technology

FRIOA01	Adaptive Compensation for Lorentz Force Detuning in Superconducting RF Cavities	140
FRIOA02	Innovative Tuner Designs For Low Beta SRF Cavities	140
FRIOA03	Recent Progress in HOM Damping from Around The World	140
FRIOA04	Power Couplers for Spiral-2	140
FRIOA05	Overview of CW Input Couplers for ERL	141
FRIOA06	Construction of cERL Cryomodules for Injector and Main Linac	141
FRIOA07	SRF Photoinjector Tests at HoBiCat	141

FRIOB — New/Emerging SRF Capability & Applications

FRIOB01	SRF Activities at Peking University	142
FRIOB02	RF and Beam Test of the DC-SRF Injector of PKU-SETF	142
FRIOB03	Chinese Plan for ADS and CSNS	143
FRIOB04	SRF Accelerator for Indian ADS Program: Present & Future Prospects	143
FRIOB05	Crab Crossing for LHC Upgrade	143
FRIOB06	The ESS Accelerator	144

Author Index

Program

25-Jul-11 08:00 – 08:30

08:00 – 08:30 MOTA — Welcome

MOTA01 Accelerators for the Future
W.F. Henning (ANL)

25-Jul-11 08:40 – 10:15

08:40 – 10:15 MOIOA — Overview of SRF Challenges
Session Chair: J. Knobloch, HZB (Berlin, Germany)

MOIOA01 Challenges in SRF Module Production for the European XFEL
D. Reschke (DESY)

MOIOA02 Advances in SRF Development for ILC
A. Yamamoto (KEK)

MOIOA03 Recent SRF Developments for ERLs
G.H. Hoffstaetter (CLASSE)

MOIOA04 SRF Challenges for Improving Operational Electron Linacs
C.E. Reece (JLAB)

25-Jul-11 10:45 – 13:00

10:45 – 13:00 MOIOB — Overview of SRF Challenges
Session Chair: J.R. Delayen, ODU (Norfolk, Virginia, USA)

MOIOB01 SRF Development for High Energy Physics
M.S. Champion (Fermilab)

MOIOB02 Advances in SRF for Low Beta Ion Linacs
S. Bousson (IPN)

MOIOB03 Advances in SRF for Neutron Sources
S.-H. Kim (ORNL)

MOIOB04 Survey of SRF Guns
S.A. Belomestnykh (BNL)

MOIOB05 Operational Experience with SRF Cavities for Light Sources
M. Jensen (Diamond)

MOIOB06 Hot Topics: Source of Quench Producing Defects
R.L. Geng (JLAB)

25-Jul-11 14:30 – 18:00

14:30 – 18:00 MOPO — Poster Session

MOPO001 Commercial Superconducting Electron Linacs
T.L. Grimm (Niowave, Inc.)

MOPO002 A Superconducting Cavity for a Flux Coupled Cyclotron That Drives a Power Plant Based on a Spent Nuclear Fuel
N. Pogue (Texas A&M University)

MOPO003 650 MHz Cryomodules for Project X at Fermilab – Requirements and Concepts
T.J. Peterson (Fermilab) R. Ghosh (RRCAT)

MOPO004 Modified SRF Photoinjector for the ELBE at HZDR
P. Murcek (HZDR) P. Kneisel (JLAB)

MOPO005 Conceptual Design of the Superconducting Proton Linac (SPL) Short Cryo-module
V. Parma (CERN) P. Dambre (IPN)

MOPO006 Status and Plans for an SRF Accelerator Test Facility at Fermilab
M.D. Church (Fermilab)

Program

- MOPO007** Test of Components for the S-DALINAC Injector Upgrade*
S.T. Sievers (TU Darmstadt)
- MOPO008** RF and SRF Layout of BERLinPro
W. Anders (HZB)
- MOPO009** Design Status of the Superconducting Driver Linac for the Facility for Radioactive Isotope Beams
M. Leitner (FRIB)
- MOPO010** Update on Module Measurements for the XFEL Prototype Modules
D. Kostin (DESY)
- MOPO011** Status of SARAF Superconducting Acceleration Module
A. Perry (Soreq NRC)
- MOPO012** Overview of ILC High Gradient Cavity R&D at Jefferson Lab
R.L. Geng (JLAB)
- MOPO013** RF Test Results from Cryomodule 1 at the Fermilab SRF Beam Test Facility
E.R. Harms (Fermilab)
- MOPO014** Design of the Fundamental Power Coupler and Photocathode Inserts for the 112 MHz Superconducting Electron Gun
T. Xin (Stony Brook University) S.A. Belomestnykh (BNL)
- MOPO015** IHEP 1.3GHz SRF Technology R&D Status
J. Gao (IHEP Beijing)
- MOPO016** Superconducting RF R&D for the Cornell ERL Main Linac
M. Liepe (CLASSE)
- MOPO017** Performance Limitation Studies on ISAC-II QWR's and e-Linac Elliptical Cavities at TRIUMF
D. Longuevergne (TRIUMF, Canada's National Laboratory for Particle and Nuclear Physics)
- MOPO018** The Upgraded Injector Cryostat-Module and Upcoming Improvements at the S-DALINAC
R. Eichhorn (TU Darmstadt)
- MOPO019** Minimizing Microphonics Detuning by Optimization of Stiffening Rings
S. Posen (CLASSE)
- MOPO020** Nine-cell Elliptical Cavity Development at TRIUMF
V. Zvyagintsev (TRIUMF, Canada's National Laboratory for Particle and Nuclear Physics) M. Ahammed (DAE/VECC) R.O. Bolgov (MEPhI) R. Edinger (PAVAC)
- MOPO021** Electromechanical Design of 704MHz β 0.65 SC Proton Cavity
H. Gassot (IPN)
- MOPO022** Higher Order Mode Properties of Superconducting Two-Spoke Cavities
C.S. Hopper (ODU) J.R. Delaysen (JLAB) R.G. Olave (Old Dominion University)
- MOPO023** Low Temperature Test of a Low-Beta Elliptical Cavity for PEFP Linac Extension
H.S. Kim (KAERI)
- MOPO024** Design of Single Spoke Resonators at Fermilab
L. Ristori (Fermilab)
- MOPO025** High-Frequency and Mechanical Basic Analysis of Conical Half-Wave Resonator
E.N. Zaplatin (FZJ) A. Kanareykin (Euclid TechLabs, LLC)
- MOPO026** $\beta = 0.285$ Half-Wave Resonator for FRIB
P.N. Ostroumov (ANL)
- MOPO027** Analysis of HOM Properties of Superconducting Parallel-Bar Deflecting/Crabbing Cavities
S.U. De Silva (ODU) A. Castilla (DCI-UG) S.U. De Silva (JLAB)
- MOPO028** Design of CW Superconducting Buncher for RIKEN RI-Beam Factory
L. Lu (RIKEN) O. Kamigaito (RIKEN Nishina Center)
- MOPO029** Some Concerns on the Development of Spoke Cavity
F.S. He (PKU/IHIP) H. Wang (JLAB)
- MOPO030** The sc cw -LINAC Demonstrator - First section of a sc cw -LINAC
V. Gettmann (HIM) K. Aulenbacher (IKP) W.A. Barth (GSI) F.D. Dziuba (IAP)
- MOPO031** Electro-Magnetic Optimization and Analyses of Etching for HIRFL Quarter-Wave Resonators
C. Zhang (IMP)

- MOPO032** Development of a Frequency Map for the WiFEL SRF Gun
R.A. Legg (JLAB) M.V. Fisher (UW-Madison/SRC) T.L. Grimm (Niowave, Inc.)
- MOPO033** Design of Superconducting Multi-Spoke Cavities for High-Velocity Applications
C.S. Hopper (ODU) J.R. Delayen (JLAB)
- MOPO034** Optimized RF Design of 704 MHz $\beta=1$ Cavity for Pulsed Proton Drivers
J. Plouin (CEA/IRFU) S. Chel (CEA/DSM/IRFU)
- MOPO035** Structural Mechanical Analysis of Superconducting CH-Cavities
M. Amberg (HIM) K. Aulenbacher (IKP) W.A. Barth (GSI) M. Busch (IAP)
- MOPO036** Design Optimization of Spoke Cavity of Energy-Recovery Linac for Non-Destructive Assay Research
M. Sawamura (JAEA) R. Nagai (JAEA/ERL)
- MOPO037** Development of Superconducting CH Cavities
F.D. Dziuba (IAP) M. Amberg (HIM) K. Aulenbacher (IKP) W.A. Barth (GSI)
- MOPO038** Development of the Demountable Damped Cavity
T. Konomi (Sokendai) F. Furuta (KEK)
- MOPO039** Low- β Triple Spoke Cavity Design Improvement for Proton Linac
H. Gassot (IPN)
- MOPO040** SRF Cavity Design for High Current Linacs
W. Xu (BNL)
- MOPO041** Conceptual Design of the $\beta = 0.86$ Cavities for the Superconducting Linac of ESS
J. Plouin (CEA/IRFU) G. Devanz (CEA/DSM/IRFU)
- MOPO042** Coupler Design for a Sample Host TE Cavity
Y. Xie (CLASSE)
- MOPO043** Mechanical Study of Superconducting Parallel-Bar Deflecting/Crabbing Cavities
H. Park (JLAB) S.U. De Silva (ODU)
- MOPO044** Electromagnetic Design Optimization of a Half-Wave Resonator
B. Mustapha (ANL)
- MOPO045** Coupled Electromagnetic and Mechanical Simulations for Half-Wave Resonator Design
J.P. Holzbauer (NSCL) J. Binkowski (FRIB)
- MOPO046** Design of a 322 MHz $\beta=0.29$ Half Wave Resonator
J. Popielarski (FRIB)
- MOPO047** HOM Cavity Design for the TRIUMF E-LINAC
P. Kolb (TRIUMF, Canada's National Laboratory for Particle and Nuclear Physics)
- MOPO048** The Dipole Steering Effect With New Ways: Shifting Inside and Outside Pole of QWR Cavity Method
J.D. Jeong (SKKU)
- MOPO049** Electro-Magnetic Optimization of a Quarter-Wave Resonator
C. Zhang (IMP)
- MOPO050** Design of a 1500 MHz Bunch Lengthening Cavity for NSLS-II
J. Rose (BNL) C.H. Boulware (Niowave, Inc.)
- MOPO051** Design for Manufacture of a Superconducting Half Wave Resonator $\beta=0.53$
S.J. Miller (FRIB)
- MOPO052** Studies on a Plunger Tuner System for a Double Spoke Cavity
J.L. Munoz (ESS-Bilbao) F.J. Bermejo (Bilbao, Faculty of Science and Technology) V. Etxebarria (University of the Basque Country, Faculty of Science and Technology) N. Garmendia (ESS Bilbao)
- MOPO053** Designs of Superconducting Parallel-Bar Deflecting Cavities for Deflecting/Crabbing Applications
J.R. Delayen (ODU) J.R. Delayen (JLAB)
- MOPO054** Superconducting 112 MHz QWR Electron Gun
S.A. Belomestnykh (BNL) C.H. Boulware (Niowave, Inc.) T. Xin (Stony Brook University)
- MOPO055** Superconducting Resonator Production for Ion Linac at Michigan State University
C. Compton (FRIB)

Program

- MOPO056** Beam Break Up Studies for Cornell's Energy Recovery Linac
N.R.A. Valles (CLASSE)
- MOPO057** Coupler Kick Studies in Cornell's 7-Cell Superconducting Cavities
N.R.A. Valles (CLASSE)
- MOPO058** Analysis of Beam Damage to FRIB Driver Linac
Y. Zhang (FRIB)
- MOPO059** Design and Test of HOM Coupler for High Current SRF Cavity
W. Xu (BNL)
- MOPO060** Using Cavity Higher Order Modes for Beam Diagnostics in Third Harmonic 3.9 GHz Accelerating Modules
N. Baboi (DESY) R.M. Jones (UMAN)
- MOPO061** Effects of Elliptically Deformed Cell Shape in the Cornell ERL Cavity
L. Xiao (SLAC) M. Liepe (CLASSE)
- MOPO062** BEPCII Superconducting RF System Operation Status
Y. Sun (IHEP Beijing)
- MOPO063** HOM Measurements with Beam at the Cornell Injector Cryomodule
S. Posen (CLASSE)
- MOPO064** Adaptive Lorentz Force Detuning Compensation in the ILC S1-G Cryomodule at KEK
W. Schappert (Fermilab) H. Hayano (KEK)
- MOPO065** Systems Testing of Cryomodules for an Ion Reaccelerator Linac
J. Popielarski (FRIB)
- MOPO066** SCREAM – Modified Code SCREAM to Simulate the Acceleration of a Pulsed Beam Through the Superconducting Linac
Y.I. Eidelman (Fermilab)
- MOPO067** CW Measurements of Cornell LLRF System at HoBiCaT
A. Neumann (HZB) S.A. Belomestnykh (BNL) J. Dobbins (CLASSE)
- MOPO068** Reliability Improvements of the Diamond Superconducting Cavities
P. Gu (Diamond)
- MOPO069** Operation Status of SRF System at SSRF
H.T. Hou (SINAP) H.T. Hou (Shanghai KEY Laboratory of Cryogenics & Superconducting RF Technology)
- MOPO070** Preliminary Test Results from 650 MHz Single Cell Medium Beta Cavities for Project X
P. Kneisel (JLAB)

25-Jul-11 18:00 – 19:00

- 18:00 – 19:00** MOIOC — Hot Topics
Source of Quench Producing Defects
Session Chair: R.L. Geng, JLAB (Newport News, Virginia, USA)

26-Jul-11 08:00 – 10:15

- 08:00 – 10:15** TUIOA — New Materials/Techniques
Session Chair: M. Liepe, Cornell University (Ithaca, New York, USA)
- TUIOA01** Atmospheric Surface Treatments to SC cavities
V. Palmieri (INFN/LNL) D. Rizzetto (Univ. degli Studi di Padova)
- TUIOA02** Multilayer Coatings: Opportunities and Challenges.
A.V. Gurevich (Old Dominion University)
- TUIOA03** Magnetic Screening of NbN Multilayers Samples
C.Z. Antoine (CEA/DSM/IRFU) A. Andreone (Naples University Federico II) Q. Famery (CEA/IRFU) G. Lamura (CNR-INFN-LAMIA) J.C. Villegier (CEA/INAC)
- TUIOA04** MgB₂ Thin Film Studies
T. Tajima (LANL) V.A. Dolgashev (SLAC) H. Inoue (KEK) A. Matsumoto (NIMS) B. Moeckly (STI) M.J. Pellin (ANL) B. Xiao (JLAB)
- TUIOA05** The Superheating Field of Niobium: Theory and Experiment
N.R.A. Valles (CLASSE)

TUIOA06 Deposition of Niobium and Other Superconducting Materials With High Power Impulse Magnetron Sputtering: Concept and First Results
A. Anders (LBNL)

26-Jul-11 10:45 – 13:15

10:45 – 13:15 TUIOB — New Materials/Techniques
Session Chair: C.Z. Antoine, CEA/DSM/IRFU (France)

TUIOB01 Energetic Condensation Growth of Nb Films
M. Krishnan (AASC) P. Maheshwari (NCSU AIF) H.L. Phillips (JLAB) K.I. Seo (NSU) Z.H. Sung (ASC)

TUIOB02 Summary of the Symposium on Ingot Nb and New Results on Fundamental Studies of Large Grain Nb
G. Ciovati (JLAB)

TUIOB03 Testing the RF Properties of Novel Super Conducting Materials
J. Guo (SLAC)

TUIOB04 Muon Spin Rotation/Relaxation Studies of Niobium for SRF applications
A. Grassellino (TRIUMF, Canada's National Laboratory for Particle and Nuclear Physics)

TUIOB05 New Approaches to Nb Thin Film Coating
S. Calatroni (CERN)

TUIOB06 Nb Films: Substrates, Nucleation & Crystal Growth
A-M. Valente-Feliciano (JLAB)

TUIOB07 Magnesium Diboride Films for SRF Cavity Applications
Y.D. Agassi (NSWC) B. Moeckly (STI) D.E. Oates (MIT)

TUIOB08 Hot Topics: Medium Field Q-Slope and Paths to High-Q Operation
W. Weingarten (CERN)

26-Jul-11 14:30 – 18:00

14:30 – 18:00 TUPO — Poster Session

TUPO001 Development of Quality Assurance Procedures for the Fast/Slow Tuners on the 1.3 GHz SRF Cavities for the SRF Accelerator Test Facility at Fermilab
Y.M. Pischnalnikov (Fermilab)

TUPO002 High Power Pulsed Tests of a $\beta=0.5$ 5-Cell 704 MHz Superconducting Cavity
J. Plouin (CEA/DSM/IRFU) W. Hügler (CERN)

TUPO003 Cooling Properties of HOM Absorber Model for cERL in Japan
M. Sawamura (Japan Atomic Energy Agency (JAEA), Gamma-ray Non-Destructive Assay Research Group) E. Cenni (Sokendai) T. Furuya (KEK) K. Shinoe (ISSP/SRL)

TUPO004 Development and Testing of Prototype Fundamental Power Couplers for FRIB Half Wave Resonators
J. Popielarski (FRIB)

TUPO005 High Power Tests of KEK-ERL Input Coupler for Main Linac Under LN₂ Condition
H. Sakai (KEK) E. Cenni (Sokendai) M. Sawamura (JAEA) K. Shinoe (ISSP/SRL)

TUPO006 High Power Couplers for the Project X Linac
S. Kazakov (Fermilab)

TUPO007 Development of STF Input Couplers for ILC
M. Satoh (KEK)

TUPO008 Vertical Test Facility for Superconducting RF Cavities at Daresbury Laboratory
R.K. Buckley (STFC/DL/ASTeC)

TUPO009 How to Increase Average Power of Main Coupler
S. Kazakov (Fermilab)

TUPO010 Conditioning the Fundamental Power Coupler for ERL SRF Gun
W. Xu (BNL) M.D. Cole (AES)

TUPO011 Coupler Cleaning Machine
W. Kaabi (LAL)

Program

- TUPO012** Niobium Electropolishing in an Aqueous, Non-Viscous HF-Free Electrolyte: A New Polishing Mechanism
M.E. Inman (Faraday Technology, Inc.) C.E. Reece (JLAB)
- TUPO013** Assembly of the International ERL Cryomodule at Daresbury Laboratory
P.A. McIntosh (STFC/DL/ASTeC) S.A. Belomestnykh (CLASSE) A. Buechner (HZDR) M.A. Cordwell (STFC/DL) J.N. Corlett (LBNL) T. Kimura (Stanford University) D. Proch (DESY)
- TUPO014** High Gradient Results of ICHIRO 9-Cell Cavity in Collaboration With KEK and Jlab
F. Furuta (KEK)
- TUPO015** Standard Procedures of ILC High Gradient Cavity Processing at Jefferson Lab
R.L. Geng (JLAB) A.C. Crawford (CLASSE)
- TUPO016** Study Correlating Niobium Surface Roughness with Surface Particle Counts
C. Compton (FRIB)
- TUPO017** Development and Scale-Up of an HF Free Electropolishing Process in Single-Cell Niobium SRF Cavities
M.E. Inman (Faraday Technology, Inc.) L.D. Cooley (Fermilab)
- TUPO018** Update of the DESY Infrastructure for Cavity Preparation
M. Schalwat (DESY)
- TUPO019** Fabrication, Tuning, Treatment and Testing of Two 3.5 Cell Photo-Injector Cavities for the ELBE Linac
A. Arnold (HZDR) G.V. Ereemeev (JLAB)
- TUPO020** CMP Polishing of a Niobium SRF Cavity
S.D. Lesiak (Cabot Microelectronics Polishing Corp) A.M. Rowe (Fermilab)
- TUPO021** Current State of Electropolishing at ANL
T. Reid (ANL)
- TUPO022** Effects of Cathode Shapes on BEP and EP During Vertical Surface Treatments on Niobium
S. Jin (PKU/IHIP) R.A. Rimmer (JLAB)
- TUPO023** Development of the Superconducting Cavity for ILC at TOSHIBA
T. Ota (Toshiba) H. Hayano (KEK)
- TUPO024** Sulfur Residues in Niobium Electropolishing
L. Zhao (The College of William and Mary) M.J. Kelley (JLAB)
- TUPO025** Integrated Cavity Processing Apparatus at Fermilab: SRF Cavity Processing R&D
C.A. Cooper (Fermilab)
- TUPO026** Nine - Cell Tesla Shape Cavities Produced From Hydroformed Cells
W. Singer (DESY) R. Crooks (Black Laboratories, L.L.C.) P. Kneisel (JLAB) I.N. Zhelezov (RAS/INR)
- TUPO027** A New Home for SRF Work at JLab—the Technology and Engineering Development Facility
C.E. Reece (JLAB)
- TUPO028** Qualification of the Second Batch Production 9-Cell Cavities Manufactured by AES and Validation of the First US Industrial Cavity Vendor for ILC
R.L. Geng (JLAB) M. Calderaro (AES) M.S. Champion (Fermilab) A.C. Crawford (CLASSE)
- TUPO029** Gradient Improvement by Removal of Identified Local Defects
R.L. Geng (JLAB) C.A. Cooper (Fermilab) H. Hayano (KEK)
- TUPO030** Status of the 9-Cell Superconducting Cavity R&D for ILC at Hitachi
T. Watanuki (Hitachi Ltd.) H. Hayano (KEK)
- TUPO031** Update on the R&D of Vertical Buffered Electropolishing on Nb Samples and SRF Single Cell Cavities
A.T. Wu (JLAB) S. Jin (PKU/IHIP)
- TUPO032** Updates on R&D of Nondestructive Inspection Systems for SRF Cavities
Y. Iwashita (Kyoto ICR) H. Hayano (KEK)
- TUPO033** Study of I-V Characteristics at Different Locations Inside a Demountable Nb SRF Cavity During Vertical BEP and EP Treatments
S. Jin (PKU/IHIP) R.A. Rimmer (JLAB)
- TUPO034** High Pressure Rinse System for Multiple SRF Cavities
R.C. Murphy (ANL)

- TUPO035** Cryogenic Test of a Two-Cell Passive SRF Cavity for NSLS-II
C.H. Boulware (Niowave, Inc.) W.K. Gash (BNL)
- TUPO036** Material for European XFEL Resonators
W. Singer (DESY)
- TUPO037** Study on Electro-Polishing Process by Niobium-Plate Sample With Artificial Pits
T. Saeki (KEK) W.A. Clemens (JLAB) P.V. Tyagi (Sokendai)
- TUPO038** Superconducting RF Cavity Development With UK Industry
A.E. Wheelhouse (STFC/DL/ASTeC)
- TUPO039** Long-Term Monitoring of 2nd-Period EP-Electrolyte in STF-EP Facility at KEK
M. Sawabe (KEK)
- TUPO040** The Status of Cavity-Fabrication Study for ILC at KEK
T. Saeki (KEK) H. Nakamura (SPS)
- TUPO041** Investigation on Cavity String Assembly and Repair
A. Matheisen (DESY)
- TUPO042** SLAC/FNAL TTF3 Coupler Assembly and Processing Experience
C. Adolphsen (SLAC) A. Lunin (Fermilab)
- TUPO043** Optimization of Ar/CL2 Plasma Parameters Used for SRF Cavity Etching
J. Upadhyay (ODU) H.L. Phillips (JLAB)
- TUPO044** Correction of a Superconducting Cavity Shape Due to Etching, Cooling Down and Tuning
V.D. Shemelin (CLASSE)
- TUPO045** Status of Investigations on Degradation of Cavities in DESY Acceleration Modules
A. Matheisen (DESY)
- TUPO046** Update on Large Grain Cavities with 45 MV/m in a Nine-Cell Cavity at DESY
D. Reschke (DESY)
- TUPO047** Progress in Developing 500MHz Nb Cavity at SINAP
J.F. Liu (SINAP) Z. Li (Shanghai KEY Laboratory of Cryogenics & Superconducting RF Technology) B. Yin (Graduate University, Chinese Academy of Sciences)
- TUPO048** Commissioning and Upgrade of Automatic Cavity Tuning Machines for the European Xfel
J.H. Thie (DESY) D. Bhogadi (Fermilab)
- TUPO049** Q0 Improvement of Large-Grain Multi-Cell Cavities by Using JLab's Standard ILC EP Processing
R.L. Geng (JLAB) K.X. Liu (PKU/IHIP)
- TUPO050** Studies on Transportation of Superconducting Resonators and Beam Position Monitors - Quadrupol Units for the XFEL Project
A. Schmidt (DESY)
- TUPO051** High-Temperature Heat Treatment Study on a Large-Grain Nb Cavity
G. Ciovati (JLAB) P. Maheswari (NCSU AIF)
- TUPO052** Fabrication and Test of 500MHz Nb Cavity for BEPCII
G.W. Wang (IHEP Beijing)
- TUPO053** Optical Inspection of SRF Cavities at Fermilab
E. Toropov (Fermilab)
- TUPO054** SRF Cavity Surface Topography From Optical Inspection
E. Toropov (Fermilab)
- TUPO055** Horizontal SRF Cavity Testing at Fermilab
A. Hocker (Fermilab)
- TUPO056** Dewar Testing of $\beta = 0.53$ Half Wave Resonators at MSU
J. Popielarski (FRIB)
- TUPO057** Buffered Chemical Polishing Development for the $\beta=0.53$ Half-Wave Resonator for the Facility for Rare Isotope Beams
L. Popielarski (FRIB)
- TUPO058** CERN SRF Assembling and Test Facilities
J.K. Chambrillon (CERN)
- TUPO059** SRF Cavity Processing and Cleanroom Facility Upgrades at Michigan State University
L. Popielarski (FRIB)

Program

- TUPO060** Dewar Testing of $\beta = 0.085$ Quarter Wave Resonators at MSU
J. Popielarski (FRIB)
- TUPO061** Preparation and Testing of the SRF Cavities for the CEBAF 12 GeV Upgrade
A. Reilly (JLAB)
- TUPO062** Vertical Electro-Polishing at CEA Saclay: Commissioning of a New Set-Up and Modeling of the Process Applied to Different Cavities
F. Eoziz (CEA/DSM/IRFU)
- TUPO063** MgB₂ Films on Metallic Substrates with Different Surface Roughness
C.G. Zhuang (TU)
- TUPO064** Large-Area MgB₂ Films by Hybrid Physical Chemical Vapor Deposition
X. Xi (TU)
- TUPO065** Economical Manufacture of Seamless High-Purity Niobium
V.M. Arrieta (Ultramet)
- TUPO066** Analysis of Recent Results from Second Sound, Temperature Mapping and Optical Inspection of 1.3 GHz Cavities at DESY
F. Schlönder (DESY)
- TUPO067** E HIE ISOLDE QWR: Progress in Magnetron and Bias Diode Sputtered Niobium Thin Film Coating
G. Lanza (CERN)
- TUPO068** Electropolishing of Niobium to Obtain Defect Free Surface
A. Chandra (Ohio State University)

26-Jul-11 18:00 – 19:00

- 18:00 – 19:00** TUIOC — Hot Topics
Medium Field Q-Slope and Paths to High-Q Operation
Session Chair: W. Weingarten, CERN (Geneva, Switzerland)

27-Jul-11 08:00 – 10:15

- 08:00 – 10:15** WEIOA — R&D/Diagnostics
Session Chair: C.E. Reece, JLAB (Newport News, Virginia, USA)
- WEIOA01** Quantitative EP Studies and Results for SRF Nb Cavity Production
H. Tian (JLAB)
- WEIOA02** Centrifugal Barrel Polishing (CBP) of SRF Cavities Worldwide
C.A. Cooper (Fermilab) B. Bullock (CLASSE) S.C. Joshi (RRCAT) A.D. Palczewski (JLAB) K. Saito (KEK)
- WEIOA03** A New Electropolishing System For Low-Beta SC Cavities
S.M. Gerbick (ANL)
- WEIOA04** Review of RF - Sample - Test Equipment and Results
T. Junginger (CERN) T. Junginger (MPI-K) C.P. Welsch (Cockcroft Institute)
- WEIOA05** X-Ray Tomography Inspection of SRF Cavities
E.R. Harms (Fermilab)
- WEIOA06** Effect of Deformation and Heat Treatment on the Thermal Conductivity of Large Grain Superconducting Niobium
S.K. Chandrasekaran (MSU) T.R. Bieler (Michigan State University) C. Compton (FRIB) N.T. Wright ((MSU))

27-Jul-11 10:45 – 13:00

- 10:45 – 13:00** WEIOB — R&D/Diagnostics/Fabrication
Session Chair: W.-D. Moeller, DESY (Hamburg, Germany)
- WEIOB01** Guided Cavity Repair with Laser, E - Beam and Grinding
G. Wu (ANL)
- WEIOB02** Cavity Inspection and Repair Techniques
K. Watanabe (KEK) Y. Iwashita (Kyoto ICR)

- WEIOB03** Improvement in Cavity Fabrication Technology and Cost Reduction Methods
K. Sennyu (MHI)
- WEIOB04** XFEL Cavity Procurement as an Example of Technology Transfer
W. Singer (DESY)
- WEIOB05** Large Grain Cavities: Fabrication, RF Results and Optical Inspection
S. Aderhold (DESY)
- WEIOB06** IHEP 1.3GHz Low-Loss Large Grain 9-cell cavity R&D for ILC
J.Y. Zhai (IHEP Beijing)

27-Jul-11 18:00 – 21:30

18:00 – 21:30 WEIOC — Banquet Special Talk

- WEIOC01** 50 Years of RF Superconductivity
H. Padamsee (Cornell University)

28-Jul-11 08:00 – 10:15

- 08:00 – 10:15** THIOA — $\beta=1$ Cavities
Session Chair: H.T. Edwards, Fermilab (Batavia, USA)
- THIOA01** Test Results of the International S1-Global Cryomodule
Y. Yamamoto (KEK) C. Adolphsen (SLAC) T.T. Arkan (Fermilab) A. Bosotti (INFN/LASA) K. Jensch (DESY)
- THIOA02** Gradient R&D in the US
J.P. Ozelis (Fermilab)
- THIOA03** Compact Superconducting Cavities for Deflecting and Crabbing Applications
J.R. Delayen (ODU)
- THIOA04** QWR for $\beta \sim 1$ Accelerators
I. Ben-Zvi (BNL)
- THIOA05** The sc cw-LINAC Demonstrator - SRF-Technology finds the way into GSI
S. Mickat (GSI) M. Amberg (HIM) K. Aulenbacher (IKP) F.D. Dziuba (IAP)
- THIOA06** Mechanical Design Considerations for $\beta=1$ Cavities
O. Capatina (CERN) S. Chel (CEA/DSM/IRFU)
- THIOA07** Single-cell SC Cavity Development in India
A. Puntambekar (RRCAT) C.A. Cooper (Fermilab) P.N. Potukuchi (IUAC) G. Wu (ANL)

28-Jul-11 10:45 – 13:00

- 10:45 – 13:00** THIOB — $\beta < 1$ Cavities
Session Chair: W. Weingarten, CERN (Geneva, Switzerland)
- THIOB01** Project X Cavity and Cryomodule Development
C.M. Ginsburg (Fermilab)
- THIOB02** Vertical Tests Results of the IFMIF Cavity Prototypes and Cryomodule Development
F. Orsini (CEA/IRFU) J. Calero (CIEMAT) E.N. Zaplatin (FZJ)
- THIOB03** Status of the ReAccelerator Facility ReA for Rare Isotopes
D. Leitner (NSCL) A. Facco (FRIB) O.K. Kester (GSI)
- THIOB04** SRF Advances for ATLAS and other $\beta < 1$ Applications
M.P. Kelly (ANL)
- THIOB05** SPL Cavity Development
G. Olry (IPN)
- THIOB06** Recent Developments in SRF at TRIUMF
R.E. Laxdal (TRIUMF, Canada's National Laboratory for Particle and Nuclear Physics) R.S. Orr (University of Toronto)
- THIOB07** HIE-ISOLDE quarter wave Nb/Cu cavity
M. Pasini (CERN) M. Pasini (Instituut voor Kern- en Stralingsfysica, K. U. Leuven)
- THIOB08** Hot topics: Recipes for 9-cell cavity fabrication and preparation
T. Saeki (KEK)

Program

28-Jul-11 14:30 – 18:00

14:30 – 18:00 THPO — Poster Session

- THPO001** Quench Simulation Using a Ring-Type Defect Model
Y. Xie (CLASSE)
- THPO002** Defect-Induced Local Heating of Superconducting Cavity Surface
Y. Morozumi (KEK)
- THPO003** Multipacting in HOM Couplers at the 1.3GHz 9-cell TESLA Type SRF Cavity
D. Kostin (DESY)
- THPO004** Electro- or Chemical- Polishing and UHV Baking of Superconducting rf Nb Cavities and Q(H) Dependencies
J. Halbritter (FZ Karlsruhe)
- THPO005** Exploration of Very High Gradient Cavities
G.V. Ereemeev (JLAB)
- THPO006** Study of Trapped Magnetic Flux in Superconducting Niobium Samples
S. Aull (HZB)
- THPO007** Novel Deflecting Cavity Design for eRHIC
Q. Wu (BNL)
- THPO008** Post-Baking Losses in Niobium Cavities Studied by Dissection
A. Romanenko (Fermilab) G. Ciovati (JLAB)
- THPO009** Quench Studies in Large and Fine Grain Nb Cavities
S. Posen (CLASSE)
- THPO010** Multipactor Studies for DIAMOND Storage Ring Cavities
S.A. Pande (Diamond)
- THPO011** Improving the Intrinsic Quality Factor of SRF Cavities by Thermal Cycling
O. Kugeler (HZB)
- THPO012** Influence of Foreign Particles on the Quality Factor of a Superconducting Cavity
V.D. Shemelin (CLASSE)
- THPO013** Investigation of 9-Cell Cavity Performance Problem by Facilities in KEK AR East 2nd Experimental Hall
K. Saito (KEK)
- THPO015** Repair SRF Cavity by Re-Melting Surface Defects via High Power Laser Technique
M. Ge (CLASSE) E. Borissov (Fermilab) G. Wu (ANL)
- THPO016** Preliminary Results on the Laser Heating Investigation of Hotspots in a Large-Grain Nb Cavity
G. Ciovati (JLAB) S. M. Anlage (UMD) A.V. Gurevich (Old Dominion University) G. Nemes (Astigmat)
- THPO017** Probing the Fundamental Limit of Niobium in High Radiofrequency Fields by Dual Mode Excitation in Superconducting Radiofrequency Cavities
G.V. Ereemeev (JLAB)
- THPO018** Quench Studies of ILC Cavities
G.V. Ereemeev (JLAB) J. Dai (PKU/IHIP)
- THPO019** Design, Construction, and Initial Test of High Spatial Resolution Thermometry Arrays for Detection of Surface Temperature Profiles on SRF Cavities in Super Fluid Helium
A.D. Palczewski (JLAB)
- THPO020** Exploration of Quench Initiation Due to Intentional Geometrical Defects in a High Magnetic Field Region of an SRF Cavity
J. Dai (PKU/IHIP) G.V. Ereemeev (JLAB)
- THPO021** Measurement of H_{c1} in Superconducting Thin Films
N.F. Haberkorn (LANL) B. Moeckly (STI)
- THPO022** Temperature and Surface Treatment Dependence of Medium Field Q-Slope
A. Romanenko (Fermilab) G. Wu (ANL)

- THPO023** External Magnetic Fields and Operating SRF Cavity
D.A. Sergatskov (Fermilab)
- THPO024** Quench Dynamics in SRF Cavities
Y.B. Maximenko (MIPT) D.A. Sergatskov (Fermilab)
- THPO025** Effects of Anodization on Field Emission on Nb Surfaces
A.T. Wu (JLAB) S. Jin (PKU/IHIP)
- THPO026** Second Sound Triangulation for SPL Cavity Quench Localization
K.C. Liao (CERN) H. Vennekate (University of Giessen, Georg-August University of Göttingen)
- THPO027** Optical Observation of Geometrical Features and Correlation With RFTest Results
J. Dai (PKU/IHIP) R.L. Geng (JLAB) K. Watanabe (KEK)
- THPO028** SIMS and TEM Analysis of Niobium Bicrystals
P. Maheswari (NCSU AIF) G. Ciovati (JLAB) M. Rigsbee (Materials Science and Engineering)
- THPO029** Commissioning Cornell OSTs for SRF Cavity Testing at JLab
G.V. Ereemeev (JLAB)
- THPO030** Microphonics Compensation for a 325MHz Single Spoke Cavity at Fermilab
W. Schappert (Fermilab)
- THPO031** Second Sound as an automated Quench Localisation Tool at DESY
F. Schlender (DESY)
- THPO032** TOF-SIMS Analysis of Hydrogen in Niobium, From 160i½K to 475i½K
P. Maheswari (NCSU AIF) G. Ciovati (JLAB) M. Rigsbee (Materials Science and Engineering)
- THPO033** Measurements of HOM Spectrum a 1.3 GHz ILC SC Cavity
T.N. Khabiboulline (Fermilab)
- THPO034** Vertical Test Results on KEK-ERL 9-Cell L-Band Superconducting Cavity
E. Cenni (Sokendai) T. Furuya (KEK) M. Sawamura (Japan Atomic Energy Agency (JAEA), Gamma-ray Non-Destructive Assay Research Group) K. Shinoe (ISSP/SRL)
- THPO035** Comparison of Field Emission at Different SRF Cavity Assembly States and Test Stands
D. Kostin (DESY)
- THPO036** A Machine for High-Resolution Inspection of SRF Cavities at JLab
R.L. Geng (JLAB)
- THPO037** Lorentz Force Detuning Compensation in Fermilab Cryomodule 1
Y.M. Pischalnikov (Fermilab)
- THPO038** Detailed Nb Surface Morphology Evolution During Electropolishing for SRF Cavity Production
H. Tian (JLAB)
- THPO039** Niobium Surface Resistance Measurement by Thermometric Method With a TE011 Cavity
G. Martinet (IPN)
- THPO040** A Wire Position Monitor System for the 1.3GHz Tesla-Style Cryomodule at the Fermilab New Muon Lab
N. Eddy (Fermilab)
- THPO041** HOM Identification and Bead Pulling on the Brookhaven ERL
H. Hahn (BNL) P. Jain (Stony Brook University)
- THPO042** Crystallographic Orientation of Epitaxial Transition Observed for Nb (BCC) on Cu and MgO (FCC) Single-Crystals
K.I. Seo (NSU) M. Krishnan (AASC) H.L. Phillips (JLAB)
- THPO043** Understanding of Suppressed Superconductivity on SRF Quality Niobium
Z.H. Sung (ASC) L.D. Cooley (Fermilab) A.V. Gurevich (Old Dominion University) P.J. Lee (NHMFL)
- THPO044** Structural Characterization of Nb Films Deposited by ECR Plasma Energetic Condensation on Crystalline Insulators
X. Zhao (JLAB) H. Baumgart (ODU) K.I. Seo (NSU)
- THPO045** Nb Surface Nonlinear Properties Under Localized High RF Magnetic Field
T.M. Tai (CNAM, UMD) S. M. Anlage (UMD)

Program

- THPO046** Characterization of Scale-Dependent Roughness of Niobium Surfaces as a Function of Surface Treatment Processes
C. Xu (The College of William and Mary) C.E. Reece (JLAB)
- THPO047** Growth Mode and Strain Effects in the Superconducting Properties of Nb Thin Films on Sapphire
C. Clavero (The College of William and Mary) C.E. Reece (JLAB)
- THPO048** RF Surface Impedance of MgB₂ Thin Films at 7.5 GHz
B. Xiao (The College of William and Mary) H.L. Phillips (JLAB) T. Tajima (LANL)
- THPO049** Atomic-Scale Characterization of Niobium for SRF Cavities Using Ultraviolet Laser-Assisted Local-Electrode Atom-Probe Tomography
Y.-J. Kim (NU) A. Romanenko (Fermilab)
- THPO050** TE Sample Host Cavities Development at Cornell
Y. Xie (CLASSE)
- THPO051** Laser Re-Melting Influence on Nb Properties: Geometrical and Chemical Aspects
A.V. Dzyuba (Fermilab) A.V. Dzyuba (NSU) M. Ge (CLASSE) G. Wu (ANL)
- THPO052** Investigation of Near-Surface Interstitial Hydrogen in Cavity-Grade Niobium
A. Romanenko (Fermilab) L.V. Goncharova (UWO)
- THPO053** Material for Fabrication of DESY Large Grain/Single Crystal Cavities
X. Singer (DESY) H.G. Brokmeier (Technische Universität Clausthal, Institut für Nichtmetallische Werkstoffe) R. Grill (Plansee Metall GmbH) F. Schoelz (W.C. Heraeus GmbH, Materials Technology Dept.)
- THPO054** Magneto-Optical and Electromagnetic Study Different Forms of Nb for SRF Application
A. Polyanskii (ASC) P.J. Lee (NHMFL) A-M. Valente-Feliciano (JLAB)
- THPO055** Investigation of Samples Separated From Prototype Cavities of the European XFEL
X. Singer (DESY) M. Hoss (W.C. Heraeus GmbH, Materials Technology Dept.)
- THPO056** Thermal-Vacuum Variations of the Surface Oxide Complex on Cu
M. Bagge-Hansen (The College of William and Mary) C.E. Reece (JLAB) K.I. Seo (NSU)
- THPO057** Superconducting DC and RF Properties of Ingot Niobium
P. Dhakal (JLAB)
- THPO058** Phase-Sensitive Nonlinear Near-Field Microwave Microscopy on MgB₂ Thin Films
B.G. Ghamsari (UMD)
- THPO059** Correlation of Microstructure, Chemical Composition and RRR-Value in High Purity Niobium (Nb-RRR)
R. Grill (Plansee Metall GmbH) M. Heilmaier (TU Darmstadt) W. Singer (DESY)
- THPO060** First Principles Investigation of Hydrogen in Niobium
D.C. Ford (Fermilab) D.C. Ford (Northwestern University) D.N. Seidman (NU)
- THPO061** Activation of Field Emitters on Clean Nb Surfaces
A. Navitski (Bergische Universität Wuppertal) D. Reschke (DESY)
- THPO062** Epitaxial Niobium Thin Films for Accelerator Cavities
W.M. Roach (The College of William and Mary) C.E. Reece (JLAB)
- THPO063** Study of the Impurity Species in Niobium Films Grown by ECR Technique Employing Secondary Ion Mass Spectrometry
A-M. Valente-Feliciano (JLAB) F.A. Stevie (NCSU AIF)
- THPO064** Structural Properties of Niobium Thin Films Deposited on Metallic Substrates by ECR Plasma Energetic Condensation
J.K. Spradlin (JLAB) D. Gu (ODU) K.I. Seo (NSU)
- THPO065** Anomalous Morphological Scaling in Epitaxial Nb Thin Films on MgO(001)
D.B. Beringer (The College of William and Mary) C.E. Reece (JLAB)
- THPO066** Stoichiometric Nb₃Sn in First Samples Coated at Cornell
S. Posen (CLASSE)
- THPO067** Characterization of Large Grain Nb Ingot Microstructure Using OIM and Laue Methods
D. Kang (Michigan State University) G. Ciovati (JLAB) C. Compton (FRIB) T.L. Grimm (Niowave, Inc.)

- THPO068** Experimental Investigation and CPFE Modeling of Single Crystal Niobium for Tube Hydroforming
A. Mapar ((MSU)) D.C. Baars (Michigan State University) C. Compton (FRIB) P. Darbandi (MSU) J.E. Murphy (University of Nevada, Reno)
- THPO069** Nb Film Growth on Crystalline and Amorphous Substrates
E.F. Valderrama (AASC) P. Maheshwari (NCSU AIF) K.I. Seo (NSU) X. Zhao (JLAB)
- THPO070** Effect of Fabricate Condition on Properties of Bi-2212 Thin Films
T.M. Nguyen (nguyenthi mua)
- THPO071** Detailed Surface Analysis of Incremental Centrifugal Barrel Polishing (CBP) and EP of Single-Crystal Niobium Samples
A.D. Palczewski (JLAB)
- THPO072** Raman Spectroscopy as a Probe of Surface Oxides and Hydrides on Niobium
J. Zasadzinski (IIT) Th. Proslie (ANL)
- THPO073** Laser Melt Smoothing of Niobium Superconducting Radio-Frequency Cavity Surfaces
S. Singaravelu (JLAB) C. Xu (The College of William and Mary)
- THPO074** NbTiN Films for SRF Multilayer Structures
A.M. Valente-Feliciano (JLAB) D. Gu (ODU) K.I. Seo (NSU)
- THPO075** Does Annealing Reduce or Remove Defects Observed After Electropolishing?
L.D. Cooley (Fermilab)
- THPO076** Measurement of the Loss Tangent and Heat Capacity of a Large Single Crystal Sapphire
N. Pogue (Texas A&M University)
- THPO077** Mo-Re Films for SRF Applications
E.F. Valderrama (AASC) P. Maheshwari (NCSU AIF) K.I. Seo (NSU) X. Zhao (JLAB)
- THPO078** Surface and Thin Film Characterization of Superconducting Multilayer Films for Application in RF Accelerator Cavities
R.K. Schulze (LANL) B. Moeckly (STI) T. Proslie (ANL) A.T. Zocco (UC)
- THPO079** Surface Preparation of Metallic Substrates for Quality SRF Thin Films
J.K. Spradlin (JLAB)

28-Jul-11 18:00 – 19:00

- 18:00 – 19:00** THIOC — Hot Topics
Hot topics: Recipes for 9-cell cavity fabrication and preparation
Session Chair: T. Saeki, KEK (Ibaraki, Japan)

29-Jul-11 08:00 – 10:15

- 08:00 – 10:15** FRIOA — SRF Technology
Session Chair: S. Noguchi, KEK (Ibaraki, Japan)
- FRIOA01** Adaptive Compensation for Lorentz Force Detuning in Superconducting RF Cavities
W. Schappert (Fermilab)
- FRIOA02** Innovative Tuner Designs For Low Beta SRF Cavities
Z.A. Conway (ANL)
- FRIOA03** Recent Progress in HOM Damping from Around The World
M. Liepe (CLASSE)
- FRIOA04** Power Couplers for Spiral-2
Y. Gijmez Martinez (LPSC) P.-E. Bernaudin (CEA/DSM/IRFU) G. Olry (IPN)
- FRIOA05** Overview of CW Input Couplers for ERL
H. Sakai (KEK)
- FRIOA06** Construction of cERL Cryomodules for Injector and Main Linac
K. Umemori (KEK) E. Cenni (Sokendai) M. Sawamura (JAEA) K. Shinoe (ISSP/SRL)
- FRIOA07** SRF Photoinjector Tests at HoBiCat
A. Neumann (HZB) P. Kneisel (JLAB) R. Nietubyc (The Andrzej Soltan Institute for Nuclear Studies, Centre Swierk) J.K. Sekutowicz (DESY) I. Will (MBI)

29-Jul-11 10:45 – 12:30

- 10:45 – 12:30** FRIOB — New/Emerging SRF Capability & Applications
Session Chair: J.E. Chen, PKU/IHIP (Beijing, People’s Republic of China)
- FRIOB01** SRF Activities at Peking University
J.K. Hao (PKU/IHIP)
- FRIOB02** RF and Beam Test of the DC-SRF Injector of PKU-SETF
F. Zhu (PKU/IHIP)
- FRIOB03** Chinese Plan for ADS and CSNS
S. Fu (IHEP Beijing) Y. He (IMP)
- FRIOB04** SRF Accelerator for Indian ADS Program: Present & Future Prospects
P. Singh (BARC)
- FRIOB05** Crab Crossing for LHC Upgrade
R. Calaga (BNL)
- FRIOB06** The ESS Accelerator
M. Lindroos (CERN) S. Peggs (ESS)

29-Jul-11 12:45 – 13:00

12:45 – 13:00 FRT — Closeout

MOIOA — Overview of SRF Challenges

Challenges in SRF Module Production for the European XFEL

The internationally organized European XFEL free-electron laser is under construction at the Deutsches Elektronen-Synchrotron (DESY). With an electron beam energy of 14 GeV the possible wavelength will be down to 0.05 nm. The project is the first large scale application of the TESLA technology developed over the last 15 years. The main linac will consist of 80 accelerator modules, i.e. 640 superconducting accelerator cavities, operated at a gradient of 24.3 MV/m. The talk describes the activities with respect to the module production within the international collaboration. The challenges and the status of final prototyping, industrialization and commissioning of new infrastructure will be presented.

D. Reschke (DESY)

MOIOA01

Advances in SRF Development for ILC

The International Linear Collider (ILC) project expects sixteen thousands 1.3 GHz, 9-cell SRF cavities with a field gradient of 35 MV/m, in order to realize an electron and positron collider with a total energy of 500 GeV. It will require thoughtful preparation for the industrialization and for advanced technical approach for a large amount of cost-effective production. For further long term scope, It will be important to make our best effort to investigate much higher field gradient and Q0 value, and to seek for further cost-effective cavity production for future energy upgrade toward 1 TeV. It may include new material and new fabrication technology. The advances in SRF cavity technology development and future prospect will be discussed.

A. Yamamoto (KEK)

MOIOA02

Recent SRF Developments for ERLs

Research and Development of SRF technology is being advanced around the world. We review developments in Europe, Asia and North America citing specifics from Helmholtz Zentrum Berlin, KEK, JLab and Cornell. These programs are designed in part to improve BBU control, power coupling and Qo which is crucial for minimizing power consumption for operation of ERLs as CW sources of high-current low-emittance beams.

G.H. Hoffstaetter, M. Tigner (CLASSE)

MOIOA03

SRF Challenges for Improving Operational Electron Linacs

The performance of the operational SRF-based electron linacs CEBAF, ELBE, and S-DALINAC continues to evolve positively. These facilities are exploiting opportunities to improve operational capability by both remediation of past limitations and also construction of new capacity using state-of-the-art designs and processes. A project to rework the weakest ten cryomodules in CEBAF was completed and enabled robust operation for physics at 6 GeV. The 12 GeV Upgrade of CEBAF is now underway and involves construction of ten new CW >100 MV cryomodules with 80 new 7-cell low-loss cell shaped fine-grained niobium cavities, all electropolished. The technical challenges associated with the preparation of these cavities will be reviewed and their performance in individual acceptance and cryomodule testing to date will be summarized. The ELBE facility at Helmholtz Zentrum Dresden Rossendorf continues to develop its source with an SRF gun system. The long-running S-DALINAC at Technische Universität Darmstadt is operating reliably, and in the framework of the injector upgrade program, a new cryomodule featuring a waveguide power coupler with low transversal fields was developed and is assembled.

C.E. Reece (JLAB)

MOIOA04

Funding: Authored by Jefferson Science Associates, LLC under U.S. DOE Contract No. DE-AC05-06OR23177.

MOIOB — Overview of SRF Challenges

MOIOB01

SRF Development for High Energy Physics

M.S. Champion (Fermilab)

Superconducting Radio-Frequency (SRF) technology has become the technology of choice for accelerator-based high energy physics (HEP) research, from the operating Large Hadron Collider to the planned Project X and International Linear Collider. The HEP community has made large investments in recent years in preparation for the construction of a SRF-based project, and the SRF community has grown commensurately. Results and ongoing efforts will be described along with some comparison to the application of SRF technology in non-HEP applications.

Funding: Supported by Fermi Research Alliance, LLC under Contract No. De-AC02-07CH11359 with the United States Department of Energy.

MOIOB02

Advances in SRF for Low Beta Ion Linacs

S. Bousson (IPN)

Projects based on ion linacs have multiplied during the last decade to follow the increasing demand of ion beams, either stable or radioactive, for application in nuclear physics or material studies. Thanks to the continuous progress in SRF (Superconducting Radio Frequency) technology, all these linacs are based on low beta superconducting cavities of different type (half-wave, quarter-wave, bulk Nb or Nb/cu) and make this particular field very active in many laboratories worldwide. In this paper, we review the most recent developments in SRF performed in the framework of FRIB, SPIRAL-2, ATLAS, SARAF, IFMIF, TRIUMF and ISOLDE.

MOIOB03

Advances in SRF for Neutron Sources

S.-H. Kim (ORNL)

There have been studies for applications of superconducting radio-frequency (SRF) technologies to the proton or deuteron accelerators to generate high intensity neutrons. The areas of interests are neutron scattering, material test and accelerator driven systems for nuclear transmutation, energy generation, isotope production, and etc. Advantages of the SRF technology for high power proton/deuteron accelerators include high operating gradient, low beam loss from large aperture size and extremely high vacuum, high RF power transfer efficiency to beam, and operational flexibility. Many technical advances of SRF technologies from various programs have been applied to the high power accelerators for meeting their missions, which enables designs, constructions, and operations of high intensity accelerators at multi-megawatts level or higher. Major large scale operational and future neutron sources using the SRF technologies are presented together with their specific merits, requirements and issues.

MOIOB04

Survey of SRF Guns

S.A. Belomestnykh (BNL)

Developing Superconducting RF (SRF) electron guns is an active field with several laboratories working on different gun designs. While the first guns were based on elliptic cavity geometries, Quarter Wave Resonator (QWR) option is gaining popularity. QWRs are especially well suited for producing beams with high charge per bunch. In this talk we will describe recent progress in developing both types of SRF guns.

Funding: Work is supported by Brookhaven Science Associates, LLC under Contract No. DE-AC02-98CH10886 with the U.S. DOE.

Operational Experience with SRF Cavities for Light Sources

Third generation light sources require modest accelerating voltages, however this is offset by a need for high reliability,

M. Jensen (Diamond)

to serve users on a continual basis with minimal interruption. The high Q of the superconducting (SC) cavities means that cavities are designed such that higher order modes are effectively damped using external loads, offering stable high current, multi-bunch operation. Fundamental mode SC cavities for light sources were initially used in CESR and KEKB, followed by Taiwan Light Source and Canadian Light Source and third harmonic systems are used for bunch lengthening at SLS and ELETTRA. The successful operation of those machines led to the choice of SC cavities in the design of Soleil, Diamond Light Source and Shanghai Synchrotron Radiation Facility, all now in operation. Additionally, Taiwan Photon Source, Pohang Light Source II and National Synchrotron Light Source II are currently in construction and all employ SC cavities. In this paper we will review recent operational experience of SC cavities in light sources and will describe recent developments related to the cavities and their auxiliary systems.

MOIOB05

Hot Topics: Source of Quench Producing Defects

Recent efforts in pushing the performance of superconducting RF niobium cavities for the International Linear Collider have resulted in two-fold progresses:

R.L. Geng (JLAB)

reduced field emission and improved quench limit in real 9-cell cavities. RF testing at cryogenic temperatures assisted with quench-detection instrumentation reveals that quench happens often times at highly localized areas inside or near the equator weld of a cavity cell, which is also the high surface magnetic field region. High-resolution optical inspection of the identified quench location makes it possible to correlate the cavity quench limit with certain types of defects. Several sources of quench producing defects are being explored. We will discuss the experimental evidence in supporting each of these sources. We will also discuss the methods of curing or preventing these defects for improved gradient limit and reduced gradient spread.

Funding: This work was authored by Jefferson Science Associates, LLC under U.S. DOE Contract No. DE-AC05-06OR23177

MOIOB06

MOPO — Poster Session

MOPO001

Commercial Superconducting Electron Linacs

T.L. Grimm, C.H. Boulware, J.L. Hollister (Niowave, Inc.)

Industry now has the capability to design, build and commission superconducting electron linacs. This capability includes the integration of the liquid helium refrigerator and the license to operate a radiation generating device. Niowave offers a broad range of commercial turnkey superconducting electron linacs with beam energies from 0.5 to 50 MeV and average beam powers from 1 W to 1 MW. The commercial linacs operate at 4.5 K with helium refrigerator loads typically less than 100 W. Operation at 4.5 K uses niobium cavities with frequencies less than about 700 MHz. The types of electron source used depend on the application and include DC, copper RF and SRF guns with cathodes based on photoemission, thermionic and field emission. There are many applications with a diverse range of uses from ultrafast electron microscopes to free electron laser to advanced x-ray sources and isotope production. Commercial developments and plans to date will be presented.

MOPO002

A Superconducting Cavity for a Flux Coupled Cyclotron That Drives a Power Plant Based on a Spent Nuclear Fuel

N. Pogue, P.M. McIntyre, A. Sattarov (Texas A&M University)

Accelerator-driven subcritical fission is a promising candidate method to destroy the long-lived actinides in spent nuclear fuel without reprocessing it. To make it economically feasible one needs an accelerator delivering a continuous 800MeV proton beam with 5-10 MW power and minimum down time. We are developing a design for a flux-coupled stack of isochronous cyclotrons (IC), in which each IC provides 3mA proton beam using a magnetic design very similar to that of the PSI IC. We have designed a superconducting cavity for each IC that would operate at 50 MHz and deliver 1MeV/turn energy gain. The lobes of the cavity are oriented parallel to the beam plane to fit into the confined space within the flux-coupled stack. The top and bottom lobes are coupled at the radial inside and outside ends to eliminate field distortions and parasitic modes that are produced if the lobes were terminated with flat ends. The approach enables us to reduce the accelerating gap and still preserve coupling between top and bottom sections of the cavity. The overall cavity is approximately 78 cm wide, 70 cm tall, and 3.2 meter long, producing a uniform accelerating field, and dissipates 9 W at 4 K.

MOPO003

650 MHz Cryomodules for Project X at Fermilab – Requirements and Concepts

T.J. Peterson, M.H. Foley, C.M. Ginsburg, C.J. Grimm, J.S. Kerby, Y. Orlov (Fermilab) R. Ghosh, G. Gilankar, A. Jain, P. Khare, P.K. Kush, A. Laxminarayanan (RRCAT)

Cryomodules containing 650 MHz superconducting niobium RF cavities and associated components (input couplers, tuners, instrumentation, etc.) will be developed for Project X, a proposed high intensity proton accelerator facility based on an H^- linear accelerator at Fermilab. This paper describes the requirements of the 650 MHz cryomodules and the implications of those requirements for the cryomodule design. Cryomodule string segmentation, integration with the cryogenic system, features for maintainability and access, piping and emergency venting considerations, pressure vessel issues, and thermal and mechanical design concepts will be described.

Modified SRF Photoinjector for the ELBE at HZDR

The superconducting radio frequency photoinjector (SRF photoinjector) with Cs₂Te cathode has been successfully operated under the collaboration of BESSY, DESY, HZDR, and MBI. In order to improve the gradient of the gun cavity and the beam quality, a new modified SRF gun (SRF-gun2008) has been designed. The main updates of the new cavity design for the new injector was published before. (ID TH-PPO022 on the SRF09 Berlin.) This cavity is being fabricated in Jefferson Lab. In this paper the ideas of the redesign of the further parts of the SRF-gun2008 will be presented. The most important issue is the special design of half-cell and choke filter. The cathode cooler is also slightly changed, which simplifies the installation of the cathode cooler in the cavity. The next update is the separation of input and output of the liquid nitrogen supply, for the purpose of the stability of the N₂ pressure as well as the better possibility of temperature measurement. Another key point is the implementation of the superconducting solenoid inside the cryomodule. The position of the solenoid can be accurately adjusted with two stepmotors, which is thermally isolated to the solenoid itself.

P. Murcek, A. Arnold, H. Buettig, D. Janssen, M. Justus, P. Michel, G.S. Staats, J. Teichert, R. Xiang (HZDR) P. Kneisel (JLAB)

MOPO004

Conceptual Design of the Superconducting Proton Linac (SPL) Short Cryo-module

The Superconducting Proton Linac (SPL) is an R&D effort conducted by CERN in partnership with other international laboratories, aimed at developing key technologies for the construction of a multi-megawatt proton linac based on state-of-the-art SRF technology, which would serve as a driver for new physics facilities such as neutrinos and radioactive ion beams. Amongst the main objectives of this effort, are the development of 704 MHz bulk niobium $\beta=1$ elliptical cavities, operating at 2 K and providing an accelerating field of 25 MV/m, and testing of a string of cavities integrated in a machine-type cryo-module. In an initial phase only 4 out of the 8 cavities of an SPL cryo-module will be tested in a $\frac{1}{2}$ length cryo-module developed for this purpose thus called the Short Cryo-module. This paper presents the conceptual design of the Short Cryo-module, highlighting its innovative principles in terms of cavity supporting and alignment, and describes the integration of cavities and their main equipment (RF couplers, helium vessels, tuners, magnetic shielding) inside the cryo-module and their assembly method. The operational scenarios and test plans are also presented and discussed.

V. Parma, P. Bestman, N. Bourcey, O. Capatina, P. Coelho Moreira de Azevedo, E. Montesinos, T. Renaglia, A. Vande Crean, W. Weingarten, L.R. Williams (CERN) P. Dambre, P. Duchesne, P. Duthil, D. Reynet, S. Rousselot (IPN)

MOPO005

Status and Plans for an SRF Accelerator Test Facility at Fermilab

A superconducting RF accelerator test facility is currently under construction at Fermilab. The accelerator will consist of an electron gun, 40 MeV injector, beam acceleration section consisting of 3 TTF-type or ILC-type cryomodules, and multiple downstream beam lines for testing diagnostics and performing beam experiments. With 3 cryomodules installed this facility will initially be capable of generating an 810 MeV electron beam with ILC beam intensity. The facility can accommodate up to 6 cryomodules for a total beam energy of 1.5 GeV. This facility will be used to test SRF cryomodules under high intensity beam conditions, RF power equipment, instrumentation, and LLRF and controls systems for future SRF accelerators such as the ILC and Project-X. This paper describes the current status and overall plans for this facility.

M.D. Church, J.R. Leibfritz, S. Nagaitsev (Fermilab)

Funding: Operated by Fermi Research Alliance, LLC under Contract # DE-AC02-07CH11359 with the U.S. Department of Energy

MOPO006

MOPO007

Test of Components for the S-DALINAC Injector Upgrade*

S.T. Sievers, J. Conrad, R. Eichhorn, R. Grewe, F. Hug, T. Kuerzeder, N. Pietralla, A. Richter (TU Darmstadt)

In 2009 a vertical bath cryostat was commissioned at the S-DALINAC. Since then, components for the new cryostat module within the framework of the injector up-

grade have been tested. Measurements have been performed to check the leakage rate of "Quick-CF" UHV flanges and the performance of piezo actors in superfluid helium have been investigated. To enlarge the scale of possible measurements at the vertical bath cryostat, systems to measure the quality factor via the decay time method and quench localisation via second sound will be implemented this year. We will report on the recent results.

Funding: *Supported by the DFG through SFB 634

MOPO008

RF and SRF Layout of BERLinPro

W. Anders, A. Jankowiak, T. Kamps, J. Knobloch, O. Kugeler, A. Neumann (HZB)

The ERL project BERLinPro is funded and now in the design phase. The planned SRF layout is described including the RF transmitters, the cryogenic in-

stallations and the configuration of the SRF modules.

Funding: Work funded by the Bundesministerium für Bildung und Forschung and Land Berlin

MOPO009

Design Status of the Superconducting Driver Linac for the Facility for Radioactive Isotope Beams

M. Leitner, C. Compton, K. Elliott, A. Facco, W. Hartung, M.J. Johnson, D. Leitner, F. Marti, S.J. Miller, J. Popielarski, L. Popielarski, J. Wei, J. Weisend, J. Wlodarczyk, Y. Xu, Y. Zhang (FRIB)

The Facility for Rare Isotope Beams (FRIB) will utilize a powerful, superconducting heavy-ion driver linac to provide stable ion beams from protons to uranium, at energies of > 200 MeV/u at a beam power of up to 400 kW. ECR ion

sources installed above ground will be used to provide highly charged ions, that will be transported into the linac tunnel approx. 10 m below ground. For the heaviest ions, two charge states will be accelerated to about 0.5 MeV/u using a room-temperature 80.5 MHz RFQ and injected into a superconducting cw linac, consisting of 114 quarter-wave (80.5 MHz) and 231 half-wavelength (322 MHz) cavities, installed inside 52 cryomodules operating at 2K. A single stripper section will be located at about 17 MeV/u (for uranium). Transverse focusing along the linac will be achieved by 9 T superconducting solenoids within the same cryostat as the superconducting rf accelerating structures. This paper describes the matured linac design, as the project is progressing towards a Department of Energy performance baseline definition in 2012. Development status of the linac subcomponents are presented with emphasis on the superconducting RF components.

Funding: This material is based upon work supported by the U.S. Department of Energy Office of Science under Cooperative Agreement DE-SC0000661

MOPO010

Update on Module Measurements for the XFEL Prototype Modules

D. Kostin, A. Goessel, K. Jensch, W.-D. Moeller, A.A. Sulimov (DESY)

The Cryo Module Test Bench (CMTB) at DESY is used since several years for the SRF module tests. Three XFEL prototypes modules, PXFEL1,2,3, were tested

on this facility. An update on the SRF modules testing activities since PXFEL1 test is presented.

Status of SARAF Superconducting Acceleration Module

Soreq Applied Research Accelerator Facility (SARAF) is based on a 176 MHz superconducting RF light ions linac, currently under commissioning at Soreq NRC. At present, the accelerator includes a Prototype Superconducting Module, containing 6 half wave resonators. In this work we present measurement results of various mechanical properties of the resonators. These results are compared to simulation results obtained using CST MWS. Beam operation results are presented as well, including a technique for the calibration of the cavity pick up probe by operating the Linac using two RF sources.

A. Perry, Y. Ben Aliz, B. Kaizer, A. Kreisel, J. Rodnizki, L. Weissman (Soreq NRC)

MOPO011

Overview of ILC High Gradient Cavity R&D at Jefferson Lab

We report on the progress of ILC high gradient cavity R&D at Jefferson Lab since the Berlin Workshop. Nine out of

ten 9-cell cavities manufactured by ACCEL/RI achieved a gradient of more than 38 MV/m at Q0 of more than $8 \cdot 10^9$ up to a second-pass processing. Four out of six 9-cell second production batch cavities manufactured by AES achieved a gradient in the range of 36-41 MV/m. The cavity quench studies are further enhanced by adopting the Cornell OST's and the KEK replica technique, in addition to the existing JLab fixed thermometry system and JLab high-resolution optical inspection machine. We have also processed and tested ILC alternate cavities including 9-cell large-grain niobium cavities and 9-cell low-loss shape (ICHIRO) cavities in collaboration with Peking University and KEK. To date, about 50 9-cell cavities have been processed and tested at JLab under the American Regional Team program in support of ILC. More than 110 ILC cavity EP cycles have been accumulated, corresponding to more than 320 hours of active EP time. More than 150 ILC cavity RF tests at cryogenic temperatures have been completed.

R.L. Geng (JLAB)

Funding: This work was authored by Jefferson Science Associates, LLC under U.S. DOE Contract No. DE-AC05-06OR23177

MOPO012

RF Test Results from Cryomodule 1 at the Fermilab SRF Beam Test Facility

Powered operation of Cryomodule 1 (CM-1) at the Fermilab SRF Beam Test Facility began in late 2010. Since then a series of tests first on the eight individual cavities and then the full cryomodule have been performed. We report on the results of these tests and lessons learned which will have an impact on future module testing at Fermilab.

E.R. Harms, J. Branlard, K. Carlson, B. Chase, E. Cullerton, C.C. Jensen, P.W. Joireman, A.L. Klebaner, T. Kubicki, M.J. Kucera, A.M. Legan, J.R. Leibfritz, A. Martinez, M.W. McGee, S. Nagaitsev, O.A. Nezhevenko, D.J. Nicklaus, H. Pfeffer, Y.M. Pischalnikov, P.S. Prieto, J. Reid, W. Schappert, V. Tupikov, P. Varghese (Fermilab)

Funding: Operated by Fermi Research Alliance, LLC under Contract No. DE-AC02-07CH11359 with the United States Department of Energy.

MOPO013

MOPO014

Design of the Fundamental Power Coupler and Photocathode Inserts for the 112 MHz Superconducting Electron Gun

T. Xin (Stony Brook University) S.A. Belomestnykh, I. Ben-Zvi, X. Chang, X. Liang, T. Rao, J. Skaritka, E. Wang, Q. Wu (BNL)

A 112MHz superconducting quarter-wave resonator electron gun will be used as the injector of the Coherent Electron Cooling (CEC) proof-of-principle experiment at BNL. Furthermore, this electron gun can be the testing cavity for various photocathodes. In this paper, we present the design of the Fundamental Power Coupler (FPC) and the cathode stalks designated to the future experiments. The axial waveguide structure FPC has the properties of tunable coupling factor and small interference to the electron beam output. The optimization of the coupling factor and the location of the FPC are discussed in detail. Two types of cathode stalks are discussed. Special shape of the stalk is applied in order to minimize the RF power loss. The location of cathode plane is also optimized to enable the extraction of low emittance beam.

Funding: Work is supported at Stony Brook University under grant DE-SC0005713 by the US DOE, at BNL by Brookhaven Science Associates, LLC under Contract No. DE-AC02-98CH10886 with the U.S. DOE.

MOPO015

IHEP 1.3GHz SRF Technology R&D Status

J. Gao, Y.L. Chi, J.P. Dai, S.P. Li, W.M. Pan, Y. Sun, J.Y. Zhai (IHEP Beijing)

1.3 GHz superconducting radio-frequency (SRF) technology is one of the key technologies for the ILC and future XFEL and ERL projects in China. With the aim to develop 1.3 GHz SRF technology, IHEP has started a program to build an SRF Accelerating Unit. This unit contains a 9-cell 1.3 GHz superconducting cavity, a short cryomodule, a high power input coupler, a tuner, a low level RF system etc. This program also includes the SRF laboratory upgrade, which will permit the unit to be built and tested at IHEP. The unit will be used for the 1.3 GHz SRF system integration study, high power horizontal test and possible beam test in the future. In this paper, we report the recent R&D status of this program. The first large grain low-loss shape 9-cell superconducting RF cavity made by IHEP reached 20 MV/m in the first vertical test. The prototype tuner and LLRF system are under test. The first 1.3 GHz high power input coupler fabrication was finished and the cryomodule is under fabrication. Several key SRF facilities (CBP, CP, HPR, optical inspection camera, pretuning machine etc) for 9-cell cavity surface treatment and pre-tuning were successfully commissioned and in operation.

MOPO016

Superconducting RF R&D for the Cornell ERL Main Linac

M. Liepe, Y. He, G.H. Hoffstaetter, S. Posen, J. Sears, V.D. Shemelin, M. Tigner, N.R.A. Valles, V. Veshcherevich (CLASSE)

Cornell University is developing the superconducting RF technology required for the construction of a 100 mA hard X-ray light source driven by an Energy-Recovery Linac. Prototype components of the 5 GeV cw SRF main linac cryomodule are under development, fabrication and testing. This work includes an optimized 7-cell SRF cavity, a broadband HOM beamline absorber, and a 5 kW cw RF input coupler. In this paper we give an overview of these activities at Cornell.

Funding: Supported by NSF award DMR-0807731.

Performance Limitation Studies on ISAC-II QWR's and e-Linac Elliptical Cavities at TRIUMF

TRIUMF has been operating successfully for several years numerous 100MHz class superconducting quarter wave resonators on the ISAC-II heavy ion linac and is now developing a 1.3 GHz activity to build the e-linac, a 50 MeV superconducting electron linac to produce radioisotopes by photofission. Several studies on cavity treatments are ongoing to both enhance ISAC-II QWR performances and to meet the requirements on the e-linac elliptical cavities. This paper will summarize the main development efforts to understand performance limitations in these cavities.

D. Longuevergne, A. Grassellino, P. Kolb, R.E. Laxdal, V. Zvyagintsev (TRIUMF, Canada's National Laboratory for Particle and Nuclear Physics)

MOPO017

The Upgraded Injector Cryostat-Module and Upcoming Improvements at the S-DALINAC

Since 1991 the superconducting Darmstadt linear accelerator S-DALINAC provides an electron beam of up to 130 MeV for nuclear and astrophysical experiments. The accelerator consists of an injector and four main linac cryostats, where the superconducting 3 GHz cavities are operated in a liquid helium bath at 2 K. For the injector upgrade program, the RF power delivered to the beam had to be increased from 500 W to 2 kW. Therefore, the coaxial power couplers have to be replaced by new waveguide couplers introducing only small transversal kicks to the beam. Consequently, modifications to the cryostat-module and had become necessary. We review on the design of the module and some interesting features and give details on the tuning of the newly built 20-cell cavities. The paper will close with an outlook towards the installation of an additional recirculation path planned in 2013.

R. Eichhorn, J. Conrad, F. Hug, M. Kleinmann, T. Kuerzeder, S.T. Sievers (TU Darmstadt)

MOPO018

Funding: This work is supported by the DFG through SFB 634

Minimizing Microphonics Detuning by Optimization of Stiffening Rings

Maintaining a constant gradient in a superconducting cavity requires can require much more power if the cavity is not driven on resonance. Significant cost savings in both power consumption and power supplies can be realized by minimizing the detuning of the cavity away from the drive frequency. One of the largest contributions to detuning is microphonics. In this paper, simulations of microphonics detuning by LHe bath pressure fluctuations in a Cornell ERL cavity are presented, and the effect of varying stiffening ring radius is investigated. The consequences of using optimal stiffening ring radii are explored as well, including bandwidth limitations in active detuning compensation due to mechanical resonances and requirements for the frequency tuner.

S. Posen, M. Liepe (CLASSE)

MOPO019

MOPO020

Nine-cell Elliptical Cavity Development at TRIUMF

V. Zvyagintsev, C.D. Beard, A. Grassellino, P. Kolb, R.E. Laxdal, D. Longuevergne, B.S. Waraich (TRIUMF, Canada's National Laboratory for Particle and Nuclear Physics) M. Ahammed (DAE/VECC) R.O. Bolgov, N.P. Sobenin (MEPhI) R. Edinger (PAVAC)

The superconducting e-Linac project at TRIUMF requires a new nine cell elliptical cavity at 1.3GHz of TESLA influenced design capable of providing a CW accelerating voltage of 10MV at 10mA of beam intensity. This corresponds to a challenging 100kW of beam loaded rf power and

a Beam Break-up (BBU) threshold in multi-pass mode of $R_d/Q \cdot QL = 10 \text{ MOhms}$. For this purpose we use two opposed CPI 60kW cw rated couplers. Another challenge is to provide HOM damping for the possibility of multi-pass ERL operation by means of end cell optimization and higher order mode (HOM) dampers. Results of the cavity design work including developments toward a passive HOM damper will be discussed.

MOPO021

Electromechanical Design of 704MHz β 0.65 SC Proton Cavity

H. Gassot, F.B. Bouly, G. Olry, S. Rousselot (IPN)

Within the framework of the EUCARD, IPN Orsay is in charge of design of a 704MHz elliptic superconducting cavity

for $\beta = 0.65$ high intensity proton linac in pulsed mode. This study offers a new option to replace the injector of the Large Hadron Collider at CERN with SPL (Superconducting Proton Linac) project. For this cavity's design, a compromise between the requirements of high technological performances and the constraint of the cavity's cost should be found. As middle beta elliptical cavity has a big ratio between equator radian and iris radian, the mechanical deformations generate important Lorentz forces detuning. As a consequence, the cavity wall thickness should be increased and one or two stiffening rings between cells are necessary. The additional cost should be imperatively minimized since more than fifty β 0.65 cavities are considered for SPL linac. To do these optimizations, the electromechanical calculations are performed via our simulation platform, which drives and links CATIA for CAD, Cast3m for mechanics and Opera3d for RF. The final design of cavity is presented in this paper.

Funding: European Coordination for Accelerator Research & Development (EuCARD)

MOPO022

Higher Order Mode Properties of Superconducting Two-Spoke Cavities

C.S. Hopper, S.J. Roof (ODU) J.R. Delayen (JLAB) R.G. Olave (Old Dominion University)

Multi-Spoke cavities lack the cylindrical symmetry that many other cavity types have, which leads to a more complex Higher Order Mode (HOM) spectrum. In

addition, spoke cavities offer a large velocity acceptance which means we must perform a detailed analysis of the particle velocity dependence for each mode's R/Q. We present here a study of the HOM properties of two-spoke cavities designed for high-velocity applications. Frequencies, R/Q and field profiles of HOMs have been calculated and are reported.

Low Temperature Test of a Low-Beta Elliptical Cavity for PEFP Linac Extension

For the future extension of the PEFP (Proton Engineering Frontier Project) proton linac, a study on the SRF technology has

H.S. Kim, Y.-S. Cho, H.-J. Kwon (KAERI)

been performed including a prototype cavity development to confirm the design of the cavity and fabrication procedures and to check the RF and mechanical properties of a low-beta elliptical cavity. The geometrical beta and resonant frequency of operating mode are 0.42 and 700 MHz, respectively. The cavity is a five-cell structure stiffened by double-ring structure to increase mechanical stability. For the vertical test of the cavity, RF system based on PLL (phase locked loop) has been prepared. If there is no magnetic shielding and operating temperature is 4.2 K, the required RF power to generate the design accelerating field of 8 MV/m is estimated to be about 320 W at critical coupling. In case single RF amplifier cannot deliver sufficient RF power, a coaxial type two-way RF combiner is under consideration. The details of the cavity test setup and results will be presented in this paper.

Funding: This work was supported by Ministry of Education, Science and Technology of the Korean Government.

MOPO023

Design of Single Spoke Resonators at Fermilab

Project X is based on a 3 GeV CW superconducting linac and is currently in the R&D phase awaiting CD-0 approval. The low-energy section of the Project X H⁻ linac (starting at 2.5 MeV) includes three

L. Ristori, S. Barbanotti, M.S. Champion, M.H. Foley, C.M. Ginsburg, I.G. Gonin, C.J. Grimm, T.N. Khabiboulline, N. Solyak, V.P. Yakovlev (Fermilab)

types of superconducting single spoke cavities operating at 325 MHz. The first three cryomodules will each house 7 SSR0 cavities at $\beta = 0.11$. The following two cryomodules will each contain 10 SSR1 cavities each at $\beta = 0.21$. The last four cryomodules will contain 11 SSR2 cavities each at $\beta = 0.4$. Single spoke cavities were selected for the linac in virtue of their higher r/Q values compared to standard Half Wave Resonator. Quarter Wave Resonators were not considered for such a high frequency. In this paper we present the decisions and analyses that lead to the final design of SSR0. Electro-magnetic and mechanical finite element analyses were performed with the purpose of optimizing the electro-magnetic design, minimizing frequency shifts due to helium bath pressure fluctuations and providing a pressure rating for the resonators that allow their use in the cryomodules.

Funding: Operated by Fermi Research Alliance, LLC under Contract No. DE-AC02-07CH11359 with the U.S. Department of Energy.

MOPO024

High-Frequency and Mechanical Basic Analysis of Conical Half-Wave Resonator

A cylindrical Half-Wave length Resonator is a proved superconducting structure In the low energy part of ac-

E.N. Zaplatin (FZJ) A. Kanareykin (Euclid TechLabs, LLC)

celerators. Accelerating efficiency in such resonator is limited by the peak RF magnetic field on the inner cavity surface. By an enlargement of the dome cavity volume containing RF magnetic field the cavity peak surface magnetic field is reduced. Additionally, this results in the power dissipation reduction. The paper reports results of cavity shape optimization and structural analysis of conical Half-Wave Resonators for $\beta=v/c=0.11$ and two resonance frequencies 325 MHz and 162.5 MHz. This Work is supported by the DOE SBIR Program, contract #DE-SC0006302.

MOPO025

MOPO026

 $\beta = 0.285$ Half-Wave Resonator for FRIB

P.N. Ostroumov, Z.A. Conway, R.L. Fischer, S.M. Gerbick, M.P. Kelly, A. Kolomiets, B. Mustapha, A. Ortega Bergado (ANL)

Isotope Beams (FRIB). The cavity design is based on recent advances in SRF technology for TEM-class structures being developed at ANL. Highly optimized EM parameters were achieved using an "hourglass" cavity shape for the HWR. This new design will be processed with a new HWR horizontal electropolishing system after all mechanical work on the cavity including the welding of the helium vessel is complete. Recently, this procedure was successfully tested on a quarter wave resonator developed for the ATLAS Upgrade which achieved peak surface fields of 70 MV/m and 10^5 mT. Following these results we propose to operate the HWR with a 2.6 MV accelerating voltage per cavity at the optimal ion velocity of $\beta = 0.285$. Fabrication of the cavity can be started immediately as soon as funding is available.

Funding: This work was supported by the U.S. Department of Energy, Office of Nuclear Physics, under Contract No. DE-AC02-06CH11357 and WFO 85Y64 Supported by Michigan State University

We have developed an optimized electromagnetic and mechanical design of a 322 MHz half-wave resonator (HWR) suitable for acceleration of ions in the post-stripper section of the Facility for Rare

MOPO027

Analysis of HOM Properties of Superconducting Parallel-Bar Deflecting/Crabbing Cavities

S.U. De Silva, M.H. Moore (ODU) A. Castilla (DCI-UG) S.U. De Silva, J.R. Delayen (JLAB)

compact design geometries. The 499 MHz deflecting cavity proposed for the Jefferson Lab 12 GeV upgrade and the 400 MHz crab cavity for the proposed LHC luminosity upgrade are two of the major applications. For high current applications the higher order modes must be damped to acceptable levels to eliminate any beam instabilities. The frequencies and R/Q of the HOMs and mode separation are evaluated and compared for different parallel-bar cavity designs.

The superconducting parallel-bar cavity is currently being considered for a number of deflecting and crabbing applications due to improved properties and

MOPO028

Design of CW Superconducting Buncher for RIKEN RI-Beam Factory

L. Lu (RIKEN) O. Kamigaito, N. Sakamoto, K. Suda, K. Yamada (RIKEN Nishina Center)

(RRC, fRC, IRC and SRC). There are two charge-stripping sections in this complex. One is located after the RRC ($\beta = 0.16$), and the other is after the fRC ($\beta = 0.32$). The stripping process causes an increase of the phase width of the beam in the following cyclotrons, which will be reduced by a longitudinal focusing device: a rebuncher. However, design of the rebuncher is challenging because the beam velocity is not so small and the required voltage is estimated to be as high as a few megavolts. We started the design study of the SRF resonator which works at the velocity of $\beta = 0.32$. Several types of the rf structure have been simulated in this initial design study: a quarter-wavelength resonator (QWR), half-wavelength resonator (HWR), double-spoke resonator, and half-H mode resonator. In addition, we examined the possibility of a new type of coupled TE-mode structure, which is expected to make the voltage distribution more uniform. Basic parameters are calculated and the feasibility is discussed in this paper.

In the RIKEN RI-Beam Factory (RIBF), very heavy ions such as uranium are accelerated with a cascade of a linac injector (RILAC2) and four booster cyclotrons

Some Concerns on the Development of Spoke Cavity

The design and optimization goal are re-considered based on the the construction and operation efficiency in the desired beta range. Some first order analytical methods as well as equivalent circuit model are applied to guide the design effort. Initial result of the EM design for the ESS requirement is reported.

F.S. He (PKU/IHIP) H. Wang (JLAB)

MOPO029

The sc cw -LINAC Demonstrator - First section of a sc cw -LINAC

The realisation of the first section of a new superconducting (sc) continuous wave (cw) LINAC is planned in 2013. The project is called "cw LINAC Demonstrator" and is financed by the Helmholtz Institute Mainz (HIM). The aim is a "full performance test" at GSI-HLI of a new 217 MHz sc CH-Cavity which is designed by the Institute of Applied Physics (IAP) of the University Frankfurt. According to an engineering study for the cryostat, a frame has been designed to support the cavity embedded by two sc solenoids. A nuclotron -suspension analog to the SIS-100 Magnets for FAIR is used, which nearly prevents the displacement of the components on the frame while cooling down. Another challenge is to reduce the magnetic field of the solenoid from 9.3 T to 50 mT at the cavity within some centimeters by moveable compensation -coils. This and other technical solutions in the cryogenic environment of the Demonstrator are presented.

V. Gettmann, M. Amberg, S. Jacke (HIM) K. Aulenbacher (IKP) W.A. Barth, S. Mickat (GSI) F.D. Dziuba, H. Podlech, U. Ratzinger (IAP)

MOPO030

Electro-Magnetic Optimization and Analyses of Etching for HIRFL Quarter-Wave Resonators

A superconducting accelerating section for SSC-linac system (injector into separated sector cyclotron) is under development at the HIRFL (heavy ion research facility of Lanzhou). Two types of superconducting quarter-wave resonators (81.25 MHz, optimum $\beta = 0.041$ and 0.085) will be used for acceleration to energies of up to 10 MeV per nucleon. The $\beta=0.041$ QWR works at the accelerating voltage of 0.75 MV and $\beta=0.085$ QWR works at 1.5 MV, in order to reach a record high performance, the EM design was carefully optimized for both cavities. A selected number of cavity geometry parameters were analyzed to see how they affect the electro-magnetic parameters of the cavity, and different influence levels of these geometry parameters are ranked. In this paper, we will also present how the etching thickness changes the frequency during the buffered chemical polishing processing, and the difference of the change for the two type cavities has been compared.

C. Zhang, W. Chang, Y. He, S.H. Zhang, H.W. Zhao (IMP)

MOPO031

MOPO032

Development of a Frequency Map for the WiFEL SRF Gun

R.A. Legg (JLAB) M.V. Fisher, K.J. Kleman (UW-Madison/SRC) T.L. Grimm, R. Jecks, B. Kuhlman (Niowave, Inc.)

SRF cavity design requires the integration of several different software and analytic tools to produce a cavity which, after production and cool down to liquid helium temperatures, has the correct resonant frequency. We describe a 'map' which starts with a cold cavity at the correct frequency and moves back through the series of production steps producing an expected resonant frequency at each step. For example, contributions to cavity deformation from vacuum and tuner loading are modeled in ANSYS and a piecewise linear fit is produced which is re-inserted into the SUPERFISH1 model to determine the new resonance point. We describe the steps and calculations used to develop the frequency map for the Wisconsin SRF electron gun and the specific initial cavity geometry.

1. J. H. Billen and L. M. Young, "POISSON/SUPERFISH on PC Compatibles" Proceedings of the 1993 Particle Accelerator Conference, Vol. 2 of 5, 790-792 (1993).

Funding: *The U of Wisc electron gun program is supported by DOE Award DE-SC0005264.

MOPO033

Design of Superconducting Multi-Spoke Cavities for High-Velocity Applications

C.S. Hopper, S.U. De Silva (ODU) J.R. Delayen (JLAB)

Superconducting spoke cavities have been designed and tested for particle velocities up to $\beta \sim 0.6$ and are currently being designed for velocities up to $\beta = 1$. We present the electromagnetic designs for two-spoke cavities operating at 325 MHz for $\beta = 0.82$ and $\beta = 1$.

MOPO034

Optimized RF Design of 704 MHz $\beta=1$ Cavity for Pulsed Proton Drivers

J. Plouin (CEA/IRFU) S. Chel, G. Devanz (CEA/DSM/IRFU)

The high energy part of the Superconducting Proton Linac (SPL) will be composed of two families of elliptical cavities, $\beta = 0.65$ and $\beta = 1$. This paper focuses on the $\beta = 1$, 5-cell cavity, whose RF design has been developed at CEA-Saclay in the frame of EUCARD (European Coordination for Accelerator Research & Development). These cavities are aimed to work in pulsed mode (50Hz, duty cycle 5%), with a beam current of 40 mA and RF peak power 1MW. Since these cavities should provide a challenging gradient of 25 MV/m, the RF design has been realized to optimize cavity efficiency and peak fields. The position of high power couplers has been determined to achieve the adequate external coupling, and the monopole High Order Modes have been identified and characterized. We have also carried out RF/mechanical simulations in order to optimize the mechanical behavior of cavity, in particular the Lorentz force detuning.

MOPO035

Structural Mechanical Analysis of Superconducting CH-Cavities

M. Amberg (HIM) K. Aulenbacher (IKP) W.A. Barth, S. Mickat (GSI) M. Busch, F.D. Dziuba, H. Podlech, U. Ratzinger (IAP)

The superconducting Crossbar-H-mode (CH)-structure has been developed and tested successfully at the Institute for Applied Physics (IAP) of Frankfurt University. It is a multi-gap drift tube cavity for the acceleration of protons and ions in the low and medium energy range based on the H210-mode. At present two types of superconducting CH-structures ($f = 325$ MHz, $\beta = 0.16$, seven cells and $f = 217$ MHz, $\beta = 0.059$, 15 cells) are under construction. For the geometrical design of superconducting cavities structural mechanical simulations are essential to predict mechanical eigenmodes and the deformation of the cavity walls due to bath pressure effects and the cavity cool-down. Therefore, several static structural and modal analyses with ANSYS Workbench have been performed. Additionally, a new concept for the dynamic frequency tuning including a novel type of a piezo based bellow-tuner has been investigated to control the frequency against microphonics and Lorentz force detuning.

Design Optimization of Spoke Cavity of Energy-Recovery Linac for Non-Destructive Assay Research

We are proposing non-destructive assay system of nuclear materials with laser Compton scattering combined with an energy-recovery linac (ERL) and a laser.

To construct this system for nuclear safeguards and security purpose, it is important to make the accelerating cavity small. The spoke cavity has advantages over the elliptical cavity to use for our proposing system. We are designing a spoke cavity favorable to compact cavity. Design optimization calculation of the spoke cavity shape is being carried out with 3D electro-magnetic field simulation code and generic algorithm. The results will be presented.

M. Sawamura, R. Hajima (JAEA) R. Nagai, N. Nishimori (JAEA/ERL)

MOPO036

Development of Superconducting CH Cavities

At present, two superconducting (sc) CH cavities are under development at the Institute for Applied Physics (IAP) of Frankfurt University. The construction of a sc 325 MHz CH cavity with 7 cells and an envisaged design gradient of 5 MV/m is almost finished. It is planned to test this cavity with beam at GSI Universal Accelerator (UNILAC), Darmstadt to show its performance as a candidate for the UNILAC upgrade. Furthermore, the 217 MHz CH structure with 15 accelerating cells and a real estate gradient of 5.1 MV/m will be the first cavity of the new sc continuous wave (cw) LINAC at GSI. This proposed cw LINAC is highly requested to fulfil the requirements of nuclear chemistry and especially for a competitive production of new Super Heavy Elements (SHE). To demonstrate the cavity capabilities under a realistic accelerator environment, a full performance test by injecting and accelerating a beam from the GSI High Charge Injector (HLI) is planned in 2013/14. The current status of both sc CH cavities is presented.

Funding: BMBF Contr. No. 06FY9089I, Helmholtz Institut Mainz (HIM), GSI

F.D. Dziuba, M. Busch, H. Podlech, U. Ratzinger (IAP) M. Amberg (HIM) K. Aulenbacher (IKP) W.A. Barth, S. Mickat (GSI)

MOPO037

Development of the Demountable Damped Cavity

We have designed a new HOM free cavity named Demountable Damped Cavity (DDC) as an ILC R&D. DDC has two design concepts. The first one is an axial symmetry to eliminate kick off effect by HOM coupler itself. DDC is applied coaxial structure along the beam axis to make strong coupling with HOM. HOM is damped on RF absorber at the end of coaxial waveguide and the accelerating mode is reflected by the choke filter mounted on the entrance of coaxial waveguide. The second concept is demountable structure which can make cleaning of end group easy in order to suppress the Q-slope problem at high field. MO sealing will be applied for the demountable joint. We have simulated the HOM damper structure, thermal structure, and the multipacting phenomena on single DDC. We have also simulated how DDC works on ICHIRO 9-cell cavity. Now we are fabricating single DDC. Cold test is also planned. In this paper, we will present the results of them.

T. Konomi (Sokendai) F. Furuta, K. Saito (KEK)

MOPO038

MOPO039

Low- β Triple Spoke Cavity Design Improvement for Proton Linac

H. Gassot, S. Bousson, G. Olry, S. Rousselot (IPN)

Within the framework of the EURISOL, IPN Orsay has proposed a 352MHz triple-spoke superconducting cavity: for the low energy section ($\beta = 0.3$) of high power proton linear accelerators. In terms of structure design, a triple-spoke superconducting cavity has a complicated geometry, 3D modelling is necessary. More, the design requires simulations which couple electromagnetism with mechanics. To perform these tasks, the mechanics simulation code CAST3M (Calcul et Analyse de Structure et Thermique par la méthode des Éléments Finis) has been linked to the electromagnetism code Opera3D via a dedicated platform, which has been developed for this purpose. This work allows the instantaneous passage from CAD (CATIA) design to mechanical calculations using Cast3m and electromagnetic simulations with Opera3D. As a consequence, the delay of design studies has been considerably reduced. The mathematical advances of the simulation platform are summarized. The electromagnetic and mechanical behaviours of the triple-spoke are presented and discussed in this paper.

Funding: EURISOL (European Isotope-Separation-On-Line Facility) supported by the 6th PCRD of the European Union

MOPO040

SRF Cavity Design for High Current Linacs

W. Xu, S.A. Belomestnykh, I. Ben-Zvi, R. Calaga, H. Hahn, E.C. Johnson, J. Kewisch (BNL)

A high current five-cell Nb superconducting cavity, called BNL3 cavity, was optimized and designed for the SPL and eRHIC. For the fundamental mode, the optimization process aimed at maximizing the R/Q of the fundamental mode and the geometry factor G under an acceptable RF field ratio level of B_{peak}/E_{acc} and E_{peak}/E_{acc} . For higher order modes, the optimization is to lower $(R/Q)_{ext}$ for dipole and quadrupole modes to suppress the beam-break-up (BBU). To extract the HOM power out of the cavity, the BNL3 cavity employs a larger beam pipe, allowing the propagation of HOMs, but not the fundamental mode. Six HOM couplers (three at each end) are used to extract large HOM power. To avoid the cross-talk between cavities, tapers are employed between the cavities. This paper presents the design of the BNL3 cavity, end groups and connection of cavities.

Funding: This work is supported by Brookhaven Science Associates, LLC under Contract No. DE-AC02-98CH10886 with the U.S. DOE.

MOPO041

Conceptual Design of the $\beta = 0.86$ Cavities for the Superconducting Linac of ESS

J. Plouin (CEA/IRFU) G. Devanz (CEA/DSM/IRFU)

CEA-Saclay is in charge of the design, the fabrication and the tests of the superconducting high beta cavities for the high energy part of the ESS (European Spallation Source) linac. This paper reports the actual status of the RF and mechanical design of these cavities. According to ESS specifications, these cavities will be 5-cells elliptical, with frequency 704 MHz and $\beta=0.86$. They will work in the pulsed mode, with a beam current initially equal to 50 mA. The target accelerating gradient is 18 MV/m on the linac, and 20 MV/m in vertical tests. For the RF design, the cavity efficiency and the peak fields were optimized, while the feasibility of the external coupling with RF power was taken into account. Attention was also paid to the HOM frequencies and impedances and to their future extraction. Coupled RF/mechanical FEM calculations have been carried out and the Lorentz detuning, critical for a pulsed mode cavity, is lowered by the insertion of stiffening rings.

Coupler Design for a Sample Host TE Cavity

A sample host niobium superconducting cavity operating at both TE012 and TE013 modes has been developed *. The cavity features a flat 3.75" diameter demountable bottom plate allowing RF testing of new materials such as Nb3Sn and MgB2. Since the surface resistance of the sample plates may vary a lot, an adjustable input coupler has been developed for this cavity. A hook shape coupler tip is designed and optimized to couple to the magnetic field of both transverse electric modes. The external Q factor, coupler heating considerations and 3D multipacting simulations using ACE3P will be discussed.

Y. Xie, M. Liepe (CLASSE)

* Y. Xie, J. Hinnefield, M. Liepe, "Design of a TE-type cavity for testing superconducting material samples", SRF2009, Berlin (2009)

Funding: Work supported by NSF and Alfred P. Sloan Foundation.

MOPO042

Mechanical Study of Superconducting Parallel-Bar Deflecting/Crabbing Cavities

The superconducting parallel-bar deflecting/crabbing cavities have improved properties compared to conventional cavity structures. It is currently being considered for number of applications. The mechanical design analysis is performed on two designs of the 499 MHz parallel-bar deflecting cavity for the Jefferson Lab 12 GeV upgrade. The main purpose of the mechanical study is to examine the structural stability of the cavities under the operating conditions in the accelerators. The study results will suggest the need for additional structural strengthening. Also the study results will help to develop a concept of the tuning method. If the cavity is to be installed in the accelerator it should satisfy a certain design parameters due to the safety requirements (for example, pressure vessel code) which are much severe condition than the actual operating condition.

H. Park, J.R. Delayen (JLAB) S.U. De Silva, H. Park (ODU)

MOPO043

Electromagnetic Design Optimization of a Half-Wave Resonator

The optimization procedure developed for the electromagnetic (EM) design of the ATLAS Upgrade quarter-wave resonator (QWR) [1] has now been successfully tested. The prototype QWR achieved record peak surface fields of 70 MV/m and 10^5 mT and is capable of providing 4.4 MV, far exceeding the design voltage of 2.5 MV. We have developed and applied a similar procedure for the EM design of a 322 MHz - beta ~ 0.29 half-wave resonator (HWR) for the medium energy section of the FRIB driver linac. The optimization path and the final results will be presented and discussed. The choice of aperture and its effect on the EM design parameters will be discussed. A comparison between equivalent half-wave and single-spoke resonators will also be presented. The transition from the electromagnetic model in MWS to the engineering model in Inventor was carefully studied as it may affect both the EM design parameters and the cavity fabrication.

B. Mustapha, Z.A. Conway, A. Kolomiets, P.N. Ostroumov (ANL)

* "Electromagnetic Optimization of a Quarter-Wave Resonator" B. Mustapha and P. Ostroumov, Proceedings of Linac-10, Tsukuba, Japan.

Funding: This work was supported by the U.S. Department of Energy, Office of Nuclear Physics, under Contract No. DE-AC02-06CH11357 and WFO 85Y64 Supported by Michigan State University

MOPO044

MOPO045

Coupled Electromagnetic and Mechanical Simulations for Half-Wave Resonator Design

J.P. Holzbauer (NSCL) J. Binkowski, A. Facco, M.J. Johnson, S.J. Miller, J. Popielarski, Y. Xu (FRIB)

Mechanical design of two Half-Wave Resonators (HWRs) at 322 MHz with optimum $\beta = v/c = 0.29$ and 0.53 is underway at Michigan State University (MSU).

These cavities are being designed for use in the Facility for Rare Isotope Beams (FRIB) driver linac. Part of this work has been the optimization of the mechanical properties to minimize Lorentz Force Detuning and helium bath pressure sensitivity while providing adequate tuning range. The simulation techniques used for this work and the resulting proposed cavity stiffening will be presented.

Funding: This material is based upon work supported by the U.S. Department of Energy Office of Science under Cooperative Agreement DE-SC0000661

MOPO046

Design of a 322 MHz $\beta=0.29$ Half Wave Resonator

J. Popielarski, J. Binkowski, C. Compton, A. Facco, J.P. Holzbauer, M. Leitner, S.J. Miller, Y. Xu (FRIB)

A medium velocity Half Wave Resonator (HWR) is in the final stages of design at Michigan State University (MSU) for use in the Facility for Rare Isotope Beams

(FRIB) driver linac. The cavity is being designed to deliver 1.9 MV accelerating voltage reliably, with on optimum $\beta=v/c=0.29$. The design effort optimizes the surface fields for reliable operation but also considers frequency stability and tunability altogether with straightforward fabrication and surface preparation procedures. The electromagnetic and mechanical design incorporate lessons learned from MSU developed 322 MHz HWR's for $\beta=0.53$, which has a similar shape.

Funding: This material is based upon work supported by the U.S. Department of Energy Office of Science under Cooperative Agreement DE-SC0000661.

MOPO047

HOM Cavity Design for the TRIUMF E-LINAC

P. Kolb, Y.-C. Chao, R.E. Laxdal, V. Zvyagintsev (TRIUMF, Canada's National Laboratory for Particle and Nuclear Physics)

The TRIUMF eLINAC, currently in its design phase, is a 50MeV electron linear accelerator and will be used for photo-fission to produce rare isotopes for experi-

ments. Future upgrade plans include an option to go to a recirculating LINAC to provide higher energies. This brings up the need to calculate the shunt impedances of higher order modes (HOM) to avoid beam instabilities and beam break up (BBU). The cavity design for a 9 cell cavity has to account for the limitations given by the desired beam current of 10mA and the layout of the recirculating path to create a high enough BBU limit. Work on the cavity design to accommodate for the HOM requirements will be presented as well as a way to reduce the shunt impedance by the use of ring dampers will be discussed.

The Dipole Steering Effect With New Ways: Shifting Inside and Outside Pole of QWR Cavity Method

In our project KoRIA (Korea Rare Isotope Accelerator), we will use QWR cavity in the ISOL Linac for the acceleration of RI

J.D. Jeong (SKKU)

beam which is from the RFQ with energy of 0.3 MeV to the 18 MeV output for further use of experiment and re-acceleration of IFF Linac. Several studies about QWR cavity, however, finds out that due to the asymmetric geometric characteristic of QWR cavity there will be un-welcome transverse forces which take a role of increasing transverse emittance within the acceleration gaps. This quadrupole terms in the transverse Lorentz force which can cause appreciable emittance growth is known as dipole steering effect. On the other hands, there has been a lot of effort to compensate this dipole steering effect such as tilting beam pipe ends, shaping beam pipe like a racetrack and shifting beam axis, etc. During the process of conceptual design of KoRIA project, we have studied about the QWR cavity and tried to compensate the dipole steering effect. In this paper we will discuss about what we did to eliminate the dipole steering effect with new ways: shifting inside and outside pole of QWR cavity method.

MOPO048

Electro-Magnetic Optimization of a Quarter-Wave Resonator

The Institute of Modern Physics (IMP) has been trying to design a highly effective accelerating quarter-wave resonator

C. Zhang, Y. He, S.H. Zhang, H.W. Zhao (IMP)

(QWR) cavity which can work at a record high voltage of 2.5 MV with as low as possible peak surface electromagnetic (EM) fields. In the cavity design, we set the goal of the optimization to minimize the peak magnetic and electric fields while still keeping good values for the R over Q and the geometric factor. Take the design of the QWR cavity with frequency of 81.25 MHz and beta of 0.085 for example, from a regular cylindrical shaped inner and outer conductor, the optimization has led them to a conic inner conductor and an elliptic outer conductor. In this paper, we will present how the cavity geometry parameters evolve in order to approach optimal EM design. The optimization also includes the internal drift tube face angle required for beam steering correction.

MOPO049

Design of a 1500 MHz Bunch Lengthening Cavity for NSLS-II

The NSLS-II is a new third generation light source being constructed at > BNL. In order to increase the Touschek lifetime and third harmonic bunch > lengthening

J. Rose, N.A. Towne (BNL) C.H. Boulware, T.L. Grimm (Niowave, Inc.)

cavity is required. A 1500 MHz passive third harmonic cavity has > been designed and fabricated. It is a coupled two-cell HOM damped SRF cavity > that can provide 1 MV of voltage in a single cryomodule. The two cell design > allows for a single tuner mechanism outside the cryostat while the room > temperature ferrite HOM dampers provide damping of all but the fundamental > zero and pi modes. Since the unwanted zero mode is strongly coupled to the > pi mode it tracks the pi mode tuning which is required for the beam induced > excitation. The design allows for the tuning of the pi mode between minimum > and required field excitation while keeping the zero mode excitation below > allowable limits. Design and initial cold test results are presented.

MOPO050

MOPO051

Design for Manufacture of a Superconducting Half Wave Resonator $\beta=0.53$

S.J. Miller, J. Binkowski, M.J. Johnson, Y. Xu (FRIB)

University (MSU) for use in a heavy ion linac. The cavity is designed to provide 3.7 MV of accelerating voltage at an optimum $\beta = v/c = 0.53$. The cavity was designed for manufacturing recommendations based on previous design as well as for stiffness, tunability, assembly, and cleaning. Finite Element Analysis simulations were performed for modal analysis, bath pressure sensitivity, Lorentz Force detuning, tuner stiffness, and tuning range. Industry prototyping is planned to confirm tolerances and fabrication processes. A tuner prototype has also been built. The helium vessel and power coupler have been designed and fabricated and will be adapted to the new cavity design.

Funding: This material is based upon work supported by the U.S. Department of Energy Office of Science under Cooperative Agreement DE-SC0000661.

A medium velocity half wave resonator has been designed at the Facility for Rare Isotope Beams (FRIB) at Michigan State

MOPO052

Studies on a Plunger Tuner System for a Double Spoke Cavity

J.L. Munoz, J. Feuchtwanger, J. Verdu (ESS-Bilbao) F.J. Bermejo (Bilbao, Faculty of Science and Technology) V. Etxebarria, J. Portilla (University of the Basque Country, Faculty of Science and Technology) N. Garmendia (ESS Bilbao)

compatible with the ESS project spoke cavities. Different tuning systems will be studied for spoke resonators, and one of them is the use of plunger tuners. In this paper, a study of this kind of tuners on DSR cavities is presented, including electromagnetic and thermal simulations. Also, for different R&D activities related to spoke cavities, ESS-Bilbao designed and built a beta 0.39 DSR model in aluminum. This model can be used to install a plunger tuner system and test LLRF devices at room temperature.

ESS-Bilbao proton linac warm section will end at 50 MeV. A cryomodule with two double spoke cavities, currently in R&D stage, will be tested at that energy. The two spoke cavity prototypes to be built (geometric beta 0.54) will be fully

MOPO053

Designs of Superconducting Parallel-Bar Deflecting Cavities for Deflecting/Crabbing ApplicationsJ.R. Delayen, A. Castilla, S.U. De Silva, M.H. Moore (ODU)
J.R. Delayen (JLAB)

being considered for a number of applications. The new parallel-bar design with curved loading elements and circular or elliptical outer conductors have improved properties compared to the designs with rectangular outer conductors. We present the designs proposed as deflecting cavities for the Jefferson Lab 12 GeV upgrade and for Project-X and as crabbing cavities for the proposed LHC luminosity upgrade and electron-ion collider at Jefferson Lab.

The superconducting parallel-bar cavity is a deflecting/crabbing cavity with attractive properties, compared to other conventional designs, that is currently

Superconducting 112 MHz QWR Electron Gun

Brookhaven National Laboratory and Niowave, Inc. have designed and fabricated a superconducting 112 MHz quarter-wave resonator (QWR) electron gun. The first cold test of the QWR cryomodule has been completed at Niowave. The

paper describes the cryomodule design, presents the cold test results, and outline plans to upgrade the cryomodule. Future experiments include studies of different photocathodes and use for the coherent electron cooling proof-of-principle experiment. Two cathode stalk options, one for multi-alkali photocathodes and the other one for a diamond-amplified photocathode, are discussed.

Funding: Work is supported at BNL by BSA, LLC under U.S. DOE Contract No. DE-AC02-98CH10886, at Stony Brook University by U.S. DOE grant DE-SC0005713, at Niowave by U.S. DOE SBIR contract No. DE-FG02-07ER84861

S.A. Belomestnykh, I. Ben-Zvi, X. Chang, T. Rao, J. Skaritka, R. Than, Q. Wu (BNL) C.H. Boulware, T.L. Grimm, B. Siegel, M.J. Winowski (Niowave, Inc.) T. Xin, L. Xue (Stony Brook University)

MOPO054

Superconducting Resonator Production for Ion Linac at Michigan State University

Superconducting quarter-wave resonators and half-wave resonators are being prototyped and fabricated at Michigan State University (MSU) in effort to support the Facility for Rare Isotope Beams (FRIB) project. FRIB requires a 200 MeV per nucleon driver linac, operating 345 resonators at two frequencies (80.5 and 322 MHz) and four betas (0.041, 0.085, 0.29, and 0.53). FRIB cavity development work is underway, with the prototyping of all four resonators, including helium vessel design, stiffening strategy, and tuner interface. In addition, the acquisition strategy for FRIB resonators is being finalized, and the technology transfer program is being initiated. The status of the resonator production effort will be presented in this paper, including an overview of the acquisition strategy for FRIB.

Funding: Work supported by US DOE Cooperative Agreement DE-SC0000661 and Michigan State University

C. Compton, A. Facco, W. Hartung, M. Hodek, M.J. Johnson, T. Kole, M. Leitner, F. Marti, D. R. Miller, S.J. Miller, J. Popielarski, L. Popielarski, J. Wei, K. Witgen, J. Wlodarczak (FRIB)

MOPO055

Beam Break Up Studies for Cornell's Energy Recovery Linac

New results are presented of beam break-up (BBU) studies for the Cornell ERL main linac. Previously, a 1.3 GHz main linac 7-cell cavity was optimized to maximize the BBU current through the accelerator. This work realistically models the ERL main linac cavity shapes by taking into account small machining variations in ellipse dimensions. Cavity shapes were simulated with uniformly distributed errors, and their higher-order mode spectrum computed. The strongest higher-order modes can cause resonant excitations in the beam which can lead to beam loss. The threshold current through the accelerator is determined resulting from a linac comprised of cavities with machining variations using particle tracking and demonstrates that the threshold current is well above the 100 mA design goal for the Cornell's Energy Recovery Linac.

N.R.A. Valles, D.S. Klein, M. Liepe (CLASSE)

MOPO056

MOPO0057

Coupler Kick Studies in Cornell's 7-Cell Superconducting Cavities

N.R.A. Valles, M. Liepe, V.D. Shemelin (CLASSE)

Cornell is developing a 5 GeV Energy Recovery Linac operating at 100 mA with very small emittances (~ 30 pm at 77 pC bunch charge) in the horizontal and vertical directions. We investigate the effect of the fundamental RF power couplers of the main linac SRF cavities on the beam using the ACE3P software package. The cavities in the ERL main linac will be operated at very high loaded quality factors of up to $6.5 \cdot 10^7$, corresponding to a full bandwidth of only 20 Hz. Cavity microphonics will detune the cavities by more than one bandwidth during operation, thereby causing a time dependent change of the coupler kick in addition to its fast oscillation at the RF frequency. In order to investigate the dependence of the coupler kick on the cavity frequency, we calculate the coupler kick given to the beam for the case of a detuned RF cavity. We show that a compensation stub geometry located opposite to the input coupler port can be optimized to reduce the overall kick given to the beam and the emittance growth caused by its time dependence.

Cornell is developing a 5 GeV Energy Recovery Linac operating at 100 mA with very small emittances (~ 30 pm at 77 pC bunch charge) in the horizontal and vertical directions. We investigate the effect of the fundamental RF power couplers of the main linac SRF cavities on the beam using the ACE3P software package. The cavities in the ERL main linac will be operated at very high loaded quality factors of up to $6.5 \cdot 10^7$, corresponding to a full bandwidth of only 20 Hz. Cavity microphonics will detune the cavities by more than one bandwidth during operation, thereby causing a time dependent change of the coupler kick in addition to its fast oscillation at the RF frequency. In order to investigate the dependence of the coupler kick on the cavity frequency, we calculate the coupler kick given to the beam for the case of a detuned RF cavity. We show that a compensation stub geometry located opposite to the input coupler port can be optimized to reduce the overall kick given to the beam and the emittance growth caused by its time dependence.

MOPO0058

Analysis of Beam Damage to FRIB Driver Linac

Y. Zhang, D. Stout, J. Wei (FRIB)

Component damage caused by particle beam is an important issue in the design of a high power accelerator, particularly a superconducting linac. The FRIB driver linac must deliver a beam on target of approximately 1 mm in diameter, increasing beam energy density significantly compared to other SRF linacs. Because dE/dx of heavy ion beam is several ten times larger than proton or electron beam, the situation is more severe: at full power, 400 kW, a uranium beam may cause accelerator structure damage in less than $40 \mu\text{s}$. A fast response machine protection system is necessary, in addition to special protection design, very careful linac beam tuning and operation. In this paper, temperature rise of niobium and stainless steel at different beam incident angles are compared, and thermal stress analyzed for nominal FRIB beam at different energy. Protection designs are also briefly discussed.

Component damage caused by particle beam is an important issue in the design of a high power accelerator, particularly a superconducting linac. The FRIB driver linac must deliver a beam on target of approximately 1 mm in diameter, increasing beam energy density significantly compared to other SRF linacs. Because dE/dx of heavy ion beam is several ten times larger than proton or electron beam, the situation is more severe: at full power, 400 kW, a uranium beam may cause accelerator structure damage in less than $40 \mu\text{s}$. A fast response machine protection system is necessary, in addition to special protection design, very careful linac beam tuning and operation. In this paper, temperature rise of niobium and stainless steel at different beam incident angles are compared, and thermal stress analyzed for nominal FRIB beam at different energy. Protection designs are also briefly discussed.

Funding: This material is based upon work supported by the U.S. Department of Energy Office of Science under Cooperative Agreement DE-SC0000661.

MOPO0059

Design and Test of HOM Coupler for High Current SRF Cavity

W. Xu, S.A. Belomestnykh, I. Ben-Zvi, H. Hahn, E.C. Johnson (BNL)

Damping higher order modes (HOMs) significantly to avoid beam instability is a challenge for the high current Energy Recovery Linac-based eRHIC at BNL. To avoid the overheating effect and high tuning sensitivity, current, a new band-stop HOM coupler is being designed at BNL. The new HOM coupler has a bandwidth of tens of MHz to reject the fundamental mode, which will avoid overheating due to fundamental frequency shifting because of cooling down. In addition, the S21 parameter of the band-pass filter is nearly flat from first higher order mode to 5 times the fundamental frequency. The simulation results showed that the new couplers effectively damp HOMs for the eRHIC cavity with enlarged beam tube diameter and 2 120° HOM couplers at each side of cavity. This paper presents the design of HOM coupler, HOM damping capacity for eRHIC cavity and prototype test results.

Damping higher order modes (HOMs) significantly to avoid beam instability is a challenge for the high current Energy Recovery Linac-based eRHIC at BNL. To avoid the overheating effect and high tuning sensitivity, current, a new band-stop HOM coupler is being designed at BNL. The new HOM coupler has a bandwidth of tens of MHz to reject the fundamental mode, which will avoid overheating due to fundamental frequency shifting because of cooling down. In addition, the S21 parameter of the band-pass filter is nearly flat from first higher order mode to 5 times the fundamental frequency. The simulation results showed that the new couplers effectively damp HOMs for the eRHIC cavity with enlarged beam tube diameter and 2 120° HOM couplers at each side of cavity. This paper presents the design of HOM coupler, HOM damping capacity for eRHIC cavity and prototype test results.

Funding: This work is supported by Brookhaven Science Associates, LLC under Contract No. DE-AC02-98CH10886 with the U.S. DOE.

Using Cavity Higher Order Modes for Beam Diagnostics in Third Harmonic 3.9 GHz Accelerating Modules

An international team is currently investigating the best way to use cavity Higher Order Modes (HOM) for beam diagnostics in 3.9 GHz cavities. HOMs are excited by charged particles when passing through an accelerating structure. Third harmonics cavities working at 3.9 GHz have been installed in FLASH and will be installed in the European XFEL to help with the bunch energy profile. The proof-of-principle of using HOMs for beam monitoring has been made at FLASH in the TESLA 1.3 GHz cavities. Since the wakefields generated in the 3.9 GHz cavities are higher, their impact on the beam should be particularly taken care of. Therefore our target is to monitor HOMs and minimize them by aligning the beam on the cavity axis. The difficulty is that, in comparison to the 1.3 GHz cavities, the HOM-spectrum is very crowded, making it difficult to identify individual modes. Also, most modes propagate through the whole cryo-module containing several cavities, making it difficult to measure local beam properties. In this paper the results of the studies made in order to identify the frequency range best suited for beam monitoring will be shown and the specs for the HOM-electronics will be discussed.

N. Baboi, P. Zhang (DESY) R.M. Jones, I.R.R. Shinton (UMAN)

Funding: This work is supported in part by the European Commission under the FP7 Research Infrastructures project EuCARD, grant agreement 227579.

MOPO060

Effects of Elliptically Deformed Cell Shape in the Cornell ERL Cavity

The Cornell ERL cavity is optimized to minimize the dipole mode BBU parameters to achieve the required high beam current (100mA). Deformations due to errors in fabrication and tuning of the accelerating mode can result in a cavity shape different from the ideal. In elliptically deformed cells, this can cause dipole mode frequency spread and splitting of the mode polarizations leading to an x-y mode coupling. To investigate these effects, we use a mesh distortion technique to generate an elliptically deformed cell cavity model as a base for studying random imperfections. Simulation results from the eigensolver Omega3P of one hundred randomly elliptically deformed cell cavities covering the first three dipole bands will be presented. The results will be used as input to the beam tracking code BMAD to calculate the impact of such imperfections on the dipole mode BBU parameters.

L. Xiao, K. Ko, K.H. Lee, C.-K. Ng (SLAC) M. Liepe, N.R.A. Valles (CLASSE)

MOPO061

BEPCII Superconducting RF System Operation Status

Two KEK-B type 500MHz Superconducting cavities have been used in BEPCII project since the end of 2006. All the maximum RF voltages have been over 1.65MV under the operation with beam power of 100 kW and beam current of 1.89GeV@800mA. During the physics collision mode operation, there is a strange phenomenon of helium gas pressure increasing with the beam current going up, which is dangerous to both cavity and cold box of cryogenics system. To search the unknown heating source, several beam tests had been made, which are HOMs power measurement, contrast of the RF power influence of coaxial coupler with Synchrotron Radiation operation mode, and the beam synchrotron light influence in different beam orbits.

Y. Sun, J.P. Dai, T.M. Huang, G. Li, Z.Q. Li, Q. Ma, W.M. Pan, P. Sha, G.W. Wang, Q.Y. Wang (IHEP Beijing)

MOPO062

MOPO063

HOM Measurements with Beam at the Cornell Injector Cryomodule

S. Posen, M. Liepe (CLASSE)

The Cornell ERL injector prototype is undergoing commissioning and testing for running unprecedented currents in an electron cw injector. This paper discusses preliminary measurements of HOMs in the injector prototype's superconducting RF cryomodule. These include HOM spectra up to 30 GHz measured via small antennae located at the HOM beam line absorbers between the SRF cavities. The spectra are compared at different beam currents and repetition rates. The shape of the spectra are compared to ABCI simulations of the loss factor spectrum of the cryomodule beam line. The total HOM power dissipated in the HOM loads was also measured with beam on, which allowed for an estimate of the loss factor. This measurement was accomplished via temperature sensors on the loads, calibrated to input power by heaters on the loads.

The Cornell ERL injector prototype is undergoing commissioning and testing for running unprecedented currents in an

MOPO064

Adaptive Lorentz Force Detuning Compensation in the ILC S1-G Cryomodule at KEK

W. Schappert, R.V. Pilipenko, Y.M. Pischalnikov (Fermilab) H. Hayano, E. Kako, S. Noguchi, N. Ohuchi, Y. Yamamoto (KEK)

The recent tests of the S1-Global cryomodule at KEK provided a unique opportunity to compare the performance of four different styles of 1.3 GHz SRF cavities and tuners under similar operating conditions. Results of adaptive LFD compensation at gradients of up to 35 MV/m for DESY/Saclay, FNAL/INFN and KEK cavity/tuner designs are compared.

The recent tests of the S1-Global cryomodule at KEK provided a unique opportunity to compare the performance of four different styles of 1.3 GHz SRF cavities

MOPO065

Systems Testing of Cryomodules for an Ion Reaccelerator Linac

J. Popielarski, S. Bricker, A. Facco, M. Hodek, J.P. Holzbauer, D. Leitner, D. Morris, S. Nash, D. Norton, G. Perdikakis, N.R. Usher, N. Verhanovitz, J. Wlodarczak (FRIB)

Michigan State University is developing, testing, and commissioning cryomodules for a superconducting linac to be used for the reacceleration of exotic ions (ReA). The first stage of ReA will accelerate ions from 0.3MeV/u to 3MeV/u for heavy ions and up to 6MeV/u for light ions. The first two cryomodules contain a total of seven quarter-wave resonators for $\beta = 0.041$. A total of five superconducting solenoids (9 T) are interspersed between resonators for focusing. The cryomodules have been fabricated and installed, with testing underway. The third cryomodule (requiring eight QWRs for $\beta = 0.085$ and three solenoids) is being fabricated. Experience so far with system performance of the cryomodules will be described in this paper. Topics will include cavity performance, magnetic shielding, microphonics, cavity tuning, input coupler performance, and thermal loads.

Michigan State University is developing, testing, and commissioning cryomodules for a superconducting linac to be used for the reacceleration of exotic ions (ReA). The first stage of ReA will accelerate ions

Funding: This material is based upon work supported by the U.S. Department of Energy Office of Science under Cooperative Agreement DE-SC0000661.

MOPO066

SCREAM – Modified Code SCREAM to Simulate the Acceleration of a Pulsed Beam Through the Superconducting Linac

Y.I. Eidelman, S. Nagaitsev, N. Solyak (Fermilab)

The code SCREAM – SuperConducting Relativistic particle Accelerator siMulation was significantly modified and improved. Some misprints in the formulae used have been fixed and a more realistic expression for the vector sum introduced. A friendly GUI allows the various parameters of the simulated problem easily and quickly to be changed. Effective control of various output data is provided. A change of various parameters during the simulation process is controlled by plotting the corresponding graphs “on the fly”. A large collection of various graphs is used to illustrate the results.

The code SCREAM – SuperConducting Relativistic particle Accelerator siMulation was significantly modified and improved.

CW Measurements of Cornell LLRF System at HoBiCaT

In Energy Recovery Linacs, such as the Cornell ERL or BERLinPro, the main linac cavities are operated in CW at low beam-loading. The choice of the external Q is given by two competing factors: The

achievable field stability and the maximum provided RF power. To determine the optimum external Q, LLRF measurements with the Cornell system were performed at HoBiCaT to study the field stability at given microphonics detuning of a TESLA cavity for different gain settings and external Q values. Stable operation at external Q up to $2 \cdot 10^8$ was demonstrated with field's phase stability of 0.02 degrees.

Funding: Work funded by the Bundesministerium für Bildung und Forschung and Land Berlin.

A. Neumann, W. Anders, R. Goergen, J. Knobloch, O. Kugeler (HZB) S.A. Belomestnykh (BNL) J. Dobbins, R.P.K. Kaplan, M. Liepe, C.R. Strohmman (CLASSE)

MOPO067

Reliability Improvements of the Diamond Superconducting Cavities

For successful operation of superconducting cavities in light sources, high reliability and minimal beam losses are essential. Diamond started operation with

users in January 2007 and since then, the Diamond storage ring superconducting cavities have been the largest single contributor to unplanned beam trips. We have dedicated extensive effort to improve our data acquisition, numerical modelling and fault analysis to improve our understanding of the main causes of the trips and how to prevent trips or reduce their frequency. In the past seven months, the performance of the cavities has improved significantly. We present here our analysis of some of the trips and their underlying causes and discuss improvements carried out.

P. Gu, M. Jensen, M. Maddock, P.J. Marten, S.A. Pande, S. Rains, A.F. Rankin, D. Spink, A.V. Watkins (Diamond)

MOPO068

Operation Status of SRF System at SSRF

SSRF has been open to users with 3.5GeV 200mA beam current in decay mode since April, 2009. The Superconducting Radio-Frequency system runs stably and reliably to support the operation of the light source with high performance. There still

however happened some kinds of trips from cavities, RF power sources, DLLRF and the utility system. Several times of cavity trips brought by cryogenic system breakdown have been treated correctly without any harmful damage to superconducting modules, and the SRF system was recovered as soon as cryogenic system was ready to keep the light source operation. Here the operation status of SRF system will be reported and methods to solve various kinds of trips from SRF system will be discussed.

H.T. Hou, Z.Q. Feng, J.F. Liu, C. Luo, Z.Y. Ma, D.Q. Mao, K. Xu, Zh.G. Zhang, S.J. Zhao, Y.B. Zhao (SINAP) **H.T. Hou**, Z. Li, X. Zheng (Shanghai KEY Laboratory of Cryogenics & Superconducting RF Technology)

MOPO069

Preliminary Test Results from 650 MHz Single Cell Medium Beta Cavities for Project X

P. Kneisel, A. Burrill, P. Kushnick, F. Marhauser, R.A. Rimmer (JLAB)

We have fabricated two single cell 650 MHz cavities of a JLab design [1], for possible project X application. Both cavities were manufactured at Jlab from

RRR>250 niobium sheet of 4 mm thickness using standard techniques such as deep drawing, EBW, BCP, hydrogen degassing heat treatment, high pressure ultrapure water rinsing and clean room assembly. A detailed description of the design and fabrication procedures is forthcoming [2]. Initially cavity #1 was – after final surface treatment by bcp – measured without any provisions for stiffening. As expected, the pressure sensitivity and the Lorentz Force detuning coefficients were quite high; however, the RF performance was very encouraging: the cavity exhibited a Q-value $> 10^{11}$ at 1.6K, corresponding to a residual resistance of < 1.5 nOhm. The initial gradient was limited to $E_{acc} \sim 18$ MV/m, limited by field emission. In a subsequent test, we are re-rinsing the cavity and are making provisions for stiffening up the cavity. By the time of this writing, this test is in progress; the results will be reported at this conference as well as results from the second cavity.

[1] F. Marhauser, JLab-TN-10-043

[2] F. Marhauser et al; IPAC 2011 to be published

Funding: This manuscript has been authored by Jefferson Science Associates, LLC under U.S. DOE Contract No. DE-AC05-06OR23177.

MOIOC — Hot Topics

Source of Quench Producing Defects

Recent efforts in pushing the performance of superconducting RF niobium cavities for the International Linear Collider have resulted in two-fold progresses: reduced field emission and improved quench limit in real 9-cell cavities. RF testing at cryogenic temperatures assisted with quench-detection instrumentation reveals that quench happens often times at highly localized areas inside or near the equator weld of a cavity cell, which is also the high surface magnetic field region. High-resolution optical inspection of the identified quench location makes it possible to correlate the cavity quench limit with certain types of defects. Several sources of quench producing defects are being explored. We will discuss the experimental evidence in supporting each of these sources. We will also discuss the methods of curing or preventing these defects for improved gradient limit and reduced gradient spread.

HOT TOPIC

TUIOA — New Materials/Techniques

TUIOA01

Athmospheric Surface Treatments to SC cavities

V. Palmieri, A.A. Rossi (INFN/LNL) D. Rizzetto (Univ. degli Studi di Padova)

V. Palmieri, D. Rizzetto, A.A. Rossi - Laboratori Nazionali di Legnaro and University of Padua After an obsessive search for the cleanest ultrahigh vacuum for

preparing niobium films, niobium nitride or A15 compounds, we have discovered that high purity sharp transition superconducting films are obtainable even without the need of vacuum by the help of atmospheric plasma torches, and not only. Atmospheric plasma treatments have already shown that can effectively contribute to the cavity cleaning. However at the moment we have set up a method for the obtainement of high purity niobium nitride without the use of vacuum pumps

TUIOA02

Multilayer Coatings: Opportunities and Challenges.

A.V. Gurevich (Old Dominion University)

The use of multilayer coatings may enable significant increase of the breakdown fields or operating temperatures of

SRF cavities by utilizing materials with the thermodynamic critical field H_c higher than $H_c = 200$ mT for Nb. However, such coating materials have shorter coherence length so the significant effects of impurities or grain boundaries on the surface resistance should be understood. In this talk I'll analyze the dynamics of penetration of vortices along grain boundaries and dissipation in a thin film coating in strong rf fields. I'll also discuss the role of impurities, in particular their contribution to the nonlinear Meissner effect which affects the surface resistance in the dirty limit. And finally I'll discuss the nonlinear response in two-band superconductors like MgB2 in which strong rf fields can cause decoupling of bands at fields $H < H_c$, which can contribute to the high-field Q slope.

Funding: DOE, Argonne National Lab. Award #313641

TUIOA03

Magnetic Screening of NbN Multilayers Samples

C.Z. Antoine (CEA/DSM/IRFU) A. Andreone (Naples University Federico II) Q. Famery, J. Leclerc (CEA/IRFU) G. Lamura (CNR-INFN-LAMIA) J.C. Villegier (CEA/INAC)

In 2006 Gurevich proposed to use nanoscale layers of superconducting materials with high values of $H_c > H_c$ (Nb) for magnetic shielding of bulk niobium to increase the field in Nb RF cavities. We

have deposited high quality "model" samples on monocrystalline sapphire substrates. A 250 nm layer of niobium figures the bulk Nb. It was coated with a single or multiple stacks of NbN layers (25 nm or 12 nm) separated by 15 nm MgO barriers, and characterized by X-rays reflectivity and DC transport measurements. DC or AC measurement of H_{C1} is an important tool for multilayers evaluation during the sample optimization phase. A clear increase of H_{C1} at low frequency is a promising indication since H_{C1} is expected to be higher in RF. We have measured the first magnetic penetration field H_P ($\sim H_{C1}$) on DC magnetization curves in a SQUID system. H_P of NbN covered samples is increased compared to Nb alone. We have also developed a set-up that allows measuring H_{C1} over a large range of field and temperature with a local probe method based on 3rd harmonic analysis. We have confirmed the screening behavior of a single 25 nm NbN layer placed on the top of a thick Nb layer.

MgB₂ Thin Film Studies

Demonstrating the idea of enhancing achievable surface magnetic field by coating multilayer thin film superconductors proposed by Gurevich is the main objective. DC magnetization measurements of 500 nm and 300 nm MgB₂ films coated on Sapphire showed an increase in the lower critical magnetic field (B_{c1}) compared to that of bulk. Also, the B_{c1} of a 300 nm film showed >200 mT at 4.5 K, which is >25 % higher than that of Nb (~145 mT). RF measurements using a 11.4 GHz pulsed Klystron and a TE₀₁₃-like mode hemispherical copper cavity with a 2-inch (50.8 mm) diameter sample, however, have shown a low quenching field of 42 mT at 4 K. From detailed data analyses together with the data on Nb quench fields these quenches were found to be thermal, not magnetic, due to a high RF resistance caused by inter-diffusion of coated materials at the interfaces. Additionally, recent results of RF surface resistance at 7.5 GHz using a calorimetric technique at JLab will also be shown.

T. Tajima, L. Civale, N.F. Haberkorn, R.K. Schulze (LANL) V.A. Dolgashev, J. Guo, D.W. Martin, S.G. Tantawi, C. Yoneda (SLAC) H. Inoue, **T. Tajima** (KEK) A. Matsumoto, E. Watanabe (NIMS) B. Moeckly (STI) M.J. Pellin, Th. Proslir (ANL) B. Xiao (JLAB)

Funding: This work is supported by the DOE Office of Nuclear Physics.

TUIOA04

The Superheating Field of Niobium: Theory and Experiment

This study discusses the superheating field of Niobium, a metastable state, which sets the upper limit of sustainable magnetic fields on the surface of a superconductors before it transitions into the normal conducting state. Current models for the superheating field are discussed, and experimental results are presented for niobium obtained through pulsed, high power measurements performed at Cornell. Material preparation is also shown to be an important parameter in exploring other regions of the superheating field, and fundamental limits are presented based upon these experimental and theoretical results.

N.R.A. Valles, M. Liepe (CLASSE)

TUIOA05

Deposition of Niobium and Other Superconducting Materials With High Power Impulse Magnetron Sputtering: Concept and First Results

Niobium coatings on copper cavities have been considered as a cost-efficient replacement of bulk niobium RF cavities, however, coatings made by magnetron sputtering have not lived up to high expectations. Energetic condensation of niobium films from the plasma phase has been tried using filtered cathodic arc plasmas, and promising RRR values were recently demonstrated. High power impulse magnetron sputtering (HIPIMS) is a promising emerging coatings technology which combines magnetron sputtering with a pulsed power approach. The magnetron is turned into a metal plasma source by using very high peak power density of ~ 1 kW/cm². In this contribution, the cavity coatings concept with HIPIMS is explained. A system with two cylindrical, movable magnetrons was set up with custom magnetrons small enough to be inserted into 1.3 GHz cavities. Preliminary data on niobium HIPIMS plasma and resulting coatings are presented. The HIPIMS approach has the potential to be extended to film systems beyond niobium, including other superconducting materials and/or multilayer systems.

A. Anders, S. Lim, R. Mendelsberg, A.V. Nollau, J.G. Wallig (LBNL)

Funding: This work was initially supported by an LDRD grant of Lawrence Berkeley National Laboratory, and by the Office of High Energy Physics, U.S. Department of Energy, under Contract No. DE-AC02-05CH11231.

TUIOA06

TUIOB — New Materials/Techniques

TUIOB01

Energetic Condensation Growth of Nb Films

M. Krishnan, C. James, E.F. Valderrama (AASC) P. Maheshwari, F.A. Stevie (NCSU AIF) H.L. Phillips, C.E. Reece, J.K. Spradlin, A-M. Valente-Feliciano, X. Zhao (JLAB) K.I. Seo (NSU) Z.H. Sung (ASC)

This paper describes Energetic Condensation Growth of Nb films using a cathodic arc plasma, whose 40-120eV ions enable sufficient surface mobility to ensure that the lowest energy state (crystalline structure with minimal defects) is

accessible to the film. Hetero-epitaxial films of Nb were grown on a-plane sapphire and MgO crystals with good superconducting properties and crystal size (10mm × 20mm) limited only by substrate size. The substrates were heated to 700 deg C and coated at 300, 500 and 700 deg C. Film thickness varied from ~0.25μm up to >3μm. Residual resistivity ratio (RRR) values (up to a record RRR-554 on MgO and RRR-328 on a-sapphire) vary with substrate annealing and deposition temperatures. XRD spectra and pole figures reveal that RRR increases as the crystal structure of the Nb film becomes more ordered, consistent with fewer defects and hence longer electron mean free path. A transition from Nb(110) to Nb(100) orientation on the MgO(100) lattice occurs at higher temperatures. SIMS depth profiles, EBSD and SEM images complement the XRD data. Crystalline structure in Nb on amorphous borosilicate substrates has implications for future, lower-cost SRF cavities.

Funding: Funded by DE-FG02-08ER85162 and DE-SC0004994. The Jefferson Science Associates, LLC effort supported by DE-AC05-06OR23177, with supplemental funding from the American Recovery and Reinvestment Act.

TUIOB02

Summary of the Symposium on Ingot Nb and New Results on Fundamental Studies of Large Grain Nb

G. Ciovati, P. Dhakal, R. Myneni (JLAB)

The First International Symposium on the Superconducting Science and Technology of Ingot Niobium was held at

Jefferson Lab in September 2010. Significant activities are taking place at laboratories and universities throughout the world to address several aspects related to the science and technology of Ingot Nb: from ingot production to mechanical, thermal and superconducting properties. A summary of the results presented at the Symposium is given in this contribution. New results on the superconducting properties and interstitial impurities content measured in large-grain Nb samples and cavities are briefly highlighted.

Funding: This manuscript has been authored by Jefferson Science Associates, LLC under U.S. DOE Contract No. DE-AC05-06OR23177

TUIOB03

Testing the RF Properties of Novel Super Conducting Materials

J. Guo (SLAC)

Development in niobium SRF cavities has resulted in successful applications among a wide range of particle accelerator projects, due to the combination of its low surface RF resistance and high quenching field. However,

new materials with better performance - especially higher quenching magnetic field - are always tempting to accelerator scientist and have attracted enormous research effort. We have developed a testing system capable to characterize both the surface RF resistance and quenching magnetic field of a superconducting material. The system uses a hemispheric resonant cavity with high quality factor and an interchangeable wall, which can host a flat sample with 2-3 inch diameter. Various samples have been tested, including Nb, MgB2 and Cu in different forms. We will present the most recent developments of the system and discuss the testing results.

Muon Spin Rotation/Relaxation Studies of Niobium for SRF applications

One of the outstanding scientific issues related to superconducting radio frequency cavities made of high-purity bulk niobium is the occurrence of field dependent losses in the walls of the niobium cavity. These losses occur at different RF field levels and pose severe limitations to the niobium technology for both CW or pulsed applications. In this presentation I will explain the results of an experiment which focused on understanding the mechanisms behind losses in the high field regime (above 80-100mT peak magnetic fields). The problem was studied utilizing the unique TRIUMF muon spin rotation (muSR) facility to investigate superconducting properties of niobium samples. In particular, the muon spin rotation experiments aimed at studying the field of first flux entry in high field Q-slope cutouts from small and large grain BCP (buffered chemical polished) 1.5GHz cavities, before and after undergoing 120C UHV-bake. The results obtained will be presented, and it will be discussed in which future direction those results lead.

A. Grassellino (TRIUMF, Canada's National Laboratory for Particle and Nuclear Physics)

TUIOB04

New Approaches to Nb Thin Film Coating

Niobium films are widely used at CERN and several other Laboratories for the coating of superconducting cavities. The performances of these cavities are highly influenced by the thin film properties, and in particular its microstructure. Energetic condensation, and in particular High Power Impulse Magnetron Sputtering (HIPIMS) gives new opportunities for conventional magnetron sputtering equipment. In this talk we will review the background on thin film performance, the motivations of the study, illustrate the experience that has been gained at CERN during the first months of operation and present the results obtained so far.

S. Calatroni, A.E. Gustafsson, M. Scheubel, W. Vollenberg (CERN)

TUIOB05

Funding: The research leading to these results has received funding from the European Commission under the FP7 Research Infrastructures grant agreement no.227579.

Nb Films: Substrates, Nucleation & Crystal Growth

Over the years, Nb/Cu technology, despite its shortcomings due to the commonly used magnetron sputtering, has positioned itself as an alternative route for the future of accelerator superconducting structures. Recently, significant progress made in the development of energetic vacuum deposition techniques is showing promise for the production of thin films tailored for SRF applications. Energetic condensation allows to improve film structure on low temperature substrates by adding energy to the film during condensation to compensate for the lack of thermally induced growth processes. Energetic condensation is characterized by a number of processes enabled by the energy of the incoming ions such as desorption of adsorbed species, enhanced mobility of surface atoms, and sub-implantation of impinging ions. All these with the nature and properties of the substrate have an important influence on the nucleation and subsequent growth of the Nb film. This paper will show how the structure and the electron mean free path (represented by residual resistance ratio values) of Nb films can be tailored on various substrates by varying the ion energy and thermal energy provided to the substrate.

A-M. Valente-Feliciano (JLAB)

TUIOB06

Funding: *Authored by Jefferson Science Associates, LLC under U.S. DOE Contract No. DE-AC05-06OR23177.

TUIOB07

Magnesium Diboride Films for SRF Cavity Applications

Y.D. Agassi (NSWC) B. Moeckly (STI) D.E. Oates (MIT)

We have explored magnesium diboride films for applications in SRF cavities. MgB_2 has a high $T_c = 40$ K and low surface resistance that, even in polycrystalline films, is comparable to niobium. It also shows the potential for higher power handling than niobium because of the higher critical fields. We report the results of measurements of the surface resistance and power handling in films deposited by the reactive-evaporation method. The measurements were made using both a stripline-resonator at 2 GHz and with a dielectric resonator at 10.7 GHz. The best results for surface resistance are 14 micro-ohm at 10.7 GHz, which scales to 0.5 micro-ohm at 2 GHz. The maximum rf magnetic field of the best film has been measured to be 300 Oe, limited by the available amplifier. We have also demonstrated a successful surface-passivation method of atomic-layer-deposited (ALD) films of Al_2O_3 and ZrO_2 . We have also demonstrated evidence that one of the two energy gaps shows unconventional symmetry with a six-fold-symmetric nodal order parameter. The implications for applications of these findings of the basic physics of the material will be discussed.

Funding: This work was supported by the Office of Naval Research

TUIOB08

Hot Topics: Medium Field Q-Slope and Paths to High-Q Operation

W. Weingarten (CERN)

Superconducting RF cavities for accelerator application offer, at least in principle, the perspective of large accelerating gradients and low RF losses. Both qualities must proceed reciprocally. Therefore, consequent to the achieved increase in accelerating gradient during recent years, the RF losses must be reduced accordingly, in order to keep the cryogenic installation at reasonable size. However, the Q-value, which describes the RF losses, did not follow the improved accelerating gradient as wished or required. The reasons are physical mechanisms, only partly understood, on top of the residual losses, that provoke a more than quadratic increase of the RF losses with the accelerating gradient (Q-slope). Cures have been identified experimentally to some extent, but both the theoretical understanding and a complete elimination of the "Q-slop" are lacking. The hot topic discussion should open the floor for a new and deeper understanding of the "Q-slop".

TUPO — Poster Session

Development of Quality Assurance Procedures for the Fast/Slow Tuners on the 1.3 GHz SRF Cavities for the SRF Accelerator Test Facility at Fermilab

The 1.3 GHz elliptical SRF cavities being prepared for cryomodules of the Fermilab SRF Accelerator Test Facility are equipped with coaxial blade tuners.

Quality Assurance tests of these tuners during initial installation, cold testing in the Horizontal Test Stand and during string assembly are described.

Y.M. Pischalnikov, S. Barbanotti, C.J. Grimm, T.N. Khabiboulline, R.V. Pilipenko, W. Schappert (Fermilab)

TUPO001

High Power Pulsed Tests of a $\beta=0.5$ 5-Cell 704 MHz Superconducting Cavity

A $\beta=0.5$ 5-cell 704 MHz cavity was developed in the framework of european R&D programs on high intensity pulsed proton injectors. Medium beta elliptical cavities are known to be sensitive to Lorentz

detuning, which can become difficult to deal with in pulsed operation. The cavity was optimized to reduce the Lorentz detuning by means of two series of rings welded around the irises, and equipped with a piezo tuning system. In order to test the cavity in pulsed mode, a power coupler with 1 MW capability was connected to the cavity. We report here on the fully equipped cavity tests at 1.8 K carried out in the horizontal cryostat Cryholab at Saclay to study its Rf and mechanical behavior in pulsed mode, mostly with 2 ms pulses at a 50 Hz repetition rate. The compensation of Lorentz force detuning has been achieved at an accelerating gradient of 13 MV/m (44 MV/m peak surface electric field).

J. Plouin, D. Braud, M. Desmons, G. Devanz, Y. Gasser, E. Jacques, O. Piquet, J.P. Poupeau, D. Roudier, P. Sahuquet (CEA/DSM/IRFU) W. Hignier, D. Valuch (CERN)

TUPO002

Cooling Properties of HOM Absorber Model for cERL in Japan

The HOM absorber model was designed and fabricated according to results of ferrites and ceramic properties measurement at low temperature. The HOM absorber model uses the RF absorber of HIP (Hot Isostatic Press) ferrite attached on

the copper base. The comb-type RF bridge is adopted at the beam pipe connection between the HIP ferrite part and the flange part. Both parts of the RF bridge are connected with a bellows to reduce the heat load into the superconducting cavity. The HOM absorbers are also required to have good thermal transmission properties to effectively remove the HOM absorption power. The HOM absorber without ferrite was used to measure the thermal properties at liquid nitrogen temperature. Prototype of HIP ferrite model was fabricated. The thermal simulation calculation was also performed. Thermal cycle test between the room temperature and 80K with a GM refrigerator was also carried out to check the thermal tolerance of the HIP ferrite.

M. Sawamura (Japan Atomic Energy Agency (JAEA), Gamma-ray Non-Destructive Assay Research Group) E. Cenni (Sokendai) T. Furuya, H. Sakai, K. Umemori (KEK) K. Shinoe (ISSP/SRL)

TUPO003

TUPO004

Development and Testing of Prototype Fundamental Power Couplers for FRIB Half Wave Resonators

J. Popielarski, P. Glennon, M. Hodek, J. Wlodarczak (FRIB)

The driver linac for the Facility for Rare Isotope Beams (FRIB) requires superconducting Half Wave Resonators to accelerate ions to 200 MeV per nucleon. The Fundamental Power Coupler (FPC) is designed to deliver up to 14 kW of RF power at 322 MHz to the resonator and the beam in CW, and to increase the resonator's control bandwidth for stable operation. With the resonator over-coupled, the mismatch creates a standing wave in the FPC and transmission line downstream of the circulator. The FPC includes an alumina vacuum barrier to allow the resonator to be under ultra-high vacuum. The FPC also serves as a thermal break between the room-temperature transmission line and the resonator at 2 K, with thermal intercepts designed to minimize the heat load to the cryoplant. The FPC design allows for some variation in the coupling, in case a larger bandwidth is needed to mitigate microphonic disturbances. The RF and mechanical design of the coupler and conditioning stand will be reviewed, and the results of high power RF conditioning and testing will be presented.

Funding: This material is based upon work supported by the U.S. Department of Energy Office of Science under Cooperative Agreement DE-SC0000661.

TUPO005

High Power Tests of KEK-ERL Input Coupler for Main Linac Under LN2 Condition

H. Sakai, T. Furuya, N. Nakamura, K. Umemori (KEK) E. Cenni (Sokendai) M. Sawamura (JAEA) K. Shinoe (ISSP/SRL)

We fabricated the prototype of an input coupler, which has two ceramic windows to keep the inside of the superconducting cavity clean, for ERL main linac and performed the high power test. Required input power is about 20kW with standing wave condition for the cavity acceleration field of 20MV/m. In this high power test, the one ceramic window, named as a cold window, was installed into the vacuum insulating chamber and cooled by liquid Nitrogen. First, the multipacting at 10kW level prevented the power increasing. By using the pulse processing method for 8 hours, power finally reached the 25kW with standing wave condition. We could also keep feeding 20kW power into coupler for 16 hours. The maximum measured temperature rises under feeding the 20 kW power to coupler were 120K near the bellows parts and these are not so severe values to operate ERL main linac. After power test, the thermal cycle test of cold window of coupler was done. After 10-times thermal cycle tests between the room temperature and liquid Nitrogen temperature, no leaks and cracks were observed. From these results of high power test, this prototype coupler satisfied our thermal and RF requirements.

TUPO006

High Power Couplers for the Project X Linac

S. Kazakov, M.S. Champion, S. Cheban, T.N. Khabiboulline, M. Kramp, Y. Orlov, O. Pronitchev, V.P. Yakovlev (Fermilab)

Project X, a multi-megawatt proton source under development at Fermi National Accelerator Laboratory. [1]. The key element of the project is a superconducting (SC) 3GV continuous wave (CW) proton linac. The linac includes 5 types of SC accelerating cavities of two frequencies.(325 and 650MHz) The cavities consume up to 30 kW average RF power and need proper main couplers. Requirements and approach to the coupler design are discussed in the report. Results of electro-dynamics and thermal simulations are presented. New cost effective schemes are described.

Development of STF Input Couplers for ILC

High power tests of the STF-Phase 1 cryomodule was carried out at KEK-STF (Superconducting RF Test facility) in 2008. Vacuum leaks at the cold ceramic window of STF-1 input couplers were found in the disassembly of the cryomodule after warm-up. It was considered that the vacuum leaks might be caused by the thermal cycles. Structures of brazing parts at a ceramic disk was investigated to reduce the thermal strain. The STF-2 input couplers with an improved brazing structure for S1-Global cryomodule was designed after the thermal cycle tests of the sample RF windows. The results of the thermal cycle tests of the sample RF windows and the high power performance of the improved STF-2 input couplers will be reported.

M. Satoh, E. Kako, S. Noguchi, T. Shishido, K. Watanabe, Y. Yamamoto (KEK)

TUPO007

Vertical Test Facility for Superconducting RF Cavities at Daresbury Laboratory

The Vertical Test Facility at Daresbury Laboratory has been recently relocated to enable it to fulfill its potential of performing high power characterization tests of Superconducting RF Cavities in the 1.3 to 3GHz range. The 250 litre, 3 Metre Dewar is capable of operation from 1.6K to 4K and has recently been used to test the first Superconducting cavity produced in the UK. This paper outlines the setup, processes and results of these tests.

R.K. Buckley, R. Bate, P. Goudket, A.R. Goulden, J.F. Orrett, S.M. Pattalwar, A.E. Wheelhouse (STFC/DL/ASTeC)

TUPO008

How to Increase Average Power of Main Coupler

New idea how to increase average power of main coupler is described.

S. Kazakov (Fermilab)

TUPO009

Conditioning the Fundamental Power Coupler for ERL SRF Gun

The 703 MHz superconducting gun for the BNL Energy Recovery Linac (ERL) prototype has two fundamental power couplers (FPCs), and each of them will deliver up to 500 kW of CW RF power. In order to prepare the couplers for high power RF service and process multipacting, the FPCs should be conditioned prior to installation into the gun cryomodule. A conditioning cart based test stand, which includes a vacuum pumping system, controllable bake-out system, diagnostics, interlocks and data log system has been designed, constructed and commissioned by collaboration of BNL and AES. This paper presents FPC conditioning cart systems and the conditioning process.

W. Xu, Z. Altinbas, S.A. Belomestnykh, I. Ben-Zvi, A. Burrill, S. Deonarine, D.M. Gassner, J.P. Jamilkowski, P. Kankiya, D. Kayran, N. Laloudakis, L. Masi, G.T. McIntyre, D. Pate, D. Phillips, T. Seda, A.N. Steszyn, T.N. Tallerico, R.J. Todd, D. Weiss, A. Zaltsman (BNL) M.D. Cole, G.J. Whitbeck (AES)

TUPO010

Funding: This work is supported by Brookhaven Science Associates, LLC under Contract No. DE-AC02-98CH10886 with the U.S. DOE.

TUPO011

Coupler Cleaning Machine

W. Kaabi, M. Lacroix, Y. Peinaud (LAL)

Today, the research on couplers focuses on the preparation techniques which are very important for conditioning and good working of couplers on cryomodules. Unfortunately, these steps take long time : 1 week for particle free cleaning and 1 week for in-situ baking, which is not acceptable for project like ILC where around 16000 couplers will have to be prepared. From this fact, we decided at LAL to propose for the EUCARD program a study to automatise the clean room cleaning. This study is the design and the production of a coupler cleaning machine "Automate de Lavage Intégré pour Coupleur Electromagnétique" : ALICE). This machine will do the usual cleaning tasks that we used to do by hands (Ultrasonic cleaning with detergent and Ultrapure water, rinsing, resistivity measurement and drying). Our goal is to reduce the processing time from 5 days to 3 hours. In the same time, this machine will reduce the risk of pollution due to human handling (8 steps turned into only one) and will permit to improve the cleaning parameters like time, temperature, ... The main challenge was to design a free particle mechanisms for the coupler motion needed in the process.

Funding: EUCARD

TUPO012

Niobium Electropolishing in an Aqueous, Non-Viscous HF-Free Electrolyte: A New Polishing MechanismM.E. Inman, T.D. Hall, E.J. Taylor (Faraday Technology, Inc.)
C.E. Reece, O. Trofimova (JLAB)

Faraday is working with the Jefferson Lab to develop an improved process for electropolishing niobium RF superconducting cavities in an electrolyte free of hydrofluoric acid, to create microscopically clean and smooth niobium surfaces on the cavity interior. Conventional electropolishing of niobium cavities is based on a viscous electrolyte with an approximately 20 micron thick diffusion layer*, containing hydrofluoric acid as a depassivation agent. The FARADAYIC Electropolishing process combines pulse reverse electric fields and aqueous, low acid, non-viscous electrolytes to control current distribution and oxide film formation during metal removal. This eliminates the need for a depassivation agent, such as hydrofluoric acid. This program is aimed at understanding this new electropolishing mechanism, and optimizing it to achieve the desired oxide formation, reduced defect density and high performance. The feasibility of the process has been demonstrated using an aqueous sulfuric acid solution in conjunction with the FARADAYIC Process to electropolish niobium to surface finishes below 1 nm over a 2 x 2 micron area.

* Hui Tian and Charles E. Reece, Evaluation of the diffusion coefficient of fluorine during the electropolishing of niobium, Phys. Rev. ST Accel. Beams, 13, 083502 (2010)

TUPO013

Assembly of the International ERL Cryomodule at Daresbury Laboratory

P.A. McIntosh, R. Bate, P. Goudket, S.M. Patalwar (STFC/DL/ASTeC) S.A. Belomestnykh, M. Liepe, H. Padamsee, P. Quigley, J. Sears, V.D. Shemelin (CLASSE) A. Buechner, F.G. Gabriel, P. Michel (HZDR) M.A. Cordwell, J. Strachan (STFC/DL) J.N. Corlett, D. Li, S.M. Lidia (LBNL) T. Kimura, T.I. Smith (Stanford University) D. Proch, J.K. Sekutowicz (DESY)

The collaborative development of an optimised cavity/cryomodule solution for application on ERL facilities is nearing completion. This paper outlines the progress of the module assembly and details the processes used for final cavity string integration. The preparation and installation of the high power couplers will be described, as will that of the HOM loads. The testing and integration of the various sub-components of the cryomodule are also detailed in this paper.

High Gradient Results of ICHIRO 9-Cell Cavity in Collaboration With KEK and Jlab

KEK and Jlab have continued S0-study collaboration on ICHIRO 9cell cavities since 2008. In 2010, we have started S0 tight loop test on ICHIRO full 9cell cavity, ICHIRO#7. Surface treatments and vertical tests have been repeated at Jlab. Maximum gradient of 40MV/m was achieved so far. We will report the results and details of this.

F. Furuta (KEK)

TUPO014

Standard Procedures of ILC High Gradient Cavity Processing at Jefferson Lab

We describe the JLab standard procedures of ILC cavity processing and handling for reproducible high gradient high

Q0 results. The procedure begins with mixing fresh electrolyte with the molar ratio of HF:H2O:H2SO4 in the range that is compatible with that in the original Siemens recipe. Three key process parameters, namely the acid flow rate, the polish cell voltage and the cavity body temperature, are identified and in control. Our experience shows that optimal EP is achieved in the continuous current oscillation mode. The appearance of current oscillation also serves as a sensitive in-situ QA/QC indicator. The "auto polishing" procedure is introduced by continuing the acid flow and cavity rotation after the voltage is shut off. This effectively reduces sulfur-bearing niobium oxide granules, an inherent contaminant of the EP process. An elaborate post-EP cleaning procedure includes low-pressure water rinsing, HOM coupler brushing and ultrasonic cleaning with detergent. The vacuum furnace heat treatment procedure is updated. A no-touch bead-pull method is established. Slow pump down is routinely applied to prevent recontamination of the cavity surface.

Funding: This work was authored by Jefferson Science Associates, LLC under U.S. DOE Contract No. DE-AC05-06OR23177

R.L. Geng (JLAB) A.C. Crawford (CLASSE)

TUPO015

Study Correlating Niobium Surface Roughness with Surface Particle Counts

A study has been initiated at Michigan State University (MSU) to relate the surface preparation of Superconducting Radio Frequency (SRF) resonators and surface particle counts, using niobium samples. During fabrication, undesired surface roughness can develop on the internal surfaces of the resonators. The final cavity finish will be product of material forming, machining, welding, chemistry, high-pressure rinsing, and handling of the niobium material. This study will document niobium samples treated with MSU standard processing procedures; first measuring the surface roughness, then polishing samples with defined techniques, processing, and measuring surface particle counts. The samples will include as received niobium, machined surfaces, welded surfaces, and surfaces with characterized surface imperfections (scratches).

Funding: Work supported by US DOE Cooperative Agreement DE-SC0000661 and Michigan State University

C. Compton, L.J. Dubbs, K. Elliott, D. R. Miller, R. Oweiss, L. Popielarski, K. Witgen (FRIB)

TUPO016

TUPO017

Development and Scale-Up of an HF Free Electropolishing Process in Single-Cell Niobium SRF Cavities

M.E. Inman, H.M. Garich, S.T. Snyder, E.J. Taylor (Faraday Technology, Inc.) L.D. Cooley, C.A. Cooper, A.M. Rowe (Fermilab)

The performance of niobium SRF cavities is strongly dependent on a microscopically smooth and clean surface, achieved using buffered chemical polishing or electropolishing, which require a viscous electrolyte containing hydrofluoric acid to achieve niobium oxide breakdown and current distribution control. An ideal polishing process would include: electrolyte free of hydrofluoric acid; control of surface roughness to less than 0.1 micron; surface free from contamination; current distribution control enabling uniform polishing; removal of at least 100 microns. Faraday is working with Fermilab to develop and scale-up the FARADAYIC Electropolishing process to achieve these conditions. FARADAYIC Electropolishing combines pulse reverse electric fields and low viscosity aqueous electrolytes to control current distribution and oxide formation during metal removal. Recent results on coupon polishing will be presented including polishing rates up to 1 micron/min, control of electrolyte temperature to below 20 C, and surface finishes less than 0.2 microns over 4 mm length scales. Construction of a single-cell cavity electropolishing apparatus at Faraday are discussed.

The performance of niobium SRF cavities is strongly dependent on a microscopically smooth and clean surface, achieved using buffered chemical polishing or electropolishing, which require a

TUPO018

Update of the DESY Infrastructure for Cavity Preparation

M. Schalwat, K. Escherich, N. Krupka, A. Matheisen, B. Petersen, N. Steinhilber-Kuehl (DESY)

The main infrastructure for preparation of superconducting cavities at DESY is the cleanroom which was set up in the early 90th of the last century. This cleanroom is completely renovated in 2009. The ground space of cleanroom class ISO 4 was enlarged from 20 to 53 m² and the areas of ISO 7 of the old cleanroom are upgraded to ISO 6 and ISO 5 standard. Areas for ultrasonic cleaning, ultrapure water rinsing and chemical surface treatment are upgraded to ISO 4 standards. Multiple vacuum connections are installed to reduce movement of cavities during string assembly. A 1200 C baking oven, fulfilling the ISO 4 requirements, is connected to the ISO 4 assembly area and allows in situ baking of multi cell s.c. resonators. For industrial cavity production it is shown that a high pressure rinsing unit driven by a turbine pump allows feeding several high pressure rinsing stands in parallel. For cost reduction of water ultra-pure production and increase the amount of water in the cavity preparation cycle a recirculation of rinsing water is investigated and under commissioning. Fixtures and tool for the assembly of the BPM Quadrupole units for XFEL modules are installed and commissioned.

The main infrastructure for preparation of superconducting cavities at DESY is the cleanroom which was set up in the early 90th of the last century. This clean-

Fabrication, Tuning, Treatment and Testing of Two 3.5 Cell Photo-Injector Cavities for the ELBE Linac

As part of a CRADA (Cooperative Research and Development Agreement) between Helmholtz-Zentrum Dresden-Rossendorf (HZDR) and Thomas Jefferson Lab National Accelerator Facility (TJNAF) we have fabricated and tested two 1.3 GHz 3.5 cell photo-injector cavities from polycrystalline RRR niobium and large grain RRR niobium, respectively.

A. Arnold, P. Murcek, J. Teichert, R. Xiang (HZDR) G.V. Ere-meev, P. Kneisel, M. Stirbet, L. Turlington (JLAB)

The cavity with the better performance will replace the presently used injector cavity in the ELBE linac*. The cavities have been fabricated and pre-tuned at TJNAF, while the more sophisticated final field tuning, the adjustment of the external couplings and the field profile measurement of transverse electric modes for RF focusing** was done at HZDR. The following standard surface treatment and the vertical test was carried out at TJNAF's production facilities. A major challenge turned out to be the rinsing of the cathode cell, which has small opening ($\approx 10\text{mm}$) to receive the cathode stalk. Another unexpected problem encountered after etching, since large visible defects appeared in the least accessible cathode cell. This contribution reports about our experiences, initial results and the on-going diagnostic work to understand and fix the problems.

* J. Teichert, et al., Proc. FEL 2010, Malmoe, Sweden, p. 453.

** V. Volkov, D. Janssen, Phys. Rev. ST Accel. Beams 11, 061302 (2008).

TUPO019

CMP Polishing of a Niobium SRF Cavity

Typical SRF cavity preparation protocol requires approximately 150 microns total of inner surface removal in two steps using an HF based electro-polishing process. The bulk removal, consumes approximately 130 microns and the final polishing step consumes an additional 20 microns.

S.D. Lesiak, D. McMullen, K. Moeggenborg (Cabot Micro-electronics Polishing Corp) A.M. Rowe (Fermilab)

The work presented in this paper discusses a technique using chemical mechanical polishing (CMP) to replace the final 20 micron HF-based electro-polishing step. CMP processing results in a significant improvement in surface roughness when compared to electro-polish processing with the added benefits of being ecologically innocuous and operationally safe. Sub-surface anomalies, attributable to previous fabrication and finishing operations, were encountered in the CMP processing of the first sample SRF cavity. Sub-surface damage is normally uncovered during the CMP process and has been used to identify the nature of the damage and point to some of the potential sources of the anomalies. The nature of CMP enables polishing without inducing sub-surface damage. The combined effects of removing sub-surface damage and a higher quality surface finish as a result of CMP processing are discussed.

TUPO020

Current State of Electropolishing at ANL

An electropolishing system for 1.3 GHz elliptical single- and 9-cell cavities is in full operation at the joint ANL/FNAL

T. Reid, S.M. Gerbick, M.P. Kelly, R.C. Murphy (ANL)

Superconducting Cavity Surface Processing Facility (SCSPF) located at Argonne. Currently, the facility is processing an average of one cavity per week. Single cell cavities are routinely achieving accelerating gradients exceeding 35 MV/m and several recent 9-cell cavities have operated in the region of 35-38 MV/m. Process improvements are continuing with the intent to improve overall yield at 35 MV/m and to improve cavity Q-values. In particular, cavity rf losses at the level of $\sim 5\text{ nOhm}$ in both the low- and medium field regions appear to be sensitive to relatively small changes in EP parameters. Some examples of this are presented here. Finally, electropolishing on dressed 9-cell cavities is being explored as a technique for recovering previously good performing bare cavities where performance has degraded, for example, after rf processing.

TUPO021

TUPO022

Effects of Cathode Shapes on BEP and EP During Vertical Surface Treatments on Niobium

S. Jin, X.Y. Lu, K. Zhao (PKU/IHIP) R.A. Rimmer, A.T. Wu (JLAB)

This paper reports the research results of effects of cathode shapes during buffered and conventional vertical electropolishing treatments for single cell superconducting radio frequency (SRF) niobium cavities. Several different cathodes shapes such as, for instance, bar, ball, ellipsoid, wheel, etc. were employed. Detailed electropolishing parameters at different locations inside a single cell SRF cavity were measured using a unique JLab home-made demountable cavity, including I-V characteristic, removal rate, surface roughness, polishing uniformity and so on. It was demonstrated that optimal polishing results could be achieved by changing the cathode shape for both BEP and EP. Implications on the electropolishing mechanism of Nb cavities for both BEP and EP based on the obtained experimental results are discussed.

Funding: Authored by Jefferson Science Associates, LLC under U.S. DOE Contract No. DE-AC05-06OR23177.

TUPO023

Development of the Superconducting Cavity for ILC at TOSHIBA

T. Ota, N. Kuroiwa, K. Mori, T. Nagafuchi, K. Nakayama, S. Nomura, J. Shibuya, Y. Tajima, T. Tosaka, M. Urata, J. Watanabe, M. Yamada (Toshiba) H. Hayano, E. Kako, S. Noguchi, T. Saeki, M. Sato, T. Shishido, K. Watanabe, A. Yamamoto, Y. Yamamoto (KEK)

TOSHIBA is developing superconducting cavity for International Linear Collider (ILC) in collaboration with High Energy Accelerator Research Organization (KEK) from 2009. We fabricated a 9-cell cavity and carried out the performance test of it at KEK in 2010. The status of superconducting cavity development for ILC at TOSHIBA is presented in this conference.

perconducting cavity development for ILC at TOSHIBA is presented in this conference.

TUPO024

Sulfur Residues in Niobium Electropolishing

L. Zhao (The College of William and Mary) M.J. Kelley, C.E. Reece, H. Tian (JLAB)

Electropolishing (EP) in sulfuric/hydrofluoric acid mixtures affords significantly greater surface smoothness than the incumbent buffered chemical polishing (BCP), making it attractive as the future baseline technology for SRF cavity manufacture. However, reported observations of particulate sulfur residues raise concern. One hypothesis is sulfate reduction to elemental sulfur at the cathode, where the measured potential drop is thermodynamically sufficient. Alternatively, the low effectiveness of the cathode's aluminum oxide surface as a hydrogen recombination catalyst could lead to accumulation of atomic hydrogen, a powerful reductant. We explored these possibilities under standard EP conditions in a small three-electrode laboratory cell. We varied aluminum cathode area to obtain different current densities (and thus overpotentials) at constant cell current. We substituted platinum, an excellent hydrogen recombination catalyst, for aluminum in some experiments. Surface of cathodes were examined with Scanning Electron Microscope (SEM). Surface composition was analyzed by Energy Dispersive X-Ray Spectroscopy (EDS) and X-Ray Photoelectron Spectroscopy (XPS).

Funding: Authored by Jefferson Science Associates, LLC under U.S. DOE Contract No. DE-AC05-06OR23177.

Integrated Cavity Processing Apparatus at Fermilab: SRF Cavity Processing R&D

A center for cavity processing R&D at Fermilab, called the Integrated Cavity Processing Apparatus, is currently in the final stages of installation and commissioning. This facility contains centrifugal barrel polishing, a horizontal electropolishing tool, a 1000°C vacuum furnace, a high pressure rinse tool utilizing ultrapure water, ISO class 4, 5 and 6 clean rooms for cavity assembly work and various other associated pieces of support equipment. All the operations are designed for single cell and nine cell 1.3 GHz Tesla type cavities except for the electropolishing tool which will initially be only for single cell use. Upgrades are currently being examined for single and five cell 650 MHz cavities. The current status of the facility and plans for future work are discussed.

C.A. Cooper, L.D. Cooley, V. Poloubotko, O. Pronitchev, A.M. Rowe, M. Wong (Fermilab)

TUPO025

Nine - Cell Tesla Shape Cavities Produced From Hydroformed Cells

Production of two types of seamless niobium tubes for hydroforming of RF cavities has been developed. The first type of tubes, developed at DESY, have been spun from sheets and flow formed. The

W. Singer, A. Ermakov, G. Kreps, A. Matheisen, X. Singer, K. Twarowski (DESY) R. Crooks (Black Laboratories, L.L.C.) P. Kneisel (JLAB) I.N. Zhelezov (RAS/INR)

second type of tubing was developed by Black Laboratories in collaboration with the company ATI Wah Chang. These longer length tubes were extruded from a heavily deformed billet, processed for a fine-grained microstructure and flow formed. Several seamless three cell units have been produced by hydroforming at DESY. Some of the units have been treated by buffered chemical polishing and RF tested at JLab. The accelerating gradient Eacc of the units exceeded in most cases 30 MV/m. Three of the 3-cell units from the first type of tubing were combined to three 9-cell niobium cavities at the company E. Zanon. The 3-cell units from extruded tubing are welded together to the fourth 9-cell cavity at JLab. All cavities are in preparation for the RF tests at DESY and JLab. Up to now two of the cavities are electropolished and tested at DESY. The first cavity reached an accelerating gradient of Eacc of ~30 MV/m, the second one ~35 MV/m.

TUPO026

A New Home for SRF Work at JLab—the Technology and Engineering Development Facility

A project is underway at Jefferson Lab to fully renovate all of the SRF research, development, fabrication, processing and assembly facilities. Initiated in 2009 and funded by the US Department of Energy's Science Laboratory Infrastructure program, this work together with construction of a new building to house JLab's Engineering Division and detector electronics group is collectively known as the Technology and Engineering Development Facility (TEDF) Project. The majority of the SRF facilities will be consolidated in a new building with 30,000 square feet (3300 m²) of work space attached to the existing Test Lab. The purpose-built facility integrates fabrication, chemistry, and cleanroom suites and cryomodule assembly lines for convenient, yet flexible operations serving multiple projects in parallel. A robust ultra-pure water system and integrated hazardous materials transfer and neutralization system are included in the project. Construction is underway and move-in is scheduled for early 2012. Project details will be presented.

C.E. Reece, A. Reilly (JLAB)

Funding: Authored by Jefferson Science Associates, LLC under U.S. DOE Contract No. DE-AC05-06OR23177.

TUPO027

TUPO0028

Qualification of the Second Batch Production 9-Cell Cavities Manufactured by AES and Validation of the First US Industrial Cavity Vendor for ILC

R.L. Geng, D. Forehand, B.A. Golden, P. Kushnick, R.B. Overton (JLAB) M. Calderaro, E. Peterson, J. Rathke (AES) M.S. Champion, J. Follkie (Fermilab) A.C. Crawford (CLASSE)

One of the major goals of ILC SRF cavity R&D is to develop industrial capabilities of cavity manufacture and processing in all three regions. In the past several years, Jefferson Lab, in collaboration

with Fermi National Accelerator Laboratory, has processed and tested all the 9-cell cavities of the first batch (4 cavities) and second batch (6 cavities) production cavities manufactured by Advanced Energy Systems Inc. (AES). Over the course, close information feedback was maintained, resulting in changes in fabrication and processing procedures. A light buffered chemical polishing was introduced, removing the weld splatters that could not be effectively removed by heavy EP alone. An 800 Celsius 2 hour vacuum furnace heat treatment procedure replaced the original 600 Celsius 10 hour procedure. Four out of the six 9-cell cavities of the second production bath achieved a gradient of 36-41 MV/m at a Q0 of more than $8 \cdot 10^9$ at 35 MV/m. This result validated AES as the first "ILC certified" industrial vendor in the US for ILC cavity manufacture. **Funding:** This work was authored by Jefferson Science Associates, LLC under U.S. DOE Contract No. DE-AC05-06OR23177

TUPO0029

Gradient Improvement by Removal of Identified Local Defects

R.L. Geng, W.A. Clemens (JLAB) C.A. Cooper (Fermilab) H. Hayano, K. Watanabe (KEK)

Recent experience of ILC cavity processing and testing at Jefferson Lab has shown that some 9-cell cavities are quench limited at a gradient in the range

of 15-25 MV/m. Further studies reveal that these quench limits are often correlated with sub-mm sized and highly localized geometrical defects at or near the equator weld. There are increasing evidence to show that these genetic defects have their origin in the material or in the electron beam welding process (for example due to weld irregularities or splatters on the RF surface and welding porosity underneath the surface). A local defect removal method has been proposed at Jefferson Lab by locally re-melting the niobium material. Several 1-cell cavities with known local defects have been treated by using the JLab local e-beam re-melting method, resulting in gradient and Q0 improvement. We also sent 9-cell cavities with known gradient limiting local defects to KEK for local grinding and to FNAL for global mechanical polishing. We report on the results of gradient improvements by removal of local defects in these cavities.

Funding: This work was authored by Jefferson Science Associates, LLC under U.S. DOE Contract No. DE-AC05-06OR23177

TUPO0030

Status of the 9-Cell Superconducting Cavity R&D for ILC at Hitachi

T. Watanuki, T. Semba, M. Watanabe (Hitachi Ltd.) H. Hayano, E. Kako, S. Noguchi, T. Saeki, T. Shishido, K. Watanabe, Y. Yamamoto (KEK)

Hitachi is developing 9-cell superconducting cavities for ILC project in collaboration with KEK. We focus on electron beam welding (EBW) and plastic forming techniques. In 2010, Hitachi's first 9-cell

cavity without HOM couplers was completed successfully. Surface treatments and performance test of the cavity were done at KEK and the accelerating gradient reached 35.2 MV/m. We have fabricated the next 9-cell cavity with HOM couplers from January 2011. We will report the fabrication procedure and test result of our first cavity and the current status of the next cavity.

Update on the R&D of Vertical Buffered Electropolishing on Nb Samples and SRF Single Cell Cavities

Electropolishing (EP) has become a popular choice as the final step of the surface removal process during the fabrication of Nb superconducting radio frequency (SRF) cavities. One of the major reasons for the choice is that Nb SRF cavities treated by EP tend to have a better chance to reach an accelerating gradient of 30MV/m or higher. This advantage of EP over BCP can at least be partially attributed to the smoother Nb surfaces that EP can produce. Recently a Nb surface removal technique called buffered electropolishing (BEP) was developed at JLab, which could produce the smoothest surface finish. In this contribution, R&D efforts of vertical BEP on Nb small samples and SRF single cell cavities since the last SRF conference in 2009 will be updated. It is shown that under a suitable condition, BEP can have a Nb removal rate as high as 10 $\mu\text{m}/\text{min}$ that is more than 25 and 5 times quicker than those of EP and BCP(112) respectively. Possible mechanisms responsible for the high Nb removal rate are proposed. Clues on the optimization of vertical BEP and EP treatments on Nb SRF cavities from recent experimental results obtained on a Nb single cell demountable cavity will be discussed.

Authored by Jefferson Science Associates, LLC under U.S. DOE Contract No. DE-AC05-06OR23177.

A.T. Wu, J.D. Mammoser, R.A. Rimmer (JLAB) S. Jin, L. Lin, X.Y. Lu, K. Zhao (PKU/IHIP)

TUPO031

Updates on R&D of Nondestructive Inspection Systems for SRF Cavities

We are developing high resolution eddy current scan and High density Tmap and X-map. The high resolution eddy current scan showed 100 μm diameter hole with 50 μm depth that was drilled on a Nb plate. The surface mount print circuit technology is applied to the high density Tmap and X-map devices, which will be ready soon to test at a vertical test bench. In addition, radiography using Xrays and neutrons are also under study. The results and status will be presented.

Y. Iwashita, H. Tongu (Kyoto ICR) H. Hayano, T. Saeki, K. Watanabe (KEK)

TUPO032

Study of I-V Characteristics at Different Locations Inside a Demountable Nb SRF Cavity During Vertical BEP and EP Treatments

For a normal superconducting radio frequency (SRF) cavity, it is hard to obtain detailed information of an electropolishing process. So, a demountable cavity was firstly made by JLab to resolve this problem. This paper reports the measurements of I-V characteristics at three different locations inside the demountable cavity during buffered electropolishing (BEP) and electropolishing (EP) treatments. The polishing plateau appeared earlier on the surface areas close to iris and later on those near equator. To find the reason for this phenomenon, the electric field distribution in the cavity was considered and simulated by means of Poisson Superfish. Correlations were found between the measured I-V characteristics and the simulated results. This implies that electric field distribution inside a SRF cavity had an important effect on the polishing processes during vertical BEP and EP.

Funding: Authored by Jefferson Science Associates, LLC under U.S. DOE Contract No. DE-AC05-06OR23177.

S. Jin, X.Y. Lu, K. Zhao (PKU/IHIP) R.A. Rimmer, A.T. Wu (JLAB)

TUPO033

TUPO034

High Pressure Rinse System for Multiple SRF Cavities

R.C. Murphy, J.D. Fuerst, S.M. Gerbick, M. Kedzie, M.P. Kelly, T. Reid (ANL)

The Physics Division SRF group at Argonne National Laboratory is building a new, high pressure rinse system for the joint ANL/FNAL Superconducting Cavity Surface Processing Facility (SCSPF). The rinsing tool can be easily reconfigured vertically or horizontally to process a variety of SRF cavity shapes and sizes including elliptical, spoke, quarter- and half-wave cavities. The system has been commissioned with a new 72 MHz $\beta=0.077$ quarter wave cavity as part of the ATLAS Intensity Upgrade at ANL. The tool is also designed to rinse 1.3 GHz elliptical single-cell and 9-cell cavities, as well as the new 650 MHz elliptical cavities under development for Project-X and Fermilab. This work was supported by the U.S. Department of Energy, Office of Nuclear Physics, under Contract No. DE-AC02-06CH11357.

Funding: This work was supported by the U.S. Department of Energy, Office of Nuclear Physics, under Contract No. DE-AC02-06CH11357.

TUPO035

Cryogenic Test of a Two-Cell Passive SRF Cavity for NSLS-II

C.H. Boulware, T.L. Grimm, C. Krizmanich, B. Kuhlman, N. Miller, B. Siegel, M.J. Winowski (Niowave, Inc.) W.K. Gash, B.N. Kosciuk, V. Ravindranath, J. Rose, S.K. Sharma, R. Sikora, N.A. Towne (BNL)

In collaboration with Brookhaven National Lab (BNL), Niowave, Inc. has built and performed the first cryogenic test on a two-cell passive SRF cavity for controlling electron bunch lengths at NSLS-II, the new 3rd generation synchrotron under construction at BNL. The structure is resonant at 1500 MHz, the third harmonic of the accelerating RF frequency. Because the cavity is powered by the beam itself, however, many frequencies could potentially be excited and higher-order modes must be strongly damped. Further, only one of the two cavity fundamental modes is used for the bunch length control, and the other mode has been carefully tuned so that it will be minimally excited by the electron bunches. The first cryogenic test has been performed to demonstrate a successful cooldown of the cavity in its cryomodule and to show that the cavity can be tuned to its operating frequency while the proper spacing between the two fundamental modes is maintained. A brief discussion of the cavity design will be presented along with some results from the cavity tuning and cryotest.

Funding: The work at Niowave has been funded by DOE SBIR grant DE-FG02-08ER85014.

TUPO036

Material for European XFEL Resonators

W. Singer, S. Arnold, A. Brinkmann, J.A. Dammann, A. Ermakov, J. Iversen, D. Klinke, M. Lengkeit, W.-D. Moeller, P. Poerschmann, X. Singer (DESY)

Twelve different types of semi-finished products will be provided by DESY to producers of European XFEL superconducting resonators. Work on material for XFEL cavities is divided into three phases

(prototyping, pre-series and series production). Two new companies (Ningxia OTIC and Plansee Metal GmbH) have been qualified as XFEL suppliers. Material is contracted to 4 companies (Ningxia OTIC, Plansee Metal GmbH, Tokyo Denkai and W.C. Heraeus). Procurement of semi-finished products includes: acceptance on producer's site, eddy current scanning of the sheets, testing for required parameters (RRR, interstitial impurity analysis, metallic impurities analysis, metallography, tensile test, hardness HV, dimensional check, surface roughness), documentation using the DESY EDM-System, marking, delivery to companies. Semi-finished products for pressure bearing sub-components of cavities have to be fabricated according Pressure Equipment Directive 97/23/EC. Qualification of material and the certification of the material producers were done by a "notified body". Appropriate infrastructure and logistic for guiding through more than 20.000 of semi-finished products has been build up.

Study on Electro-Polishing Process by Niobium-Plate Sample With Artificial Pits

The Electro-polishing (EP) process is the best candidate of final surface-treatment for the production of ILC cavities. Nevertheless, the development of defects on the inner-surface of the Superconducting RF cavity during EP process has not been studied by experimental method. We made artificial pits on the surface of a Nb-plate sample and observed the development of the pit-shapes after each step of 30um-EP process where 120um was removed by EP in total. This article describes the results of this EP-test of Nb-sample with artificial pits.

T. Saeki, H. Hayano, S. Kato, M. Nishiwaki, M. Sawabe (KEK)
W.A. Clemens, R.L. Geng, R. Manus (JLAB) P.V. Tyagi (Sokendai)

TUPO037

Superconducting RF Cavity Development With UK Industry

As part of a STFC Industrial Programme Support Scheme (PIPSS) grant Daresbury Laboratory and Shakespeare Engineering Ltd have fabricated, processed and tested a single cell 1.3 GHz superconducting RF cavity, in collaboration with Jefferson Laboratory. The overall aim of the project through a knowledge exchange programme was to develop the capability of UK industry to fabricate and process a single cell niobium superconducting cavity, as part of a long term strategy to enable UK industry to address the large potential market for superconducting RF structures. As a means of measuring the performance of the fabrication and processing an objective of the programme of work was to achieve an accelerating gradient of greater than 15 MV/m at an unloaded quality factor of 1.0×10^{10} or better. Three cavities were fabricated by Shakespeare Engineering, and electron beam welded at Jefferson Laboratory in the USA. Processing and testing of the cavities was then performed both at Jefferson Laboratory and at Daresbury Laboratory. The fabrication and process methods are discussed in this paper along with the results obtained from the testing performed in the vertical test facilities.

A.E. Wheelhouse, R. Bate, R.K. Buckley, P. Goudket, A.R. Goulden, P.A. McIntosh, J.F. Orrett (STFC/DL/ASTeC)

TUPO038

Long-Term Monitoring of 2nd-Period EP-Electrolyte in STF-EP Facility at KEK

We have constructed an Electro-polishing (EP) Facility in the Superconducting RF Test Facility (STF) at KEK at the end of 2007. We have begun to operate the EP facility since 2008 and performed the EP process of cavity about 140 times up to now. During this period, we exchanged EP-electrolyte twice in the 2,000L tank. We are performing EP processes with the 3rd-period EP-electrolyte at the present moment. By this report, we report the long-term monitoring results of the 2nd-period EP-electrolyte used from May, 2009 to July, 2010.

M. Sawabe, H. Hayano, A. Komiya, H. Monjushiro, T. Saeki, M. Satou (KEK)

TUPO039

The Status of Cavity-Fabrication Study for ILC at KEK

We are constructing a new cavity-fabrication facility at KEK from 2009. In the facility, we have installed a deep-drawing machine, a half-cup trimming machine, an electron-beam welding machine, and a chemical etching room in one place. We started the fabrication study of 9-cell cavity for ILC from 2009 using this facility. The study is focusing on the cost reduction in the mass production of 9-cell cavities in ILC. This article reports the current status of cavity-fabrication study in the facility.

T. Saeki, Y. Ajima, K. Enami, H. Hayano, H. Inoue, E. Kako, S. Kato, S. Noguchi, M. Satoh, T. Shishido, A. Terashima, N. Toge, K. Ueno, Y. Watanabe, S. Yamaguchi, A. Yamamoto, Y. Yamamoto, K. Yokoya (KEK) H. Nakamura, K. Nohara, M. Shinohara, N. Kawabata (SPS)

TUPO040

TUPO041

Investigation on Cavity String Assembly and Repair

A. Matheisen, B. Horst, van der, S. Saegbarth, P. Schilling, M. Schmoekel, N. Steinhau-Kuehl, H. Weitkaemper (DESY)

At DESY several cavity strings for modules of the flash accelerator and studies on XFEL prototypes are completed. In some modules cavities have been exchanged for upgrade of applicable module gradients or exchange of resonators that showing performance degradation in the module test. Assembly and repair sequences and quality control plans for cavity string are developed and applied. From module srting PXFEL3 six out of eight cavities are removed and handed over to CEA Saclay for training of string and module assembly. On two of these cavities the procedures for assembly and exchange of cavities in cavity strings are crosschecked. These cavities are tested at 2 K removaed from string without additional treatments to cross check assembly and repair sequences.

TUPO042

SLAC/FNAL TTF3 Coupler Assembly and Processing Experience

C. Adolphsen, A.A. Haase, C.D. Nantista, J. Tice, F. Wang (SLAC) A. Lunin, K.S. Premo (Fermilab)

The TTF3-style coupler is typically used to power 1.3 GHz TESLA-type superconducting cavities. For the US ILC program, parts purchased in industry for such couplers are received at SLAC where they are inspected, cleaned, assembled as pairs in a Class 10 cleanroom, pumped down, baked at 150 degC and rf processed. The pairs are then shipped to FNAL and installed in cavities that are then tested at input power levels up to 300 kW. This paper describes the coupler results to date including improvements to the procedures and efforts to mitigate problems that have been encountered. Also progress on building a cold coupler section without e-beam welding is presented.

Funding: Work supported by the U.S. Department of Energy under contract number DE-AC02-76SF00515

TUPO043

Optimization of Ar/CL2 Plasma Parameters Used for SRF Cavity Etching

J. Upadhyay, M. Nikolić, S. Popovic, L. Vuskovic (ODU) H.L. Phillips, A-M. Valente-Feliciano (JLAB)

We are pursuing the development of environmentally friendly dry etching of superconducting radio frequency (SRF) cavities in Ar/CL2 discharges. It has been proven with flat samples that the bulk Niobium (Nb) removal rate and the surface roughness after plasma etchings are equal to or better than wet etching processes. The plasma properties inside the single cell SRF cavity depend on frequency, pressure and power. To understand the plasma properties and chemical kinetics of plasma etching process inside a single cell cavity, we are using a specially-designed cavity with 20 sample holders symmetrically distributed over the cell. These holders are being used for Nb coupon etching as well as diagnostic ports. Multiple optical probes with optical fibers have been utilized for emission spectroscopy measurements. A power supply in the radio frequency regime (100 MHz) and another power supply in the microwave frequency regime (2.45 GHz) are used to produce plasma inside the cavity. The plasma parameters at different pressures and power levels in combination with the analysis of the Nb sample etched will be used to determine the adequate frequency regime for plasma etching of Nb cavities.

TUPO044

Correction of a Superconducting Cavity Shape Due to Etching, Cooling Down and Tuning

V.D. Shemelin (CLASSE)

Corrections of shape needed for an SRF cavity after fabrication are presented in a convenient form with a possibility to take into account different technological procedures, such as etching, cooling down and pre-loading.

Funding: Supported by NSF award DMR-0807731

Status of Investigations on Degradation of Cavities in DESY Acceleration Modules

In the last decade the degradation of cavity acceleration gradients is observed frequently in module RF tests, after the assembly and installation of complete accelerator modules. In some cases no explanation for these degradations could be found from quality control records, assembly procedure protocols or notes from observers. On the PXFEL3 module quench limitations without indication of field emission loading is observed at two cavities. Boundary conditions like storage of resonators, cleaning process for ISO 4 clean room as well as the assembly processes and handling of the resonators are under investigation. The two degraded cavities of module PXFEL 3 are removed from the cavity string and studied intensively. The actual status of our research is presented.

A. Matheisen, B. Horst, van der, D. Kostin, N. Krupka, S. Saegbarth, M. Schalwat, P. Schilling, M. Schmoekel, H. Weitkaemper (DESY)

TUPO045

Update on Large Grain Cavities with 45 MV/m in a Nine-Cell Cavity at DESY

Since 2009 a series of eight nine-cell cavities (AC151 – AC158) of TESLA shape fabricated of large grain (LG) niobium material is under preparation and test at DESY. In a first step all cavities were tested after a BCP treatment. In a second step additional electro polishing is applied to all cavities. In this paper the treatment will be discussed and a first excellent result of AC155 will be reported.

D. Reschke, S. Aderhold, A. Goessel, J. Iversen, S. Karstensen, D. Kostin, G. Kreps, A. Matheisen, W.-D. Moeller, F. Schlander, W. Singer, X. Singer, N. Steinhau-Kuehl, A.A. Sulimov, K. Twarowski (DESY)

TUPO046

Progress in Developing 500MHz Nb Cavity at SINAP

The SRF system has been operated for 3 years since the final acceptance test of 500MHz superconducting module in 2008. The R&D on niobium superconducting cavity at SINAP has been carried out to reach some exciting results. The whole fabrication procedure on developing a 500MHz single cell cavity including the deep-drawing, electron beam welding, surface processing and vertical testing will be reported in detail. The final vertical test results show that the fabricated niobium cavity has a good performance of reaching as high as 10MV/m accelerating gradient and quality factor better than $4 \cdot 10^8$.

J.F. Liu, Z.Q. Feng, H.T. Hou, C. Luo, Z.Y. Ma, D.Q. Mao, Zh.G. Zhang, S.J. Zhao, Y.B. Zhao (SINAP) Z. Li, **J.F. Liu**, H. Yu, X. Zheng (Shanghai KEY Laboratory of Cryogenics & Superconducting RF Technology) B. Yin (Graduate University, Chinese Academy of Sciences)

TUPO047

TUPO0048

Commissioning and Upgrade of Automatic Cavity Tuning Machines for the European Xfel

J.H. Thie, A. Goessel, J. Iversen, D. Klinke, G. Kreps, W.-D. Moeller, C. Mueller, H.-B. Peters, A.A. Sulimov, D. Tischhauser (DESY) D. Bhogadi, R.H. Carcagno, T.N. Khabiboulline, S. Kotelnikov, A. Makulski, R. Nehring, J.M. Nogiec, W. Schapert, C. Sylvester (Fermilab)

Four new tuning machines were developed and built in a collaborating effort among FNAL, KEK and DESY. Two machines were commissioned at DESY in a close teamwork with FNAL. For several months, these machines have been used regularly for the automatic tuning

of different types of cavities for FLASH. Due to this operating experience and the requirements for the European XFEL cavity Specification, it was necessary to implement the following improvements: improve the precision of the eccentricity measurement; change the tuning sequence according to the different production stages in the cavity fabrication and preparation process; review and change the machine access procedures according to the safety aspects of the EC Directive of Machinery. These improvements required changes in both the mechanical parts developed by DESY and the electronics and software developed by FNAL. We report in detail about the commissioning, our tuning experience and the necessary improvements.

TUPO0049

Q0 Improvement of Large-Grain Multi-Cell Cavities by Using JLab's Standard ILC EP Processing

R.L. Geng, G.V. Ereemeev, P. Kneisel (JLAB) K.X. Liu, X.Y. Lu, K. Zhao (PKU/IHIP)

As reported previously at the Berlin workshop, applying the JLab standard ILC EP recipe on previously BCP etched fine-grain multi-cell cavities results in

improvement both in gradient and Q0. We recently had the opportunity to experiment with two 1300 MHz 9-cell large-gain niobium cavities manufacture by JLab and Peking University. Both cavities were initially BCP etched and further processed by using JLab's standard ILC EP recipe. Due to fabrication defects, these two cavities only reached a gradient in the range of 20-30 MV/m. Interestingly both cavities demonstrated significant Q0 improvement in the gradient range of 15-20 MV/m. At 2K, a Q0 value of $2 \cdot 10^{10}$ is achieved at 20 MV/m. At a reduced temperature of 1.8K, a Q0 value of $3 \cdot 10^{10}$ is achieved at 20 MV/m. These results suggest that a possible path for obtaining higher Q0 in the medium gradient range is to use the large-grain material for cavity fabrication and EP and low temperature bake for cavity processing.

Funding: This work was authored by Jefferson Science Associates, LLC under U.S. DOE Contract No. DE-AC05-06OR23177

TUPO0050

Studies on Transportation of Superconducting Resonators and Beam Position Monitors - Quadrupol Units for the XFEL Project

A. Schmidt, R. Bandelmann, H. Brueck, A. Matheisen, J. Schaffran (DESY)

For the XFEL project industrial companies in Germany and Italy are in charge of the cavity fabrication and preparation.

For the radio frequency acceptance test at 2 K at DESY these cavities have to be transported to the DESY site in Hamburg without losing the performance. The XFEL Beam position monitor and Quadrupol units (BQU) are completed in the DESY clean room. The Cavities and the BQU are handed out in the status "ready for assembly" to the string assembly site at CEA Saclay. To ensure that the transports over European routes do not influence the performance of cavities or are origin of particulates inside the BQU, individual transport boxes for super conduction cavities and transport fixtures for the BQU and are designed and tested.

High-Temperature Heat Treatment Study on a Large-Grain Nb Cavity

Improvement of the cavity performance by a high-temperature heat-treatment without subsequent chemical etching have been reported for large-grain Nb

cavities treated by buffered chemical polishing, as well as for a fine-grain cavity treated by vertical electropolishing [1]. Changes in the quality factor, Q_0 , and maximum peak surface magnetic field achieved in a large-grain Nb single-cell cavity have been determined as a function of the heat treatment temperature, between 600 °C and 1200 °C. The highest Q_0 improvement of about 30% was obtained after heat-treatment at 800 °C-1000 °C. Measurements by secondary ion mass spectrometry on large-grain samples heat-treated with the cavity showed large reduction of hydrogen concentration after heat treatment.

[1] G. Ciovati, G. Myneni, F. Stevie, P. Maheshwari, and D. Griffis, Phys. Rev. ST Accel. Beams 13, 022002 (2010)

Funding: This manuscript has been authored by Jefferson Science Associates, LLC under U.S. DOE Contract No. DE-AC05-06OR23177

G. Ciovati, P. Dhakal, R. Myneni (JLAB) P. Maheswari, F.A. Stevie (NCSU AIF)

TUPO051

Fabrication and Test of 500MHz Nb Cavity for BEPCII

In order to ensure the stable operation of BEPCII, we had began a superconducting accelerator unit in IHEP 3 years ago. The

development and test of 500MHz Nb cavity, which is the key component of the unit, are introduced in this article. The fabrication of three Nb cavities has been finished, and the post-processing and vertical test of the 1st cavity have been completed, too. The technology of fabrication, electron beam welding (EBW), post-processing has been developed. Meanwhile, the related facilities has been improved, too.

G.W. Wang (IHEP Beijing)

TUPO052

Optical Inspection of SRF Cavities at Fermilab

The production of an SRF cavity includes a string of multiple treatments at different facilities before the cavity can be RF-

tested in a cryogenic system. Many of the processing steps change the cavity surface and affect the RF performance of the cavity. Interjection of optical inspections between these steps provides us with an instant feedback on the processes involved as well as giving us new insight on the mechanisms responsible for forming surface abnormalities. The major drawback of inclusion of frequent optical inspections is the increased amount of time and labor in the cavity production cycle. An optical inspection of equatorial and iris welds of a 1.3GHz TESLA-shape cavity produces about two thousand pictures. We developed an automated procedure where a computer takes over the most of the routine operations including adjusting the camera focus. With that automation, the inspection currently takes about three hours and little operator time. We will describe the developed system including the focusing algorithm and discuss the ways to further optimize the procedure.

E. Toropov, D.A. Sergatskov (Fermilab)

TUPO053

TUPO054

SRF Cavity Surface Topography From Optical Inspection

E. Toropov, D.A. Sergatskov (Fermilab)

Characteristics of the cavity surface geometry such as roughness affect cavity performance. The optical cavity inspection system at Fermilab allows us to obtain pictures of cavity surface at different lightning conditions. By analyzing the images of some fixed location inside the cavity taken while the light source moves progressively along the axis we can deduce some topographical information of that surface. In the large-grain cavities after BCP, grains are oriented at distinct angles to the surface and, therefore, reflect light in different directions. We developed a simple algorithm to calculate the angle distribution of the grains and thus to estimate the roughness. We discuss this method and the results of the analysis of the actual cavity surface.

TUPO055

Horizontal SRF Cavity Testing at Fermilab

A. Hocker, E.R. Harms, A. Lunin, A.I. Sukhanov (Fermilab)

Fermilab makes use of a single-cavity test cryostat to assess the performance of dressed superconducting RF cavities using pulsed high-power RF before they are assembled into a cryomodule. Cavity performance is evaluated in terms of accelerating gradient, unloaded quality factor, and field emission. The functionality of auxiliary components such as tuners and fundamental power couplers is also verified. The latest results from extensive testing of nine-cell 1.3 GHz cavities are presented here, along with a discussion of future extensions of the horizontal test program to include 650 MHz cavities and continuous wave testing.

Funding: U.S. Department of Energy, Contract No. DE-AC02-07CH11359

TUPO056

Dewar Testing of $\beta = 0.53$ Half Wave Resonators at MSU

J. Popielarski, A. Facco, W. Hartung, J. Wlodarczak (FRIB)

Michigan State University is developing quarter wave and half wave resonators to accelerate stable ions to 200 MeV per nucleon or higher for the Facility for Rare Isotope Beams (FRIB). The final stage of acceleration is done with half wave resonators designed for an optimum velocity of $\beta = v/c = 0.53$, with a resonant frequency of 322 MHz. Five resonators have been constructed so far, with the first prototype fabricated by MSU staff and the remaining four fabricated in cooperation with industrial partners. Over 150 additional resonators for $\beta = 0.53$ are required for the FRIB linac. Results of Dewar testing to characterize the RF performance of the resonators will be presented in this paper.

Funding: This material is based upon work supported by the U.S. Department of Energy Office of Science under Cooperative Agreement DE-SC0000661.

Buffered Chemical Polishing Development for the $\beta=0.53$ Half-Wave Resonator for the Facility for Rare Isotope Beams

The $\beta=0.53$ half wave resonator is being developed for the Facility for Rare Isotope Beams. One MSU prototype resonator and four industry made resonators have been fabricated. The proposed surface treatment is buffered chemical polishing (BCP) and high pressure rinsing with ultra pure water. The BCP process is being optimized to achieve resonator performance goals during certification testing. Research is focused on the improvement of the damaged layer removal (uniformity), the heat exchanger design, and the quality of BCP acid solution. Several etches have been completed on the half wave resonators and process data, such as removal rate, temperature profiles, and niobium concentration in solution collected. The process data was studied versus the vertical test results; maximum accelerating voltage, quality factor and field emission onset voltage. The chemistry fixture development and process data versus test results will be presented.

L. Popielarski, L.J. Dubbs, K. Elliott, I.M. Malloch, R. Oweiss, J. Popielarski (FRIB)

Funding: This material is based upon work supported by the U.S. Department of Energy Office of Science under Cooperative Agreement DE-SC0000661.

TUPO057

CERN SRF Assembling and Test Facilities

CERN is currently upgrading and refurbishing its RF and cryogenic facilities in the SM18 assembly hall with the aim of testing SRF cavities and cryo-modules of various provenience. They concern new and spare cavities for the HIE-ISOLDE upgrade, SPL study and LHC collider. These projects require a redistribution of space, refurbishment of cleanrooms, modification of SRF test stands, of vertical cryostats and of the lHe supply line. This poster presents the specifications of the refurbished facility and the technical choices required for the assembling, processing and testing of superconducting RF cavities.

J.K. Chambrillon, O. Brunner, P. Maesen, O. Pirotte, M. Therasse, B. Vullierme, W. Weingarten (CERN)

SRF Cavity Processing and Cleanroom Facility Upgrades at Michigan State University

The Michigan State University (MSU) Superconducting Radio Frequency (SRF) cavity processing and coldmass assembly infrastructure is being upgraded to meet

L. Popielarski, L.J. Dubbs, K. Elliott, I.M. Malloch, R. Oweiss, M. Williams (FRIB)

the production needs of multiple SRF projects, including the driver linac for the Facility for Rare Isotope Beams and the MSU Reaccelerator. The objective is to modify the current infrastructure to increase throughput and optimize the process workflow, while minimizing impact to the overall preproduction schedule. Facility upgrades include a cleanroom addition, chemistry room addition, part etching lab, cleanroom preparation area, and a new ultra pure water system. New handling fixtures and specialized tools are being implemented. Methods are being developed to streamline the workflow, increase repeatability, enhance process safety and reduce cross contamination and waste. The proposed work center layout, process capabilities, optimized workflow strategies, and plans for continuous improvement will be presented.

Funding: This material is based upon work supported by the U.S. Department of Energy Office of Science under Cooperative Agreement DE-SC0000661.

TUPO058

TUPO059

TUPO060

Dewar Testing of $\beta = 0.085$ Quarter Wave Resonators at MSU

J. Popielarski, A. Facco, W. Hartung, J. Wlodarczak (FRIB)

Michigan State University is developing and testing quarter wave resonators for a superconducting linac which will be used to reaccelerate exotic ions to 3 MeV per nucleon or higher (ReA3). Eight quarter wave resonators with an optimum velocity of $\beta = v/c = 0.085$ and a resonant frequency of 80.5 MHz are required for the third cryomodule, which will complete the first stage of the reaccelerator linac. Approximately 100 additional $\beta = 0.085$ resonators of the same design will be required for the Facility for Rare Isotope Beams (FRIB). Results of Dewar testing to characterize the RF performance of the resonators will be presented in this paper.

Funding: This material is based upon work supported by the U.S. Department of Energy Office of Science under Cooperative Agreement DE-SC0000661.

TUPO061

Preparation and Testing of the SRF Cavities for the CEBAF 12 GeV Upgrade

A. Reilly, T. Bass, A. Burrill, G.K. Davis, F. Marhauser, C.E. Reece, M. Stirbet (JLAB)

80 new 7-cell, LL cell-shaped cavities are required for the CEBAF 12 GeV Upgrade project. In addition to ten pre-production units fabricated at JLab, the full set of commercially-produced cavities have been delivered. An efficient processing routine, which includes a controlled 30 micron EP, has been established to transform these cavities into qualified 8-cavity strings. This work began in 2010 and will run through the end of 2011. The realized cavity performance consistently exceeds project requirements and also the maximum useful gradient in CEBAF: 25 MV/m. We will describe the cavity processing and preparation protocols and summarize test results obtained to date.

Funding: Authored by Jefferson Science Associates, LLC under U.S. DOE Contract No. DE-AC05-06OR23177.

TUPO062

Vertical Electro-Polishing at CEA Saclay: Commissioning of a New Set-Up and Modeling of the Process Applied to Different CavitiesF. Eoziz¹/₂nou, S. Chel, Y. Gasser, J.P. Poupeau, C. Servouin, Z. Wang (CEA/DSM/IRFU)

High performance required for elliptical low beta cavity makes the electro-polishing desirable for their surface treatment. For large dimension cavities, the EP treatment in vertical configuration (abbreviated as VEP) is more appropriate. A VEP set-up has been designed at Saclay for the electro-polishing of such cavities. The electrolyte will be circulating and the process automated, including several safety procedures. Chosen equipment will make it possible to use a wide range of parameters (voltage, flowrate, temperature, nitrogen inerting) with R&D purpose in mind. R&D will guide the choice of adapted parameters in such configuration. In addition, VEP has been modeled using COMSOL software with 2D axi - symmetry configuration for 2 different cavities: - 9Cell ILC cavity - Proton 5Cell cavity for SPL accelerator. Different cathodes have been designed to optimize the fluid and the electric field distribution during VEP. Respective results will be presented. At last, importance of the size of the cavity will be commented.

Funding: We acknowledge the support of the Eucard, ILC HiGrade and ASTRE programs.

MgB₂ Films on Metallic Substrates with Different Surface Roughness

For coating RF cavities with MgB₂ films, a suitable metallic substrate material and appropriate surface roughness need to be

C.G. Zhuang, K. Chen, A. Krick, Q.Y. Lei, T. Tan, X. Xi (TU)

investigated. Here we report the properties of MgB₂ films grown by hybrid physical-chemical vapor deposition on different metallic substrates, Nb, stainless steel, Mo, and Ta, with different degrees of surface roughness. Using mechanical polishing, the root-mean-square (RMS) roughness of the Nb surface is reduced to below 5nm. The surface morphology of the MgB₂ films shows significant improvement in uniformity and reduction of RMS roughness as the substrate roughness is reduced. Superconducting properties and microwave properties of these films will be discussed. The comparison of the films on different metallic substrates is also presented.

Funding: This work is supported by DOE under grant No. DE-SC0004410.

TUPO063

Large-Area MgB₂ Films by Hybrid Physical Chemical Vapor Deposition

Large-area MgB₂ films with 2" diameter are fabricated by hybrid physical chemical vapor deposition. Their properties

X. Xi, K. Chen, A. Krick, Q.Y. Lei, T. Tan, C.G. Zhuang (TU)

are characterized by x-ray diffraction, atomic force microscopy, scanning electron microscopy, and transport measurements. Films on c-cut sapphire wafers grow epitaxially with c-axis normal to the substrate surface. Films grown on niobium wafers are polycrystalline with random orientations among the grains. The superconducting properties of the films are tested by dicing the 2" inch wafers into 8mm x 8mm small pieces. The uniformities of T_c and J_c(H) with field up to 9T across the wafers are measured. The superconducting properties of the polycrystalline films on niobium are compared to those of the epitaxial films on sapphire. The RF properties of the MgB₂ films will be discussed.

Funding: This work is supported by DOE under grant No. DE-SC0004410.

TUPO064

Economical Manufacture of Seamless High-Purity Niobium

Ultramet continues to develop a fabrication methodology to construct high-performance (RRR>200), seamless niobium superconducting radio frequency (SRF) cavity cells on low-cost removable mandrels utilizing advanced chemical vapor deposition (CVD) technologies. Optimization of the CVD niobium material and process to improve as-deposited niobium purity levels has resulted in the consistent rapid deposition of RRR>200 niobium at structural thicknesses suitable for accelerator applications. Boundary layer material applications on removable low-cost mandrels used successfully in previous work were further optimized and characterized. Basic CVD niobium joining/welding capabilities have been demonstrated as a potential alternative to electron beam welding, and preliminary mechanical and microstructural characterization of the joined area were performed.

V.M. Arrieta, S.R. McNeal (Ultramet)

Funding: U.S. Department of Energy, Small Business Innovation Research (SBIR) program, grants DE-FG02-05ER84175 and DE-SC0002721

TUPO065

TUPO066

Analysis of Recent Results from Second Sound, Temperature Mapping and Optical Inspection of 1.3 GHz Cavities at DESY

F. Schländer, S. Aderhold, D. Reschke, K. Twarowski (DESY)

DESY is preparing for the delivery of some 600 superconducting 9-cell cavities for the European XFEL. Analysing the history and recorded data of recently tested cavities gives important evidence for proper treatment, preparation and handling of cavities. The experience given by temperature mapping, the Second Sound technique and optical inspection will be compared and an overview of the results obtained so far will be given in this report.

TUPO067

E HIE ISOLDE QWR: Progress in Magnetron and Bias Diode Sputtered Niobium Thin Film Coating

G. Lanza, S. Calatroni, O. Capatina, B. Delaup, L. Marques Antunes Ferreira, M. Pasini, M. Therasse (CERN)

The R&D program for coating the Quarter Wave Resonator for the HIE-ISOLDE project started at CERN in 2008. Since then the CERN facilities for surface treatment and niobium coating have been upgraded and adapted to improve process reproducibility. Two coating techniques, Magnetron Sputtering and Bias Diode Sputtering have been tested and are being optimized to achieve the required film quality and thickness homogeneity. This poster shows the two sputtering configurations, as well as the results of the surface treatments and coatings. Details of the latest RF test are presented.

CERN

CH - 1211 Geneva 23

TUPO068

Electropolishing of Niobium to Obtain Defect Free Surface

A. Chandra, G. Frankel, M. Sumption (Ohio State University)

The SRF cavities needs to have a good surface finish to achieve maximum performance. Surface defects like grain boundaries, bumps and pits limit the maximum field gradients achieved. Electropolishing (EP) is commonly used as a final surface finishing process. Acid concentration, stirring, temperature and amount of material removed are the parameters expected to affect the surface finish and their effect is studied using flat Nb specimens. Optical microscope, SEM and optical profilometer have been used to characterize the level of surface finish obtained. The mechanism of EP is not fully understood. To explore the mechanism and parameters necessary for optimum surface finish, an electrolytic cell made of 99.999% pure Al has been designed which also serves as the counter electrode. The mechanism involves the formation of a viscous layer on the Nb surface. There is evidence for the formation of this film in electrochemical experiment results and optical observations. The film is in fact critical to the EP mechanism as it has been found that the surface is pitted where a stable viscous film can not be formed.

Funding: This work supported by United States Department of Energy Grant DE-SC0004217

TUIOC — Hot Topics

Medium Field Q-Slope and Paths to High-Q Operation

Superconducting RF cavities for accelerator application offer, at least in principle, the perspective of large accelerating gradients and low RF losses. Both qualities must proceed reciprocally. Therefore, consequent to the achieved increase in accelerating gradient during recent years, the RF losses must be reduced accordingly, in order to keep the cryogenic installation at reasonable size. However, the Q-value, which describes the RF losses, did not follow the improved accelerating gradient as wished or required. The reasons are physical mechanisms, only partly understood, on top of the residual losses, that provoke a more than quadratic increase of the RF losses with the accelerating gradient (Q-slope). Cures have been identified experimentally to some extent, but both the theoretical understanding and a complete elimination of the "Q-slop" are lacking. The hot topic discussion should open the floor for a new and deeper understanding of the "Q-slop".

HOT TOPIC

WEIOA — R&D/Diagnostics

WEIOA01

Quantitative EP Studies and Results for SRF Nb Cavity Production

H. Tian, C.E. Reece (JLAB)

To achieve high performance and reliability, which is essential for Nb SRF cavities production, it is important for us to understand Nb EP in detail so that we can tailor it to the best effect. The analytical tools of electrochemistry and surface topography are the means of developing such understanding. In this talk, the recent incorporation of analytic electrochemical techniques into the development of well controlled protocols for Nb EP will be reported, such as using three electrode method for polarization curve measurements, EIS to understand the mechanism of EP, and RDE to study the diffusion coefficient of active species of F ions, and the related diffusion layers etc. In parallel, investigations for monitoring scale-dependent Nb surface morphology evolution under different Nb EP parameters, which is expected to lead to matrix a best EP parameter and have a predictive power to describe the Nb surface evolution during EP will be demonstrated. Early lessons learned that are relevant to Nb cavities will be introduced, and directions for the future are aimed at well control, high reproducibility, efficient, and geometry independent EP process for coming SRF-based projects.

WEIOA02

Centrifugal Barrel Polishing (CBP) of SRF Cavities Worldwide

C.A. Cooper (Fermilab) B. Bullock (CLASSE) S.C. Joshi (RRCAT)
A.D. Palczewski (JLAB) K. Saito (KEK)

Much interest was generated in the mid to late 1990s in an alternative cavity surface processing technique called CBP, that mechanically polishes the inside of SRF cavities by rotating them at high speeds while filled with abrasive media. This work, which was originally done at KEK by Kenji Saito & Tamawo Higuchi, has received renewed interest recently because of work done at Fermilab which has produced mirror like finishes on the 1.3 GHz Tesla-type cavity SRF surface. In addition to Fermilab & KEK, Cornell, Jefferson Lab and RRCAT are all exploring CBP as a cavity processing technique. CBP is interesting as a cavity processing technique because it removes defects associated with the manufacturing process, it can yield surface finishes (Ra) on the order of 10s of nanometers, it is a simple technology that could transfer easily to industry, it could help increase cavity yields and it requires less acid than other techniques. Recent progress and the current status of CBP as a baseline and repair technique will be discussed.

WEIOA03

A New Electropolishing System For Low-Beta SC Cavities

S.M. Gerbick, M.P. Kelly, R.C. Murphy, T. Reid (ANL)

A new electropolishing system designed for a completed low-beta niobium SC cavity with integral helium vessel was installed and operated at Argonne National Laboratory. The design was based on that used for the electropolishing of 1.3 GHz 9-cell elliptical cavities for the global ILC development effort at ANL, with the addition of direct water cooling to the cavity surface. This design also allows for repeated chemistry on the cavity, if needed, without producing the rougher surface associated with buffered chemical polishing.

Review of RF - Sample - Test Equipment and Results

The surface resistance of superconducting samples can be derived from the heat dissipation under RF exposure. This requires challenging and sometimes opposing design constraints. The samples shall be small and easily exchangeable. The RF magnetic field on the sample surface shall be large and homogeneous. It must not be limited by the host cavity. A calorimetric technique enables precise measurements and has therefore recently gained much interest. One of the devices exploiting this technique at multiple frequencies is the Quadrupole Resonator. Its measurement capabilities and limitations are discussed and compared with similar devices. Results on bulk niobium and niobium film on copper samples are presented. It is shown how different contributions to the surface resistance depend on temperature, applied RF magnetic field and frequency. Furthermore measurements of the maximum RF magnetic field as a function of temperature and frequency in pulsed and CW operation are presented.

T. Junginger, W. Weingarten (CERN) **T. Junginger** (MPI-K)
C.P. Welsch (Cockcroft Institute)

The RF magnetic field on the sample surface shall be large and homogeneous. It must not be limited by the host cavity. A calorimetric technique enables precise measurements and has therefore recently gained much interest. One of the devices exploiting this technique at multiple frequencies is the Quadrupole Resonator. Its measurement capabilities and limitations are discussed and compared with similar devices. Results on bulk niobium and niobium film on copper samples are presented. It is shown how different contributions to the surface resistance depend on temperature, applied RF magnetic field and frequency. Furthermore measurements of the maximum RF magnetic field as a function of temperature and frequency in pulsed and CW operation are presented.

Funding: Work supported by the German Doctoral Students program of the Federal Ministry of Education and Research (BMBF)

WEIOA04

X-Ray Tomography Inspection of SRF Cavities

Performance issues with superconducting cavities and a desire for an enhanced non-invasive view of the interior of a cavity compared to that provided by optical means has led us to inspection using 3-dimensional X-ray tomography. This technique has provided the necessary view of suspected faults in Higher Order Mode couplers. This success naturally leads to determining if x-ray inspection of welds and other potential cavity defects might prove to be helpful during cavity fabrication. Results of x-ray scans from commercial vendors and potential for this technique will be presented.

E.R. Harms, H.T. Edwards (Fermilab)

This success naturally leads to determining if x-ray inspection of welds and other potential cavity defects might prove to be helpful during cavity fabrication. Results of x-ray scans from commercial vendors and potential for this technique will be presented.

Funding: Operated by Fermi Research Alliance, LLC under Contract No. DE-AC02-07CH11359 with the United States Department of Energy.

WEIOA05

Effect of Deformation and Heat Treatment on the Thermal Conductivity of Large Grain Superconducting Niobium

Superconducting radio frequency cavity fabrication involves large-scale deformation of niobium at room temperature, exposing the material to engineering strains as large as 40%. Deforming metals introduces dislocations in the bulk material, resulting in changes in microstructure and thermophysical response. Deformation and the resulting dislocations in niobium have been shown to alter the thermal conductivity, especially at temperatures below 3 K where phonons dominate heat conduction. With the increased number of high-energy physics applications requiring cavities to operate at temperatures of about 2 K, improved understanding of the variation of phonon conduction between 1.6 K and 3 K will aid in design for these applications. Thermal conductivity measurements have been performed on niobium specimens from several large grain ingot discs with varying RRR and Ta content. The effect of 1% to 20% uniaxial straining and several recovery heat treatment protocols on the electron and phonon conduction regimes of the superconducting niobium specimens is presented. The effects of RRR and Ta content of the parent material on the thermal conductivity of the specimens are also discussed.

S.K. Chandrasekaran (MSU) T.R. Bieler (Michigan State University) C. Compton (FRIB) N.T. Wright ((MSU))

Deforming metals introduces dislocations in the bulk material, resulting in changes in microstructure and thermophysical response. Deformation and the resulting dislocations in niobium have been shown to alter the thermal conductivity, especially at temperatures below 3 K where phonons dominate heat conduction. With the increased number of high-energy physics applications requiring cavities to operate at temperatures of about 2 K, improved understanding of the variation of phonon conduction between 1.6 K and 3 K will aid in design for these applications. Thermal conductivity measurements have been performed on niobium specimens from several large grain ingot discs with varying RRR and Ta content. The effect of 1% to 20% uniaxial straining and several recovery heat treatment protocols on the electron and phonon conduction regimes of the superconducting niobium specimens is presented. The effects of RRR and Ta content of the parent material on the thermal conductivity of the specimens are also discussed.

Funding: This work was supported by the U.S. Department of Energy, Office of High Energy Physics, through Grant No. DE-S0004222.

WEIOA06

WEIOB — R&D/Diagnostics/Fabrication

WEIOB01

Guided Cavity Repair with Laser, E - Beam and Grinding

G. Wu (ANL)

Recent cavity processing statistics indicate that the development of RF superconductivity has reached a stage where more and more cavities were limited by quench and not by field emissions. The combination of high resolution optical inspection, cavity quench detection and surface replica revealed more than half of the cavity quenches were limited by identifiable surface features, namely pits or bumps. The quench field ranged from 12.7 MV/m up to 42 MV/m. Several methods have been explored in various laboratories to remove the surface features. Those included the laser re-melting, Electron beam re-melting and local mechanical grinding. This paper reports the latest development of those guided repair technologies and their benefits to improve cavity performances.

Funding: Work supported by U.S. Department of Energy under contract # DEAC02-07CH11359

WEIOB02

Cavity Inspection and Repair Techniques

K. Watanabe, H. Hayano (KEK) Y. Iwashita (Kyoto ICR)

The cavity inspection and repair techniques are important to study a quality control of the superconducting rf cavity for better yield with high accelerating gradient. A high-resolution camera system was developed for optical inspection in 2008. It enables 2-D analysis by image processing on inner surface of the cavity. Therefore, the cause to limit the cavity performance can be categorized into a geometrical defect or an assembly work and the surface treatment. In addition, by performing the optical inspection at each treatment, we can obtain an information when a defect appeared. The cavities that quenched at the low field were inspected. One or few geometrical defects were found around quench location on some of these cavities. It is a possibility that the cavity performance can be recovered by removing the geometrical defect at the quench location. A local grinding machine was developed for this purpose. This method was tested on the 9-cell cavities, and we succeeded to recover the cavity performance with combination of local grinding and light EP. The method and results of the cavity inspection as well as the replica techniques will be presented in this talk.

WEIOB03

Improvement in Cavity Fabrication Technology and Cost Reduction Methods

K. Sennyu, H. Hara, H. Hitomi, K. Kanaoka, T. Yanagisawa (MHI)

Cavity fabrication method with new forming technology and Laser welding technology are reported. 1.3GHz 9-cell cavity with Laser welding technology for stiffener and flange joint is achieved 29 MV/m at vertical test at KEK and 1.3GHz 2-cell seamless dumbbell cavity are fabricated at MHI for verifying the fabrication method. These are reported in detail. Some other fabrication technology for cost reduction and stable quality are introduced.

XFEL Cavity Procurement as an Example of Technology Transfer

Procurement of superconducting RF cavities for the European XFEL consists of two phases. The preparation phase for the European XFEL cavity production includes: qualification of high purity niobium vendors and potential cavity producers; accommodation of the TESLA cavity design to the XFEL demands; establishing the XFEL treatment process, work out and check the strategy of preparation for the vertical acceptance test; define the documentation and prompt data transfer, qualification of created infrastructure, cavity acceptance criteria and tests. A detailed specification has been worked out on the basis of ca. 50 prototype cavities. Production of 600 cavities is currently contracted on the principle "build to print"; the cavity material will be provided by DESY. DESY will supply vendors with machine for cavity tuning at room temperature and equipment for RF measurement of dumb bells and end groups. The cavity with helium tank has to be built as a component according Pressure Equipment Directive (PED) 97/23/EC. The contracted "notified body" will supervise the material qualification and procurement. Monitoring of the vendor's work will be executed by DESY and INFN (Milano) team.

W. Singer (DESY)

WEIOB04

Large Grain Cavities: Fabrication, RF Results and Optical Inspection

SRF cavities produced from large grain niobium material have been investigated as an alternative to the standard fine

grain material in the past years. While many single cell cavities have been prepared and successfully tested, the number of large grain 9-cell cavities available at the laboratories worldwide is still small. The worldwide experience and results with fabrication, treatment and testing will be compared. At DESY, a batch of eight large grain 9-cell cavities has been processed and tested recently, in addition to three cavities that had been processed and tested earlier. The surface preparation process has been closely followed by optical inspection in-between all treatment steps that include surface removal. Several of the vertical RF tests have been done with T-mapping and/or second sound measurements for determination of the quench location. The results after a first treatment cycle with BCP and a second treatment cycle with EP will be presented.

S. Aderhold (DESY)

WEIOB05

IHEP 1.3GHz Low-Loss Large Grain 9-cell cavity R&D for ILC

The combination of the low-loss shape and large grain niobium material is expected to be the possible way to achieve higher gradient and lower cost for ILC 9-cell cavities, and will be essential for the ILC 1 TeV upgrade. As the key component of the "IHEP 1.3 GHz SRF Accelerating Unit Project", a low-loss shape 9-cell cavity using Ningxia large grain niobium (IHEP-01) was fabricated and surface treated (CBP, CP, annealing, pre-tuning) at IHEP. The cavity reached 20 MV/m in the first vertical test at KEK STF on July 2010. The quench locations were found by T-mapping and optical inspection. Equator defects were removed by further CBP treatment. Second vertical test on this cavity was done at JLAB recently after 2nd processing at IHEP. This paper reports the latest result of the vertical test and surface diagnostics.

J.Y. Zhai, J.P. Dai, J. Gao, D.Z. Li, Z.Q. Li, Z.C. Liu, Q.Y. Wang, T.X. Zhao (IHEP Beijing)

WEIOB06

THIOA — $\beta=1$ Cavities

THIOA01

Test Results of the International S1-Global Cryomodule

Y. Yamamoto, M. Akemoto, S. Fukuda, K. Hara, H. Hayano, N. Higashi, E. Kako, H. Katagiri, Y. Kojima, Y. Kondo, T. Matsumoto, H. Matsushita, S. Michizono, T. Miura, H. Nakai, H. Nakajima, K. Nakanishi, S. Noguchi, N. Ohuchi, T. Saeki, M. Satoh, T. Shidara, T. Shishido, T. Takenaka, A. Terashima, N. Toge, K. Tsuchiya, K. Watanabe, S. Yamaguchi, A. Yamamoto, K. Yokoya, M. Yoshida (KEK) C. Adolphsen, C.D. Nantista (SLAC) T.T. Arkan, S. Barbanotti, M.A. Battistoni, H. Carter, M.S. Champion, A. Hocker, R.D. Kephart, J.S. Kerby, D.V. Mitchell, T.J. Peterson, Y.M. Pischalnikov, M.C. Ross, W. Schappert, B.E. Smith (Fermilab) A. Bosotti, C. Pagani, R. Papparella, P. Pierini (INFN/LASA) K. Jensch, D. Kostin, L. Lilje, A. Matheisen, W.-D. Moeller, P. Schilling, M. Schmoekel, N.J. Walker, H. Weise (DESY)

S1-Global collaborative project by joint efforts of INFN, DESY, FNAL, SLAC and KEK, finished successfully at KEK- STF on February in 2011, is a crucial project for ILC. For this project, 8 SRF cavities, 2 from DESY, 2 from FNAL and 4 from KEK, were installed into one cryomodule with the thermal shields and the cooling pipes of liquid helium and nitrogen, cooled down to 2K totally three times, and cold-tested by using the three different frequency tuning systems (Blade tuner from INFN/FNAL, Saclay tuner from DESY and Slide-Jack tuner from KEK) and two types of input couplers (TTF III from DESY and STF#2 from

KEK). During the cold test with high power, cavity performance, LFD (Lorentz Force Detuning) compensation by Piezo actuator, simultaneous 7 SRF cavities operation, dynamic heating loss measurement including static loss and DRFS (Distributed RF Scheme) operation with LLRF (Low Level RF) feedback system, were established successfully. In this talk, the results of the S1-Global cryomodule test are reported, discussed and summarized.

THIOA02

Gradient R&D in the US

J.P. Ozelis (Fermilab)

Over the past few years, significant effort has been made to systematically improve multi-cell cavity accelerating gradients,

driven in large part by the requirements of the ILC, for which the reproducible achievement of high gradients is a prerequisite. Substantial progress has been made by teams at Cornell University, Fermilab, and Jefferson Lab, in pushing gradients to higher values and in achieving this performance on a more regular basis. Development of improved diagnostic/inspection techniques along with the utilization of both localized and global repair tools have helped enable this improvement. Likewise, processing and assembly procedures that led to a lower incidence of field emission have facilitated this progress. The present status of cavity performance will be presented along with its evolution, and examples of the role the aforementioned techniques and tools have played in achieving this performance.

Funding: cOperated by Fermi Research Alliance, LLC under Contract No. DE-AC02-07CH11359 with the United States Department of Energy.

THIOA03

Compact Superconducting Cavities for Deflecting and Crabbing Applications

J.R. Delayen (ODU)

There is increasing interest in using superconducting cavities as rf separators (e.g. Jefferson Lab 12 GeV upgrade and

Fermilab Project X) or as crabbing systems to increase the luminosity in colliders (e.g. LHC upgrade and electron-ion colliders). Several of these applications have severe dimensional constraints that would prevent the use of cavities operating in the TM110 mode. A number of compact designs for deflecting/crabbing cavities have been designed and are under development; their properties are presented.

QWR for $\beta \sim 1$ Accelerators

The Superconducting Quarter Wave Resonator (QWR) was developed first for heavy ion acceleration in 1981 and became highly successful and widespread in low β linacs. Recently the QWR has been adapted for a variety of applications for high particle velocity, near $\beta=1$. The applications are varied, from the use in a relativistic hadron storage ring, to photocathode electron guns and crab cavities. In this work I will describe these applications, and how they benefit from the rather unique properties of this resonator, such as the Higher Order Mode spectrum, the electro-mechanical stability and the compact size.

Funding: Work supported by Brookhaven Science Associates, LLC under Contract No. DE-AC02-98CH10886 with the U.S. Department of Energy.

I. Ben-Zvi (BNL)

THIOA04

The sc cw-LINAC Demonstrator - SRF-Technology finds the way into GSI

A new superconducting (sc) continuous wave (cw) LINAC at GSI is desired by a broad community of future users. Especially the Super Heavy Elements (SHE) program at GSI and HIM benefits highly from such a dedicated machine. A conceptual layout of an sc cw-LINAC was worked out at the Institute for Applied Physics (IAP) at Frankfurt University. Here the key component, an sc Crossbar-H (CH) cavity, was developed recently. The multi-gap cavity is operated at 217 MHz and provides gradients of 5.1 MV/m at a total length of 0.69 m. The first section of the proposed cw-LINAC comprising a sc CH-cavity embedded by two sc solenoids is financed by HIM as a Demonstrator. One important milestone of the project is a full performance test with beam of the Demonstrator in 2013/14 at the GSI High Charge Injector (HLI). With the demonstrator the srf-technology finds the way to GSI. The tests would be the first of an sc multi-gap structure with heavy ions being an important milestone towards the proposed cw-LINAC.

S. Mickat, W.A. Barth, L.A. Dahl, M. Kaiser, W. Vinzenz (GSI) M. Amberg, V. Gettmann, S. Jacke, **S. Mickat** (HIM) K. Aulenbacher (IKP) F.D. Dziuba, D. Mäder, H. Podlech, U. Ratzinger (IAP)

THIOA05

Mechanical Design Considerations for $\beta=1$ Cavities

The Superconducting Proton Linac (SPL) is an R&D effort coordinated by CERN in partnership with other international laboratories, aimed at developing key technologies for the construction of a multi-megawatt proton linac based on state-of-the-art RF superconducting technology, which would serve as a driver for new physics facilities such as neutrinos and Radioactive Ion Beam (RIB). Amongst the main objectives of this R&D effort, is the development of 704 MHz bulk niobium $\beta=1$ elliptical cavities, operating at 2 K with a maximum accelerating field of 25 MV/m, and the testing of a string of cavities integrated in a machine-type cryomodule. The R&D program concerning the elliptical $\beta=1$ cavities fabricated from niobium sheets explores new mechanical design and new fabrication methods. The paper presents several opportunities for design optimization that were identified, such as a comparison between stainless steel helium vessel versus NbTi/Ti transitions to a titanium helium vessel. Different mechanical design aspects, including cryogenic considerations, and fabrication aspects were analyzed and the results are discussed.

O. Capatina, G. Arnau-Izquierdo, S. Atieh, I. Aviles Santillana, S. Calatroni, T. Junginger, V. Parma, T. Renaglia, T. Tardy, N. Valverde Alonso, W. Weingarten (CERN) S. Chel, G. Devanz, J. Plouin (CEA/DSM/IRFU)

THIOA06

Single-cell SC Cavity Development in India

A. Puntambekar, J. Dwivedi, P.D. Gupta, S.C. Joshi, G. Mundra, P. Shrivastava (RRCAT) C.A. Cooper, M.H. Foley, T.N. Khabiboulline, C.S. Mishra, J.P. Ozelis, A.M. Rowe (Fermilab) P.N. Potukuchi (IUAC) G. Wu (ANL)

Under Indian Institutions and Fermilab Collaboration (IIFC), Raja Ramanna Centre for Advanced Technology (RRCAT) Indore, India has initiated the development of SCRF cavity technology in collaboration with Fermi National Accelerator Laboratory (FNAL) USA. The R & D efforts are focused on the proposed Project-X accelerator complex at FNAL and High Intensity Proton Accelerator activities in India. As an initial effort, two prototype 1.3 GHz single cell bulk niobium cavities have been developed in collaboration with the Inter University Accelerator Centre (IUAC), New Delhi. Learning from the experience gained and the initial results of these prototypes (achieving $E_{acc} \sim 23$ MV/m), two more improved 1.3 GHz single cell cavities are being developed. These two improved single cell cavities will also be processed and tested at FNAL. Development of a 1.3 GHz, 5-cell SCRF cavity with simple end groups, development of end group, and fabrication of a single -cell 650 MHz ($\beta=0.9$) prototype cavity are being undertaken as the next stage in these efforts. This paper will present the development and test results on the 1.3 GHz single cell cavities and status of the ongoing work.

THIOB — $\beta < 1$ Cavities

Project X Cavity and Cryomodule Development

Project X is a proposed multi-MW proton accelerator facility based on an H^- linear accelerator using SRF technology at Fermilab. The Project X 3-GeV CW linac requires the development of two families of SRF cavities at 325 and 650 MHz, to accelerate 1 mA of average H^- beam current in the energy range 2.5-160 MeV, and 160-3000 MeV, respectively. The cavities must support possible acceleration of up to 4 mA beam current. The baseline design calls for three types of SRF single-spoke resonators at 325 MHz having betas of 0.11, 0.22, and 0.42, and two types of SRF five-cell elliptical cavities having betas of 0.61 and 0.9. The electromagnetic and mechanical cavity designs are well underway and prototype tests for some cavity designs have started. Due to CW operation, the heat load on the cryogenic system is substantial; and for purposes of cryogenic system design, the dynamic heat load is limited to 250 W at 2K per cryomodule. The anticipated heat loads for the 650 MHz section lead to stringent requirements on cavity unloaded quality factor Q_0 , and on cryogenic aspects of the cryomodule design. Status and plans for the Project X cavity and cryomodule development will be described.

C.M. Ginsburg, M.S. Champion (Fermilab)

Funding: Work supported in part by the U.S. Department of Energy under Contract No. DE-AC02-07CH11359.

Vertical Tests Results of the IFMIF Cavity Prototypes and Cryomodule Development

In the framework of the International Fusion Materials Irradiation Facility (IFMIF), which consists of two high power CW accelerator drivers, each delivering a 125 mA deuteron beam at 40 MeV, an accelerator prototype is presently under design for the first phase of the project. A superconducting option has been chosen for the 5 MeV RF Linac, based on a cryomodule composed of 8 low-beta Half Wave Resonators, 8 Solenoid Packages and 8 RF couplers. This presentation will mainly focus on the HWR development: realization and vertical tests of the two HWR prototypes will be presented, including the validation tests of the innovating cold tuning system, located in the central region of the cavity (results with tuning system are expected for the conference). In addition, the 1st cryomodule current design will be also discussed.

F. Orsini, N. Bazin, P. Bosland, P. Bredy, P. Carbonnier, G. Disset, N. Grouas, P. Hardy, V.M. Hennion, H. Jenhani, J. Migne, Y. Penichot, J. Plouin, J. Relland, B. Renard, D. Roudier (CEA/IRFU) J. Calero, F.M. De Aragon, J.L. Gutierrez, I. Podadera Aliseda, S. Sanz, F. Toral, J.G.S. de la Gama (CIEMAT) E.N. Zaplatin (FZJ)

THIOB01

THIOB02

THIOB03

Status of the ReAccelerator Facility ReA for Rare Isotopes

D. Leitner, D. Morris, S. Nash, G. Perdikakis, N.R. Usher (NSCL) A. Facco, M. Hodek, J. Popielarski, W. Wittmer, X. Wu, Q. Zhao (FRIB) O.K. Kester (GSI)

The Facility for Rare Isotope Beams (FRIB) at Michigan State University (MSU) is currently in the preliminary design phase. FRIB consists of a heavy ion driver LINAC, followed by a fragmentation target station, and a ReAccelerator facility (ReA). In its final configuration, ReA will provide heavy ion beams from 0.3 MeV/u to 12 MeV/u for heaviest ions and up to 20 MeV/u for light ions. While FRIB plans to start conventional construction in 2012, the first stage of ReA is already under commissioning and will be connected to the Coupled Cyclotron Facility at MSU end of 2012. The front end of the accelerator consists of a gas stopper, an Electron Beam Ion Trap (EBIT) charge state booster, a room temperature RFQ, followed by a short SRF LINAC, which contains seven $\beta=0.041$, eight $\beta=0.085$ QWR cavities, and eight 9T focusing solenoids. ReA serves as prototyping test bed for the FRIB cryomodule development since FRIB utilizes similar cavities as installed on ReA. An overview and status of the ReA facility will be presented. The presentation will focus on the testing, beam commissioning, and operational experience of the first $\beta=0.041$ cryomodules.

The Facility for Rare Isotope Beams (FRIB) at Michigan State University (MSU) is currently in the preliminary design phase. FRIB consists of a heavy ion driver LINAC, followed by a fragmentation

THIOB04

SRF Advances for ATLAS and other $\beta < 1$ Applications

M.P. Kelly, Z.A. Conway, S.M. Gerbick, M. Kedzie, R.C. Murphy, B. Mustapha, P.N. Ostroumov, T. Reid (ANL)

linac with large acceptance and minimal beam losses. Cavities will be installed into ATLAS in 2012 as the beam intensity upgrade, but are also intended for the next generation of ion linacs to be used in basic and applied science and technology. State-of-the-art cavity designs and fabrication techniques developed at ANL have been applied to the construction of the first prototype. Tests of the prototype 72 MHz QWR demonstrate the highest performance achieved to date for this class of cavity designed to cover the velocity range $0.06 < \beta < 0.12$. The cavity has very low RF losses and the highest accelerating gradients ever achieved for any quarter-wave structure. Indeed, the accelerating voltage of 4.3 MV is roughly four times higher than that reported for the best SC cavities in this velocity range currently in operation at any facility worldwide. Also, this demonstrated 4.3 MV accelerating voltage substantially exceeds the 2.5 MV design voltage.

The guiding principle for the design of the new 72 MHz quarter wave SC cavities at Argonne was to provide the maximum possible accelerating gradient along the

THIOB05

SPL Cavity Development

G. Olry (IPN)

The Superconducting Proton Linac (SPL) is planned as a 4MW machine in pulsed operation at CERN. Two families (beat = 0.65 and $\beta = 1.0$) of 5 cell superconducting elliptical cavities, operating at 704.4 MHz, will be used to accelerate H⁻ beam from 160 MeV up to 5 GeV. One of the main challenge is the nominal gradient required for both cavities type: 19 MV/m for the $\beta=0.65$ and 25 MV/m for the $\beta=1$. Several prototypes of elliptical cavities have been studied by different laboratories (CERN, CEA/Saclay, BNL, IPN Orsay) through a large collaboration (EuCARD program, French and US in-kind contribution. . .) and are now ready for fabrication. First of all, we will present the work done on RF and mechanical optimizations as well as the studies on HOMs. Then, we will give an overview of the short-cryomodule design, housing four $\beta=1.0$ cavities, which should be tested at CERN.

The Superconducting Proton Linac (SPL) is planned as a 4MW machine in pulsed operation at CERN. Two families (beat =

Recents Developments in SRF at TRIUMF

The TRIUMF SRF program follows three basic paths: the support of the existing installed superconducting heavy ion linac with forty quarter wave cavities, the development of infrastructure and cavities for the new e-Linac project at 1.3GHz

R.E. Laxdal, C.D. Beard, A. Grassellino, P. Kolb, D. Longueveergne, V. Zvyagintsev (TRIUMF, Canada's National Laboratory for Particle and Nuclear Physics) R.S. Orr, W. Trischuk (University of Toronto)

and fundamental studies to support student projects. Work on the quarter waves primarily involves determining optimum processing steps to improve cavity performance. The e-Linac cavity is a variant of the Tesla nine cell cavity modified to allow the acceleration of 10mA in cw mode. Fundamental studies on RRR niobium have been done at the Muon Spin Resonance facility at TRIUMF to characterize the flux of first entry for different processing of the niobium. The program will be summarized.

THIOB06

HIE-ISOLDE quarter wave Nb/Cu cavity

The HIE-ISOLDE project aims at the energy boost of the radio active beams produced in the ISOLDE facility from 3 MeV/u up to 5.5 MeV/u in a first stage and 10 MeV/u as ultimate installation.

M. Pasini, S. Calatroni, O. Capatina, A. D'Elia, M.A. Fraser, M. Therasse (CERN) **M. Pasini** (Instituut voor Kern- en Stralingsfysica, K. U. Leuven)

The beam acceleration is mainly achieved by employing 20 Nb sputtered Quarter Wave Resonator at $\beta = 0.1$ for which an R&D program has started. RF and mechanical design as well as the latest results of the sputtering process are reported in this paper.

THIOB07

Hot topics: Recipes for 9-cell cavity fabrication and preparation

In the mass production of International Linear Collider (ILC), about 16,000 9-cell SRF cavities must be produced for the linac.

T. Saeki (KEK)

The current recipe of 9-cell cavity production is not enough for the required cost reduction for ILC. Various ideas for the cost reduction of 9-cell cavity fabrication would be discussed in this presentation. As the final surface treatment of 9-cell cavity, the Electro-Polishing (EP) is the best candidate to realize high yield rate for high-gradient performance. However, the laboratories in the world are still using different EP parameter-sets for various reasons. In this presentation, the comparison of EP parameters among laboratories would be done and how we can reach to the best parameter sets would be discussed.

THIOB08

THPO — Poster Session

THPO001

Quench Simulation Using a Ring-Type Defect Model

Y. Xie, M. Liepe, H. Padamsee (CLASSE)

A 2 dimensional ring-type defect thermal feedback model has been improved by including magnetic field enhancement at the pit edge. Latest simulation results show that there is a thermally stable state below the quench field with part of edge becoming normal conducting, which can explain pre-heating phenomenon observed in thermometry measurements. 3D magnetic field enhancement calculations of pit structures using Omega3P shows angular non-uniform field enhancement around the edge. Those findings will be incorporated into a 3D finite ring-type defect thermal codes.

Funding: Work supported by NSF and Alfred P. Sloan Foundation.

THPO002

Defect-Induced Local Heating of Superconducting Cavity Surface

Y. Morozumi (KEK)

The limitation of the accelerating gradient is one of the current major issues with high gradient superconducting RF accelerator structures such as the ILC accelerating cavities. Field emission and thermal breakdown due to surface imperfections tend to limit the gradient performance. Some kind of surface defects are suspects responsible for thermal breakdown of superconducting RF cavities. Profilometry-based realistic high-fidelity modeling of field enhancement will be presented. Evaluation of local heating at surface defects and analysis of thermal behavior will be discussed in comparison with experimental evidences.

THPO003

Multipacting in HOM Couplers at the 1.3GHz 9-cell TESLA Type SRF Cavity

D. Kostin, Th. Buettner, W.-D. Moeller, J.K. Sekutowicz (DESY)

During the XFEL prototype module tests on the module test stand at DESY RF power measurement anomaly on the high order mode (HOM) couplers on the cavity operating frequency was detected and investigated. HOM coupler multipacting, predicted by the analytical simulations, was found to be the source of the anomalous signal peak. TESLA type SRF cavity HOM coupler multipacting simulations and observations are presented, compared and discussed.

Electro- or Chemical- Polishing and UHV Baking of Superconducting rf Nb Cavities and Q(H) Dependencies

Standard treatments to achieve excellent high rf power Nb accelerator cavities after machining are electro polishing (EP, >0.050mm), buffered chemical polishing (BCP, ~0.01mm), or subsequent ~120°C (>10h) UHV baking (LTB)[1-4]. LFQ and HFQ have been discussed in detail in [2,4], here we concentrate on oxidation and on MFQ described by $\Delta R(H) = R1H/H_c + R2(H/H_c)^2$, where R1 is related to hysteresis weak link, flux losses and R2 is mainly related to heating [3]. The observed differences between BCP, EP and LTB can be related to differences in Nb₂O₅/NbO_x/Nb interfaces. For example: by BCP oxidation the repeated Nb₂O₅-crystallite nucleation creates DS, weak links and injects O into larger depth [2] where the weak links strengthen MFQ [1,3]; by EP the repeated Nb₂O₅-crystallite nucleation is missing and so O sticks to the surface and less DSs and weak links are created resulting in less MFQ [1]; and by LTB at, and adjacent to, Nb surfaces O precipitates enforcing MFQ and LTB, enhancing H_{c3} and reducing, e.g. RBCS(T, <15GHz) [1-4]. Depending on details to be discussed these intermingled LTB effects after EP may reduce or enhance R(T, <GHz, <20MeV/m).

[1] A.Romanenko et al., PAC'11

[2] A.S.Dhvale, Symp. Techn. of Nb., JLAB, Sept. 2010

[3] G.Ciovati et al., PhysicaC 441,57(2006)

[4] J.Halbritter, SRF09-TUPPO089 (Berlin, 2009), p.450

J. Halbritter (FZ Karlsruhe)

THPO004

Exploration of Very High Gradient Cavities

Several of the 9-cell ILC cavities processed at Jlab within ongoing ILC R&D program have shown interesting

behavior at high fields, such as mode mixing and sudden field emission turn-on during quench. Equipped with thermometry and OST system for quench detection, we couple our RF measurements with local dissipation measurements. In this contribution we report on our findings with high gradient SRF cavities.

G.V. Ereemeev (JLAB)

THPO005

Study of Trapped Magnetic Flux in Superconducting Niobium Samples

Trapped magnetic flux is known to be one cause of residual losses in an SRF cavity.

An ambient magnetic field is trapped in

the material when lattice defects inhibit the expulsion of the field during the transition into the Meissner phase. We measured the fraction of trapped magnetic flux in niobium samples with different treatment histories, such as BCP and tempering. The differences between single crystal and polycrystalline material as well as the influence of local temperature gradients and different cooling rates were investigated. In addition, the progression of the release of a trapped field during warm up was studied. It was found that different fractions of an applied field were trapped due to heat treatment. Differences between single crystal and polycrystalline material were also observed. Additionally, single crystal samples showed a logarithmic dependency on the cooling rate. It was demonstrated that a local temperature gradient produces an additional magnetic field which has impact on the flux trapping.

S. Aull, J. Knobloch, O. Kugeler (HZB)

THPO006

THPO007

Novel Deflecting Cavity Design for eRHIC

Q. Wu, S.A. Belomestnykh, I. Ben-Zvi (BNL)

BNL (eRHIC), there is a demand for crab cavities. In this article, we will present a novel design of the deflecting/crabbing 200 MHz superconducting RF cavity that will fulfill the requirements of eRHIC. The quarter-wave resonator structure of the new cavity possesses many advantages, such as compact size, high Rt/Q , the absence of same order mode and lower order mode, and easy higher order mode damping. We will present the properties and characteristics of the new cavity in detail.

Funding: Work is supported by Brookhaven Science Associates, LLC under Contract No. DE-AC02-98CH10886 with the U.S. DOE.

To prevent significant loss of the luminosity due to large crossing angle in the future ERL based Electron Ion Collider at

THPO008

Post-Baking Losses in Niobium Cavities Studied by Dissection

A. Romanenko, L.D. Cooley, G. Wu (Fermilab) G. Ciovati (JLAB)

absence of the high field Q-slope there are still a few localized sources of dissipation. Identification of these areas along with the high field quench location followed by dissection and surface analysis of the resulting coupons allowed to gain insight into possible mechanisms of these effects, and will be reported in this contribution.

Thermometry investigations on electropolished cavities, which underwent mild baking, and are limited by a localized quench at 150-200 mT, show that in the

THPO009

Quench Studies in Large and Fine Grain Nb Cavities

S. Posen, M. Liepe, N.R.A. Valles (CLASSE)

MV/m, tested in continuous wave mode. Studies were carried out on both fine grain and large grain cavities in ILC and Cornell Re-entrant shape geometries. The quenches were located by triangulation using Cornell oscillating superleak transducers and then cavities were optically inspected to determine the surface conditions of the cavity at the quench location. For quench locations exhibiting topological defects, surface molds were created and investigated using 3-D profilometry techniques.

This work investigates the causes of quenches in several niobium 1.3 GHz single-cell cavities performing above 20

THPO010

Multipactor Studies for DIAMOND Storage Ring Cavities

S.A. Pande, M. Jensen (Diamond)

499.654 MHz. The cavities are suffering from a significant number of trips due to a sudden loss of accelerating field believed to be caused by Multipacting. It is observed that operating the cavities at lower voltages reduces the trip frequency significantly. In order to estimate the multipacting thresholds and to determine safe (multipactor free) parameter zones, we have initiated a detailed simulation study of multipacting in the cavities and the coupling waveguide. The cavities have fixed coupling, and therefore the match of the cavities varies with beam current, radiation loss and cavity voltage. A change in any of these parameters leads to a different standing wave in the waveguide. This requires the simulations to account for the different operating conditions. In addition to the waveguide and the cavity cell, the simulations also indicate the possibility of multipactor in the connecting beam tubes. In this paper, we summarise the results of our simulations obtained using CST Studio PIC and Tracking solvers.

The Diamond storage ring is presently operating with two CESR type Superconducting (SC) RF cavities operating at

Improving the Intrinsic Quality Factor of SRF Cavities by Thermal Cycling

We investigated the influence of the cooling gradients near T_c on the obtained Q_0 values of a TESLA cavity. Measurements

O. Kugeler, W. Anders, J. Knobloch, A. Neumann (HZB)

were performed in the HoBiCaT test stand by briefly warming the cavity above T_c via He depletion inside the cryovessel and subsequent cooling. The temperature was measured at different points at the cavity and the cryo-tank. It turned out that there is a correlation between obtained Q_0 and the time lag between the first transition of a thermo-sensor through T_c and the last transition of a sensor through T_c which is interpreted as a local gradient. We have observed no correlation to the cooling speed, i.e. different temperature gradients in time. The findings could help explain the large fluctuations in measured Q values in different test-stands, and even open up pathways to devising a cooling scheme to obtain higher Q values "for free".

THPO011

Influence of Foreign Particles on the Quality Factor of a Superconducting Cavity

The quality factor of superconducting (SC) cavities of the Cornell Energy Recovery Linac (ERL) Injector measured in its

V.D. Shemelin, G.H. Hoffstaetter (CLASSE)

horizontal cryostat appears systematically lower than in vertical tests. Furthermore, this lower value of the Q factor is scattered in a range of about Here, an explanation of these effects is presented taking into account contamination of the cavities by microscopic particles of ferrite used in the higher order mode (HOM) loads and other particles present in the vicinity of cavities during assembly of the horizontal cryostat. The average Q degradation and the scatter of Q values are used to estimate the size and the number of contaminants per cavity. We also analyze, which materials have relevant contaminants.

Funding: Supported by NSF award DMR-0807731.

THPO012

Investigation of 9-Cell Cavity Performance Problem by Facilities in KEK AR East 2nd Experimental Hall

So far our 9-cell cavity performance is often suffered from field emission. We are investigating our facilities at the KEK AR

K. Saito (KEK)

East 2nd experimental hall. We examined two points of view post EP/BCP cleaning and particle contamination. Particle contamination problem has been found in our HPR system, cavity assembly, and vacuum evacuation procedure. We have taken cures against these problems. We will report about these problems and the cured results on cavity performance in this paper.

THPO013

Repair SRF Cavity by Re-Melting Surface Defects via High Power Laser Technique

As the field emission is gradually under control in recent SRF activities, cavity performance is limited by hard quench in the most case. Surface defect has been identified as one of main reasons caused

M. Ge (CLASSE) E. Borissov, L.D. Cooley, D.T. Hicks, T.H. Nicol, J.P. Ozelis, J. Ruan, D.A. Sergatskov (Fermilab) G. Wu (ANL)

cavity quench scattering cavity accelerating gradient from 12 MV/m to 40 MV/m. Laser processing is able to re-shape the steep flaws to be flat and smooth surface. In Fermilab, a sophisticated laser repair system has been built for 1.3GHz low performance SRF cavity which is limited by surface defect. The pit in a 1.3GHz single-cell cavity was re-melted by high power laser pulse, cavity took 30 μm light Electropolishing after that. The gradient achieved 39MV/m in initial run; after another 30 μm Electropolishing, it achieved 40 MV/m. The improved laser repair system is able to re-melt the surface defect in one meter long 9-cell SRF cavity. It successfully re-melted a pit in 9-cell SRF cavity TB9ACC017.

THPO015

THPO016

Preliminary Results on the Laser Heating Investigation of Hotspots in a Large-Grain Nb Cavity

G. Ciovati, C. Baldwin, G. Cheng, R. J. Flood, K. Jordan, P. Kneisel, M.L. Morrone, L. Turlington, K.M. Wilson, S. Zhang (JLAB) S. M. Anlage (UMD) A.V. Gurevich (Old Dominion University) G. Nemes (Astigmat)

Magnetic vortices pinned near the inner surface of SRF Nb cavities are a possible source of RF hotspots, frequently observed by temperature mapping of the cavities outer surface at RF surface magnetic fields of about 100 mT. Theoretically,

we expect that the thermal gradient provided by a 10 W green laser shining on the inner cavity surface at the RF hotspot locations can move pinned vortices to different pinning locations. The experimental apparatus to send the beam onto the inner surface of a photoinjector-type large-grain Nb cavity is described. Preliminary results on the changes in thermal maps observed after applying the laser heating are also reported.

THPO017

Probing the Fundamental Limit of Niobium in High Radiofrequency Fields by Dual Mode Excitation in Superconducting Radiofrequency Cavities

G.V. Ereemeev, R.L. Geng, A.D. Palczewski (JLAB)

We have studied thermal breakdown in several multicell superconducting radiofrequency cavity by simultaneous excitation of two TM₀₁₀ passband modes. Unlike measurements done in the past, which indicated a clear thermal nature of the breakdown, our measurements present a more complex picture with interplay of both thermal and magnetic effects. JLab LG-1 that we studied was limited at 40.5 MV/m, corresponding to B_{peak} = 173 mT, in 8pi9 mode. Dual mode measurements on this quench indicate that this quench is not purely magnetic, and so we conclude that this field is not the fundamental limit in SRF cavities.

Funding: *Authored by Jefferson Science Associates, LLC under U.S. DOE Contract No. DE-AC05-06OR23177.

Funding: *Authored by Jefferson Science Associates, LLC under U.S. DOE Contract No. DE-AC05-06OR23177.

THPO018

Quench Studies of ILC Cavities

G.V. Ereemeev, R.L. Geng, A.D. Palczewski (JLAB) J. Dai (PKU/IHIP)

Quench limits accelerating gradient in SRF cavities to a gradient lower than theoretically expected for superconducting niobium. Identification of the quenching site with thermometry and OST, optical inspection, and replica of the culprit is an ongoing effort at Jefferson Lab aimed at better understanding of this limiting phenomenon. In this contribution we present our finding with several SRF cavities that were limited by quench.

Funding: *Authored by Jefferson Science Associates, LLC under U.S. DOE Contract No. DE-AC05-06OR23177

Funding: *Authored by Jefferson Science Associates, LLC under U.S. DOE Contract No. DE-AC05-06OR23177

Design, Construction, and Initial Test of High Spatial Resolution Thermometry Arrays for Detection of Surface Temperature Profiles on SRF Cavities in Super Fluid Helium

We designed and built two high resolution (0.6-0.55mm special resolution [1.1-1.2mm separation]) thermometry arrays

A.D. Palczewski, G.V. Eremeev, R.L. Geng (JLAB)

prototypes out of the Allen Bradley 90-120 Ω 1/8 watt resistor to measure surface temperature profiles on SRF cavities. One array was designed to be physically flexible and conform to any location on a SRF cavity; the other was modeled after the common G-10/stycast 2850 thermometer and designed to fit on the equator of an ILC (Tesla 1.3GHz) SRF cavity. We will discuss the advantages and disadvantages of each array and their construction. In addition we will present a case study of the arrays performance on a real SRF cavity TB9NR001. TB9NR001 presented a unique opportunity to test the performance of each array as it contained a dual (4mm separation) cat eye defect which conventional methods such as OST (Oscillating Superleak second-sound Transducers) and full coverage thermometry mapping were unable to distinguish between. We will discuss the new arrays ability to distinguish between the two defects and their preheating performance. **Funding:** Authored by Jefferson Science Associates, LLC under U.S. DOE Contract No. DE-AC05-06OR23177.

THPO019

Exploration of Quench Initiation Due to Intentional Geometrical Defects in a High Magnetic Field Region of an SRF Cavity

A computer program which was used to simulate and analyze the thermal behaviors of SRF cavities has been developed

J. Dai, K. Zhao (PKU/IHIP) G.V. Eremeev, R.L. Geng (JLAB)

at Jefferson Lab using C++ code. This code was also used to verify the quench initiation due to geometrical defects in high magnetic field region of SRF cavities. We built a CEBAF single cell cavity with 4 artificial defects near equator, and this cavity has been tested with T-mapping. The preheating behavior and quench initiation analysis of this cavity will be presented here using the computer program.

daijin@pku.edu.cn

Funding: *Authored by Jefferson Science Associates, LLC under U.S. DOE Contract No. DE-AC05-06OR23177

THPO020

Measurement of Hc1 in Superconducting Thin Films

Superconducting radio frequency (SRF) cavities are the leading technology for particle accelerators. Niobium cavities are the core of many existing accelerators

N.F. Haberkorn, L. Civale, M. Hawley, Q.X. Jia, R.K. Schulze, T. Tajima, Y.Y. Zhang (LANL) B. Moeckly (STI)

and will be used in several future systems currently under construction or design. The performance of Nb Cavities has been continuously improved over many years, but presently this technology is approaching the fundamental limit set by the superconducting critical field of bulk Nb, around 2000 Oe. Gurevich [Appl. Phys. Lett. 88, 012511 (2006)] suggests that performance (maximum accelerating field) of Nb cavities could be extended by covering the internal walls with a superconductor / insulator multilayer. The central idea is that when the thickness of the superconducting layer is smaller than the penetration depth, a size effect results in an increase of the lower critical field Hc1 where the vortex penetration becomes favorable. In this work we explore the enhancement of the Hc1 on MgB2, Nb, and MoN thin films of different thickness. Preliminary results indicate an enhancement of Hc1 in comparison with bulk values, up to values exceeding those currently achievable in Nb cavities.

Funding: This work was supported by 2010 DOE Early Career Award (T. Tajima), DOE Office of Nuclear Physics, and the US DOE, Office of Basic Energy Sciences (Division of Materials Sciences and Engineering)

THPO021

THPO022

Temperature and Surface Treatment Dependence of Medium Field Q-Slope

A. Romanenko, J.P. Ozelis (Fermilab) G. Wu (ANL)

the cavity quality factors. RF measurements at bath temperatures ranging from 1.6 to 2.3K were performed on a number of 1.3 GHz single cell elliptical TESLA shape cavities of fine grain size after different surface treatments (BCP, tumbling, EP, before and after mild baking and HF rinsing) in the preliminary search for the optimum surface preparation technique at medium surface fields.

Significant cost-affecting factor in the projected continuous wave (CW) accelerators such as Project X is determined by

THPO023

External Magnetic Fields and Operating SRF Cavity

D.A. Sergatskov, T.N. Khabiboulline, R.L. Madrak, J.P. Ozelis, I. Terechkine (Fermilab)

surface resistance. This effect was extensively studied, is well understood by now and results in stringent requirements for an ambient magnetic field on the surface of an SRF cavity. The situation is quite different when magnetic field is applied to a cavity already in the superconducting state. During normal operation the bulk of the superconducting Nb should protect the RF surface of the cavity from fields on the outside. So we expect that the requirements on an external magnetic field applied to an operating cavity could be significantly relaxed. One possible failure mode is when the cavity quenches while the external field is applied. The magnetic field would penetrate through a normal zone formed during the quench and can get trapped during the subsequent post-quench cooling. We studied the effects of an external magnetic field applied to an operating SRF cavity and report the results.

When an SRF cavity is undergoing a transition to the superconducting state in an external magnetic field it traps some of the flux which results in an increase of

Funding: The work herein has been performed at Fermilab, which is operated by Fermi Research Alliance, LLC under Contract No. DE-AC02-07CH11359 with the United States Department of Energy.

THPO024

Quench Dynamics in SRF Cavities

Y.B. Maximenko (MIPT) D.A. Sergatskov, V.P. Yakovlev (Fermilab)

Funding: The work herein has been performed at Fermilab, which is operated by Fermi Research Alliance, LLC under Contract No. DE-AC02-07CH11359 with the United States Department of Energy.

We have developed a time-dependent model of quench process in an SRF cavity. We discuss peculiarities of the numerical solution and the results of simulation.

Effects of Anodization on Field Emission on Nb Surfaces

Minimization of field emission on the inner surfaces of niobium (Nb) superconducting radio frequency (SRF) cavities is highly desirable for SRF community. Previous experimental results [1] seemed to imply that the threshold of field emission was related to the thickness of Nb surface oxide layers. In this contribution, a more detailed study on the influences of the surface oxide layers on the field emission on Nb surfaces will be reported. By anodization technique, the thickness of the surface pentoxide layer was varied from 3nm up to 460nm. These samples were measured by means of a home-made scanning field emission microscope (SFEM). The emitters detected by SFEM were characterized using a scanning electron microscope together with an energy dispersive x-ray analyzer. Attempts were made to try to correlate the results from SFEM measurements with surface morphology and oxide thickness of Nb samples and chemical composition and geographic shape of the emitters. The SFEM results were also analyzed employing a model based on the classic electromagnetic theory. Possibly implications for Nb SRF cavity applications from this study will be discussed.

A.T. Wu, R.A. Rimmer (JLAB) S. Jin, X.Y. Lu, K. Zhao (PKU/IHIP)

Authored by Jefferson Science Associates, LLC under U.S. DOE Contract No. DE-AC05-06OR23177.

THPO025

Second Sound Triangulation for SPL Cavity Quench Localization

Second sound is a temperature wave which travels at a speed of $\sim 20\text{m/s}$ in superfluid helium. The second sound detector is a so-called oscillating superleak transducer (OST), initially provided by Cornell-CLASSE, and thereafter manufactured at CERN. It contains a flexible porous membrane for transmitting and blocking the movement of the superfluid and normalfluid components of the second sound wave. From the measured speed of this wave and by determining the travel time between the quench event and several OSTs an alternative method is offered to localize the quench site by triangulation. Several surface mount devices (thick film chip resistors) are used to simulate the quench spot in a cavity. Given the heat pulse and the location of the installed OSTs, the temperature dependence of the second sound velocity is determined under different experimental conditions and compared with previous results and a theoretical curve. The second sound triangulation will be finally used to diagnose quench locations of the Superconducting Proton Linac test cavities (704MHz) at CERN.

K.C. Liao, C. Balle, J. Bremer, T. Junginger, W. Vollenberg, W. Weingarten (CERN) H. Vennekate (University of Gi \ddot{u} ttingen, Georg-August University of Gi \ddot{u} ttingen)

THPO026

Optical Observation of Geometrical Features and Correlation With RF Test Results

Three kinds of geometrical features analysis techniques were adopted in association with cavity gradient R&D at Jefferson Lab: (1) Feature shape analysis by Kyoto camera system; (2) 3D shape analysis using a HIROX KH-7700 High Resolution Digital-Video Microscopy System; (3) Replica technique plus surface profiler for profile measurement of geometrical features. Up to now, many features were found in two nine cell SRF cavities: PKU2 from Peking University in China and NR1 from Niowave-Roark in America. Both of them have been RF tested at 2K. The shape analysis of geometrical surface features and correlation with RF test results using a thermal analysis code will be presented here.

J. Dai, K. Zhao (PKU/IHIP) R.L. Geng (JLAB) K. Watanabe (KEK)

daijin@pku.edu.cn

Funding: *Authored by Jefferson Science Associates, LLC under U.S. DOE Contract No. DE-AC05-06OR23177.

THPO027

THPO028

SIMS and TEM Analysis of Niobium Bicrystals

P. Maheswari, A.D. Batchelor, D.P. Griffis, F.A. Stevie, C. Zhou (NCSU AIF) G. Ciovati, R. Myneni (JLAB) M. Rigsbee (Materials Science and Engineering)

The behaviour of interstitial impurities (C, O, N, H) on the Nb surface with respect to grain boundaries may affect cavity performance. Large grain Nb makes possible the selection of bicrystal samples with a well defined grain boundary. In this work, Dynamic SIMS was used to analyze two Nb bicrystal samples, one of them heat treated and the other non heat treated (control). H levels were found to be higher for the non heat treated sample and a difference in the H intensity and sputtering rate was also observed across the grain boundary for both the samples. TEM results showed that the bicrystal interface showed no discontinuity and the oxide layer was uniform across the grain boundary for both the samples. TOF-SIMS imaging was also performed to analyze the distribution of the impurities across the grain boundary in both the samples. C was observed to be segregated along the grain boundary for the control sample, while H and O showed a difference in signal intensity across the grain boundary. Crystal orientation appears to have an important role in the observed sputtering rate and impurity ion signal differences both across the grain boundary and between samples

The behaviour of interstitial impurities (C, O, N, H) on the Nb surface with respect to grain boundaries may affect cavity performance. Large grain Nb makes possible the selection of bicrystal samples with a well defined grain boundary. In this work, Dynamic SIMS was used to analyze two Nb bicrystal samples, one of them heat treated and the other non heat treated (control). H levels were found to be higher for the non heat treated sample and a difference in the H intensity and sputtering rate was also observed across the grain boundary for both the samples. TEM results showed that the bicrystal interface showed no discontinuity and the oxide layer was uniform across the grain boundary for both the samples. TOF-SIMS imaging was also performed to analyze the distribution of the impurities across the grain boundary in both the samples. C was observed to be segregated along the grain boundary for the control sample, while H and O showed a difference in signal intensity across the grain boundary. Crystal orientation appears to have an important role in the observed sputtering rate and impurity ion signal differences both across the grain boundary and between samples

THPO029

Commissioning Cornell OSTs for SRF Cavity Testing at JLab

G.V. Eremeev (JLAB)

Understanding the current quench limitations in SRF cavities is a topic essential for any SRF accelerator that requires high fields. This understanding crucially depends on correct and precise quench identification. Second sound quench detection in superfluid liquid helium with oscillating superleak transducers is a technique recently applied at Cornell University as a fast and versatile method for quench identification in SRF cavities. Having adopted Cornell design, we report in this contribution on our experience with OST for quench identification in different cavities at JLab.

Authored by Jefferson Science Associates, LLC under U.S. DOE Contract No. DE-AC05-06OR23177.

Funding: Authored by Jefferson Science Associates, LLC under U.S. DOE Contract No. DE-AC05-06OR23177.

Understanding the current quench limitations in SRF cavities is a topic essential for any SRF accelerator that requires high fields. This understanding crucially depends on correct and precise quench identification. Second sound quench detection in superfluid liquid helium with oscillating superleak transducers is a technique recently applied at Cornell University as a fast and versatile method for quench identification in SRF cavities. Having adopted Cornell design, we report in this contribution on our experience with OST for quench identification in different cavities at JLab.

THPO030

Microphonics Compensation for a 325MHz Single Spoke Cavity at Fermilab

W. Schappert, Y.M. Pischalnikov (Fermilab)

Microphonics compensation for these cavities are presented.

Fermilab is developing 325MHz CW narrow-bandwidth spoke cavities for the proposed Project X. The first results of active microphonics compensation for these cavities are presented.

Second Sound as an automated Quench Localisation Tool at DESY

The understanding of local thermal breakdown ("quench") in superconducting RF cavities is still a challenge.

F. Schlander, E. Elsen, D. Reschke (DESY)

An easy way to find these heat spots is to measure the Second Sound in superfluid helium. This detection technique has been examined in several institutes. At DESY there are currently two vertical bath cryostats where cold RF tests with a cavity mounted in a cryostat insert can be done. At all of the four inserts the Second Sound setup consisting of eight Oscillating Superleak Transducers (OSTs) is mounted. These are connected to amplifier electronics and the measured signals are fed into an ADC to be read out with MATLAB. Within MATLAB the location is derived from the measured propagation times. The present system is already in use on a regular basis. An automated setup which will be implemented into the usual RF measurements is under development and the current status will be described.

Funding: This work is supported by the Commission of the European Communities under the 7th Framework Programme "Construction of New Infrastructures – Preparatory Phase", contract number 206711.

THPO031

TOF-SIMS Analysis of Hydrogen in Niobium, From 160i½K to 475i½K

Niobium (Nb) is the material of choice for superconducting radio frequency (SRF) cavities due to its high critical temperature and critical magnetic field. Interstitial impurity elements such as H directly

P. Maheswari, A.D. Batchelor, D.P. Griffis, F.A. Stevie, C. Zhou (NCSU AIF) G. Ciovati, R. Myneni (JLAB) M. Rigsbee (Materials Science and Engineering)

influence the efficiency of these cavities. Quantification of H in Nb is difficult since H is extremely mobile in Nb with a very high diffusion coefficient even at room temperature. In the presented work, Time of Flight Secondary Ion Mass Spectrometry (TOF-SIMS) was used to characterize H in Nb over a wide temperature range (160i½K to 475i½K) in situ to check for changes in mobility. Multiple experiments showed that as the specimen temperature is decreased below 300 i½K, the H/Nb intensity changes by first increasing and then decreasing drastically at temperatures below 200i½K. As specimen temperature is increased from 300i½K to 450i½K, the H/Nb intensity decreases. Remarkably, the H intensity with respect to Nb increases with time at 475i½K (approximately 200oC). Correlation between this data and the H-Nb phase diagram appears to account for the H behaviour.

THPO032

Measurements of HOM Spectrum a 1.3 GHz ILC SC Cavity

Frequency spectrum stability measurements were done in scope High Order Modes (HOM) damping study in the

T.N. Khabiboulline, N. Solyak, V.P. Yakovlev (Fermilab)

Project-X accelerator, a superconducting linac developing currently at Fermilab. Possibility of the cavity design without HOM couplers is under consideration. Dumping of resonance excitation of high order modes with high shunt impedance is proposed by of detuning dangerous mode frequency of the cavity. Results of detuning HOM spectrum of 1.3 GHz cavities at 2K in Horizontal Test Station of Fermilab are presented.

THPO033

THPO034

Vertical Test Results on KEK-ERL 9-Cell L-Band Superconducting Cavity

E. Cenni (Sokendai) T. Furuya, H. Sakai, K. Umemori (KEK)
M. Sawamura (Japan Atomic Energy Agency (JAEA), Gamma-ray Non-Destructive Assay Research Group) K. Shinoe (ISSP/SRL)

In order to develop the Energy Recovery Linac at KEK, we are studying the performance of two prototype L-band superconducting cavities by means of vertical tests. After annealing, electro polishing, high pressure rinsing and baking, several

vertical tests has been performed and the cavities have been inspected through rotating X-ray and temperature mapping system. The performance limiting factor has been found to be the field emissions. We have observed X-ray emission and temperature raise along the cavity wall. The quench locations have been determined with a good agreement between X-ray and temperature sensors. During vertical test we have experienced some interesting phenomena such as quality factor degradation and X-ray burst. In the first case the degradation was observed even at low field, however we recovered it with a warming up to room temperature without additional surface treatment. In the latter case new emitters have suddenly appeared after some quenches. They remained in the same location also after the warming up. The cavities have fulfilled the requirement for the KEK-ERL main linac reaching an accelerating field of more than 20 MV/m.

THPO035

Comparison of Field Emission at Different SRF Cavity Assembly States and Test Stands

D. Kostin, A. Goessel, V. Gubarev, W.-D. Moeller, D. Reschke,
K. Twarowski (DESY)

SRF cavity Field Emission (FE) presents a major diagnostics instrument on the cavity performance, save the FE levels differ significantly from one cavity test setup to

another, making the analysis difficult. A comparison study complimented with a direct calibration of FE in the cavities tested with different auxillaries and test stands (vertical / horizontal / module) is presented and discussed.

THPO036

A Machine for High-Resolution Inspection of SRF Cavities at JLab

R.L. Geng, T. Goodman (JLAB)

A new high-resolution cavity inspection machine has been built at JLab, integrating a KEK/Kyoto camera system with a

JLab built system based on a long-distance microscope. This system has been a working horse in support the on-going ILC cavity gradient R&D. More recently, this machine has been also used to inspect small aperture cavities including some 1497 MHz 7-cell CEBAF upgrade cavities and S-band single-cell crab cavities, demonstrating the capability and flexibility of the machine. We will describe the detailed features of the inspection machine along with some exemplary inspection results.

Funding: This work was authored by Jefferson Science Associates, LLC under U.S. DOE Contract No. DE-AC05-06OR23177

THPO037

Lorentz Force Detuning Compensation in Fermilab Cryomodule 1

Y.M. Pischalnikov, B. Chase, E.R. Harms, W. Schappert (Fermilab)

Cryomodule 1 of the Fermilab SRF Accelerator Test Facility has recently been commissioned. First results are presented from the simultaneous compensation of

Lorentz force detuning in all eight of the 1.3 GHz Tesla style superconducting cavities.

Detailed Nb Surface Morphology Evolution During Electropolishing for SRF Cavity Production

Electropolishing is currently an important part of attaining the best performance of SRF cavities. We endeavor to develop sufficient understanding of the process dynamics to gain predictive power over specific topographies subjected to controlled electropolishing conditions. This work examines the evolution of highly reproducible Nb surface morphology produced by centrifugal barrel polishing of fine-grain and single-crystal material as this material is electropolished under different well-controlled conditions. The morphology evolution of Nb surface has been described using a combined approach of scaling analysis and predictions of the electropolishing theory. Our results shows that electropolishing at low temperature helps to smooth out the surface feature scales within the diffusion layer and to reduce the kinetics-controlled surface etching. A preliminary computational model has been developed that simulates the evolution of specific topography of a niobium surface under parametrized conditions. This work is expected to lead to the direct linking of starting surface morphology specification, specific processing protocol, and consistently attained finished surface condition.

H. Tian, C.E. Reece (JLAB)

THPO038

Niobium Surface Resistance Measurement by Thermometric Method With a TE011 Cavity

Bulk niobium single-cell cavities of ILC type reach almost the theoretical limit of accelerating gradient. In order to enhance the maximum accelerating field of SRF cavities or/and increase the unloaded quality factor, further investigations on thin film technology namely coating processes and new superconducting materials alternative to bulk niobium are carried out. A dedicated TE011 cavity with removable end plate has been built in order to measure surface resistance of various superconducting materials subjected to RF field. A precise thermometric method is used for this purpose. In this paper, we present the first results obtained with bulk niobium sample.

G. Martinet, M. Fouaidy, N. Hammoudi (IPN)

THPO039

A Wire Position Monitor System for the 1.3GHz Tesla-Style Cryomodule at the Fermilab New Muon Lab

A wire position monitor system was put in place to monitor the motion of the 300mm return pipe in the first 1.3GHz Tesla-style cryomodule currently under RF testing at the Fermilab New Muon Lab. An overview of the system is given along with initial results including cooldown and subsequent testing.

N. Eddy, B.J. Fellenz, A. Semenov, D.C. Voy, M. Wendt (Fermilab)

Funding: Operated by Fermi Research Alliance LLC under contract #DE-AC02-07CH11359 with the US Department of Energy.

THPO040

THPO041

HOM Identification and Bead Pulling on the Brookhaven ERL

H. Hahn, W. Xu (BNL) P. Jain, E.C. Johnson (Stony Brook University)

Several past measurements of the Brookhaven ERL at superconducting temperature produced a long list of higher order modes (HOMs). The Niobium 5-cell cavity is terminated with HOM ferrite dampers that successfully reduce the Q-factors to tolerable levels. However, a number of undamped resonances with $Q \sim 10^6$ were found at 4 K and their mode identification remained as a goal for this paper. The approach taken here consists of different measurements on a copper cavity replica of the ERL which can be compared with Microwave Studio computer simulations. Several different S21 transmission measurements are used, including those taken from the fundamental input coupler to the pick-up probe across the cavity, between probes in a single cell, and between beam-position monitor probes in the beam tubes. These measurements are supported by bead pulling with a metallic needle, which is calibrated in the fundamental mode. This paper presents results for the first two dipole bands with the prototypical 958 MHz trapped mode, the high Q quadrupole band, the first beam tube resonances, and other as yet to be identified resonances.

Funding: Work supported by Brookhaven Science Associates, LLC under Contract No. DE-AC02-98CH10886 with the U.S. DOE and by the DOE grant DE-SC0002496 to Stony Brook University

THPO042

Crystallographic Orientation of Epitaxial Transition Observed for Nb (BCC) on Cu and MgO (FCC) Single-Crystals

K.I. Seo (NSU) M. Krishnan, E.F. Valderrama (AASC) H.L. Phillips, C.E. Reece, J.K. Spradlin, A-M. Valente-Feliciano, X. Zhao (JLAB)

Niobium thin films were grown on (001) MgO (or Cu) single-crystal using a coaxial energetic deposition. The quality of the substrate surface and epitaxial Nb layers were investigated by the XRD and pole figure measurements. Depending on growth temperature, in-plane XRD show Kurdjumov-Sachs (KS) as well as Nishiyama-Wassermann (NW) epitaxial relationships for (110) and (001) Nb on (001) MgO. Calculation of the interface energy in rigid lattice models finds one KS and two NW minima. For the NW case the optimal atomic diameter ratio $d_{bcc}/d_{fcc}=0.866$ and 1.061 , whereas for the KS case it is at $d_{bcc}/d_{fcc}=0.919$. Transitions of this type are usually induced by a change in the lattice parameter ratio resulting from a relaxation process in the early stage of the growth.

THPO043

Understanding of Suppressed Superconductivity on SRF Quality Niobium

Z.H. Sung, D.C. Larbalestier, A. Polyanskii (ASC) L.D. Cooley, A. Romanenko (Fermilab) A.V. Gurevich (Old Dominion University) P.J. Lee (NHMFL)

By using transport current measurement, μ Hall probes and magneto optical imaging to high-purity SRF quality niobium coupons, we have shown that GBs (grain boundaries) in Nb can be responsible for significant degradation in superconducting properties. We have shown that GBs can preferentially admit flux penetration when the plane of a GB is aligned parallel or close to parallel to the vector of the external field magnet field and that the initial GB FF can be characterized as a single vortex row and breakdown of superconductivity in SRF Nb can be significantly accelerated by multiple rows of GB flux flow at high field regions, above $H_{c1} \sim 150-180$ mT. We also find that local work-hardening produced by continuously crossed rolled mechanical deformation on Nb can cause localized suppression of surface superconductivity and enhance bulk pinning properties, which would result in performance degradation in SRF cavities. We are extending this study to coupons directly isolated from hot and cold spots on a single Nb cavity in order to further understand whether suppression of RF superconductivity is triggered by surface properties or intrinsic bulk properties, or both

Funding: The work at the Applied Superconductivity Center was supported by the US DOE under grants DE-FG02-07ER41451, FNAL PO 570362, and the State of Florida

Structural Characterization of Nb Films Deposited by ECR Plasma Energetic Condensation on Crystalline Insulators

An energetic condensation thin film coating technique with an electron cyclotron resonance (ECR) induced plasma ion source is used to deposit Nb thin films on crystalline insulating substrates, such as a-plane and c-plane sapphire (Al₂O₃) and on magnesium oxide, MgO (100), (110), and (111). Heteroepitaxial Nb films were produced by ECR deposition with regulated substrate temperature. The residual resistance ratio (RRR) of about 1 micron thick films reach unprecedented values (350 - 450) on a-plane (11-20) sapphire substrates. The epitaxial relationship of Nb/crystalline substrate is found to be strongly influenced by the substrate bias voltage (adding to the initial Nb⁺ kinetic energy), the substrate crystalline orientation, and heating conditions. At low substrate temperature, the Nb films demonstrated non-epitaxial crystalline textures, revealed by XRD Pole Figure technique and Electron Backscattering Diffraction (EBSD). The texture might be caused by "Volmer-Weber" growth mode, i.e. island growth, at low surface adatom mobility. This study shows that the film's crystal structural character has great impact on its RRR/T_c value.

X. Zhao, H.L. Phillips, C.E. Reece, J.K. Spradlin, A-M. Valente-Feliciano (JLAB) H. Baumgart, D. Gu (ODU) K.I. Seo (NSU)

Funding: Authored by Jefferson Science Associates, LLC under U.S. DOE Contract No. DE-AC05-06OR23177.

Nb Surface Nonlinear Properties Under Localized High RF Magnetic Field

Despite much effort, Nb Superconducting Radio Frequency (SRF) cavities often do not reach their theoretical accelerating gradient potential because of defects on the Nb surface which locally reduce the RF critical field. Therefore there is an urgent need to develop a qualitative and quantitative understanding of the effects of these defects on the electromagnetic properties of Nb. A scanning microscope with the capability of measuring the local surface critical fields and nonlinear response from superconductors in sub-micron areas is a candidate for diagnosing the problems limiting the performance of SRF cavities. In order to achieve this goal, a localized and nearly 200 mTesla RF magnetic field, created by a magnetic write head, is integrated into our nonlinear-Meissner-effect scanning microwave microscope [1]. A sputtered Nb film (thickness=300 nm) is measured at a fixed location and shows a temperature-dependent vortex penetration field from the nonlinear measurements. Further improvement of this nonlinear microscopy with a 3D scanning system will map out the surface critical field on Nb, and compare to the independently determined defect structure.

T.M. Tai, B.G. Ghamsari (CNAM, UMD) S. M. Anlage (UMD)

[1] Tamin Tai, et al., "Nonlinear Near-Field Microwave Microscope For RF Defect Localization in Superconductors," IEEE Trans. Appl. Supercond., June, 2011 (in press). arXiv:1008.2948.

Funding: We acknowledge the support of DOE/HEP under contract # DESC0004950.

THPO044

THPO045

THPO046

Characterization of Scale-Dependent Roughness of Niobium Surfaces as a Function of Surface Treatment Processes

C. Xu, M.J. Kelley (The College of William and Mary) C.E. Reece, H. Tian (JLAB)

Micro-roughness is attributed to be a critical issue for realizing optimum performance of Superconducting Radio Frequency (SRF) cavities. Several surface processing methods such as chemical, mechanical and plasma, are used to obtain relatively smooth surfaces. Among those process methods, Buffered Chemical Polish (BCP) and Electro-Polishing (EP) are most commonly used in current niobium cavity production. The Power Spectral Density (PSD) of surface height data provides a more thorough description to the topography than a simple R_q (RMS) measurement and reveals useful information including fractal and superstructure contributions. Polishing duration and temperature can have predictable effects on the evolution of such features at different scale regions in PSD spectrum. 1 dimensional average PSD functions derived from morphologies of niobium surfaces treated by BCP and EP with different controlled starting conditions and durations have been fitted with a combination of fractal, K-correlation and shifted Gaussian models, to extract characteristic parameters at different spatial harmonic scales.

Funding: Authored by Jefferson Science Associates, LLC under U.S. DOE Contract No. DE-AC05-06OR23177.

THPO047

Growth Mode and Strain Effects in the Superconducting Properties of Nb Thin Films on Sapphire

C. Clavero, D.B. Beringer, R.A. Lukaszew, W.M. Roach, R. Skuza (The College of William and Mary) C.E. Reece (JLAB)

Superconducting thin films and multilayers have attracted the attention of the scientific community due to the promise of overcoming the maximum field gradients that SRF cavities can withstand, pushing them above 100 MeV/m*. Nevertheless, in order to achieve the desired properties, special attention needs to be devoted to the epitaxy and growth mode of such thin films, taking into account multiple aspects such as crystalline quality, lattice strain, grain size, etc. We present a complete correlation between morphology, structure and superconducting properties such as critical field, critical temperature and complex susceptibility for single crystal Nb(110) thin films sputter deposited on a-plane sapphire substrates. The influence of strain and grain boundaries in the superconducting transition is analyzed in detail, since the lattice mismatch between Nb and sapphire induces strain in the first atomic layers and may affect the superconducting properties of the thin films. AC susceptibility techniques allow us to identify the dissipative effects in the lattice associated with the presence of defects, thus allowing us to tune the growth conditions to minimize their effect.

*A. Gurevich, Applied Physics Letters 88 (1), 012511 (2006).

Funding: Defense Threat Reduction Agency: HDTRA1-10⁻¹-0072; Department of Energy: DE-AC05-06OR23177

RF Surface Impedance of MgB₂ Thin Films at 7.5 GHz

The Surface Impedance Characterization (SIC) system in Jefferson Lab can presently make direct calorimetric RF surface impedance measurements on the central 0.8 cm² area of 5 cm diameter disk samples from 2 to 20 K exposed to RF magnetic fields up to 14 mT at 7.5 GHz. MgB₂ thin films from STI/LANL were deposited on 5 cm diameter Nb disks using reactive evaporation technique. We will report the results of measurements on these samples using the SIC system. The data will be interpreted based on BCS theory as the temperature-dependent properties suggest evaluation of the T_c, energy gap, penetration depth, mean free path and coherence length.

Funding: Authored by Jefferson Science Associates, LLC under U.S. DOE Contract No. DE-AC05-06OR23177

B. Xiao, M.J. Kelley (The College of William and Mary) H.L. Phillips, C.E. Reece (JLAB) T. Tajima (LANL)

THPO048

Atomic-Scale Characterization of Niobium for SRF Cavities Using Ultraviolet Laser-Assisted Local-Electrode Atom-Probe Tomography

Niobium is the metal of choice for superconducting radio-frequency (SRF) cavities for the International Linear Collider

due to the highest critical temperature (T_c = 9.2 K) of any element in the periodic table and can be plastically deformed into complex geometries. Differences in surface chemistry from bulk niobium are believed to determine the performance of SRF cavities, such as the high-field Q (quality factor) drop. In this study, the surface chemistry of niobium was characterized utilizing ultraviolet (UV) laser-assisted local-electrode atom-probe (LEAP) tomography employing picosecond laser pulsing together with transmission electron microscopy (TEM). The superior spatial resolution and analytical sensitivity of a LEAP tomograph permits us to determine the surface composition on an atom-by-atom and atomic layer-by-layer basis. The three-dimensional reconstructions from three-dimensional LEAP tomographic analyses demonstrate different behaviors for oxygen and hydrogen atoms in pure niobium.

Funding: This research was supported by Fermi Lab. and the USDOE. The LEAP tomograph was purchased with funding from the NSF-MRI (Grant No. DMR 0420532) and ONR-DURIP (Grant No. N00014-0400798) programs.

Y.-J. Kim, D.N. Seidman (NU) A. Romanenko (Fermilab)

THPO049

TE Sample Host Cavities Development at Cornell

In order to measure surface resistance of new materials other than niobium such as Nb₃Sn and MgB₂, two sample host niobium cavities operating at TE modes have been developed at Cornell University. The first one is a 6GHz pillbox TE011 cavity modified from an older vision enabling testing 2.75" diameter flat sample plates*. The second one is an optimized mushroom-shape niobium cavity operating at both 4GHz TE012 and 6GHz TE013 modes for 3.75" diameter flat sample plates**. First results from the commissioning of the two TE cavities will be reported.

* D. Rubin et al., Phys. Rev. B 38, 6538(1988)

** Y. Xie, J. Hinnfield, M. Liepe, "Design of a TE-type cavity for testing superconducting material samples", SRF2009, Berlin (2009)

Funding: Work supported by NSF and Alfred P. Sloan Foundation

Y. Xie, M. Liepe (CLASSE)

THPO050

THPO051

Laser Re-Melting Influence on Nb Properties: Geometrical and Chemical Aspects

A.V. Dzyuba, L.D. Cooley, E. Toropov (Fermilab) A.V. Dzyuba (NSU) M. Ge (CLASSE) G. Wu (ANL)

We present recent results on Laser re-melting system used to smoothen niobium surfaces of superconducting RF cavities in order to overcome quench. In

the work we studied both chemical and geometrical aspects of the melting by means of electron backscattered diffraction microscopy and laser confocal microscopy. BCP, EP and HF impacts have been investigated on both single and large grain niobium samples. Appropriate post processing has been suggested.

THPO052

Investigation of Near-Surface Interstitial Hydrogen in Cavity-Grade Niobium

A. Romanenko (Fermilab) L.V. Goncharova (UWO)

Details of the distribution of near-surface hydrogen in niobium cavities is important for research into mechanisms affect-

ing quality factor dependence on the magnitude of surface fields. We utilized an elastic recoil detection technique to extract the distribution of hydrogen with depth resolution of order one nanometer in samples, which underwent different treatments similar to the ones with the known effect on cavity performance. Results of this study and possible implications are reported.

THPO053

Material for Fabrication of DESY Large Grain/Single Crystal Cavities

X. Singer, J. Iversen, W. Singer, K. Twarowski (DESY) H.G. Brokmeier (Technische Universität Clausthal, Institut für Nichtmetallische Werkstoffe) R. Grill (Plansee Metall GmbH) F. Schoelz, B. Spaniol (W.C. Heraeus GmbH, Materials Technology Dept.)

Material for large grain LG and single crystal SC cavities of TESLA shape has been developed in collaboration with industry. One of the aspects of LG material was electron beam melting of the ingots with required structure. The second was slicing of the discs cost effectively with

tight thickness tolerances, high surface quality and high purity. Surface and structural properties of SC on the LG discs are investigated. Measurements of the crystal orientation on the LG discs of three companies have been done by complete penetration using synchrotron radiation. Two LG material features have been stressed in cavity production: the influence of the LG crystal orientation on the anisotropic behavior during deep drawing and the impact of pronounced steps at grain boundaries on cavity behavior. 11 LG 9-cell cavities of XFEL-like shape are fabricated. The procedure of increasing the crystal size by rolling of LG discs and cut out of SC discs, followed by subsequent forming and welding without destroying of the SC structure, was developed. A method of fabrication of single crystal cavities was proposed. Several SC cavities with different crystal orientations were produced.

Magneto-Optical and Electromagnetic Study Different Forms of Nb for SRF Application

In order to understand the properties of different forms of Nb for cavity applications we investigated pure bulk polycrystalline Nb as well as thin bi-crystal films grown on STO substrates. Thin film Nb is potentially useful for our electrical and magnetic characterization of SRF Nb because of its high volume to thickness ratio. In polycrystalline bulk Nb, Magneto-Optical imaging showed regular magnetic flux behavior across the full sample width except for when the plane of the GBs (grain boundaries) was parallel to the direction of the external magnetic field. In thin films of Nb at temperature above 7 K we also observed regular flux penetration from the edges of the films and earlier flux penetration at the GBs than in the grains. However, below 7 K the regular flux penetration triggers a dendritic flux instability obscuring any inhomogeneous flux behavior. We contrast such behavior with that found for bulk high purity Nb. From MO images we were able to pattern peculiarities of flux behavior at different temperatures and magnetic field and, as a result, calculate the critical current in the grains and across the GB in both form of Nb.

A. Polyanskii, D.C. LARBALÉSTIER, Z.H. SUNG (ASC) P.J. LEE (NHMFL) A-M. Valente-Feliciano (JLAB)

Funding: The work at the Applied Superconductivity Center was supported by the US DOE under grants DE-FG02-07ER41451, FNAL PO 570362, and the State of Florida

Investigation of Samples Separated From Prototype Cavities of the European XFEL

XFEL prototype cavities fabricated in industry and treated at DESY mainly meet the specification. Few cavities demonstrated low performance (13-20 MV/m) limited by thermal breakdown. The T-map analysis detected quench areas mainly close to the equator. Optical inspection by high resolution camera allowed tracking the several stages of preparation (as received, after the main electropolishing EP, after RF test) and in some cases makes possible monitoring the evolution of defects. In order to understand the nature of reduced performance and get more detailed information on the origin of defects, some samples have been extracted from four cavities and investigated by light microscope, 3D-microscope, SEM, EDX and Auger spectroscopy. Several surface flaws with sizes from a few μm to hundreds of μm have been detected. The defects can be grouped in four categories. The first category of defects indicates foreign elements (often with increased content of carbon). Deviation from smooth surface profile characterizes the second type of defects (holes, bumps). Damaged surface areas at high pressure water rinsing and etching pits belong to the third and fourth category of defects.

X. Singer, S. Aderhold, A. Ermakov, D. Reschke, W. Singer, K. Twarowski (DESY) M. Hoss (W.C. Heraeus GmbH, Materials Technology Dept.)

Thermal-Vacuum Variations of the Surface Oxide Complex on Cu

The surface chemistry of Cu is the most critical factor in the initial kinetics of Nb deposition, primarily because the degree of Cu oxidation may vary from a sub-chemisorbed layer to a complete oxidation state of CuO (cupric), thus providing a spectrum of conditions that influence the nucleation and growth of the thin film. To date, the oxidation of Cu has been thoroughly investigated under a variety of environments, from high pressure to ultrahigh vacuum, but the specific state of the surface oxide complex as a function of temperature and environmental pressure has not been studied. The predominant native oxide on Cu is Cu₂O (cuprous) which, in bulk or sufficient thickness, is stable until 1230°C where it begins to decompose. However, a thin film native oxide (<10 nm) on bulk Cu begins to decompose at temperatures far lower than 1230°C. In this note, we report the stability of surface Cu₂O as well as the variation in surface chemistry of the Cu surface over the range of 25 – 900°C in a low pressure environment.

M. Bagge-Hansen, R.A. Outlaw (The College of William and Mary) C.E. Reece, J.K. Spradlin, A-M. Valente-Feliciano (JLAB) K.I. Seo (NSU)

THPO054

THPO055

THPO056

THPO0057

Superconducting DC and RF Properties of Ingot Niobium

P. Dhakal, G. Ciovati, P. Kneisel, R. Myneni (JLAB)

Recently [1, 2], the DC and low frequency magnetic and thermal properties of large-grain niobium samples subjected to different chemical and heat treatment were measured. Here, we extend the similar study to the cylindrical hollow rods of larger diameter, fabricated from new niobium ingots, manufactured by CBMM. The results confirm the influence of chemical and heat-treatment processes on the superconducting properties, with no significant dependence on the impurity concentrations in the original ingots. Furthermore, RF properties such as the surface resistance and quench field of the niobium rods were measured using a TE011 cavity. The hollow niobium rod is the center conductor of this cavity, converting it to a coaxial cavity. The quench field is limited by the critical heat flux through the rods' cooling channel.

[1] Mondal et al., SRF 2009, Berlin, 2009.

[2] Dhavale et al., Proc. of the First Int. Symp. on the Superconducting Sci. and Tech. of Ingot Niobium, AIP Conference Proceedings 1352, p. 119 (2011).

THPO0058

Phase-Sensitive Nonlinear Near-Field Microwave Microscopy on MgB₂ Thin Films

B.G. Ghamsari, S. M. Anlage, T.M. Tai (UMD)

MgB₂ has recently attracted much attention as a coating for Nb to enhance the RF critical field in Superconducting Radio Frequency (SRF) cavities. However the surface properties of MgB₂, including its intrinsic nonlinearities as well as various types of defects, can limit the RF performance of such cavities. This work presents phase-sensitive nonlinear near-field microwave microscopy on MgB₂ films. An intense localized RF magnetic field is induced on the surface of MgB₂ films by means of a magnetic write head, and the amplitude and phase of the third harmonic voltage generated by the film are measured. Power and temperature dependence of the third harmonic response are studied to identify the dominant mechanism of nonlinearity in the film under different operating conditions, and a phenomenological model is developed to relate the nonlinear response to the local critical RF field. The method could be generalized by scanning the probe over the sample, and possibly over various defects, to generate a map of the critical RF field and enable classification of different types of defects in terms of their effect on the RF performance of MgB₂.

Funding: We acknowledge the support of DOE/HEP under contract #DESC0004950, the Office of Naval Research/UMD Appel Center, task D10 (Award No. N000140911190), and CNAM.

THPO0059

Correlation of Microstructure, Chemical Composition and RRR-Value in High Purity Niobium (Nb-RRR)

R. Grill, W. Simader (Plansee Metall GmbH) M. Heilmaier, D. Janda (TU Darmstadt) W. Singer, X. Singer (DESY)

For manufacturing of Nb-RRR sheet material a thorough understanding of material properties and niobium metallurgy is necessary to meet the required regarding material properties as specified for the XFEL project. Especially for the RRR value it is known, that residual stresses, and increased levels of vacancy and impurity concentrations, and dislocation densities after the final heat treatment can cause a severe degradation of the RRR value. Also, a comprehensive understanding of the influence of further microstructural properties (e.g. different textures due to rolling operations and annealing, dislocation substructures, etc.) on the RRR-value is lacking. For specimens having RRR-values in the range of 360 to 430, the crystallographic texture has been investigated and correlated with the measured RRR values. Furthermore, the possible influence of different impurity levels on the RRR value was calculated, compared with the measured values and discussed with regard to the current material specification for the XFEL project.

First Principles Investigation of Hydrogen in Niobium

Niobium hydride is a contributor to degraded niobium SRF cavity performance by Q-slope and Q-disease. Hydrogen is easily absorbed into niobium when the

protective oxide layer is disturbed, such as during electropolishing and chemical treatments, and the structure and distribution of hydrogen in niobium is altered during other processing steps such as baking. To optimize cavity performance and production efficiency, it is important to understand the structures of hydrogen in niobium, including the interactions of hydrogen with structural defects and other impurities such as oxygen. In this study density functional theory was used to evaluate these interactions. Hydrogen was examined as a dissolved interstitial impurity and in ordered niobium-hydride phases; and the interactions between hydrogen, niobium, vacancies on niobium sites, and oxygen dissolved in niobium were evaluated. The results yield information about the thermodynamic, electronic, magnetic, and geometric properties of these systems, which lead to important implications concerning the mobilities of impurities and vacancies in niobium and the precipitation of phases that are detrimental to cavity performance.

D.C. Ford, L.D. Cooley (Fermilab) **D.C. Ford** (Northwestern University) D.N. Seidman (NU)

THPO060

Activation of Field Emitters on Clean Nb Surfaces

Systematic investigations of the enhanced field emission (EFE) from surface irregularities of typical EP and HPR treated Nb samples revealed an exponential increase of the emitter site density N with the initial onset surface field ($E_{on} = 80-160$ MV/m) and a strong activation effect, i.e. the final occurrence of EFE at 2-4 times lower E_{on} relevant for superconducting XFEL and ILC cavities. Possible explanations for this activation are breakdown across the surface oxide, surface erosion by a local microplasma or de/adsorption effects. Such emitter activation might also be caused by the usual baking or rf power processing of cavities. Therefore, we have started a systematic test series with large-grain Nb samples based on correlated field emission microscopy (FESM) and high-resolution SEM investigations before and after heating at temperatures between 122 and 800°C. As expected, we have obtained slightly ($\times 2$) increased N after baking and strongly ($\times 10$) after heating at 800°C. Moreover, the E_{on} of the activated emitters is reduced down to 40 MV/m. Most emitters could be identified by SEM as microscratches. We will discuss the impact of these results on the EFE of SRF cavities.

A. Navitski, S. Lagotzky, G. Mueller (Bergische Universität Wuppertal) D. Reschke, X. Singer (DESY)

Funding: Funded by Helmholtz-Allianz 'Physics at the Terascale' and das BMBF-Verbundprojekt 05H09PX5.

THPO061

THPO062

Epitaxial Niobium Thin Films for Accelerator Cavities

W.M. Roach, D.B. Beringer, C. Clavero, R.A. Lukaszew (The College of William and Mary) C.E. Reece (JLAB)

SRF technology used in linear accelerators is based on bulk Nb cavities that have high cost and are approaching the maximum field gradients they can withstand*.

Thus, development of a suitable alternative to bulk Nb is needed. Attempts have been made to implement Nb-coated Cu cavities since the thermal conductivity of Cu is better than bulk Nb**. Our studies show that the transport properties of Nb, in particular the residual resistance ratio (RRR), are better when epitaxially grown on crystalline ceramics (i.e. MgO and Al₂O₃) compared to Cu templates. Since grain boundaries are one of the main obstacles to superconducting transport, we show how the increased number of crystallographic domains that can occur during epitaxial Nb growth onto Cu surfaces leading to higher density of grain boundaries can explain our results. We propose a route to improved performance while maintaining thermal efficiency by using seed-layers on Cu templates that can decrease grain boundary density. We will show our correlated studies of microstructure and surface morphology and the resulting transport/susceptibility properties illustrating possible mechanisms to improve cavity performance of such films.

* P. Kneisel et al., Proceedings of 2005 Particle Accelerator Conference, Knoxville, TN, TPPT076 (2005).

** S. Calatroni, Physica C 441, 95 (2006).

Funding: Defense Threat Reduction Agency: HDTRA1-10¹-0072 Department of Energy: DE-AC05-06OR23177

THPO063

Study of the Impurity Species in Niobium Films Grown by ECR Technique Employing Secondary Ion Mass Spectrometry

A-M. Valente-Feliciano, C.E. Reece, A.T. Wu, X. Zhao (JLAB) F.A. Stevie (NCSU AIF)

One attractive path is to use a thin film deposition technique to fabricate Nb films on Cu or other appropriate substrates instead of using bulk Nb to fabri-

cate Nb SRF cavities. It is known that the physical properties of Nb films can be affected by their impurity species and concentrations. In this contribution, a study of the impurity species in niobium films grown by electron cyclotron resonance plasma energetic deposition technique employing Secondary Ion Mass Spectrometry (SIMS) is reported. Measurements were performed on Nb films deposited on Al₂O₃ and MgO substrates using Cs⁺ and O₂⁺ primary beams. The obtained results were compared with those obtained on a standard bulk Nb sample treated by buffered chemical polishing. It was found that under suitable deposition conditions H content could be significantly lower in Nb films than that in the standard Nb bulk materials. Depth profiling by O₂⁺ found that substrate elements, such as Al and Mg, have different distributions from the film/substrate interface toward the top layer of film. Possible implications of the obtained experimental results towards the RF properties of the Nb films will be discussed.

Funding: Authored by Jefferson Science Associates, LLC under U.S. DOE Contract No. DE-AC05-06OR23177.

Structural Properties of Niobium Thin Films Deposited on Metallic Substrates by ECR Plasma Energetic Condensation

Particle accelerator technologies rely on SRF cavities to create the accelerating gradient for beam lines. Solid niobium cavities are widely employed throughout the community despite high material, fabrication, and operation cost. New thin film technologies are being explored for the suitability of niobium coatings for accelerating cavities. Thin layers of high-quality niobium would be deposited on a base material that has lower material and fabrication cost. Copper is a strong candidate for the cavity base due to availability, cost, machinability, and potentially improved performance characteristics of the niobium SRF surface. Initial results of TEM, EBSD and XRD analyses of niobium thin films grown on copper substrates under controlled conditions are presented to demonstrate the feasibility of the technology and establish lower limits of performance characteristics. Correlation of RRR data with the structure of niobium thin films will demonstrate the importance of thin film structural quality.

Funding: Authored by Jefferson Science Associates, LLC under U.S. DOE Contract No. DE-AC05-06OR23177.

J.K. Spradlin, H.L. Phillips, C.E. Reece, A-M. Valente-Feliciano, X. Zhao (JLAB) D. Gu (ODU) K.I. Seo (NSU)

THPO064

Anomalous Morphological Scaling in Epitaxial Nb Thin Films on MgO(001)

Surface and interface roughness are critical factors in determining the technological viability of many systems, in particular the development of next-generation superconducting radio frequency (SRF) cavities. Thus, we have undertaken a systematic effort to investigate the surface evolution of epitaxially grown Nb thin films under specific deposition conditions. This is important since ongoing efforts to improve cavity's performance have considered the possibility of multi-layered thin film coatings* as an alternative to the current bulk Nb technology. We examined the surface morphology of epitaxial Nb films grown on MgO at different stages during growth and applied dynamical scaling analysis to the surface features. Our thin film nucleation and growth kinetics studies are relevant since thin films may differ from bulk systems due to limited material supply as well as stress contributions from lattice mismatch with the substrate. This can induce significant surface roughness which can in turn lead to undesirable effects for SRF applications. Our studies may offer a venue to minimize these drawbacks by suitable choice of thin film growth parameters and substrates.

* A. Gurevich, Appl. Phys. Lett. 88, 012511 (2006).

Funding: Department of Energy: DE-AC05-06OR23177 Defense Threat Reduction Agency: HD-TRA1-10-1-0072

D.B. Beringer, C. Clavero, R.A. Lukaszew, W.M. Roach (The College of William and Mary) C.E. Reece (JLAB)

THPO065

Stoichiometric Nb₃Sn in First Samples Coated at Cornell

A cavity coated with the superconductor Nb₃Sn theoretically will be able to reach more than twice the maximum accelerating field of Nb in a cavity under the same operating conditions and will have a much lower BCS surface resistance at a given temperature. The SRF group at Cornell has recently developed facilities to fabricate Nb₃Sn on Nb. The first samples have been coated, and several tests have been performed to characterize them. Results presented include SEM images of the surface, anodization tests, a critical temperature measurement, a test for RRR degradation, and stoichiometry measurements using EDS and XPS.

S. Posen, M. Liepe (CLASSE)

THPO066

THPO067

Characterization of Large Grain Nb Ingot Microstructure Using OIM and Laue Methods

D. Kang, D.C. Baars, T.R. Bieler (Michigan State University)
G. Ciovati (JLAB) C. Compton (FRIB) T.L. Grimm, A.A. Kolka
(Niowave, Inc.)

Large grain niobium is being examined for fabricating superconducting radiofrequency cavities as an alternative to using rolled sheet with fine grains. It is desirable to know the grain orientations of a

niobium ingot slice before fabrication, as this allows heterogeneous strain and surface roughness effects arising from etching to be anticipated. Characterization of grain orientations has been done using orientation imaging microscopy (OIM), which requires destructive extraction of pieces from an ingot slice. Use of a Laue camera allows nondestructive characterization of grain orientations, a process useful for evaluating slices and deformation during the manufacturing process. Five ingot slices from CBMM, Ningxia, and Heraeus are compared. One set of slices was deformed into a half cell and the deformation processes that cause crystal rotations have been investigated and compared with analytical predictions. The five ingot slices are compared in terms of their grain orientations and grain boundary misorientations, indicating no obvious commonalities, which suggests that grain orientations develop randomly during solidification.

Funding: This work was supported by the U.S. Department of Energy, Office of High Energy Physics, through Grant No. DE-S0004222.

THPO068

Experimental Investigation and CPFEM Modeling of Single Crystal Niobium for Tube Hydroforming

A. Mapar ((MSU)) D.C. Baars, T.R. Bieler, D. Kang (Michigan State University) C. Compton (FRIB) P. Darbandi, F. Pourboghra (MSU) J.E. Murphy (University of Nevada, Reno)

To optimize the manufacturing process and to increase the performance of niobium cavities, mechanical behavior of single crystal niobium was investigated using tensile tests. The crystal orientation of the specimen was recorded before and after the testing. The flow stress of the single crystal niobium showed a significant and complex dependence on the crystal orientation. This phenomenon has led to the conclusion that the Schmid's law does not apply to this material, as it does to FCC materials. Considering the plastic anisotropy due to the non-planar distribution of screw dislocation cores, the authors are developing a new crystal plasticity model for the single crystal niobium. An optimized crystal plasticity material model based on combined constraints was recently used to identify orientation dependent critical resolved shear stresses and work hardening parameters for Nb single crystal. Progress toward validating this single crystal model for different crystal orientations will be presented. This will lead to the ability to use the CPFEM model in conjunction with a commercial FE code to simulate the tube bulging of Nb single/multi crystal tubes.

Funding: This work was supported by the U.S. Department of Energy, Office of High Energy Physics, through Grant No. DE-S0004222, and through a research contract with Fermi National Laboratory.

Nb Film Growth on Crystalline and Amorphous Substrates

This paper describes Energetic Condensation Growth of Nb films using a cathodic arc plasma on crystalline (a- and c-sapphire, MgO) and amorphous (borosilicate) substrates. The crystal substrates were heated to 700 deg C and subsequently coated at 300, 500 and 700 deg C. Film thickness varied from $\sim 0.25\mu\text{m}$ up to $>3\mu\text{m}$. The borosilicate substrate was preheated to 700 deg C but coated at 500 deg C. XRD spectra (Bragg-Brentano) and pole figures show a change in crystal structure on c-sapphire from textured (with twin-symmetry) to hetero-epitaxial as the temperature is increased. RRR=43 was measured on c-sapphire which is lower than RRR=200 on a-sapphire and 541 on MgO. On borosilicate, the (110) and (220) planes of Nb show sharper spectra at higher temperatures with an increase to RRR=31 at 500 deg C. The growth of crystalline Nb on an amorphous substrate is driven by energetic (40-120eV) ions from the cathodic arc plasma. The significance of crystal structure on amorphous substrates has implications for future, lower-cost SRF cavities. SIMS data show the role of impurities on crystal growth and RRR.

E.F. Valderrama, C. James, M. Krishnan (AASC) P. Maheshwari, F.A. Stevie (NCSU AIF) K.I. Seo (NSU) X. Zhao (JLAB)

Funding: Funded by DE-FG02-08ER85162 and DE-SC0004994. The Jefferson Science Associates, LLC effort supported by DE-AC05-06OR23177, with supplemental funding from the American Recovery and Reinvestment Act.

THPO069

Effect of Fabricate Condition on Properties of Bi-2212 Thin Films

High-quality epitaxial c-axis oriented Bi-2212 thin films were deposited on single crystalline (100) MgO substrate using Pulsed Laser Deposition. The results show that these films are good quality with c-axis orientation and epitaxial growth, good electrical and magnetic properties. The critical current density J_c was found to be strongly dependent on the temperature and magnetic field. The critical current density for the film growth with the best deposition conditions ($J_c=6.3 \times 10^6$ A/cm² in 0.5T magnetic field at 5 K). The onset temperature for superconducting transition T_c -onset = 95K and the temperature for zero resistivity T_c -zero=80K.

T.M. Nguyen (nguyenthi mua)

THPO070

Detailed Surface Analysis of Incremental Centrifugal Barrel Polishing (CBP) and EP of Single-Crystal Niobium Samples

We performed Centrifugal Barrel Polishing (CBP) on single crystal niobium samples housed in a stainless steel sample holder following a polishing recipe recently developed at FNAL [*]. We were able to obtain a mirror-like finish after the final stage of tumbling, although some defects and imbedded particles remain. Our presentation will discuss the initial results from the coupon study, including qualitative and quantitative analysis of the surface characteristics from each step in the CBP process, followed by HPR and well controlled incremental EP. These will include surface roughness, size and character of contaminants, surface crystal structure, and overall finish. We will discuss how the surface characteristics should guide the SRF community in exploiting or adapting the Fermi recipe; including why minimal subsequent EP is needed, and possible places for modification of the recipe to reduce polishing time.

A.D. Palczewski, C.E. Reece, H. Tian, O. Trofimova (JLAB)

* CA Cooper, LD Cooley, "Mirror Smooth Superconducting RF Cavities by Mechanical Polishing with Minimal Acid Use," <http://lss.fnal.gov/archive/2011/pub/fermilab-pub-11-032-td.pdf>, (May 31, 2011)

Funding: This work is authored by Jefferson Science Associates, LLC under U.S. DOE Contract No. DE-AC05-06OR23177.

THPO071

THPO0072

Raman Spectroscopy as a Probe of Surface Oxides and Hydrides on Niobium

J. Zasadzinski (IIT) Th. Proslie (ANL)

to identify surface oxides and hydrides on annealed, recrystallized foils of high purity Nb and on single crystals of cavity grade Nb. Cold worked regions of the Nb foil as well as rough regions near grain boundaries showed clear evidence of ordered hydride phases which were identified by VASP phonon calculations. Cold worked regions also displayed enhanced surface paramagnetism. Surface enhanced Raman spectra have also been obtained using 1.0 nm Au depositon. The SERS spectra reveal hydride molecular species which are not observable by conventional Raman. These results indicate that Raman is a useful probe of Nb surfaces relevant for cavity performance

Funding: ANL, FNAL

Raman microscopy/spectroscopy has been used in conjunction with AFM, tunneling and magnetic susceptibility

THPO0073

Laser Melt Smoothing of Niobium Superconducting Radio-Frequency Cavity Surfaces

S. Singaravelu, M.J. Kelley, J.M. Klopff, G.A. Krafft (JLAB) C. Xu (The College of William and Mary)

Superconducting Radio Frequency (SRF) niobium cavities are at the heart of an increasing number of particle accelerators. Their performance is dominated by a several nm thick layer at the interior surface. Maximizing the smoothness of this surface is critical and aggressive chemical treatments are now employed to this end. We describe laser-induced surface melting as an alternative "greener" approach. Modeling predicts the surface temperature as a function of per-pulse energy density. Guided selection of laser parameters achieves melting that reduces the surface roughness and may also mitigate surface damage from the fabrication process. The resulting topography was examined by SEM, and AFM. PSD spectra computed from AFM data were used for studying the topography of the treated niobium.

Superconducting Radio Frequency (SRF) niobium cavities are at the heart of an increasing number of particle accelerators. Their performance is dominated by a several nm thick layer at the interior surface.

THPO0074

NbTiN Films for SRF Multilayer Structures

A-M. Valente-Feliciano, H.L. Phillips, C.E. Reece, J.K. Spradlin, X. Zhao (JLAB) D. Gu (ODU) K.I. Seo (NSU)

For the past three decades, bulk niobium has been the material of choice for SRF cavities applications. In the recent years, RF cavities performances have approached the theoretical limit for bulk niobium. For further improvement of RF cavity performance for future accelerator projects, an interesting alternative has been recently proposed by Alex Gurevich with the Superconductor-Insulator-Superconductor multilayer approach, using the benefit of the higher critical field Hc2 of higher-Tc superconductors without being limited with their lower Hc1. JLab is pursuing this approach with the development of multilayer structures based on NbTiN via magnetron sputtering and High Power Impulse Magnetron Sputtering (HiPIMS). Insulators such as, AlN, Al2O3 and MgO are being investigated as candidates for the insulator layers. This paper present the preliminary results on the characteristics of NbTiN and insulator layers and a first attempt of a NbTiN-based multilayer structure on bulk Nb and thick Nb films.

For the past three decades, bulk niobium has been the material of choice for SRF cavities applications. In the recent years, RF cavities performances have approached the theoretical limit for bulk niobium.

Funding: Authored by Jefferson Science Associates, LLC under U.S. DOE Contract No. DE-AC05-06OR23177.

Does Annealing Reduce or Remove Defects Observed After Electropolishing?

Fermilab has been studying the effect of cold work on the electropolishing of niobium. Since most cavities are electropolished (EP) without recovering the cold work of deep-drawing half cells or the strains induced by welding, this study could shed light on mechanisms by which defects in cavities form during EP. Our past work showed marked increase in the tendencies for pitting when the niobium piece was cold worked, repeatedly dipped into an electrolyte to form a meniscus, or otherwise agitated. Welding itself did not seem to exacerbate pitting. In the present work, annealing in a vacuum furnace was used to recover cold work prior to EP for both plain and welded coupons. Changes in pitting tendencies will be discussed. We also introduce a new instrument, laser confocal scanning microscopy, which permits pitting to be assessed over areas much larger than profilometry does, which helps us analyze large coupons.

L.D. Cooley, D. Burk, D.T. Hicks, R. Schuessler, C. Thompson (Fermilab)

Funding: Work supported by the U.S. Department of Energy under contract No. DE-AC02-07CH11359.

THPO075

Measurement of the Loss Tangent and Heat Capacity of a Large Single Crystal Sapphire

A high-gradient test cavity is being developed to test wafer samples of advanced SRF surfaces at gradients to or beyond the BCS limit of Nb. The cavity design employs dielectric loading by a large high-purity sapphire crystal. As a first step towards construction we set out to measure the loss tangent of such a large HEMEX-grade sapphire crystal. The crystal was inserted into a single-cell CEBAF cavity equipped with couplers to operate in the TE₀₁ mode so that the electric field was localized within the sapphire. Cold testing of the cavity, without the sapphire and numerical simulations, verified that the unloaded Q of the cavity was adequate to accurate measurement of the sapphire loss tangent down to 10⁻¹⁰. Several Q measurements were made of the sapphire-loaded cavity in a variety of conditions. The temperature dependence of the sapphire's loss tangent and heat capacity were measured. The implications of these results for the high-gradient wafer test cavity design are reported.

N. Pogue, P.M. McIntyre, A. Sattarov (Texas A&M University)

Funding: DOE Grant - DEFG0210ER41650

THPO076

Mo-Re Films for SRF Applications

Single (sintered composite Mo₃:Re₁) and dual targets of Mo/Re were used to grow superconducting films of Mo:Re, using cathodic arc plasmas. Sharp superconducting transitions (at up to 13K) were observed in ~1 μm thick films deposited on a-sapphire and MgO crystals. The measured RRR (defined as the ratio of resistivity at 300K to that at 14K) in the best films was 6, which is higher than measured by others at higher annealing temperatures. XRD (Bragg-Brentano spectra) revealed a single sharp peak of Mo-Re (611) plane, from the composite Mo₃:Re₁ film. SIMS measurements revealed the role of impurity concentrations on superconducting properties. For the dual-target films, stoichiometry was controlled by varying the current to each cathode. The XRD spectra in this case showed the (330) plane of Mo-Re; hetero-epitaxial growth of Mo-Re depends upon the stoichiometry of the film. This dual-target approach allows other compound films (e.g. Nb₃Sn, MgB₂ etc.) to be grown in a single-step. For SRF cavity applications, the RRR should be increased to >100, which is our next goal.

E.F. Valderrama, C. James, M. Krishnan (AASC) P. Maheshwari, F.A. Stevie (NCSU AIF) K.I. Seo (NSU) X. Zhao (JLAB)

Funding: Funded by DE-FG02-08ER85162 and DE-SC0004994. The Jefferson Science Associates, LLC effort supported by DE-AC05-06OR23177, with supplemental funding from the American Recovery and Reinvestment Act

THPO077

THPO0078

Surface and Thin Film Characterization of Superconducting Multilayer Films for Application in RF Accelerator Cavities

R.K. Schulze, L. Civale, N.F. Haberkorn, M. Hawley, T. Tajima, Y.Y. Zhang (LANL) B. Moeckly (STI) T. Prolier (ANL) A.T. Zocco (UC)

Application of multilayer ultra-thin films on the surfaces of Nb superconducting RF cavities shows promise in substantially improving the performance of superconducting RF cavities into the 100

MV/m range. The materials science challenges associated with producing complex multilayer films, particularly for conformal application on the interior 3D surfaces of RF cavities are substantial. Here we present surface and thin film analysis of two candidate superconducting materials, MgB₂ and NbN, along with multilayers produced with alternating superconductor and dielectric ultra-thin films. We report on the analysis methods and describe results from a variety of thin film samples. The materials stability, μ and nano structure, chemistry, and thin film morphology are highly dependent on methods and parameters used in the thin film deposition. From our analysis, important factors for producing quality film materials include chemical stoichiometry, impurity content, deposition temperature, substrate surface condition, and choice of dielectric material. These factors will be discussed in the context of the production methods used for these ultra-thin superconducting film structures.

Funding: DOE Early Career Award (Tajima) and the US DOE Office of Nuclear Physics

THPO0079

Surface Preparation of Metallic Substrates for Quality SRF Thin Films

J.K. Spradlin, O. Trofimova, A-M. Valente-Feliciano (JLAB)

Surface preparation is an essential prerequisite for thin film depositions. Rough or chemically impure surfaces adversely

affect the nature of the thin film. Understanding the properties of the substrate and how they influence the quality of the thin film is necessary to transfer thin film deposition technologies to SRF cavity applications. A substrate that is flat, has sufficient grain size, and is chemically pure is the ideal starting point for thin film depositions. A method for copper substrate preparation is reviewed for niobium thin film deposition that provides epitaxy on large and fine grain copper as well as single crystal copper. Preliminary data on niobium and aluminum substrate preparation will also be included.

Funding: Authored by Jefferson Science Associates, LLC under U.S. DOE Contract No. DE-AC05-06OR23177.

THIOC — Hot Topics

Recipes for 9-cell cavity fabrication and preparation

In the mass production of International Linear Collider (ILC), about 16,000 9-cell SRF cavities must be produced for the linac. The current recipe of 9-cell cavity production is not enough for the required cost reduction for ILC. Various ideas for the cost reduction of 9-cell cavity fabrication would be discussed in this presentation. As the final surface treatment of 9-cell cavity, the Electro-Polishing (EP) is the best candidate to realize high yield rate for high-gradient performance. However, the laboratories in the world are still using different EP parameter-sets for various reasons. In this presentation, the comparison of EP parameters among laboratories would be done and how we can reach to the best parameter sets would be discussed.

HOT TOPIC

FRIOA — SRF Technology

FRIOA01

Adaptive Compensation for Lorentz Force Detuning in Superconducting RF Cavities

W. Schappert, Y.M. Pischalnikov (Fermilab)

The Lorentz force can dynamically detune pulsed Superconducting RF cavities and considerable additional RF power can be required to maintain the accelerating gradient if no effort is made to compensate. Fermilab has developed an adaptive compensation system for cavities in the Horizontal Test Stand, in the SRF Accelerator Test Facility, and for the proposed Project X.

FRIOA02

Innovative Tuner Designs For Low Beta SRF Cavities

Z.A. Conway (ANL)

This presentation will give an overview of innovative low-beta ($0.05 < \beta < 0.6$) cavity frequency tuners for heavy-ion accelerators. These cavities typically operate with microphonic induced frequency perturbations which are a significant fraction of the loaded bandwidth. If uncompensated these frequency variations may unnecessarily increase the RF power required to stabilize the phase and amplitude of the cavity RF fields. Several tuner designs with operating details will be reviewed.

FRIOA03

Recent Progress in HOM Damping from Around The World

M. Liepe (CLASSE)

Continuous progress in SRF technology is pushing the beam parameter envelope for SRF linacs towards higher currents and shorter bunch lengths. Therefore, the demands on the HOM dampers used in these SRF linacs are increasing continuously, and Higher-Order-Mode (HOM) damping remains a very active field of research and development. Different HOM damping concepts have been developed and improved over the last years to support high power handling and broadband HOM damping. In this paper we give an overview of recent progress on antenna, waveguide, and beamline HOM dampers.

FRIOA04

Power Couplers for Spiral-2

Y. Güzmez Martınez, T. Cabanel, J. Giraud, R. Micoud, M. Migliore, J. Morfin, F. Vezzu (LPSC) P.-E. Bernaudin, P. Bosland (CEA/DSM/IRFU) G. Olry (IPN)

The Spiral 2 facility is in construction phase. The driver is a super-conducting linac composed of two types of QWR cavities, $\beta = 0.07$ and 0.12 operated at 88 MHz. Each cavity is fed by a Radio-Frequency antenna coupler designed to accept up to 40kW CW. The tests of the prototype couplers have been successfully achieved in the two types of cavities. The manufacturing is finished and the processing of the 26 couplers is under way. We report the technological choices and the major issues of the process, including the absence of TiN plating. We present the main results of the tests and the processing of the couplers.

Overview of CW Input Couplers for ERL

Various efforts for SRF R&D are in progress all over the world for ERL construction. CW input coupler develop-

H. Sakai (KEK)

ment is one of the key issues for realizing the stable ERL operation. For injector, high power handling is necessary to feed the CW RF power to continuous high current beam acceleration. Furthermore, the soft injector beam should not be disturbed by coupler kick. Thanks to energy recovery, a little power is needed for main linac. However, this feeding average power is also higher than that of the pulsed operation like XFEL or ILC to keep the accelerating field stably under the microphonics of cryomodule. Therefore, it is important for both coupler cases, not to leak the large heat load to He temperature and to avoid the continuous multipacting barriers. In addition, variable coupling is desirable for several beam operations. As a result, many new coupler designs were proposed and developed until now. In this paper, we present the various options and technical issues of ERL input coupler for both injector and main linac. Then we review existing designs associated with R&D testing and summarize the experience and progress in each laboratory around the world.

FRIOA05

Construction of cERL Cryomodules for Injector and Main Linac

The Compact ERL (cERL) project is advanced in Japan. Its aim is to demonstrate the circulation of 100 mA electron beams with energy of 35-200 MeV. Superconducting cavities are key components for realizing ERL. At injector part, electron beams are accelerated up to 5-10 MeV by three 2-cell cavities. Prototype 2-cell cavities show excellent performance of about 40 MV/m. However, heating problem exists on HOM couplers. Improvement of cooling is essential for stable CW operation. Input coupler is another big issue. High power test stand was constructed using a 300 kW klystron. Prototype couplers could deliver from several tens to a hundred kW of RF power. At main linac part, HOM damped 9-cell cavities are applied. Two prototype cavities were manufactured. Initially their performance was limited by field emission. But it was overcome and they reached to more than 20 MV/m. A prototype input coupler is also fabricated for main linac. It successfully propagates 25 kW standing wave and also thermal cycle tests were passed. Prototype HOM absorbers are also fabricated and several tests were carried out. For both parts, cryomodules are under construction. They will be completed in 2012.

K. Umemori, T. Furuya, E. Kako, S. Noguchi, H. Sakai, M. Satoh, T. Shishido, K. Watanabe, Y. Yamamoto (KEK) E. Cenni (Sokendai) M. Sawamura (JAEA) K. Shinoe (ISSP/SRL)

FRIOA06

SRF Photoinjector Tests at HoBiCat

In collaboration with JLab, DESY and the A. Soltan Institute HZB developed a fully superconducting photo-injector as a first step towards a high average current electron source for the BERLinPro ERL. This set up consists of a 1.6 cell superconducting gun cavity with a lead cathode plasma-arc deposited on the half cell backwall and a superconducting solenoid. The system, including a warm diagnostic beam-line section, was recently installed in the HoBiCaT horizontal cavity test cryostat to study beam dynamics within the ERL parameter range. In this talk the first series of RF tests will be presented, including Q measurements, dark current studies, field stability and beam energy measurements.

A. Neumann, W. Anders, R. Barday, A. Frahm, A. Jankowiak, T. Kamps, S. Klauke, J. Knobloch, O. Kugeler, A.N. Matveenko, T. Quast, J. Rudolph, M. Schenk, S.G. Schubert, M. Schuster, J. Voelker (HZB) P. Kneisel (JLAB) R. Nietubyc (The Andrzej Soltan Institute for Nuclear Studies, Centre Swierk) J.K. Sekutowicz (DESY) I. Will (MBI)

Funding: Work funded by the Bundesministerium für Bildung und Forschung and Land Berlin.

FRIOA07

FRIOB — New/Emerging SRF Capability & Applications

FRIOB01

SRF Activities at Peking University

J.K. Hao, J.E. Chen, L. Lin, K.X. Liu, X.Y. Lu, S.W. Quan, B.C. Zhang, K. Zhao, F. Zhu (PKU/IHIP)

Superconducting RF technology has been developed at Peking University for more than 20 years. In the recent years, the researches are mainly focused on pro-

ducing high performance superconducting cavities and installing the DC-SRF photocathode injector as well as related 2K cryogenic facility and other auxiliary equipment. The cavities designed and fabricated by Peking University mainly include TESLA type 9-cell cavities, 1.3 GHz 5-cell cavity for high current electron beam acceleration and 450 MHz spoke cavity for low energy proton acceleration. Vertical tests of the cavities indicate that the cavities show good performances and can be used for superconducting accelerators. The gradient of a 9-cell TESLA type cavity with end groups (PKU3) reaches 28.6 MV/m. To promote the industrialization process in China, a new company, Ningxia Orient Superconductor Technology Co., Ltd., was founded jointly by Ningxia OTIC and Peking University in 2011. The goal of this company is to produce various types of superconducting cavities and pure niobium materials with high quality.

Funding: Work supported by the Major State Basic Research Development Program of China (Grant No. 2008CB817706 and 2011CB808303).

FRIOB02

RF and Beam Test of the DC-SRF Injector of PKU-SETF

F. Zhu, J.E. Chen, J.K. Hao, L. Lin, K.X. Liu, S.W. Quan, K. Zhao (PKU/IHIP)

DC-SRF photocathode injector developed by Peking University is a good candidate for obtaining high average current, low emittance, short electron beam

pulse. Much progress has been made on the 3.5-cell cavity DC-SRF injector since SRF2009. The assembling of the cryomodule was completed with the 3.5-cell SRF cavity which has an accelerating gradient of 23.5MV/m in the vertical test. The preliminary RF experiment has been carried out soon after the installation and commissioning of 2K cryogenic system was finished. The accelerating gradient of the cavity is 11.5MV/m in a horizontal cold test and the Q_{ext} is 6×10^6 . The limitation of the gradient is mainly from our present low RF power source. Higher gradient is expected with a new 20kW solid state RF power source which will be delivered to Peking University soon. The result of preliminary beam loading test of the DC-SRF injector will also be presented in this paper.

Funding: Supported by Major State Basic Research Development Program(973 Program 2011CB808302) and National Natural Science Foundation of China (11075007)

Chinese Plan for ADS and CSNS

High intensity proton accelerator now has two major applications in China: one is Accelerator Driven Subcritical System for nuclear waste transmutation and another is spallation neutron source. A basic research program on ADS started in 2000 in China. Recently a Chinese roadmap for long-term development of ADS was proposed by Chinese Academy of Sciences and the first budget of about \$260M has been approved for ADS key technology R&D. It includes a CW proton linac consisting of a room-temperature RFQ and superconducting spoke cavities. The ADS R&D program started in the first half of 2011. The almost same amount of budget has also been approved for the project of China Spallation Neutron Source (CSNS) and it is going to be launched in September 2011. CSNS accelerator consists of a room-temperature H^- linac and a rapid-cycling synchrotron with beam power of 100kW. It will be upgraded to 500kW beam power in future by adding some superconducting cavities to the linac. So superconducting RF accelerator technology becomes a major research direction in high intensity proton accelerator field in China. This paper will introduce these two programs and present the related R&D activities.

S. Fu, H. Chen, Y.L. Chi, S.X. Fang, L. Ma, W.M. Pan, J. Tang, C. Zhang (IHEP Beijing) Y. He, H.W. Zhao (IMP)

FRIOB03

SRF Accelerator for Indian ADS Program: Present & Future Prospects

Accelerator Driven Systems (ADS) have evoked lot of interest the world over because of their capability to incinerate the MA (minor actinides) and LLFP (long-lived fission products) radiotoxic waste and utilization of Thorium as an alternative nuclear fuel. One of the main sub-systems of the ADS is a high energy and high current CW proton Accelerator. The accelerator for ADS should have high efficiency and reliability and very low beam losses to allow hands-on maintenance. With this criteria, the physics studies has been done for a 1 GeV, 30 mA proton Linac, using NC structures upto 100 MeV followed by Superconducting elliptical cavities, which accelerate the beam from 100 MeV to 1 GeV. We are also studying the configuration where superconducting spoke resonators are used to accelerate the proton beam from 3-200 MeV followed by elliptical cavities for 200 MeV to 1 GeV.

P. Singh (BARC)

Funding: Bhabha Atomic Research Centre, Mumbai, India

FRIOB04

Crab Crossing for LHC Upgrade

The LHC luminosity upgrade aims at reducing the collision point betas by a factor of 2-3 of the design value. Consequently the Piwinski angle is increased well beyond 1 to keep a normalized beam separation in the common focusing channels, thus diminishing the benefit of the beta* reduction. Crab cavities will not only recover this luminosity loss but also enable luminosity levelling, a vital ingredient for the upgrade. The baseline scenario for a crab crossing implementation in the LHC, primarily focusing on the RF cavity development is presented. Constraints from aperture, impedance and machine protection are also highlighted.

R. Calaga (BNL)

Funding: This work partially supported by the US Department of Energy through the US-LARP and by the European Coordination for Accelerator Research and Development (EuCARD) under the FP7.

FRIOB05

The ESS Accelerator

M. Lindroos (CERN) S. Peggs (ESS)

In 2003 the joint European effort to design a European Spallation Source resulted in a set of detailed design reports. Lund was

agreed as the site in 2009. A company, ESS AB, has been created to design, build and operate ESS. A collaboration has been formed for the accelerator work and an update project has been agreed and financed. Detailed planning for the prototyping in a Prepare-to-build (P2B) project has also started. The current status of the Design Update project for the accelerator will be presented, together with an outline of future work. The baseline for the updated design delivers 5 MW of 2.5 GeV protons to a single target, in 2.86 ms long pulses with a 14 Hz repetition rate. The linac will have a normal conducting front end with an ion source, an RFQ and a DTL. The superconducting part starts with spoke cavities followed by two families of elliptical cavities. It will be the first time that spoke cavities are used in a major accelerator. Work is being done to optimize the energy efficiency and to make further use of the heat from the cooling water coming out of the facility. Finally, potential future upgrades of power and intensity are considered.

Submitted on behalf of the ESS Accelerator Collaboration

Author Index

A

- Aderhold, S. TUP0046, TUP0066, *WEIOB05*, THP0055
 Adolphsen, C. *TUP0042*, THIOA01
 Agassi, Y.D. *TUIOB07*
 Ahammed, M. MOP0020
 Ajima, Y. TUP0040
 Akemoto, M. THIOA01
 Altinbas, Z. TUP0010
 Amberg, M. MOP0030, *MOP0035*, MOP0037, THIOA05
 Anders, A. *TUIOA06*
 Anders, W. *MOP0008*, MOP0067, THP0011, FRIOA07
 Andreone, A. TUIOA03
 Anlage, S. M. THP0016, THP0045, THP0058
 Antoine, C.Z. *TUIOA03*
 Arkan, T.T. THIOA01
 Arnau-Izquierdo, G. THIOA06
 Arnold, A. MOP0004, *TUP0019*
 Arnold, S. TUP0036
 Arrieta, V.M. *TUP0065*
 Atieh, S. THIOA06
 Aulenbacher, K. MOP0030, MOP0035, MOP0037, THIOA05
 Aull, S. *THP0006*
 Aviles Santillana, I. THIOA06

B

- Baars, D.C. THP0067, THP0068
 Baboi, N. *MOP0060*
 Bagge-Hansen, M. *THP0056*
 Baldwin, C. THP0016
 Balle, C. THP0026
 Bandelmann, R. TUP0050
 Barbanotti, S. MOP0024, TUP0001, THIOA01
 Barday, R. FRIOA07
 Barth, W.A. MOP0030, MOP0035, MOP0037, THIOA05
 Bass, T. TUP0061
 Batchelor, A.D. THP0028, THP0032
 Bate, R. TUP0008, TUP0013, TUP0038
 Battistoni, M.A. THIOA01
 Baumgart, H. THP0044
 Bazin, N. THIOB02
 Beard, C.D. MOP0020, THIOB06
 Belomestnykh, S.A. *MOIOB04*, MOP0014, MOP0040, *MOP0054*, MOP0059, MOP0067, TUP0010, THP0007, TUP0013
 Ben Aliz, Y. MOP0011
 Ben-Zvi, I. MOP0014, MOP0040, MOP0054, MOP0059, TUP0010, *THIOA04*, THP0007
 Beringer, D.B. THP0047, THP0062, *THP0065*
 Bermejo, F.J. MOP0052
 Bernaudin, P.-E. FRIOA04
 Bestman, P. MOP0005
 Bhogadi, D. TUP0048
 Bieler, T.R. *WEIOA06*, THP0067, THP0068
 Binkowski, J. MOP0045, MOP0046, MOP0051
 Bolgov, R.O. MOP0020
 Borissov, E. THP0015
 Bosland, P. FRIOA04, THIOB02
 Bosotti, A. THIOA01
 Boulware, C.H. MOP0001, MOP0050, MOP0054, *TUP0035*
 Bouly, F.B. MOP0021
 Bourcey, N. MOP0005
 Bousson, S. *MOIOB02*, MOP0039
 Branlard, J. MOP0013
 Braud, D. TUP0002
 Bredy, P. THIOB02
 Bremer, J. THP0026
 Bricker, S. MOP0065
 Brinkmann, A. TUP0036
 Brokmeier, H.G. THP0053
 Brueck, H. TUP0050
 Brunner, O. TUP0058
 Buckley, R.K. *TUP0008*, TUP0038
 Büchner, A. TUP0013
 Büttig, H. MOP0004
 Buettner, Th. THP0003
 Bullock, B. *WEIOA02*
 Burk, D. THP0075
 Burrill, A. TUP0010, MOP0070, TUP0061
 Busch, M. MOP0035, MOP0037

C

- Cabanel, T. FRIOA04
 Calaga, R. MOP0040, *FRIOB05*
 Calatroni, S. *TUIOB05*, TUP0067, THIOA06, THIOB07
 Calderaro, M. TUP0028
 Calero, J. THIOB02
 Capatina, O. MOP0005, TUP0067, *THIOA06*, THIOB07
 Carbonnier, P. THIOB02
 Carcagno, R.H. TUP0048
 Carlson, K. MOP0013
 Carter, H. THIOA01
 Castilla, A. MOP0027, MOP0053
 Cenni, E. TUP0003, TUP0005, *THP0034*, FRIOA06
 Chambrillon, J.K. *TUP0058*
 Champion, M.S. *MOIOB01*, MOP0024, TUP0006, TUP0028, THIOA01, THIOB01
 Chandra, A. *TUP0068*
 Chandrasekaran, S.K. *WEIOA06*
 Chang, W. MOP0031
 Chang, X. MOP0014, MOP0054
 Chao, Y.-C. MOP0047
 Chase, B. MOP0013, THP0037
 Cheban, S. TUP0006
 Chel, S. MOP0034, TUP0062, THIOA06
 Chen, H. FRIOB03
 Chen, J.E. FRIOB01, FRIOB02
 Chen, K. TUP0063, TUP0064
 Cheng, G. THP0016
 Chi, Y.L. MOP0015, FRIOB03
 Cho, Y.-S. MOP0023
 Church, M.D. *MOP0006*
 Ciovati, G. *TUIOB02*, *TUP0051*, THP0008, *THP0016*, THP0028, THP0032, THP0057, THP0067
 Civale, L. *TUIOA04*, THP0021, THP0078
 Clavero, C. *THP0047*, THP0062, THP0065

Author Index

- Clemens, W.A. TUP0029, TUP0037
 Coelho Moreira de Azevedo, P. MOP0005
 Cole, M.D. TUP0010
 Compton, C. MOP0009, MOP0046, *MOP0055*,
TUP0016, WEIOA06, THP0067,
 THP0068
 Conrad, J. MOP0007, MOP0018
 Conway, Z.A. MOP0026, MOP0044, THIOB04,
FRIOA02
 Cooley, L.D. TUP0017, TUP0025, THP0008,
 THP0015, THP0043, THP0051,
 THP0060, *THP0075*
 Cooper, C.A. TUP0017, *TUP0025*, TUP0029,
WEIOA02, THIOA07
 Cordwell, M.A. TUP0013
 Corlett, J.N. TUP0013
 Crawford, A.C. TUP0015, TUP0028
 Crooks, R. TUP0026
 Cullerton, E. MOP0013
- D**
- Dahl, L.A. THIOA05
 Dai, J. THP0018, *THP0020*, *THP0027*
 Dai, J.P. MOP0015, MOP0062, WEIOB06
 Dambre, P. MOP0005
 Dammann, J.A. TUP0036
 Darbandi, P. THP0068
 Davis, G.K. TUP0061
 De Aragon, F.M. THIOB02
 de la Gama, J.G.S. THIOB02
 De Silva, S.U. *MOP0027*, *MOP0027*, MOP0033,
 MOP0043, MOP0053
 Delaup, B. TUP0067
 Delayen, J.R. MOP0022, MOP0027, MOP0033,
 MOP0043, *MOP0053*, *MOP0053*,
THIOA03
 D'Elia, A. THIOB07
 Deonaraine, S. TUP0010
 Desmons, M. TUP0002
 Devanz, G. MOP0034, MOP0041, TUP0002,
 THIOA06
 Dhakal, P. TUIOB02, TUP0051, *THP0057*
 Disset, G. THIOB02
 Dobbins, J. MOP0067
 Dolgashev, V.A. TUIOA04
 Dubbs, L.J. TUP0016, TUP0057, TUP0059
 Duchesne, P. MOP0005
 Duthil, P. MOP0005
 Dwivedi, J. THIOA07
 Dziuba, F.D. MOP0030, MOP0035, *MOP0037*,
 THIOA05
 Dziuba, A.V. *THP0051*, *THP0051*
- E**
- Eddy, N. *THP0040*
 Edinger, R. MOP0020
 Edwards, H.T. WEIOA05
 Eichhorn, R. MOP0007, *MOP0018*
 Eidelman, Y.I. *MOP0066*
 Elliott, K. MOP0009, TUP0016, TUP0057,
 TUP0059
 Elsen, E. THP0031
 Enami, K. TUP0040
 Eozénou, F. *TUP0062*
- Eremeev, G.V. TUP0019, TUP0049, *THP0005*,
THP0017, *THP0018*, THP0019,
 THP0020, *THP0029*
 Ermakov, A. TUP0026, TUP0036, THP0055
 Escherich, K. TUP0018
 Etxebarria, V. MOP0052
- F**
- Facco, A. MOP0009, MOP0045, MOP0046,
 MOP0055, MOP0065, TUP0056,
 TUP0060, THIOB03
 Famery, Q. TUIOA03
 Fang, S.X. FRIOB03
 Fellenz, B.J. THP0040
 Feng, Z.Q. MOP0069, TUP0047
 Feuchtwanger, J. MOP0052
 Fischer, R.L. MOP0026
 Fisher, M.V. MOP0032
 Flood, R. J. THP0016
 Foley, M.H. MOP0003, MOP0024, THIOA07
 Follkie, J. TUP0028
 Ford, D.C. *THP0060*, *THP0060*
 Forehand, D. TUP0028
 Fouaidy, M. THP0039
 Frahm, A. FRIOA07
 Frankel, G. TUP0068
 Fraser, M.A. THIOB07
 Fu, S. *FRIOB03*
 Fuerst, J.D. TUP0034
 Fukuda, S. THIOA01
 Furuta, F. MOP0038, *TUP0014*
 Furuya, T. TUP0003, TUP0005, THP0034,
 FRIOA06
- G**
- Gabriel, F.G. TUP0013
 Gao, J. *MOP0015*, WEIOB06
 Garich, H.M. TUP0017
 Garmendia, N. MOP0052
 Gash, W.K. TUP0035
 Gasser, Y. TUP0002, TUP0062
 Gassner, D.M. TUP0010
 Gassot, H. *MOP0021*, *MOP0039*
 Ge, M. *THP0015*, THP0051
 Geng, R.L. *MOIOB06*, *MOP0012*, *TUP0015*,
TUP0028, *TUP0029*, TUP0037,
TUP0049, THP0017, THP0018,
 THP0019, THP0020, THP0027,
THP0036
 Gerbick, S.M. MOP0026, TUP0021, TUP0034,
WEIOA03, THIOB04
 Gettmann, V. *MOP0030*, THIOA05
 Ghamsari, B.G. THP0045, *THP0058*
 Ghosh, R. MOP0003
 Gilankar, G. MOP0003
 Ginsburg, C.M. MOP0003, MOP0024, *THIOB01*
 Giraud, J. FRIOA04
 Glennon, P. TUP0004
 Görgen, R. MOP0067
 Gössel, A. MOP0010, TUP0046, TUP0048,
 THP0035
 Golden, B.A. TUP0028
 Gómez Martínez, Y. *FRIOA04*
 Goncharova, L.V. THP0052

Gonin, I.G. MOP0024
 Goodman, T. THP0036
 Goudket, P. TUP0008, TUP0013, TUP0038
 Goulden, A.R. TUP0008, TUP0038
 Grassellino, A. MOP0017, MOP0020, *TUIOB04*,
 THIOB06
 Grewe, R. MOP0007
 Griffis, D.P. THP0028, THP0032
 Grill, R. THP0053, *THP0059*
 Grimm, C.J. MOP0003, MOP0024, TUP0001
 Grimm, T.L. *MOP0001*, MOP0032, MOP0050,
 MOP0054, TUP0035, THP0067
 THIOB02
 Grouas, N. THP0044, THP0064, THP0074
 Gu, D. *MOP0068*
 Gu, P. THP0035
 Gubarev, V. TUIOA04, *TUIOB03*
 Guo, J. THIOA07
 Gupta, P.D. *TUIOA02*, THP0016, THP0043
 Gurevich, A.V. TUIOB05
 Gustafsson, A.E. THIOB02
 Gutiérrez, J.L.

H

Haase, A.A. TUP0042
 Haberkorn, N.F. TUIOA04, *THP0021*, THP0078
 Hahn, H. MOP0040, MOP0059, *THP0041*
 Hajima, R. MOP0036
 Halbritter, J. *THP0004*
 Hall, T.D. TUP0012
 Hammoudi, N. THP0039
 Hao, J.K. *FRIOB01*, FRIOB02
 Hara, H. WEIOB03
 Hara, K. THIOA01
 Hardy, P. THIOB02
 Harms, E.R. *MOP0013*, TUP0055, *WEIOA05*,
 THP0037
 Hartung, W. MOP0009, MOP0055, TUP0056,
 TUP0060
 Hawley, M. THP0021, THP0078
 Hayano, H. MOP0064, TUP0023, TUP0029,
 TUP0030, TUP0032, TUP0037,
 TUP0039, TUP0040, WEIOB02,
 THIOA01
 He, F.S. *MOP0029*
 He, Y. MOP0016, MOP0031, MOP0049,
 FRIOB03
 Heilmaier, M. THP0059
 Henning, W.F. *MOTA01*
 Hennion, V.M. THIOB02
 Hicks, D.T. THP0015, THP0075
 Higashi, N. THIOA01
 Hitomi, H. WEIOB03
 Hocker, A. *TUP0055*, THIOA01
 Hodek, M. MOP0055, MOP0065, TUP0004,
 THIOB03
 Höfle, W. TUP0002
 Hoffstaetter, G.H. *MOIOA03*, MOP0016, THP0012
 Hollister, J.L. MOP0001
 Holzbauer, J.P. MOP0046, MOP0065, *MOP0045*
 Hopper, C.S. *MOP0022*, *MOP0033*
 Horst, van der, B. TUP0041, TUP0045
 Hoss, M. THP0055
 Hou, H.T. *MOP0069*, *MOP0069*, TUP0047
 Huang, T.M. MOP0062
 Hug, F. MOP0007, MOP0018

I

Inman, M.E. *TUP0012*, *TUP0017*
 Inoue, H. TUIOA04, TUP0040
 Iversen, J. TUP0036, TUP0046, TUP0048,
 THP0053
 Iwashita, Y. *TUP0032*, WEIOB02

J

Jacke, S. MOP0030, THIOA05
 Jacques, E. TUP0002
 Jain, A. MOP0003
 Jain, P. THP0041
 James, C. TUIOB01, THP0069, THP0077
 Jamilkowski, J.P. TUP0010
 Janda, D. THP0059
 Jankowiak, A. MOP0008, FRIOA07
 Janssen, D. MOP0004
 Jecks, R. MOP0032
 Jenhani, H. THIOB02
 Jensch, K. MOP0010, THIOA01
 Jensen, C.C. MOP0013
 Jensen, M. *MOIOB05*, MOP0068, THP0010
 Jeong, J.D. *MOP0048*
 Jia, Q.X. THP0021
 Jin, S. *TUP0022*, TUP0031, *TUP0033*,
 THP0025
 Johnson, E.C. MOP0040, MOP0059, THP0041
 Johnson, M.J. MOP0009, MOP0045, MOP0051,
 MOP0055
 Joireman, P.W. MOP0013
 Jones, R.M. MOP0060
 Jordan, K. THP0016
 Joshi, S.C. WEIOA02, THIOA07
 Junginger, T. *WEIOA04*, THIOA06, THP0026,
WEIOA04
 Justus, M. MOP0004

K

Kaabi, W. *TUP0011*
 Kaiser, M. THIOA05
 Kaizer, B. MOP0011
 Kako, E. MOP0064, TUP0007, TUP0023,
 TUP0030, TUP0040, FRIOA06,
 THIOA01
 Kamigaito, O. MOP0028
 Kamps, T. MOP0008, FRIOA07
 Kanaoka, K. WEIOB03
 Kanareykin, A. MOP0025
 Kang, D. *THP0067*, THP0068
 Kankiya, P. TUP0010
 Kaplan, R.P.K. MOP0067
 Karstensen, S. TUP0046
 Katagiri, H. THIOA01
 Kato, S. TUP0037, TUP0040
 kawabata, N. TUP0040
 Kayran, D. TUP0010
 Kazakov, S. *TUP0006*, *TUP0009*
 Kedzie, M. TUP0034, THIOB04
 Kelley, M.J. TUP0024, THP0073, THP0046,
 THP0048
 Kelly, M.P. MOP0026, TUP0021, TUP0034,
 WEIOA03, *THIOB04*

Author Index

- Kephart, R.D. THIOA01
 Kerby, J.S. MOP0003, THIOA01
 Kester, O.K. THIOB03
 Kewisch, J. MOP0040
 Khabiboulline, T.N. MOP0024, TUP0001, TUP0006,
 TUP0048, THIOA07, THP0023,
THP0033
 Khare, P. MOP0003
 Kim, H.S. *MOP0023*
 Kim, S.-H. *MOIOB03*
 Kim, Y.-J. *THP0049*
 Kimura, T. TUP0013
 Klauke, S. FRIOA07
 Klebaner, A.L. MOP0013
 Klein, D.S. MOP0056
 Kleinmann, M. MOP0018
 Kleman, K.J. MOP0032
 Klinke, D. TUP0036, TUP0048
 Klopf, J.M. THP0073
 Kneisel, P. MOP0004, *MOP0070*, TUP0019,
 TUP0026, TUP0049, THP0016,
 THP0057, FRIOA07
 Knobloch, J. MOP0008, MOP0067, THP0006,
 THP0011, FRIOA07
 Ko, K. MOP0061
 Kojima, Y. THIOA01
 Kolb, P. MOP0017, MOP0020, *MOP0047*,
 THIOB06
 Kole, T. MOP0055
 Kolka, A.A. THP0067
 Kolomiets, A. MOP0026, MOP0044
 Komiya, A. TUP0039
 Kondo, Y. THIOA01
 Konomi, T. *MOP0038*
 Kosciuk, B.N. TUP0035
 Kostin, D. *MOP0010*, TUP0045, TUP0046,
THP0003, *THP0035*, THIOA01
 Kotelnikov, S. TUP0048
 Krafft, G.A. THP0073
 Kramp, M. TUP0006
 Kreisel, A. MOP0011
 Kreps, G. TUP0026, TUP0046, TUP0048
 Krick, A. TUP0063, TUP0064
 Krishnan, M. *TUIOB01*, THP0042, THP0069,
 THP0077
 Krizmanich, C. TUP0035
 Krupka, N. TUP0018, TUP0045
 Kubicki, T. MOP0013
 Kucera, M.J. MOP0013
 Kürzeder, T. MOP0007, MOP0018
 Kugeler, O. MOP0008, MOP0067, THP0006,
THP0011, FRIOA07
 Kuhlman, B. MOP0032, TUP0035
 Kuroiwa, N. TUP0023
 Kush, P.K. MOP0003
 Kushnick, P. MOP0070, TUP0028
 Kwon, H.-J. MOP0023
- L**
- Lacroix, M. TUP0011
 Lagotzky, S. THP0061
 Laloudakis, N. TUP0010
 Lamura, G. TUIOA03
 Lanza, G. *TUP0067*
 Larbalestier, D.C. THP0043, THP0054
 Laxdal, R.E. MOP0017, MOP0020, MOP0047,
 THIOB06
 Laxminarayanan, A. *THIOB06*
 MOP0003
 Leclerc, J. TUIOA03
 Lee, K.H. MOP0061
 Lee, P.J. THP0043, THP0054
 Legan, A.M. MOP0013
 Legg, R.A. *MOP0032*
 Lei, Q.Y. TUP0063, TUP0064
 Leibfritz, J.R. MOP0006, MOP0013
 Leitner, D. MOP0009, MOP0065, *THIOB03*
 Leitner, M. *MOP0009*, MOP0046, MOP0055
 Lengkeit, M. TUP0036
 Lesiak, S.D. *TUP0020*
 Li, D. TUP0013
 Li, D.Z. WEIOB06
 Li, G. MOP0062
 Li, S.P. MOP0015
 Li, Z. MOP0069, TUP0047
 Li, Z.Q. MOP0062, WEIOB06
 MOP0014
 Liao, K.C. *THP0026*
 Lidia, S.M. TUP0013
 Liepe, M. *MOP0016*, MOP0019, MOP0042,
 MOP0056, MOP0057, MOP0061,
 MOP0063, MOP0067, TUIOA05,
 TUP0013, THP0001, THP0009,
 THP0050, THP0066, *FRIOA03*
 THIOA01
 Lilje, L. TUIOA06
 Lim, S. TUP0031, FRIOB01, FRIOB02
 Lin, L. *FRIOB06*
 Lindroos, M. *TUP0047*, MOP0069, *TUP0047*
 Liu, J.F. TUP0049, FRIOB01, FRIOB02
 Liu, K.X. WEIOB06
 Liu, Z.C. *MOP0017*, MOP0020, THIOB06
 Longuevergne, D. *MOP0028*
 Lu, L. TUP0022, TUP0031, TUP0033,
 TUP0049, THP0025, FRIOB01
 Lu, X.Y. THP0047, THP0062, THP0065
 TUP0042, TUP0055
 MOP0069, TUP0047
- M**
- Ma, L. FRIOB03
 Ma, Q. MOP0062
 Ma, Z.Y. MOP0069, TUP0047
 Maddock, M. MOP0068
 Madrak, R.L. THP0023
 Mäder, D. THIOA05
 Maesen, P. TUP0058
 Maheshwari, P. TUIOB01, THP0069, THP0077
 Maheswari, P. TUP0051, *THP0028*, *THP0032*
 TUP0048
 Malloch, I.M. TUP0057, TUP0059
 Mammosser, J.D. TUP0031
 Manus, R. TUP0037
 Mao, D.Q. MOP0069, TUP0047
 Mapar, A. *THP0068*
 Marhauser, F. MOP0070, TUP0061
 Marques Antunes Ferreira, L. TUP0067
 Marten, P.J. MOP0068
 Marti, F. MOP0009, MOP0055
 Martin, D.W. TUIOA04
 Martinet, G. *THP0039*
 Martinez, A. MOP0013
 Masi, L. TUP0010

Matheisen, A.	TUP0018, TUP0026, <i>TUP0041</i> , <i>TUP0045</i> , TUP0046, TUP0050, THIOA01	Nash, S.	MOP0065, THIOB03 <i>THP0061</i>
Matsumoto, A.	TUIOA04	Navitski, A.	TUP0048
Matsumoto, T.	THIOA01	Nehring, R.	THP0016
Matsushita, H.	THIOA01	Nemes, G.	MOP0008, <i>MOP0067</i> , THP0011, <i>FRIOA07</i>
Matveenko, A.N.	FRIOA07	Neumann, A.	MOP0013
Maximenko, Y.B.	<i>THP0024</i>	Nezhevenko, O.A.	MOP0061
McGee, M.W.	MOP0013	Ng, C.-K.	<i>THP0070</i>
McIntosh, P.A.	<i>TUP0013</i> , TUP0038	Nguyen, T.M.	MOP0013
McIntyre, G.T.	TUP0010	Nicklaus, D.J.	THP0015
McIntyre, P.M.	MOP0002, THP0076	Nicol, T.H.	FRIOA07
McMullen, D.	TUP0020	Nietubyc, R.	TUP0043
McNeal, S.R.	TUP0065	Nikolić, M.	MOP0036
Mendelsberg, R.	TUIOA06	Nishimori, N.	TUP0037
Michel, P.	MOP0004, TUP0013	Nishiwaki, M.	TUP0048
Michizono, S.	THIOA01	Nogiec, J.M.	MOP0064, TUP0007, TUP0023, TUP0030, TUP0040, FRIOA06, THIOA01
Mickat, S.	MOP0030, MOP0035, MOP0037, <i>THIOA05</i> , <i>THIOA05</i>	Noguchi, S.	TUP0040
Micoud, R.	FRIOA04	Nohara, K.	TUIOA06
Migliore, M.	FRIOA04	Nollau, A.V.	TUP0023
Migne, J.	THIOB02	Nomura, S.	MOP0065
Miller, D. R.	MOP0055, TUP0016	Norton, D.	
Miller, N.	TUP0035		
Miller, S.J.	MOP0009, MOP0045, MOP0046, <i>MOP0051</i> , MOP0055		
Mishra, C.S.	THIOA07		
Mitchell, D.V.	THIOA01		
Miura, T.	THIOA01		
Moeckly, B.	TUIOA04, TUIOB07, THP0021, THP0078		
Moeggenborg, K.	TUP0020		
Möller, W.-D.	MOP0010, TUP0036, TUP0046, TUP0048, THP0003, THP0035, THIOA01		
Monjushiro, H.	TUP0039		
Montesinos, E.	MOP0005		
Moore, M.H.	MOP0027, MOP0053		
Morfin, J.	FRIOA04		
Mori, K.	TUP0023		
Morozumi, Y.	<i>THP0002</i>		
Morris, D.	MOP0065, THIOB03		
Morrone, M.L.	THP0016		
Mueller, C.	TUP0048		
Müller, G.	THP0061		
Mundra, G.	THIOA07		
Munoz, J.L.	<i>MOP0052</i>		
Murcek, P.	<i>MOP0004</i> , TUP0019		
Murphy, J.E.	THP0068		
Murphy, R.C.	TUP0021, <i>TUP0034</i> , WEIOA03, THIOB04		
Mustapha, B.	MOP0026, <i>MOP0044</i> , THIOB04		
Myneni, R.	TUIOB02, TUP0051, THP0028, THP0032, THP0057		
N			
Nagafuchi, T.	TUP0023		
Nagai, R.	MOP0036		
Nagaitsev, S.	MOP0006, MOP0066, MOP0013		
Nakai, H.	THIOA01		
Nakajima, H.	THIOA01		
Nakamura, H.	TUP0040		
Nakamura, N.	TUP0005		
Nakanishi, K.	THIOA01		
Nakayama, K.	TUP0023		
Nantista, C.D.	TUP0042, THIOA01		
		Oates, D.E.	TUIOB07
		Ohuchi, N.	MOP0064, THIOA01
		Olave, R.G.	MOP0022
		Olry, G.	MOP0021, MOP0039, <i>THIOB05</i> , FRIOA04
		Orlov, Y.	MOP0003, TUP0006
		Orr, R.S.	THIOB06
		Orrett, J.F.	TUP0008, TUP0038
		Orsini, F.	<i>THIOB02</i>
		Ortega Bergado, A.	MOP0026
		Ostroumov, P.N.	<i>MOP0026</i> , MOP0044, THIOB04 <i>TUP0023</i>
		Ota, T.	THP0056
		Outlaw, R.A.	TUP0028
		Overton, R.B.	TUP0016, TUP0057, TUP0059 <i>THIOA02</i> , THIOA07, THP0015, THP0022, THP0023
		Oweiss, R.	
		Ozelis, J.P.	
		P	
		Padamsee, H.	TUP0013, THP0001, <i>WEIOCO1</i> THIOA01
		Pagani, C.	WEIOA02, THP0017, THP0018, <i>THP0019</i> , <i>THP0071</i>
		Palczewski, A.D.	<i>TUIOA01</i>
		Palmieri, V.	MOP0015, MOP0062, FRIOB03 MOP0068, <i>THP0010</i>
		Pan, W.M.	THIOA01
		Pande, S.A.	<i>MOP0043</i> , <i>MOP0043</i> <i>MOP0005</i> , THIOA06
		Paparella, R.	TUP0067, <i>THIOB07</i> , <i>THIOB07</i>
		Park, H.	TUP0010
		Parma, V.	TUP0008, TUP0013
		Pasini, M.	FRIOB06
		Pate, D.	TUP0011
		Pattalwar, S.M.	TUIOA04
		Peggs, S.	THIOB02
		Peinaud, Y.	MOP0065, THIOB03 <i>MOP0011</i>
		Pellin, M.J.	TUP0048
		Penichot, Y.	
		Perdikakis, G.	
		Perry, A.	
		Peters, H.-B.	

Author Index

- Petersen, B. TUP0018
 Peterson, E. TUP0028
 Peterson, T.J. *MOP0003*, THIOA01
 Pfeffer, H. MOP0013
 Phillips, D. TUP0010
 Phillips, H.L. TUIOB01, TUP0043, THP0042,
 THP0044, THP0048, THP0064,
 THP0074
 THIOA01
 Pierini, P. MOP0007
 Pietralla, N. MOP0064, TUP0001
 Pilipenko, R.V. TUP0002
 Piquet, O. TUP0058
 Pirotte, O. MOP0064, *TUP0001*, MOP0013,
 THP0030, *THP0037*, FRIOA01,
 THIOA01
 Pischalnikov, Y.M. *TUP0002*, THIOA06, *MOP0034*,
MOP0041, THIOB02
 Plouin, J. THIOB02
 Podadera Aliseda, I. MOP0030, MOP0035, MOP0037,
 THIOA05
 Podlech, H. TUP0036
 Poerschmann, P. *MOP0002*, *THP0076*
 Pogue, N. TUP0025
 Poloubotko, V. THP0043, *THP0054*
 Polyanskii, A. MOP0009, MOP0045, *MOP0046*,
MOP0065, *TUP0004*, MOP0055,
TUP0056, TUP0057, *TUP0060*,
 THIOB03
 Popielarski, J. MOP0009, MOP0055, TUP0016,
TUP0057, *TUP0059*
 Popielarski, L. TUP0043
 Popović, S. MOP0052
 Portilla, J. MOP0016, *MOP0019*, *MOP0063*,
THP0009, *THP0066*
 Posen, S. THIOA07
 Potukuchi, P.N. TUP0002, TUP0062
 Poupeau, J.P. THP0068
 Pourboghraat, F. TUP0042
 Premo, K.S. MOP0013
 Prieto, P.S. TUP0013
 Proch, D. THP0078
 Prolier, T. TUP0006, TUP0025
 Pronitchev, O. TUIOA04, THP0072
 Proslie, Th. *THIOA07*
 Puntambekar, A. THP0063, THP0064, THP0065,
 THP0071, THP0074
 MOP0013
TUP0021, TUP0034, WEIOA03,
 THIOB04
 TUP0027, *TUP0061*
 THIOB02
 MOP0005, THIOA06
 THIOB02
MOIOA01, *TUP0046*, TUP0066,
 THP0031, THP0035, THP0055,
 THP0061
 MOP0005
 MOP0007
 THP0028, THP0032
 MOP0070, TUP0022, TUP0031,
 TUP0033, THP0025
MOP0024
 TUIOA01
 THP0047, *THP0062*, THP0065
 MOP0011
THP0008, *THP0022*, THP0043,
 THP0049, *THP0052*
 MOP0022
MOP0050, TUP0035
 THIOA01
 TUIOA01
 TUP0002, THIOB02
 MOP0005, MOP0021, MOP0039
 TUP0017, TUP0020, TUP0025,
 THIOA07
 THP0015
 FRIOA07
 Reid, J.
 Reid, T.
 Reilly, A.
 Relland, J.
 Renaglia, T.
 Renard, B.
 Reschke, D.
 Reynet, D.
 Richter, A.
 Rigsbee, M.
 Rimmer, R.A.
 Ristori, L.
 Rizzetto, D.
 Roach, W.M.
 Rodnizki, J.
 Romanenko, A.
 Roof, S.J.
 Rose, J.
 Ross, M.C.
 Rossi, A.A.
 Roudier, D.
 Rousselot, S.
 Rowe, A.M.
 Ruan, J.
 Rudolph, J.
 S
 Saegerbarth, S. TUP0041, TUP0045
 Saeki, T. TUP0023, TUP0030, TUP0032,
TUP0037, TUP0039, *TUP0040*,
THIOB08, THIOA01
 TUP0002
 MOP0038, WEIOA02, *THP0013*
 TUP0003, *TUP0005*, THP0034,
FRIOA05, FRIOA06
 MOP0028
 THIOB02
 TUP0023
TUP0007, TUP0040, FRIOA06,
 THIOA01
 TUP0039
 MOP0002, THP0076
 TUP0037, *TUP0039*
MOP0036, TUP0005, FRIOA06,
TUP0003, THP0034
 TUP0050
TUP0018, TUP0045
MOP0064, TUP0001, MOP0013,
 TUP0048, *THP0030*, THP0037,
FRIOA01, THIOA01
 FRIOA07
 TUIOB05
 TUP0041, TUP0045, THIOA01
 TUP0046, *TUP0066*, *THP0031*
TUP0050
 TUP0041, TUP0045, THIOA01
 THP0053
 FRIOA07
 Schaffran, J.
 Schalwat, M.
 Schappert, W.
 Schenk, M.
 Scheubel, M.
 Schilling, P.
 Schlander, F.
 Schmidt, A.
 Schmökel, M.
 Schölz, F.
 Schubert, S.G.

Q

- Quan, S.W. FRIOB01, FRIOB02
 Quast, T. FRIOA07
 Quigley, P. TUP0013

R

- Rains, S. MOP0068
 Rankin, A.F. MOP0068
 Rao, T. MOP0014, MOP0054
 Rathke, J. TUP0028
 Ratzinger, U. MOP0030, MOP0035, MOP0037,
 THIOA05
 Ravindranath, V. TUP0035
 Reece, C.E. *MOIOA04*, TUIOB01, TUP0012,
 TUP0024, *TUP0027*, TUP0061,
 WEIOA01, THP0038, THP0042,
 THP0044, THP0046, THP0047,
 THP0048, THP0056, THP0062,

Author Index

Vande Crean, A. MOP0005
 Varghese, P. MOP0013
 Vennekate, H. THP0026
 Verdu, J. MOP0052
 Verhanovitz, N. MOP0065
 Veshcherevich, V. MOP0016
 Vezzu, F. FRIOA04
 Villegier, J.C. TUIOA03
 Vinzenz, W. THIOA05
 Völker, J. FRIOA07
 Vollenberg, W. TUIOB05, THP0026
 Voy, D.C. THP0040
 Vullierme, B. TUP0058
 Vušković, L. TUP0043

W

Walker, N.J. THIOA01
 Wallig, J.G. TUIOA06
 Wang, E. MOP0014
 Wang, F. TUP0042
 Wang, G.W. MOP0062, TUP0052
 Wang, H. MOP0029
 Wang, Q.Y. MOP0062, WEIOB06
 Wang, Z. TUP0062
 Waraich, B.S. MOP0020
 Watanabe, E. TUIOA04
 Watanabe, J. TUP0023
 Watanabe, K. TUP0007, TUP0029, TUP0030,
 TUP0032, TUP0023, WEIOB02,
 THP0027, THIOA01, FRIOA06
 Watanabe, M. TUP0030
 Watanabe, Y. TUP0040
 Watanuki, T. TUP0030
 Watkins, A.V. MOP0068
 Wei, J. MOP0009, MOP0058, MOP0055
 Weingarten, W. MOP0005, TUIOB08, TUP0058,
 WEIOA04, THP0026, THIOA06
 Weise, H. THIOA01
 Weisend, J. MOP0009
 Weiss, D. TUP0010
 Weissman, L. MOP0011
 Weitkämper, H. TUP0041, TUP0045
 Welsch, C.P. WEIOA04
 Wendt, M. THP0040
 Wheelhouse, A.E. TUP0008, TUP0038
 Whitbeck, G.J. TUP0010
 Will, I. FRIOA07
 Williams, L.R. MOP0005
 Williams, M. TUP0059
 Wilson, K.M. THP0016
 Winowski, M.J. MOP0054, TUP0035
 Witgen, K. MOP0055, TUP0016
 Wittmer, W. THIOB03
 Wlodarczak, J. MOP0009, TUP0004, MOP0055,
 MOP0065, TUP0056, TUP0060
 Wong, M. TUP0025
 Wright, N.T. WEIOA06
 Wu, A.T. TUP0022, TUP0031, TUP0033,
 THP0025, THP0063
 Wu, G. WEIOB01, THP0015, THP0022,
 THP0051, THIOA07, THP0008
 Wu, Q. MOP0014, MOP0054, THP0007
 Wu, X. THIOB03

X

Xi, X. TUP0063, TUP0064
 Xiang, R. MOP0004, TUP0019
 Xiao, B. TUIOA04, THP0048
 Xiao, L. MOP0061
 Xie, Y. MOP0042, THP0001, THP0050
 Xin, T. MOP0014, MOP0054
 Xu, C. THP0046, THP0073
 Xu, K. MOP0069
 Xu, W. MOP0040, MOP0059, TUP0010,
 THP0041
 Xu, Y. MOP0009, MOP0045, MOP0046,
 MOP0051
 Xue, L. MOP0054

Y

Yakovlev, V.P. MOP0024, TUP0006, THP0024,
 THP0033
 Yamada, K. MOP0028
 Yamada, M. TUP0023
 Yamaguchi, S. TUP0040, THIOA01
 Yamamoto, A. MOP0042, TUP0023, TUP0040,
 THIOA01
 Yamamoto, Y. MOP0064, TUP0007, TUP0030,
 TUP0023, TUP0040, THIOA01,
 FRIOA06
 Yanagisawa, T. WEIOB03
 Yin, B. TUP0047
 Yokoya, K. TUP0040, THIOA01
 Yoneda, C. TUIOA04
 Yoshida, M. THIOA01
 Yu, H. TUP0047

Z

Zaltsman, A. TUP0010
 Zaplatin, E.N. MOP0025, THIOB02
 Zasadzinski, J. THP0072
 Zhai, J.Y. MOP0015, WEIOB06
 Zhang, B.C. FRIOB01
 Zhang, C. FRIOB03, MOP0031, MOP0049
 Zhang, P. MOP0060
 Zhang, S. THP0016
 Zhang, S.H. MOP0031, MOP0049
 Zhang, Y. MOP0009, MOP0058
 Zhang, Y.Y. THP0021, THP0078
 Zhang, Zh.G. MOP0069, TUP0047
 Zhao, H.W. MOP0031, MOP0049, FRIOB03
 Zhao, K. TUP0022, TUP0031, TUP0033,
 TUP0049, THP0020, THP0025,
 THP0027, FRIOB01, FRIOB02
 Zhao, L. TUP0024
 Zhao, Q. THIOB03
 Zhao, S.J. MOP0069, TUP0047
 Zhao, T.X. WEIOB06
 Zhao, X. TUIOB01, THP0042, THP0044,
 THP0063, THP0064, THP0069,
 THP0074, THP0077
 Zhao, Y.B. MOP0069, TUP0047
 Zhelezov, I.N. TUP0026
 Zheng, X. MOP0069, TUP0047
 Zhou, C. THP0028, THP0032
 Zhu, F. FRIOB01, FRIOB02

Zhuang, C.G.	<i>TUP0063</i> , TUP0064
Zocco, A.T.	THP0078
Zvyagintsev, V.	MOP0017, <i>MOP0020</i> , MOP0047, THIOB06

LIST OF REGISTRANTS

Last Updated 7/18/2011

1.	Sebastian Aderhold	DESY, Hamburg	sebastian.aderhold@desy.de
2.	Chris Adolphsen	SLAC National Accelerator Laboratory	star@slac.stanford.edu
3.	Yehoshua Dan Agassi	Naval Surface Warfare Center, Carderock Division	yehoshua.agassi@navy.mil
4.	Michael Amberg	Helmholtz Institut Mainz	amberg@iap.uni-frankfurt.de
5.	Andre Anders	Lawrence Berkeley National Laboratory	aanders@lbl.gov
6.	Wolfgang Anders	Helmholtz-Zentrum Berlin	wolfgang.anders@helmholtz-berlin.de
7.	Claire Antoine	CEA Saclay	claire.antoine@cea.fr
8.	Tug Arkan	Fermi National Accelerator Laboratory	arkan@fnal.gov
9.	Andre Arnold	Helmholtz-Zentrum Dresden-Rossendorf	a.arnold@hzdr.de
10.	Victor Arrieta	Ultramet	victor.arrieta@ultramet.com
11.	Sarah Aull	Helmholtz-Zentrum Berlin	sarah.aull@helmholtz-berlin.de
12.	Nicoleta Baboi	DESY, Hamburg	nicoleta.baboi@desy.de
13.	Leo Bellantoni	Fermi National Accelerator Laboratory	bellanto@fnal.gov
14.	Sergey Belomestnykh	Brookhaven National Laboratory	sbelomestnykh@bnl.gov
15.	Ilan Ben-Zvi	Brookhaven National Laboratory	benzvi@bnl.gov
16.	Stephane Berry	CEA Saclay	stephane.berry@cea.fr
17.	Stephane Bethuys	Thales Electron Devices	stephane.bethuys@thalesgroup.com
18.	Wilhelm Bialowons	DESY, Hamburg	wilhelm.bialowons@desy.de
19.	Thomas Bieler	Michigan State University	bieler@egr.msu.edu
20.	Theresa Boehl	The Cryogenic Society of America	theresa@cryogenicsociety.org
21.	John Boger	U. S. Department of Energy	john.boger2@science.doe.gov
22.	Chase Boulware	Niowave, Inc	boulware@niowaveinc.com
23.	Sebastien Bousson	IPN Orsay	bousson@ipno.in2p3.fr
24.	Daniel Bowring	Lawrence Berkeley National Laboratory	dbowring@lbl.gov
25.	Rachael Buckley	STFC Daresbury Laboratory	rachael.buckley@stfc.ac.uk
26.	John Buttles	Bailey Tool & Mfg. Co.	jbuttles@baileytool.com
27.	Rama Calaga	Brookhaven National Laboratory	rcalaga@bnl.gov
28.	Sergio Calatroni	CERN	sergio.calatroni@cern.ch
29.	Ofelia Capatina	CERN	ofelia.capatina@cern.ch
30.	Ruben Carcagno	Fermi National Accelerator Laboratory	ruben@fnal.gov
31.	Kermit Carlson	Fermi National Accelerator Laboratory	kermit@fnal.gov
32.	John Carwardine	Argonne National Laboratory	gml@aps.anl.gov
33.	Enrico Cenni	The Graduate University for Advanced Studies, Sokendai- KEK	enrico@post.kek.jp

34.	Yong-Chul Chae	Argonne National Laboratory	chae@aps.anl.gov
35.	Janic Chambrillon	CERN	janic.kevin.chambrillon@cern.ch
36.	Mark Champion	Fermi National Accelerator Laboratory	champion@fnal.gov
37.	Ashwini Chandra	The Ohio State University	chandra.54@osu.edu
38.	Saravan Kumar Chandrasekaran	Michigan State University	chandras@nscl.msu.edu
39.	Wei Chang	Institute of Modern Physics, Chinese Academy of Sciences	chang@impcas.ac.cn
40.	Jia-er Chen	Peking University	chenje@pku.edu.cn
41.	Micheal Church	Fermi National Accelerator Laboratory	church@fnal.gov
42.	Edmond Ciapala	CERN	edmond.ciapala@cern.ch
43.	Gianluigi Ciovati	Thomas Jefferson National Accelerator Facility	gciovati@jlab.org
44.	Paulo Coelho Moreira de Azevedo	CERN	pcoelhom@cern.ch
45.	Chris Compton	Michigan State University	compton@frib.msu.edu
46.	Zachary Conway	Argonne National Laboratory	zconway@anl.gov
47.	Lance Cooley	Fermi National Accelerator Laboratory	ldcooley@fnal.gov
48.	Charlie Cooper	Fermi National Accelerator Laboratory	ccooper@fnal.gov
49.	Jim Crisp	Michigan State University	crisp@frib.msu.edu
50.	Jin Dai	Peking University Institute of Heavy Ion Physics	daijin@pku.edu.cn
51.	Steven Daley		stevedaley@comcast.net
52.	Kirk Davis	Thomas Jefferson National Accelerator Facility	kdavis@jlab.org
53.	Subashini De Silva	Old Dominion University	sdesilva@jlab.org
54.	Brian Deimling	Niowave, Inc	deimling@niowaveinc.com
55.	Jean Delayen	Old Dominion University	jdelayen@odu.edu
56.	Pashupati Dhakal	Thomas Jefferson National Accelerator Facility	dhakal@jlab.org
57.	Nandhini Dhanaraj	Fermi National Accelerator Laboratory	dhanaraj@fnal.gov
58.	Lindsay Dubbs	Michigan State University / Facility for Rare Isotope Beams	dubbs@frib.msu.edu
59.	John V. Dugan Jr.	SPAFOA	jackdugan@cox.net
60.	Florian Dziuba	Goethe-Universität	
61.	Alexander Dzyuba	Fermi National Accelerator Laboratory	dzyuba@fnal.gov
62.	Nathan Eddy	Fermi National Accelerator Laboratory	eddy@fnal.gov
63.	Ralf Edinger	PAVAC Energy Corp.	edinger@pavac.com
64.	Donald A. Edwards		daedwards11@me.com
65.	Helen Edwards	Fermi National Accelerator Laboratory	hedwards@fnal.gov
66.	Ralf Eichhorn	S-DALINAC	eichhorn@ikp.tu-darmstadt.de
67.	Yury Eidelman	Fermi National Accelerator Laboratory	eidelyur@fnal.gov

68.	Ahmed El-Nakeeb	Cairo University	ahmdmokhtar@yahoo.com
69.	Kyle Elliot	Michigan State University	elliott@nscl.msu.edu
70.	Fabien Eozénou	CEA Saclay	fabien.eozenou@cea.fr
71.	Grigory Ereemeev	Thomas Jefferson National Accelerator Facility	grigory@jlab.org
72.	Alberto Facco	Michigan State University	facco@frib.msu.edu
73.	Joshua Feingold	Thomas Jefferson National Accelerator Facility	feingold@jlab.org
74.	He Feisi	Thomas Jefferson National Accelerator Facility	feisi@jlab.org
75.	Richard Fischer	Argonne National Laboratory	rfischer@anl.gov
76.	Mike Fisher	University of Wisconsin, Madison	mfisher@src.wisc.edu
77.	Michael Foley	Fermi National Accelerator Laboratory	foleymh@fnal.gov
78.	Denise Ford	Northwestern University	dford@fnal.gov
79.	Pedro Frigola	RadiaBeam Technologies	frigola@radiabeam.com
80.	Shinian Fu	Institute of High Energy Physics, CAS	fusn@ihep.ac.cn
81.	Joel Fuerst	Argonne National Laboratory	fuerst@anl.gov
82.	Fumio Furuta	KEK	fumio.furuta@gmail.com
83.	Huimin Gassot	IPN Orsay	gassot@ipno.in2p3.fr
84.	Mingqi Ge	Cornell University	mg574@cornell.edu
85.	Rong-Li Geng	Thomas Jefferson National Accelerator Facility	geng@jlab.org
86.	Scott Gerbick	Argonne National Laboratory	gerbick@anl.gov
87.	Viktor Gettmann	GSI Helmholtzzentrum für Schwerionenforschung GmbH	v.gettmann@gsi.de
88.	Behnood Ghamsari	University of Maryland	ghamsari@umd.edu
89.	Eric Giguët	Thales Electron Devices	eric.giguët@thalesgroup.com
90.	Camille Ginsburg	Fermi National Accelerator Laboratory	ginsburg@fnal.gov
91.	Yolanda Gomez Martinez	LPSC / CNRS	gomez@lpsc.in2p3.fr
92.	Ivan Gonin	Fermi National Accelerator Laboratory	gonin@fnal.gov
93.	Philippe Goudket	STFC Daresbury Laboratory	philippe.goudket@stfc.ac.uk
94.	Andrew Goulden	STFC Daresbury Laboratory	andy.goulden@stfc.ac.uk
95.	Krishnaswamy Gounder	DTRA	krishnaswamy.gounder_contractor@dtra.mil
96.	Robert Grill	Plansee SE	robert.grill@plansee.com
97.	Chuck Grimm	Fermi National Accelerator Laboratory	grimm@fnal.gov
98.	Terry Grimm	Niowave, Inc.	grimm@niowaveinc.com
99.	Pengda Gu	Diamond Light Source Ltd.	pengda.gu@diamond.ac.uk
100.	Jiquan Guo	SLAC National Accelerator Laboratory	jqguo@slac.stanford.edu
101.	Alex Gurevich	Old Dominion University	gurevich@odu.edu
102.	Nestor Haberkorn	Los Alamos National Laboratory	nhaberkorn@lanl.gov

103. Harald Hahn	Brookhaven National Laboratory	hahn@bnl.gov
104. Jiankui Hao	Peking University	jkhao@pku.edu.cn
105. Lee Harle	Michigan State University	harle@frib.msu.edu
106. Elvin Harms	Fermi National Accelerator Laboratory	harms@fnal.gov
107. Douglas Hartman	Everson Tesla, Inc.	dhartman@eversontesla.com
108. Mohamed Hassan	Fermi National Accelerator Laboratory	mhassan@fnal.gov
109. Hitoshi Hayano	KEK	hitoshi.hayano@kek.jp
110. Shoubo He	Institute of Modern Physics, Chinese Academy of Sciences	heshb@impcas.ac.cn
111. Yuan He	Institute of Modern Physics, Chinese Academy of Sciences	hey@impcas.ac.cn
112. Robert Heine	Institut für Kernphysik	heine@kph.uni-mainz.de
113. Matthew Hendricks	Argonne National Laboratory	hendricks@anl.gov
114. Walter F. Henning	Argonne National Laboratory	wfhenning@anl.gov
115. Leah Hesla	Fermi National Accelerator Laboratory	leah@fnal.gov
116. Andy Hocker	Fermi National Accelerator Laboratory	hocker@fnal.gov
117. Georg Hoffstaetter	Cornell University	georg.hoffstaetter@cornell.edu
118. Jerry Hollister	Niowave, Inc	hollister@niowaveinc.com
119. Douglas Holmes	Advanced Energy Systems, Inc.	doug_holmes@mail.aesys.net
120. Stephen Holmes	Fermi National Accelerator Laboratory	holmes@fnal.gov
121. Jeremiah Holzbauer	Michigan State University	holzbaue@nscl.msu.edu
122. Christopher Hopper	Old Dominion University	chopp002@odu.edu
123. Doug Horan	Argonne National Laboratory	horan@aps.anl.gov
124. Zvi Horvitz	NRC Soreq	zvihor@soreq.gov.il
125. Laurie Huget	The Cryogenic Society of America	laurie@cryogenicsociety.org
126. Warner Huget	The Cryogenic Society of America	
127. Maria Inman	Faraday Technology, Inc.	mariaainman@faradaytechnology.com
128. Yoshihisa Iwashita	Kyoto University	iwashita@kyticr.kuicr.kyoto-u.ac.jp
129. Puneet Jain	Brookhaven National Laboratory	puneet.jain@stonybrook.edu
130. Jaeho Jang	POSTECH	remedios@postech.ac.kr
131. Randall Jecks II	Niowave, Inc	jecks@niowaveinc.com
132. Morten Jensen	Diamond Light Source Ltd.	morten.jensen@diamond.ac.uk
133. Song Jin	Thomas Jefferson National Accelerator Facility / Peking University	songjin@jlab.org
134. Elliott Johnson	Brookhaven National Laboratory	johnsone@bnl.gov
135. Matt Johnson	Michigan State University	mjohnson@frib.msu.edu
136. Rolland Johnson	Muons, Inc.	roljohn@aol.com
137. Tobias Junginger	CERN, MPIK	Tobias.Junginger@cern.ch
138. Walid Kaabi	LAL-CNRS	kaabi@lal.in2p3.fr
139. Eiji Kako	KEK	eiji.kako@kek.jp

140. Joshua Kaluzny	Argonne National Laboratory	kaluzny@aps.anl.gov
141. Di Kang	Michigan State University	kangdi@msu.edu
142. Valery Kapin	Fermi National Accelerator Laboratory	kapin@fnal.gov
143. Sergey Kazakov	Fermi National Accelerator Laboratory	skazakov@fnal.gov
144. Mark Kedzie	Argonne National Laboratory	mkedzie@anl.gov
145. Michael Kelly	Argonne National Laboratory	mkelly@anl.gov
146. Robert Kephart	Fermi National Accelerator Laboratory	kephart@fnal.gov
147. Jim Kerby	Fermi National Accelerator Laboratory	kerby@fnal.gov
148. Timergali Khabiboulline	Fermi National Accelerator Laboratory	khabibul@fnal.gov
149. Maxim Kharitonov	Rutgers University	maxx@physics.rutgers.edu
150. Han-Sung Kim	Korea Atomic Energy Research Institute	kimhs@kaeri.re.kr
151. Min Jeong Kim	Fermi National Accelerator Laboratory	mjkim@fnal.gov
152. Sang-Ho Kim	Oak Ridge National Laboratory	kimsh@ornl.gov
153. Sang-hoon Kim	POSTECH	khan777@postech.ac.kr
154. YoonJun Kim	Northwestern University	yjkim@northwestern.edu
155. Young-Kee Kim	University of Chicago / Fermi National Accelerator Laboratory	ykkim@fnal.gov
156. Arkadiy Klebaner	Fermi National Accelerator Laboratory	klebaner@fnal.gov
157. Daniel Klinke	DESY, Hamburg	daniel.klinke@desy.de
158. Jeffrey Klug	Argonne National Laboratory	jklug@anl.gov
159. Jens Knobloch	Helmholtz-Zentrum Berlin	knobloch@helmholtz-berlin.de
160. Philipp Kolb	TRIUMF	kolb@triumf.ca
161. Taro Konomi	The Graduated University for Advanced Studies	konomi@post.kek.jp
162. Denis Kostin	DESY, Hamburg	denis.kostin@desy.de
163. Alexey Koveshnikov	TRIUMF	akovesh@triumf.ca
164. Frank Krawczyk	Los Alamos National Laboratory	fkrawczyk@lanl.gov
165. Arik Kreisel	Soreq NRC	arikk40@gmail.com
166. Mahadevan Krishnan	Alameda Applied Sciences Corporation	krishnan@aasc.net
167. Richard Kriske	University of Minnesota	kris0022@umn.edu
168. Oliver Kugeler	Helmholtz-Zentrum-Berlin	oliver.kugeler@helmholtz-berlin.de
169. Robert Kustom	Advanced Photon Source / Argonne National Laboratory	rlk@aps.anl.gov
170. Mickaël Lacroix	CNRS	lacroix@lal.in2p3.fr
171. Giulia Lanza	CERN	giulia.lanza@cern.ch
172. Robert Laxdal	TRIUMF	lax@triumf.ca
173. Robert Legg	Thomas Jefferson National Accelerator Facility / University of Wisconsin, Madison	rlegg@jlab.org

174. Jerry Leibfritz	Fermi National Accelerator Laboratory	leibfritz@fnal.gov
175. Daniela Leitner	Michigan State University	leitnerd@nscl.msu.edu
176. Matthaeus Leitner	Michigan State University	jkebler@msu.edu
177. Xue Liang	Stony Brook University	liangx@bnl.gov
178. Kitty Chia-Chi Liao	CERN	kitty.liao@cern.ch
179. Matthias Liepe	Cornell University	mul2@cornell.edu
180. Fareh Lin	Old Dominion University	flin@odu.edu
181. Mats Lindroos	European Spallation Source ESS AB	mats.lindroos@esss.se
182. Jie Liu	Argonne National Laboratory	jieliu@aps.anl.gov
183. Yunfeng Liu	Ningxia Orient Superconductor Technology Co., Ltd.	liuyunfeng@otic.com.cn
184. David Longuevergne	TRIUMF	longueve@triumf.ca
185. Liang Lu	RIKEN	luliang@riken.jp
186. R. Ale Lukaszew	College of William and Mary	ralukaszew@wm.edu
187. Andrei Lunin	Fermi National Accelerator Laboratory	lunin@fnal.gov
188. Xing Luo		starluo8688@yahoo.com.cn
189. Yong Luo	Argonne National Laboratory	yluo@phy.anl.gov
190. Steve MacDonald	Argonne National Laboratory	macdonald@anl.gov
191. Robyn Madrak	Fermi National Accelerator Laboratory	madrak@fnal.gov
192. Prateek Maheshwari	North Carolina State University	pmahesh@ncsu.edu
193. Aboozar Mapar	Michigan State University	maparabo@msu.edu
194. Frank Marhauser	Muons, Inc.	frank@muonsinc.com
195. Felix Marti	Michigan State University	marti@nscl.msu.edu
196. Guillaume Martinet	IPN Orsay	martinet@ipno.in2p3.fr
197. Axel Matheisen	DESY, Hamburg	axel.matheisen@desy.de
198. Yulia Maximenko	Fermi National Accelerator Laboratory	joulem@gmail.com
199. David McGinnis	Fermi National Accelerator Laboratory	mcginnis@fnal.gov
200. Peter McIntosh	STFC Daresbury Laboratory	peter.mcintosh@stfc.ac.uk
201. Shawn McNeal	Ultramet	shawn.mcneal@ultramet.com
202. James McVea	Thales Components Corporation	jmcvea@tccus.com
203. Dave Meidlinger	Advanced Energy Systems, Inc.	dmeidlinger@mail.aesys.net
204. Sascha Mickat	GSI Helmholtzzentrum für Schwerionenforschung GmbH	s.mickat@gsi.de
205. Kim Miller	Argonne National Laboratory	kimomof2@gmail.com
206. Sam Miller	Michigan State University	millers@nscl.msu.edu
207. Shekhar Mishra	Fermi National Accelerator Laboratory	mishra@fnal.gov
208. Wolf-Dietrich Moeller	DESY, Hamburg	wolf-dietrich.moeller@desy.de
209. Juan Luis Munoz	ESS-Bilbao	jlmunoz@essbilbao.org
210. Petr Murcek	HZDR	p.murcek@hzdr.de
211. Ryan Murphy	Argonne National Laboratory	rmurphy@anl.gov

212. Brahim Mustapha	Argonne National Laboratory	brahim@anl.gov
213. Alireza Nassiri	Argonne National Laboratory	nassiri@aps.anl.gov
214. Aliaksandr Navitski	Bergische Universität Wuppertal	navitski@uni-wuppertal.de
215. George R. Neil	Thomas Jefferson National Accelerator Facility	neil@jlab.org
216. Tony Nelson	ATI Wah Chang	tony.nelson@atimetals.com
217. Richard Neuhaus		wc00612@cityofchicago.org
218. Axel Neumann	Helmholtz Zentrum Berlin	axel.neumann@helmholtz-berlin.de
219. Tom Nicol	Fermi National Accelerator Laboratory	tnicol@fnal.gov
220. Chet Nieter	Tech-X Corporation	nieter@txcorp.com
221. Kiyokazu Nishimura	Izumi Techno Corp.	izumitechno@chime.ocn.ne.jp
222. Shuichi Noguchi	KEK	shuichi.noguchi@kek.jp
223. Jim Norem	Argonne National Laboratory	norem@anl.gov
224. Daniel Oates	Lincoln Laboratory Massachusetts Institute of Technology	oates@ll.mit.edu
225. Guillaume Olry	IPN Orsay	olry@ipno.in2p3.fr
226. Kenneth Olsen	SPAFOA	kenolsen7@aol.com
227. Fabienne Orsini	CEA Saclay	forsini@cea.fr
228. Arturo Ortega Bergado	Argonne National Laboratory	abergado@phy.anl.gov
229. Dwight Osha	C.F. Roark Welding & Engineering Co. Inc.	dosha@roarkfab.com
230. Peter Ostroumov	Argonne National Laboratory	ostroumov@anl.gov
231. Tomoko Ota	Toshiba Corporation	tomoko.ota@toshiba.co.jp
232. Joe Ozelis	Fermi National Accelerator Laboratory	ozelis@fnal.gov
233. Hasan Padamsee	Cornell University	hsp3@cornell.edu
234. Carlo Pagani	University of Milano / INFN	carlo.pagani@mi.infn.it
235. Ari Palczewski	Thomas Jefferson National Accelerator Facility	ari@jlab.org
236. Vincenzo Palmieri	INFN LNL	vincenzo.palmieri@lnl.infn.it
237. Weimin Pan	IHEP, Beijing	panwm@ihep.ac.cn
238. Shivaji Apparao Pande	Diamond Light Source Ltd.	shivaji.pande@diamond.ac.uk
239. Richard Pardo	Argonne National Laboratory	pardo@phy.anl.gov
240. Vittorio Parma	CERN	vittorio.parma@cern.ch
241. Matteo Pasini	CERN	matteo.pasini@cern.ch
242. Dan Paskvan	Argonne National Laboratory	dpaskvan@anl.gov
243. Ronak Patel	Fermi National Accelerator Laboratory	rapatel@fnal.gov
244. Yann Peinaud	CNRS	peinaud@lal.in2p3.fr
245. Michael Peiniger	RI Research Instruments GmbH	michael.peiniger@research-instruments.de
246. Michael Pekeler	RI Research Instruments GmbH	michael.pekeler@research-instruments.de
247. Michael Pellin	Argonne National Laboratory	pellin@anl.gov
248. Amichay Perry	Soreq NRC	imperrya@gmail.com
249. Edward Peterson	Advanced Energy Systems, Inc.	ed_peterson@mail.aesys.net
250. Tom Peterson	Fermi National Accelerator Laboratory	tommy@fnal.gov

251. Larry Phillips	Thomas Jefferson National Accelerator Facility	phillips@jlab.org
252. Roman Pilipenko	Fermi National Accelerator Laboratory	pilipen@fnal.gov
253. Yuriy Pischalnikov	Fermi National Accelerator Laboratory	pischaln@fnal.gov
254. Juliette Plouin	CEA Saclay	juliette.plouin@cea.fr
255. Nathaniel Pogue	Texas A&M University	npogue@physics.tamu.edu
256. Anatolii Polyanskii	National High Magnetic Field Laboratory / Florida State University	polyanskii@asc.magnet.fsu.edu
257. John Popielarski	Michigan State University	popielar@nscl.msu.edu
258. Laura Popielarski	Michigan State University	popiela@nscl.msu.edu
259. Milorad Popovic	Fermi National Accelerator Laboratory	popovic@fnal.gov
260. Sam Posen	Cornell University	sep93@cornell.edu
261. Tom Powers	Thomas Jefferson National Accelerator Facility	powers@jalb.org
262. Burkhard Prause	RI Research Instruments GmbH	burkhard.prause@research-instruments.de
263. Ken Premo	Fermi National Accelerator Laboratory	premo@fnal.gov
264. Oleg Pronitchev	Fermi National Accelerator Laboratory	olegp@fnal.gov
265. Thomas Proslie	Argonne National Laboratory	prolier@anl.gov
266. Avinash Puntambekar	RRCAT, Indore	avinash@rrcat.gov.in, avinash@fnal.gov
267. Alessandro Ratti	Lawrence Berkeley National Laboratory	aratti@lbl.gov
268. Charles Reece	Thomas Jefferson National Accelerator Facility	reece@jlab.org
269. Thomas Reid	Argonne National Laboratory	treid@anl.gov
270. Tony Reilly	Thomas Jefferson National Accelerator Facility	areilly@jlab.org
271. Detlef Reschke	DESY, Hamburg	detlef.reschke@desy.de
272. Leonardo Ristori	Fermi National Accelerator Laboratory	leoristo@fnal.gov
273. Jordan Roark	C.F. Roark Welding & Engineering Co. Inc.	jroark@roarkfab.com
274. Ted Roark	C.F. Roark Welding & Engineering Co. Inc.	troark@roarkfab.com
275. Alexander Romanenko	Fermi National Accelerator Laboratory	aroman@fnal.gov
276. James Rose	Brookhaven National Laboratory	rose@bnl.gov
277. Marc Ross	Fermi National Accelerator Laboratory	mcrec@fnal.gov
278. Antonio Alessandro Rossi	INFN LNL	antonio.rossi@lnl.infn.it
279. Allan Rowe	Fermi National Accelerator Laboratory	arowe@fnal.gov
280. Roger Ruber	Uppsala University	ruber@cern.ch
281. Takayuki Saeki	KEK	takayuki.saeki@kek.jp

282. Arun Saini	University of Delhi / Fermi National Accelerator Laboratory	asaini@fnal.gov
283. Kenji Saito	KEK	kenji.saito@kek.jp
284. Hiroshi Sakai	KEK	sakai.hiroshi@kek.jp
285. Masaru Sawamura	Japan Atomic Energy Agency	sawamura.masaru@jaea.go.jp
286. Marco Schalwat	DESY	marco.schalwat@desy.de
287. Warren Schappert	Fermi National Accelerator Laboratory	warren@fnal.gov
288. Karl-Martin Schirm	CERN	karl.schirm@cern.ch
289. Felix Schlander	DESY, Hamburg	felix.schlander@desy.de
290. Andreas Schmidt	DESY, Hamburg	andreas.schmidt@desy.de
291. Manuela Schmoekel	DESY	manuela.schmoekel@desy.de
292. Roland Schulze	Los Alamos National Laboratory	rkschulze@lanl.gov
293. Jacek Sekutowicz	DESY, Hamburg	jacek.sekutowicz@desy.de
294. Tomoyuki Semba	Hitachi Ltd.	tomoyuki.semba.au@hitachi.com
295. Katsuya Sennyu	Mitsubishi Heavy Industries, Ltd.	katsuya_sennyu@mhi.co.jp
296. Dmitri Sergatskov	Fermi National Accelerator Laboratory	das@fnal.gov
297. Sergey Sharamentov	Argonne National Laboratory	sharamentov@phy.anl.gov
298. Bruce Shelton	Parsons	bruce.shelton@parsons.com
299. Valery Shemelin	Cornell University	vs65@cornell.edu
300. SeungWook Shin	SungKyunKwan University	shace@skku.edu
301. Sven Sievers	S-DALINAC	sievers@ikp.tu-darmstadt.de
302. Senthilraja Singaravelu	Old Dominion University	singarav@jlab.org
303. Waldemar Singer	DESY, Hamburg	waldemar.singer@desy.de
304. Xenia Singer	DESY, Hamburg	xenia.singer@desy.de
305. Pitamber Singh	Bhabha Atomic Research Centre	psingh@barc.gov.in
306. Alexei Smirnov	RadiaBeam Technologies	asmirnov@radiabeam.com
307. Nikolay Solyak	Fermi National Accelerator Laboratory	solyak@fnal.gov
308. Bernd Spaniol	W. C. Heraeus GmbH	bernd.spaniol@heraeus.com
309. Richard Stanek	Fermi National Accelerator Laboratory	rstanek@fnal.gov
310. Alexander Sukhanov	Fermi National Accelerator Laboratory	ais@fnal.gov
311. Yi Sun	IHEP, Beijing	suny@ihep.ac.cn
312. ZuHawn Sung	NHMFL-ASC	zsung@asc.magnet.fsu.edu
313. Michael Syphers	Michigan State University	syphers@msu.edu
314. Tamin Tai	University of Maryland, College Park	tamin@umd.edu
315. Tsuyoshi Tajima	Los Alamos National Laboratory	tajima@lanl.gov
316. E.J. Taylor	Faraday Technology, Inc.	jenningsstaylor@faradaytechnology.com
317. Mathieu Therasse	CERN	mathieu.therasse@cern.ch
318. Nguyen Thi Mua	Hanoi University of Prevention and Fight Fire	muadongminh@gmail.com
319. Jan-Hendrik Thie	DESY, Hamburg	jan-hendrik.thie@desy.de

320. Hui Tian	Thomas Jefferson National Accelerator Facility	huit02@jlab.org
321. Evgeny Toropov	Fermi National Accelerator Laboratory	etoropov@fnal.gov
322. Todd Treado	CPI	todd.treado@cpil.com
323. Kensei Umemori	KEK	kensei.umemori@kek.jp
324. Hiroaki Umezawa	Tokyo Denkai Co., Ltd.	omezawa@tokyodenkai.co.jp
325. Janardan Upadhyay	Thomas Jefferson National Accelerator Facility	upadhyay@jlab.org
326. John Urbin	Linde Cryogenics	john.urbin@lppusa.com
327. Enrique Valderrama	Alameda Applied Sciences Corporation	valderrama@aasc.net
328. Anne-Marie Valente-Feliciano	Thomas Jefferson National Accelerator Facility	valente@jlab.org
329. Nicholas Valles	Cornell University	nrv5@cornell.edu
330. Birte van der Horst	DESY	birte.van.der.horst@desy.de
331. Philip Varghese	Fermi National Accelerator Laboratory	varghese@fnal.gov
332. Hanspeter Vogel	RI Research Instruments GmbH	hanspeter.vogel@research-instruments.de
333. Geoff Waldschmidt	Argonne National Laboratory	waldschm@aps.anl.gov
334. Guangwei Wang	IHEP, Beijing	wanggw@ihep.ac.cn
335. Jinsong Wang	Ningxia Orient Superconductor Technology Co., Ltd.	wangjs@cnmnc.com
336. Ken Watanabe	KEK	kenw@post.kek.jp
337. Wolfgang Weingarten	CERN	wolfgang.weingarten@cern.ch
338. Manfred Wendt	Fermi National Accelerator Laboratory	manfred@fnal.gov
339. Mark Wiseman	Thomas Jefferson National Accelerator Facility	
340. Jon Wlodarczyk	Michigan State University	wlodarcz@nscl.msu.edu
341. Genfa Wu	Argonne National Laboratory	genfa@aps.anl.gov
342. Qiong Wu	Brookhaven National Laboratory	qiowu@bnl.gov
343. Xiaoxing Xi	Temple University	xiaoxing@temple.edu
344. Binping Xiao	College of William and Mary	bpx@jlab.org
345. Liling Xiao	SLAC National Accelerator Laboratory	liling@slac.stanford.edu
346. Yi Xie	Cornell Laboratory for Accelerator-based Sciences and Education (CLASSE)	yx39@cornell.edu
347. Tianmu Xin	Stony Brook University	tianmux@gmail.com
348. Pingran Xiong	Institute of Modern Physics, Chinese Academy of Sciences	xiongpr@impcas.ac.cn
349. Chen Xu	Thomas Jefferson National Accelerator Facility	xuchen@jlab.org
350. Mengxin Xu	Institute of Modern Physics, Chinese Academy of Sciences	xumx@impcas.ac.cn
351. Tracy Xu	Michigan State University	xut@nscl.msu.edu
352. Wencan Xu	Brookhaven National Laboratory	wxu@BNL.gov

353. Vyacheslav Yakovlev	Fermi National Accelerator Laboratory	yakovlev@fnal.gov
354. Kazunari Yamada	RIKEN Nishina Center	nari-yamada@riken.jp
355. Akira Yamamoto	KEK	akira.yamamoto@kek.jp
356. Yasuchika Yamamoto	KEK	yasuchika.yamamoto@kek.jp
357. Victor Yarba	Fermi National Accelerator Laboratory	yarba@fnal.gov
358. Muralidhar Yeddulla	Brookhaven National Laboratory	myeddulla@bnl.gov
359. Richard York	Michigan State University	york@frib.msu.edu
360. Weiming Yue	Institute of Modern Physics, Chinese Academy of Sciences	yueweiming@impcas.ac.cn
361. Alex Zaltsman	Brookhaven National Laboratory	zaltsman@bnl.gov
362. Evgeny Zaplatin	Forschungszentrum Juelich	e.zaplatine@fz-juelich.de
363. John Zasadzinski	Illinois Institute of Technology	zasadzinski@iit.edu
364. Jiyuan Zhai	IHEP, Beijing	zhaijy@ihep.ac.cn
365. Cong Zhang	Institute of Modern Physics, Chinese Academy of Sciences	afeng.cong@gmail.com
366. Yan Zhang	Michigan State University	zhangy@frib.msu.edu
367. Hongwei Zhao	Institute of Modern Physics, Chinese Academy of Sciences	zhaohw@impcas.ac.cn
368. Hongyun Zhao	Ningxia Orient Superconductor Technology Co., Ltd.	zhaohongyun@otic.com.cn
369. Liang Zhao	Thomas Jefferson National Accelerator Facility	lzhao@jlab.org
370. Tongxian Zhao	IHEP, Beijing	zhaotx@ihep.ac.cn
371. Xin Zhao	Thomas Jefferson National Accelerator Facility	xinzhao@jlab.org
372. Feng Zhu	Peking University	zhufeng7726@pku.edu.cn
373. Chenggang Zhuang	Temple University	cuz4@temple.edu
374. Vladimir Zvyagintsev	TRIUMF	zvyagint@triumf.ca